Maurocalcine, un nouveau vecteur de pénétration cellulaire pour la délivrance cellulaire de composés imperméables

Narendra Ram Maraheru Sonnappa

UNIVERSITE JOSEPH FOURIER- GRENOBLE 1

Ecole Doctorale Chimie et Sciences du Vivant

THESE

Pour obtenir le grade de

DOCTEUR DE L'UNIVERSITE JOSEPH FOURIER

Discipline: NEUROSCIENCES

Maurocalcine, un nouveau vecteur de pénétration cellulaire pour la délivrance cellulaire de composés imperméables

Présenté et soutenu publiquement par,

Narendra RAM

Le 16 Octobre 2008

Devant le jury compose de,

Pr. Gilles FAURY, Président

Dr. Gilles DIVITA, Rapporteur

Dr. Alain JOLIOT, Rapporteur

Dr. Jean-Luc COLL, Examinateur

Dr. Hervé DARBON, Examinateur

Dr. Michel DE WAARD, Directeur

UNIVERSITY JOSEPH FOURIER- GRENOBLE 1

Doctoral School of Chemistry and Life Sciences

A THESIS SUBMITTED FOR THE DEGREE OF

DOCTOR OF PHILOSOPHY

DISCIPLINE: NEUROSCIENCES

FROM THE UNIVERSITY OF JOSEPH FOURIER- GRENOBLE

Maurocalcine is a new cell penetration vector for the *in vitro* and *in vivo* delivery of cell impermeable cargoes

Presented by,

Narendra RAM

On 16th October 2008

Members of the jury,

Pr. Gilles FAURY, President

Dr. Gilles DIVITA, Reviewer

Dr. Alain JOLIOT, Reviewer

Dr. Jean-Luc COLL, Examiner

Dr. Hervé DARBON, Examiner

Dr. Michel DE WAARD, Director

SUMMARY

Maurocalcine (MCa) is a 33 mer peptide toxin initially isolated from the venom of Tunisian scorpion *Scorpio maurus palmatus.* Since then, it can be produced by chemical synthesis without structural alteration. This peptide triggers interest for three main reasons. First, it has sequence homology with a calcium channel domain involved in excitation–contraction coupling and helps in unravelling the mechanistic basis of Ca^{2+} mobilization from the sarcoplasmic reticulum. Second, MCa is a powerful activator of the ryanodine receptor, thereby triggering calcium release from intracellular stores. Finally, it is of technological value because of its ability to carry cell-impermeable compounds across the plasma membrane. In this study, I have designed novel more potent analogues of maurocalcine, either by point mutation, or by substitution of cysteine residues, which possess better or equal cell penetration efficiencies, limited cell toxicity and no pharmacological activity on ryanodine receptor. I have analyzed the interaction of these analogues with membrane lipids and glycosaminoglycans and their role in cell penetration. Cell entry pathway of MCa occurs through macropinocytosis, atleast when coupled to streptavidin.

Keywords: Maurocalcine, ryanodine receptor, glycosaminoglycans, macropinocytosis.

RESUME

La maurocalcine (MCa) est un peptide/toxin de 33 acides aminés initialement isolé du venin d'un scorpion Tunisien *Scorpio maurus palmatus*. Depuis ce travail pionnier, la molécule a pu être produite par synthèse chimique sans altération structurale. Trois raisons font que ce peptide est particulièrement intéressant. D'une part, il présente une homologie de séquence avec un domaine de canal calcium dépendant du potentiel qui est impliqué dans le couplage excitation-contraction. Cette homologie est utile pour déchiffrer les bases mécanistiques de la mobilisation calcium du réticulum sarcoplasmique. D'autre part, la MCa est un activateur puissant du récepteur à la ryanodine, déclenchant de cette manière la libération de calcium des stocks intracellulaires. Finalement, ce peptide a une valeur technologique en raison de sa capacité à transporter des composés imperméables au travers de la membrane plasmique. Dans ce travail de thèse, j'ai planifié de nouveaux analogues plus efficaces de la maurocalcine, soit par des substitutions uniques d'acides aminés ou en remplaçant l'ensemble des cystéines par des acides aminés isostériques. Ces analogues possèdent des efficacités de pénétration cellulaire équivalente ou supérieure, présentent des toxicités cellulaires limitées et n'ont pas d'activités pharmacologiques sur le récepteur à la ryanodine. J'ai analysé l'interaction de ces analogues avec des lipides membranaires et des glycosaminoglycans de surface, et le rôle de ces composants dans la pénétration cellulaire de la MCa. L'entrée cellulaire de la MCa se produit par macropinocytose quand ce peptide se fixe à la streptavidine.

Mots clés : Maurocalcine, récepteur à la ryanodine, glycosaminoglycans, macropinocytose.

TABLE OF CONTENTS

LIST OF FIGURES AND TABLES

Figures

Tables

LIST OF ABREVIATIONS

ACE	Angiotensin-converting enzyme
AD	Alzheimers disease
ADP	Adenosine diphosphate
ATP	Adenosine-5'-triphosphate
BBB	Blood brain barrier
BjTx	Buthotus judaicus toxin
Ca^{2+}	Calcium
CaM	Calmodulin
CHO	Chinese hamster ovary
CAE	Clathrin-mediated endocytosis
CPPs	Cell-penetrating peptides
CRC	Calcium release channel
CSQ	Calsequestrin
DHPR	Dihydropyridine receptor
EC	Excitation-contraction
eNOS	Endothelial nitric oxide synthase
ER	Endoplasmic reticulum
FITC	Fluorescein isothiocyanate
FKBP	FK binding proteins
GAGs	Glycoaminoglycans
GDNF	Glial cell derived neurotrophic factor
Gly	Glycine
GPI	Glycosylphosphatidylinositol
HCa	Hemicalcine

HSPGs	Heparan sulphate proteoglycans
IP_3Rs	Inositol trisphosphate receptors
$IpTx_a$	Imperatoxin A
K^+	Potasium ion
LDH	Lactate dehyrogenase
MCa	Maurocalcine
MRI	Magnetic resonance imaging
MTPs	Membrane transduction peptides
MTS	Mitochondrial targeting Signal
MTT	3-(4, 5-dimethylthiazol-2-yl)-2, 5-diphenyl-tetrazolium bromide
Na^+	Sodium ion
NDAP	Nicotinamide adenine dinucleotide phosphate
NLS	Nuclear localization signal
NO	Nitric oxide
ONs	Oligonucleotides
PcTX1	Psalmotoxin 1
PGs	Proteoglycans
PKA	Protein kinase A
PNA	Peptide nucleic acid
PTDs	Protein transduction domains
ROS	Reactive oxygen spescies
RyR	Ryanodine receptor
RyTx	Ryanotoxin
SR	Sarcoplasmic reticulum

Amino acids

Ala, A	Alanine	Leu, L	Leucine
Arg, R	Arginine	Lys, K	Lysine
Asn, N	Asparagine	Met, M	Methionine
Asp, D	Aspartic acid	Phe, F	Phenylalanine
Cys, C	Cysteine	Pro, P	Proline
Glu, E	Glutamic acid	Ser, S	Serine
Gln, Q	Glutamine	Thr, T	Threonine
Gly, G	Glycine	Trp, W	Tryptophan
His, H	Histidine	Tyr, Y	Tyrosine
Ile, I	Isoleucine	Val, V	Valine

I. INTRODUCTION

The cell membrane, also called plasma membrane, is a fluid mosaic of proteins, carbohydrates and lipids, leading to the formation of an almost impermeable barrier for the movement of hydrophilic molecules into the cell. As a result of its impermeable nature to hydrophilic compounds, the cell membrane also restricts access of many potent pharmaceutical agents to their targets inside the cell. Among the various strategies being used over the past for the delivery of molecules across the cellular membrane, use of cell penetrating peptides as vectors is gaining momentum.

The present thesis concentrates on cell penetrating peptide, namely maurocalcine (MCa), a unique toxin with its pharmacological target *in vivo*, the ryanodine receptor (RyR) localized inside the cells. Herein, studies have been made to design new analogues of MCa either by point mutation or substitution of cysteine residues, possessing better or equal cell penetration efficiencies, no cell toxicity and no pharmacological activity on RyR. Further more, the mechanistic interaction of MCa with membrane lipids and glycosaminoglycans and the pathway required for the cell translocation have been studied.

II. REVIEW OF LITERATURE

1. Ryanodine receptors

1.1 The mechanics of calcium transport

Calcium is a highly versatile intercellular signal that regulates various biological processes in cells that include contraction, secretion, synaptic transmission, fertilization, proliferation, nuclear pore regulation, metabolism, exocytosis and transcription. Cytosolic Ca^{2+} levels in cells are modulated by different types of Ca^{2+} transporters like ion channels, exchangers and pumps (Berridge et al., 2003). In most of the cells, the primary intracellular Ca^{2+} storage/release organelle is the endoplasmic reticulum (ER). In striated muscles, it is the sarcoplasmic reticulum (SR). The ER and SR contain two multigene families of intracellular Ca^{2+} -release channel (CRC) proteins, namely the ryanodine receptors (RyRs) and inositol trisphosphate receptors (IP_3Rs) that have been extensively characterized over the past. The RyR and IP_3R display significant amount of amino acid identity, and this homology is most marked in the sequences that form the channel pores. Though both RyR and IP_3R are regulated by calcium, they still have their own distinguishing functional attributes like IP_3R activity requires the presence of inositol 1, 4, 5-triphosphate while RyR activity is coupled to a voltage sensor in the plasma membrane of some tissues, such as skeletal muscle.

1.2 Ryanodine receptors: Structure and function

Excitation-contraction (EC) coupling in striated muscle (Figure 1) is the process by which an electrical impulse is transformed into contraction. At the molecular level, EC coupling is the process where membrane depolarization induces conformational changes in dihydropyridine receptor (DHPR) that lead to activation of RyR of SR membrane, which further leads to the release of intracellular calcium ions from SR, which in turn triggers the contraction of myosin and actin filaments within the cell (Proenza et al., 2002; Protasi et al., 2002; Tanabe et al., 1990b).

RyRs (Figure 2) are around 2200-kDa homotetrameric complexes of four ≈ 565-kDa subunits, forming a central pore. This channel is localized at the membrane of the ER with the

bulk of its sequence localized in the cytoplasm. They have large N-terminal cytoplasmic domains that modulate the gating of the channel pore located in the C-terminus (Galvan et al., 1999). Further studies have defined three different RyR isoforms.

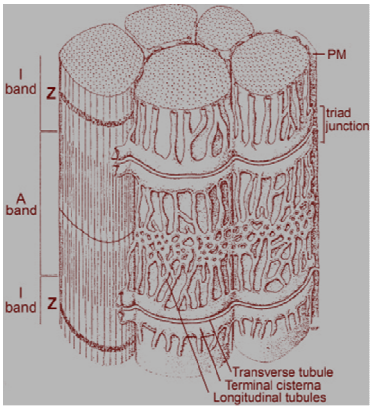

Figure 1: Mammalian striated muscle fiber*. Two transverse tubules innervate one sarcomere. The transverse tubules are invaginations of the sarcolemma, close to the line where the A and I bands meet. Two terminal cisternae of SR are junctionally associated with one transverse tubule and connect with the longitudinal sarcotubules of SR located around the A band. The tripartite structure, seen in cross-section of two terminal cisternae flanking the transverse tubule, constitutes a triad (Fleischer, 2008).*

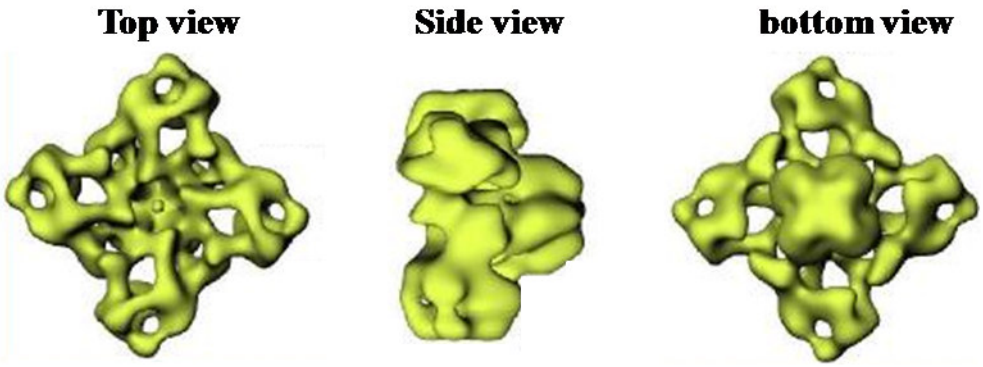

Figure 2: Ryanodine receptor. *Three-dimensional surface representation of RyR using cryo-electron microscopy and image enhancement. Left, transverse tubule face; middle, side view and right, terminal cisternae face (Fleischer, 2008).*

1.3 RyR isoforms

Molecular cloning studies have defined three different isoforms of RyR in mammals, namely RyR1, RyR2 and RyR3. All three are encoded by different genes present on different chromosomes (Marks, 1996; Mikami et al., 1989; Takeshima, 1993; Takeshima et al., 1989). In mammalian striated muscles, the expression of the different RyR protein isoforms is tissue specific. RyR1 is the predominant RyR isoform in the skeletal muscle (Coronado et al., 1994; McPherson and Campbell, 1993; Ogawa, 1994). RyR2 is most abundant in cardiac muscles and RyR3 is found in striated muscles but in relatively low levels (Froemming et al., 2000; Sutko et al., 1991). RyR isoforms are also found to be expressed in other tissues. Expression of all the three isoforms of RyR proteins are reported in smooth muscles (Ledbetter et al., 1994; Marks et al., 1989), cerebrum (Furuichi et al., 1994; Hakamata et al., 1992) and cerebellum (Martin et al., 1998).

Non-mammalian skeletal muscles contain nearly equal amounts of two different RyR isoforms, namely α-RyR and β-RyR which are homologous to mammalian RyR1 and RyR3, respectively (Airey et al., 1993; Lai et al., 1992; Murayama and Ogawa, 1992). In these organisms, both the isoforms are present in approximately equal amounts in contrast to the predominant expression of RyR1 in mammals.

The three RyR isoforms share ≈ 70% homology (Nakai et al., 1990). Analysis of the primary amino acid sequences suggests that the membrane-spanning domains of the RyR are clustered near its COOH terminus (Blazev et al., 2001; Zhao et al., 1999) and has also revealed several consensus ligand binding and phosphorylation motifs.

1.4 Regulation of RyR

RyR channels are regulated by various cellular processes, physiological agents, pharmacological drugs and different closely associated proteins that are discussed below.

1.4.1 Cytosolic Ca2+

The influence of Ca^{2+} on the RyR is quite complex. The Ca^{2+} activates, inhibits and also conducts through the channel. Activation of RyR occurs at low concentrations of Ca^{2+} (1-10 μM)

and inhibition at higher concentrations (1-10 mM). RyR channel isoforms do not behave similarly in response to Ca^{2+} levels (Copello et al., 1997; Laver et al., 1995). RyR1 channel is almost totally inhibited at 1 mM Ca^{2+} but the other two isoforms, RyR2 and RyR3, require much higher concentrations of Ca^{2+} (Bull and Marengo, 1993; Chen et al., 1998; Chu et al., 1993). The physiological role of these very high levels of Ca^{2+} inhibition is not very well understood.

1.4.2 ATP and Mg^{2+}

Cytosolic Mg^{2+} is a potent inhibitor of RyR (Copello et al., 2002; Laver et al., 1997; Smith et al., 1985), whereas ATP is an effective activator of RyR channel (Sonnleitner et al., 1997; Xu et al., 1996). Again the action of ATP and Mg^{2+} on RyR channel isoforms is specific. RyR1 is much more sensitive to ATP and Mg^{2+} than RyR2 and RyR3 (Jeyakumar et al., 1998). The action of Mg^{2+} is quite complicated since it may compete with Ca^{2+} both at the activation site (Laver et al., 1997) and also at the Ca^{2+} inhibition site (Copello et al., 2002), thereby shifting the Ca^{2+} sensitivity of the channel. In the presence of ATP and Mg^{2+}, RyR1 requires less Ca^{2+} to activate than in their absence (Takeshima et al., 1998).

1.4.3 Cyclic ADP-ribose

Cyclic ADP-ribose (cADPR) is a metabolite of NADP that dramatically activates mammalian RyR channels (Meszaros et al., 1993). However, studies later suggested only minor effects of cADPR on RyR (Sitsapesan and Williams, 1995) and in some cases, no impact was reported (Fruen et al., 1994). Studies also suggested that two closely associated proteins, calmodulin and FK-506 binding protein (Lee, 1997), are required for the effect of cADPR on RyR. cADPR, in some cases, also appeared to activate the Ca^{2+}-ATPase, which indirectly activated the RyR channel (Lukyanenko et al., 2001). Overall, the direct action of cADPR on RyR channels seems to be controversial.

1.4.4 Phosphorylation/dephosphorylation

RyR is a macromolecular complex that contains many consensus phosphorylation sites. The effect of exogenously applied kinases and phosphatases on RyR channel has been reported (Hain et al., 1995; Lokuta et al., 1995; Marx et al., 2000). Protein kinase A (PKA) activates RyR (Coronado et al., 1994) and this observation is consistent with the fact that PKA significantly

increases depolarization-induced Ca^{2+} release from SR vesicles (Igami et al., 1999). Reports suggest that RyR2 is also activated by PKA (Hain et al., 1995), whereas others suggest that PKA destabilizes RyR2 channel opening through phosphorylation-induced dissociation of FKBP12.6 protein (Marx et al., 2000). The differences in these finding would probably result from different experimental setup altogether.

1.4.5 Ryanodine

Ryanodine is a plant alkaloid found naturally in the stem and roots of *Ryania speciosa* (Elison and Jenden, 1967; Jenden and Fairhurst, 1969). Stepwise studies made over a period of time with respect to ryanodine include : (i) purification of ryanodine binding protein (Campbell et al., 1987; Fleischer et al., 1985; Hymel et al., 1988), (ii) visualization of purified tetrameric complex through electron microscopy (Inui et al., 1987; Lai et al., 1988) and (iii) incorporation of the ryanodine binding receptor into lipid bilayers, demonstrated that this receptor is an ion channel (Imagawa et al., 1987). All these initial findings demonstrated that the receptor is the SR Ca^{2+} release channel in striated muscles (Fill and Coronado, 1988; Fleischer and Inui, 1989). Ryanodine, as an alkaloid, binds with high affinity to RyR (Fabiato, 1985; Frank and Sleator, 1975). High affinity [^{3}H] -ryanodine turned out to be usefull in identifying different isoforms of RyR (Sutko et al., 1997).

1.4.6 Caffeine

Caffeine is one among the group of stimulants called methylxanthine, or xanthine that occur naturally in plants. It is known to activate Ca^{2+} release through the activation of RyR at millimolar concentrations. It is also reported that caffeine increases the sensitivity of endogenous RyR to modulators, such as Ca^{2+} and ATP, leading to increased channel activity (Rousseau et al., 1988).

1.4.7 JTV-519

JTV-519, also known as K201, is a 1 , 4-benzothiazepine derivative that shares a high degree of structural similarity with the voltage-dependent L-type Ca^{2+} channel blocker diltiazem (Tse et al., 2001). K201 inhibits diastolic SR Ca^{2+} leak and increases calstabin (FKBP) binding to RyR (Lehnart et al., 2004). Numerous studies have shown that K201 possesses cardioprotective

and anti-arrhythmic properties because of its ability to inhibit Ca^{2+} leak (Inagaki et al., 2000). Further more, studies have proposed that K201 inhibits SR Ca^{2+} leak by restoring the binding of FKBP12.6 to RyR2. The exact role of FKBP12.6 is not very well understood, but it is believed to stabilize the closed state of RyR2 channel (Kohno et al., 2003).

1.5 Regulation of RyR by associated proteins

There are large numbers of different proteins that are associated with RyR channels and also these play a role in the modulation of this channel. However not all these proteins have been thoroughly studied. A brief summary of how some of the proteins interact and modulate the RyR channel is summarized below.

1.5.1 Calmodulin

Calmodulin (CaM) is a ubiquitous, calcium-binding protein that can bind to and regulate a multitude of different protein targets, thereby affecting many different cellular functions. CaM was the first protein that was found to interact with single RyR channels in lipid bilayers (Smith et al., 1989). At low Ca^{2+} levels, CaM activates both RyR1 and RyR2 channels, but in the presence of high Ca^{2+} levels, it inhibits these channels (Fruen et al., 1994; Tripathy et al., 1995). As far as reports with RyR2 are concerned, CaM has always an inhibitory effect (Fruen et al., 1994). This modulation of RyR channel involves direct interaction of CaM-RyR and is not dependent on ATP (Smith et al., 1989). CaM also appears to bind to voltage-dependent Ca^{2+} channels of the plasma membrane, the dihydropyridine receptor (DHPR) of skeletal muscles, and has a series of structural consequences between DHPR and RyR1 interactions (Hamilton et al., 2000).

1.5.2 Calsequestrin (CSQ)

Calsequestrin is the major calcium sequestering protein in the SR and it forms a quaternary complex with the RyR. It has been suggested that Ca^{2+} and pH-dependent conformational changes in calsequestrin modulate RyR channel activity (Hidalgo et al., 1996). Calsequestrin is known to be located in the direct vicinity of RyR (Franzini-Armstrong et al., 1987), binds to triadin and junctin (Figure 3) and forms a quaternary complex that controls Ca^{2+} release (Wang et al., 1998). Again, there are conflicting reports with regard to the activity of

calsequestrin on RyR. Lipid bilayer studies suggest that calsequestrin activates the RyR channel (Kawasaki and Kasai, 1994) but there is one study mentioning that calsequestrin inhibits the RyR channel (Beard et al., 2002). Thus, the role of calsequestrin on RyR channel needs further more studies.

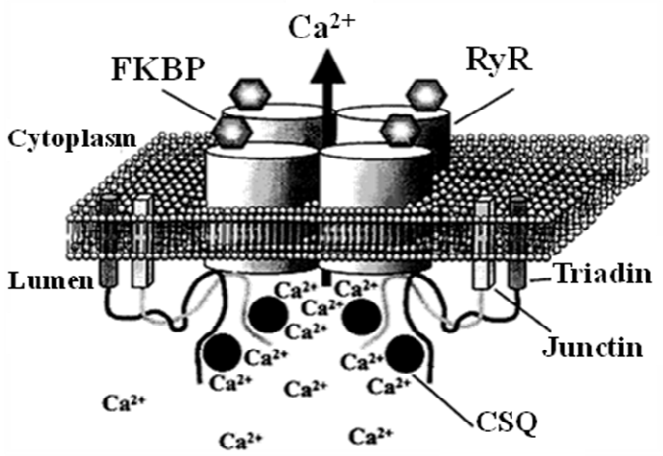

Figure 3: RyR Ca2+-release complex. *RyR receptor is composed of four subunits that form the channel, which is associated with various proteins that function to modulate its opening. Some of the associated proteins FKBP, CSQ, triadin and junction are represented in the figure.*

1.5.3 FK-506 binding proteins

FK-506 is an immunosuppressive drug that binds to FK-506 binding protein (FKBP). Depending on the molecular mass, FKBP members are named as FKBP12 and FKBP12.6. FKBP12 also known as calstabin 1 is a 108 amino acid protein that shares 85% sequence identity with FKBP12.6, (calstabin 2). Both FKBP12 and FKBP12.6 associate with RyR1, RyR2 and RyR3 proteins in apparent stoichiometric proportions (Figure 3) and thus there are four FKBPs bound to each RyR channel complex (Timerman et al., 1993; Timerman et al., 1996). Reports suggest that removal of FKBP12 from RyR1 channel activates the channel (Ahern et al., 1994; Barg et al., 1997) but the impact of FKBP on RyR2 is not very well understood. Some suggest that removal of FKBP12.6 from RyR2 channel activates the channel (Xiao et al., 1997) and other report that FKBP12.6 removal has no impact on the RyR2 channel (Barg et al., 1997). The FKBP12-binding domain of RyR1 is mapped to its central regulatory domain between amino acids 2401-2840 (Bultynck et al., 2001), whereby the valylprolyl residue was shown to be critical

for establishing high affinity FKBP12 interaction (Gaburjakova et al., 2001). Though the interaction of FKBPs with RyR2 and RyR3 (Murayama et al., 1999) have been demonstrated, their interaction sites have not yet been determined and characterized very well. Some of the controversial reports regarding FKBP modulation of RyR1 channel indicate that the removal of FKBP12 leads to uncoupling of DHPR-RyR1 interaction suggesting that FKBP12 may be a physical coupler between RyR1 and DHPR (Lamb and Stephenson, 1996).

1.5.4 DHPR-loop peptide

The functional interaction of the voltage-dependent Ca^{2+} channel of the plasma membrane, the dihydropyridine receptor (DHPR) with RyR in striated muscles, is commonly thought to produce Excitation-Contraction (EC) coupling (Tanabe et al., 1990a; Tanabe et al., 1993). Depolarization of the plasma membrane induces conformational changes in DHPR that leads to activation of RyR channel in the SR membrane. This activation of RyR leads to massive Ca^{2+} release from the SR which in turn initiates contraction. The interaction of DHPR-RyR is tissue specific. In skeletal muscles, the interaction is thought to be a physical link between two proteins, whereas in cardiac muscles, it is the influx of Ca^{2+} through muscle that activates the RyR2 channel. The cytoplasmic II-III loop of skeletal DHPR α1-subunit is required for the functional interaction of DHPR with RyR1 (Tanabe et al., 1990a). Peptide fragments that correspond to the II-III loop activate single RyR channel function and interestingly, different regions of the peptide have different actions on RyR1 channel (Lu et al., 1994). Peptide A corresponds to a functional domain of the II-III loop that is known to activate RyR1 channel (Dulhunty et al., 1999), whereas peptide C, another domain of the same II-III loop blocks the activating action of peptide A (Gurrola et al., 1999). In one of controversial report, using a chimeric DHPR, lacking the peptide A region, expressed in myotubes lacking endogenous DHPR, normal EC coupling was observed (Grabner et al., 1999). Structural similarities of some of the reported scorpion peptide toxins with peptide A and their ability to bind and activate RyR (Samso et al., 1999), is altogether opening a new insight in the study of domain A and scorpion toxins which is discussed in detail in the following chapter.

2. Venom toxins

2.1 Introduction

Toxins found in venoms are often around 10- to 70-mer peptides with high density of disulphide bonds. Often people name them as toxin peptides, but it would be more appropriate to designate them as *small proteins,* since they possesses secondary structures like α- helices, β-sheets and turns.

Toxins are usually evolved as part of defensive or prey capture strategies. As a consequence, they predominantly act on key physiological systems. The major systems that are targeted by the toxins are the neuromuscular system, the neuronal system and the cardiovascular system. Within these systems, toxins target a considerable number of macromolecules, including the ion channels, hormone receptors, enzymes and transporters. However, toxins possess a number of basic characteristics that we would like drugs to possess which include potency and specificity. Thus, toxins have become subject of interest as they form an invaluable source of pharmacological agents.

2.2 Venom biodiversity

Venomous animals have evolved a large array of peptide toxins, many of which are bioactive. Their small size, relative ease of synthesis, structural stability and target specificity make them important pharmacological probes. It is estimated that more than 50,000 conopeptides from cone snails exist, of which less than 0.1% have been characterized pharmacologically. The ones which are characterized are found to be active on diverse range of ion channels and receptors associated with pain signaling pathways (Lewis and Garcia, 2003). Similarly, considering the diversity of venom peptides found in spiders, snakes, sea anemones and scorpions, it requires lots of work to characterize them pharmacologically. Traditionally, assay-directed fractionation was used to identify peptides of interest present amongst the large number of related molecules in the venom. Recent developments of novel high-throughput assays for the diversity of targets, along with improved separation and sequencing capabilities has simplified peptide isolation and characterization (Lewis, 2000; Lewis et al., 2000; Olivera et al., 1984).

Furthermore these peptides are characterized across multiple targets both *in vitro* and *in vivo* using chemically synthesized peptides.

2.3 Pharmacology of venom peptides

2.3.1 Ion-channel peptides

Several venom peptides have been characterized over the past for their pharmacological targets or activity. A wide range of different voltage-sensitive calcium channel peptides are characterized from the venom of cone snails (Olivera et al., 1987), spiders (Mintz et al., 1991; Newcomb et al., 1998) and snakes (de Weille et al., 1991). The α-conotoxins are a class of small peptides that inhibit nicotinic acetylcholine receptors similar to snake α-neurotoxins (McIntosh et al., 1999) and are being used as analgesics (Sandall et al., 2003). Voltage-sensitive sodium channels are crucial for the functioning of the nervous system and it is not surprising that a number of venom peptides from spider (Nicholson et al., 1994; Omecinsky et al., 1996), sea anemone (Vincent et al., 1980), coral (Gonoi et al., 1986), scorpions (Possani et al., 1999) and cone snails (Cruz et al., 1985; Fainzilber et al., 1994) have evolved to target these channels. Psalmotoxin 1 (PcTX1) is one such example that is a potent and specific blocker of proton-gated sodium channel. It was isolated from the venom of the South American tarantula *Psalmopoeus cambridgei* (Escoubas et al., 2000). Potassium channels are a large and diverse family of proteins that are implicated in the regulation of many cellular functions. Of the several potassium-channel-blocking peptides identified so far, only few have shown promising results *in vivo.* Multiple sclerosis is a disease of the central nervous system and is characterized by disseminated patches of demyelination in the brain and spinal cord which results in multiple and varied neurological disorders. ShK, a 35-residue polypeptide toxin from sea anemone *Stichodactyla helianthus,* is known to block voltage-gated Kv1.3 potassium channels and has been found to be effective against multiple sclerosis (Suarez-Kurtz et al., 1999).

2.3.2 Venom peptides useful in cardiovascular disease

Several venom peptides are being used against cardiovascular diseases, one such example is captoprill, an antihypertensive agent that essentially inhibits angiotensin-converting enzyme (ACE). ACE is a vasoconstrictor associated with hypertension and an essential enzyme for the

production of angiotensin (Dei Cas et al., 2003). Another classical example that is in preclinical development as a novel anti-bleeding agent for use in open heart surgery is Textilinin, a novel antifibrinolytic serine protease inhibitor from the venom of common brown snake (Filippovich et al., 2002).

2.3.3 Venom peptides useful in treating cerebrovascular accident

A stroke, or cerebrovascular accident (CVA), occurs when blood supply to part of the brain is disrupted, causing brain cells to die. When blood flow to the brain is impaired, oxygen and glucose cannot be delivered to the brain. Ancrod from the venom of Malayan pit viper and batroxobin from the venom of *Bothrops atrox moojeni* reduces this neurological deficits by enzymatically cleaving the blood fibrinogen (Bell, 1997) when used in the early stages of stroke (Samsa et al., 2002).

2.3.4 Venom peptides useful in diabetes

Diabetes mellitus, is a syndrome characterized by disordered metabolism and abnormally high blood sugar resulting from insufficient levels of the insulin hormone. Exendin-4 peptide from the venom of *Heloderma suspectum*, is presently in phase III clinical trials for the treatment of type 2 diabetes (Eng et al., 1992) and this peptide shares structural homology with another toxin namely α-latrotoxin, from the black widow spider that has been found to be useful in the treatment of alzheimers disease (Perry and Greig, 2002). Paralleling to these latest developments, further applications regarding toxins are emerging that are of technological nature and are discussed in the later chapters.

2.4 Scorpion toxins

2.4.1 The Scorpions

2.4.1.1 Diversity and classification

Scorpions are one of the most ancient groups of animals on earth with about more than 400 millions of years of evolution and approximately 1,500 different species. During this lengthy evolutionary period, they have largely preserved their morphology and have adapted to survive in a wide variety of habitats including tropical forests, rain forests, grasslands, temperate forests, deserts and even snow covered mountains. Scorpions belonging to family Buthidae are represented by the genera *Androctonus, Buthus, Mesobuthus, Buthotus, Parabuthus* and *Leirus* located in North Africa, Asia and India. *Centruroides* are located in USA, Mexico, and Central America. *Tityus* are found in South America and *Uroplectes* in Africa (Debont et al., 1998; Hancock, 2001).

2.4.2 The scorpion venom

2.4.2.1 Composition and classification

Scorpions are interesting organisms because of the fact that their venoms contain molecules of medical importance. Advanced methods of fractionation, chromatography and peptide sequencing have made it possible to characterize the venom components. The basic steps involved in the characterization of venom is the identification of peptide toxins, analyses of their structure, function and targets (Favreau et al., 2006). Scorpion venoms contain a variety of biologically active components that include enzymes, peptides, nucleotides, lipids, mucoproteins and biogenic amines. The best studied components are the polypeptides that are active on the ion channels and receptors (Catterall, 1980; Garcia et al., 1997; Valdivia et al., 1992). Some of the criteria's that are being used to classify the scorpion toxins are based on their molecular size as long chain toxins and short chain toxins; according to activity on distinct animals as mammal-specific toxins, insect-specific toxins and crustaceans-specific toxins; based on the mechanism of action as neurotoxins and cytotoxins; and toxins with disulphide bridges and without disulphide bridges. Toxins with disulphide bridges are usually active on ion channels. Those without disulphide bridges are important bioactive peptides that have been discovered recently. Based on

the action on ion channels, four different families of scorpion venom toxins have been defined namely: Na^+- channel toxins (Catterall, 1980), K^+-channel toxins (Carbone et al., 1982; Miller et al., 1985), Cl^--channel toxins (DeBin et al., 1993) and Ca^{2+}-channel toxins (Valdivia et al., 1992). Na^+- channel toxins belong to long chain scorpion toxins consisting of 60-80 amino acids with four disulphide bridges. To date, around 230 primary structures of Na^+- channel scorpion toxins have been determined (Srinivasan et al., 2002). K^+-channel toxins are composed of 20-70 amino acids and generally compacted by three disulphide bridges. Based on their molecular size and location of cysteine residues, K^+-channel scorpion toxins are further classified as α-KTx, β-KTx, and γ-KTx (Tytgat et al., 1999). Further few short-chains K^+-channel scorpion toxins from the venoms of *Heterometrus fulvipes* are designated as kappa-KTx because of the presence of a novel bihelical scaffold (Chagot et al., 2005). Maurotoxin (MTX), a 34-residue toxin initially isolated from the venom of the scorpion *Scorpio maurus* palmatus is found to be active on several K^+-channel targets namely, apamin-sensitive small conductance Ca^{2+}-activated K^+ (SK) channels (Kharrat et al., 1996; Kharrat et al., 1997), intermediate conductance Ca^{2+}-activated K^+ (IK) channels (Castle et al., 2003), and several types of voltage-gated Kv channels (*Shaker* B and Kv1.2) (Carlier et al., 2000). MTX does not block the Kv1.1 channel type, whereas it is moderately active on Kv1.3 (Fajloun et al., 2000b). Cl^- channel scorpion toxins are usually low molecular weight peptides consisting of 35-38 amino acids with four disulphide bridges. One remarkable Cl^- channel scorpion toxin is chlorotoxin. It has been purified from *Leiurus quinquestriatus* and blocks the channel in the epithelium of mouse. It binds specifically to Cl^- channels in glia cells. Kurtoxin from *Parabuthus transvaalicus* binds with high affinity and inhibits Ca^{2+}-channel by modifying the voltage-dependent gating (Lopez-Gonzalez et al., 2003). Many of the scorpion toxins are active on intracellular calcium release channel, the ryanodine receptor which is discussed below in detail.

2.4.3 Scorpion toxins active on ryanodine receptor

2.4.3.1 Imperatoxin A ($IpTx_a$)

$IpTx_a$, a 33- amino acid peptide was the first discovered member of an ever growing family of scorpion toxins active on the RyR and initially purified from *Pandinus imperator* (Valdivia et al., 1992). This peptide has three cysteine residues that stabilize its three-dimensional

structure by forming disulphide bridges (Zamudio et al., 1997). $IpTx_a$, was found to increase [^{3}H]-ryanodine binding on skeletal muscle RyR, but not on the cardiac RyR, although it induces the appearance of long-lived subconductance states in both isoforms (Tripathy et al., 1998). $IpTx_a$ shares similar structural and functional properties with peptide A (Figure 5) Later on, it was showed that peptide A of the II-III loop of DHPR (Glu^{666}-Leu^{690}) binds to the same RyR1 site as $IpTx_a$. Using [^{125}I]-labelled $IpTx_a$, it was found that $IpTx_a$ binds on RyR1 with nanomolar affinity, whereas peptide A interacts at micromolar concentrations (Gurrola et al., 1999).

2.4.3.2 Ryanotoxin (RyTx)

RyTx is a 11.4-kDa peptide from the venom of the scorpion *Buthotus judiacus* that induces changes in ryanodine receptors of rabbit SR. RyTx was found to increase the binding affinity of [^{3}H]-ryanodine in a reversible manner with a 50% effective dose at 0.16 μM. Results also suggested that binding sites for ryanotoxin and ryanodine were different and thought to be useful in identifying domains coupling the ryanodine receptor to the voltage sensor, or domains affecting the gating and conductance of the ryanodine receptor channel (Morrissette et al., 1996).

2.4.3.3 Hemicalcine (HCa)

HCa is a 33-mer peptide toxin isolated from *Hemiscorpius lepturus*, which is the most dangerous scorpion of Khuzestan, the south-west, hot and humid province of Iran. Of all scorpion stings, 10–15% during the hot season and almost all cases during the winter are due to *H. lepturus*. These observations are based on a sample of 2534 patients who brought a scorpion specimen to a medical centre while seeking treatment (Radmanesh, 1990). This peptide is active on ryanodine sensitive Ca^{2+} channels, as it increases [^{3}H]-ryanodine binding on RyR1 and triggers Ca^{2+} release from SR. It shares 85 and 91% sequence identity with four other scorpion toxins active on RyR, namely maurocalcine, imperatoxin A, opicalcine 1 and opicalcine 2 (Shahbazzadeh et al., 2007).

2.4.3.4 *Buthotus judaicus* toxin (BjTx)

Buthotus judaicus toxin 1 (BjTx-1) and toxin 2 (BjTx-2) are two novel peptides purified from the venom of the scorpion *Buthotus judaicus* and found to be active on RyR. Their amino acid sequences differ only in 1 residue out of 28 wherein residue 16 corresponds to Lys in BjTx-1

and Ile in BjTx-2. Despite slight differences in EC_{50}, both toxins increase the binding of [^{3}H]-ryanodine to RyR1 at micromolar concentrations but had no effect on RyR2. Three-dimensional structural modeling reveals a cluster of positively charged residues (Lys^{11} to Lys^{16}) as a prominent structural motif of both BjTx-1 and BjTx-2 (Zhu et al., 2004).

2.4.3.5 BmK-PL

BmK-PL is a peptide toxin isolated from the venom of Chinese scorpion *Buthus martensi Karsch*. This toxin was found to stimulate Ca^{2+}-release channel activity of SR by an indirect mechanism, that does not involve direct interaction of the toxin with RyR, but possibly by binding to an associated protein such as triadin (Kuniyasu et al., 1999).

2.4.3.6 Maurocalcine (MCa)

MCa is a 33 amino acid residue peptide toxin isolated from the scorpion *Scorpio maurus palmatus*. Three similar peptides have been isolated or cloned from the venoms of different scorpions: $IpTx_a$ (El-Hayek and Ikemoto, 1998), that shares 82% sequence identity with MCa, and both opicalcine 1 and 2 (Zhu et al., 2003), from the scorpion *Opistophthalmus carinatus*, that show 91% and 88% sequence identities with MCa, respectively.

A  **B** 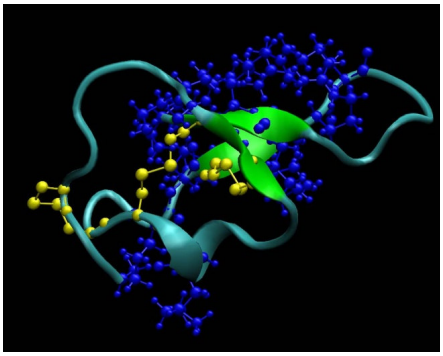

Figure 4: (A) Scorpio maurus palmatus *(Shachak and Brand, 1983),* ***(B) 3-D structure of MCa.*** *The structure was drawn by VMD1.8.6 software. Blue represents the basic amino acids and yellow the disulfide bridges.*

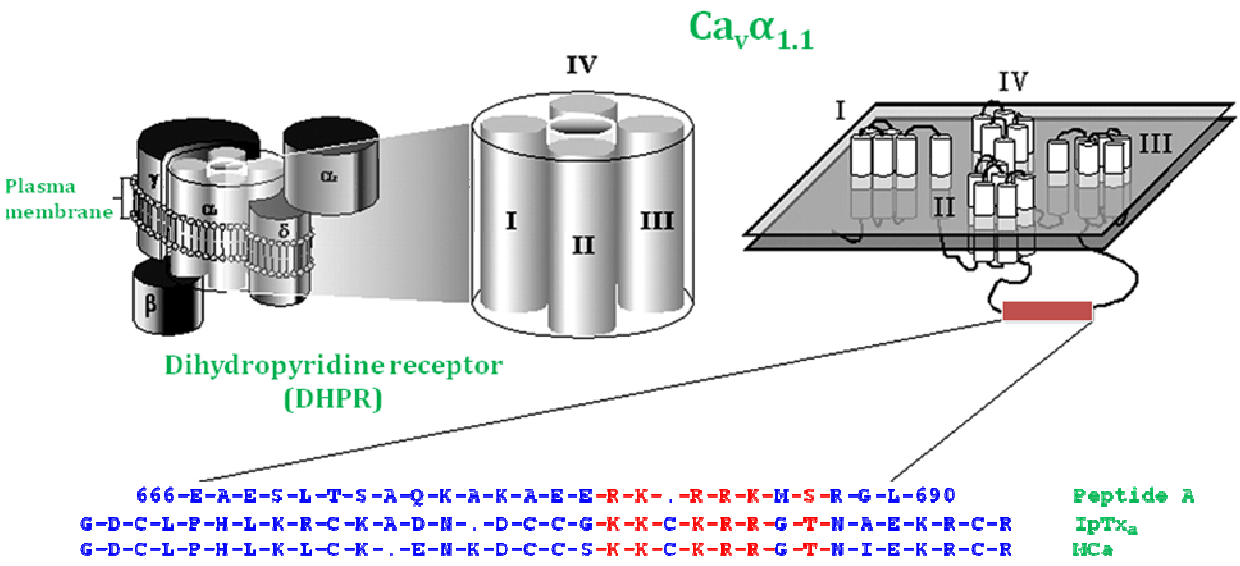

Figure 5: Sequence alignment of peptide A, IpTxa, and MCa. *Schematic representation of the DHPR complex illustrating the subunit composition. MCa has sequence similarities with domain A of the II–III loop from the $Ca_v\alpha_{1.1}$ subunit of DHPR and with $IpTx_a$, another scorpion toxin (Esteve et al., 2003)*

MCa triggers interest for three main reasons. Firstly, MCa is a powerful activator of the ryanodine receptor (RyR) (Figure 6), thereby triggering calcium release from intracellular stores (Chen et al., 2003; Esteve et al., 2003). MCa binds with nanomolar affinity onto RyR1, a calcium channel from the sarcoplasmic reticulum (SR), and generates greater channel opening probability interspersed with long-lasting openings in a mode of sub-conductance state (Fajloun et al., 2000a). Using a set of RyR1 fragments, two discrete domains of RyR1 responsible for its interaction with MCa were identified. MCa was found to bind to two discrete RyR1 regions encompassing residues 1021-1631 and 3201-3661, respectively. The second site was further restricted to amino acids 3351-3507. (Altafaj et al., 2005). MCa also interacts directly with RyR2 with an apparent affinity of 150 nM and found to bind to two domains of RyR2, which are homologous with those previously identified on RyR1. The effect of MCa binding to RyR2 was evaluated by [^{3}H]-ryanodine binding experiments, Ca^{2+} release measurements from cardiac

sarcoplasmic reticulum vesicles and single-channel recordings, showing that MCa has no effect on the open probability or on the RyR2 channel conductance level (Altafaj et al., 2007).

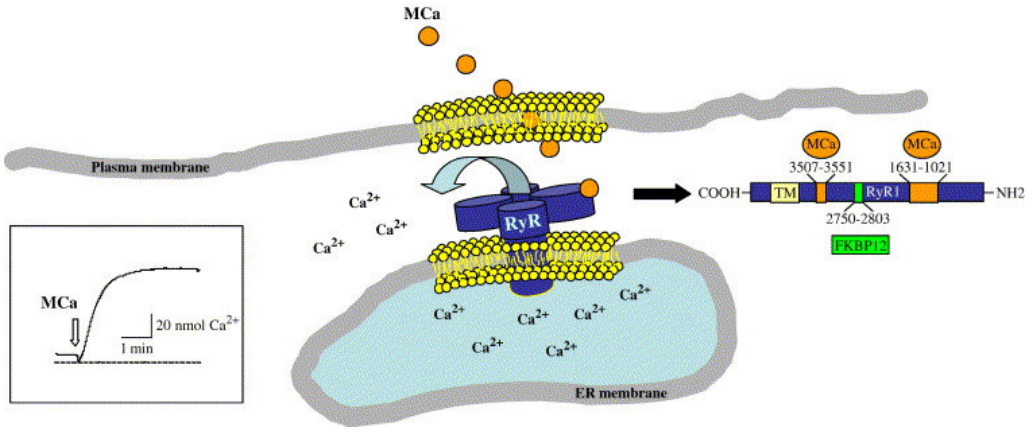

Figure 6: Schematic drawing of the ryanodine receptor. *RyR is a calcium channel localized in the membrane of the endoplasmic reticulum. Its function is to produce calcium release from this internal calcium stock. MCa has a well identified binding site on RyR that is localized on the cytoplasmic side of the channel. Binding of MCa to its site on RyR triggers calcium release from endoplasmic reticulum vesicles and Ca^{2+}release can be measured by the change in fluorescence intensity of a calcium indicato,r as shown here (Boisseau et al., 2006).*

Secondly, MCa has a unique sequence homology with a cytoplasmic domain of the pore-forming subunit of the skeletal muscle DHPR (Figure 5). This homology implicates a DHPR region that is well known for its involvement in the mechanical coupling between the DHPR and RyR1, a process whereby a modification in membrane potential is sensed by the DHPR, transmitted to RyR, and produces internal calcium release followed by muscle contraction. It is therefore expected that a close examination of the cellular effects of MCa on the process of excitation-contraction coupling may reveal intimate details of the mechanistic aspects linking the functioning of the DHPR to that of RyR. In that sense, a role of domain A in the termination of calcium release upon membrane repolarisation has been proposed through the use of MCa (Pouvreau et al., 2006).

Third, MCa appears unique in the field of scorpion toxins for its ability to cross the plasma membrane; this raises considerable technological interest in the peptide and is discussed in detail in the later chapter.

3. Membrane transport

3.1 Introduction

The Plasma membrane is a dynamic structure that separates the chemically distinct intracellular cytoplasm from the extracellular environment and also regulates the entry and exit of small and large molecules. Small molecules such as amino acids, sugars, ions and nutrients can cross the plasma membrane through the action of integral membrane protein pumps or channels (Figure 7). For the uptake of larger molecules, cells have developed a process termed as endocytosis.

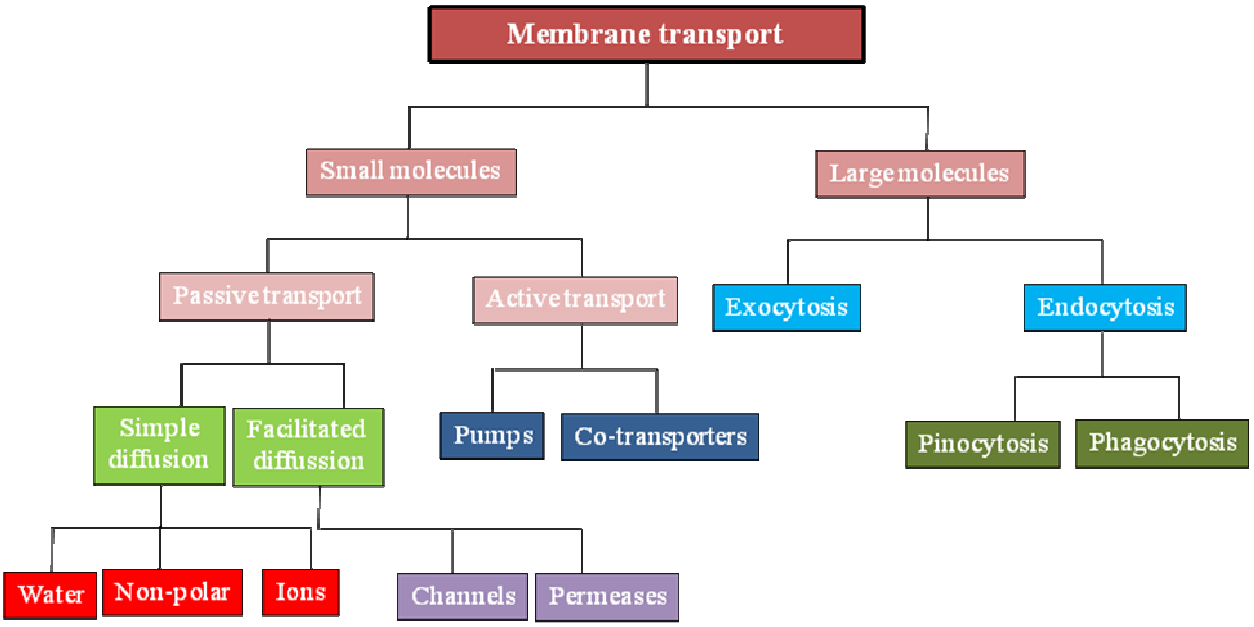

Figure 7: Classification system of membrane transport.

3.2 Endocytosis

Endocytosis is a basic cellular process that is used by cells to internalize a variety of molecules. Macromolecules are carried into the cells by vesicles formed by the invagination of the membrane. These vesicles are pinched-off into the cytoplasm. Since the macromolecules can be quite diverse, understanding the different pathways that mediate their internalization and how these pathways are regulated is important for many areas of cell and developmental biology.

Endocytosis occurs by multiple mechanisms that fall into two broad categories, phagocytosis or "cell eating" and pinocytosis or "cell drinking" (Figure 8).

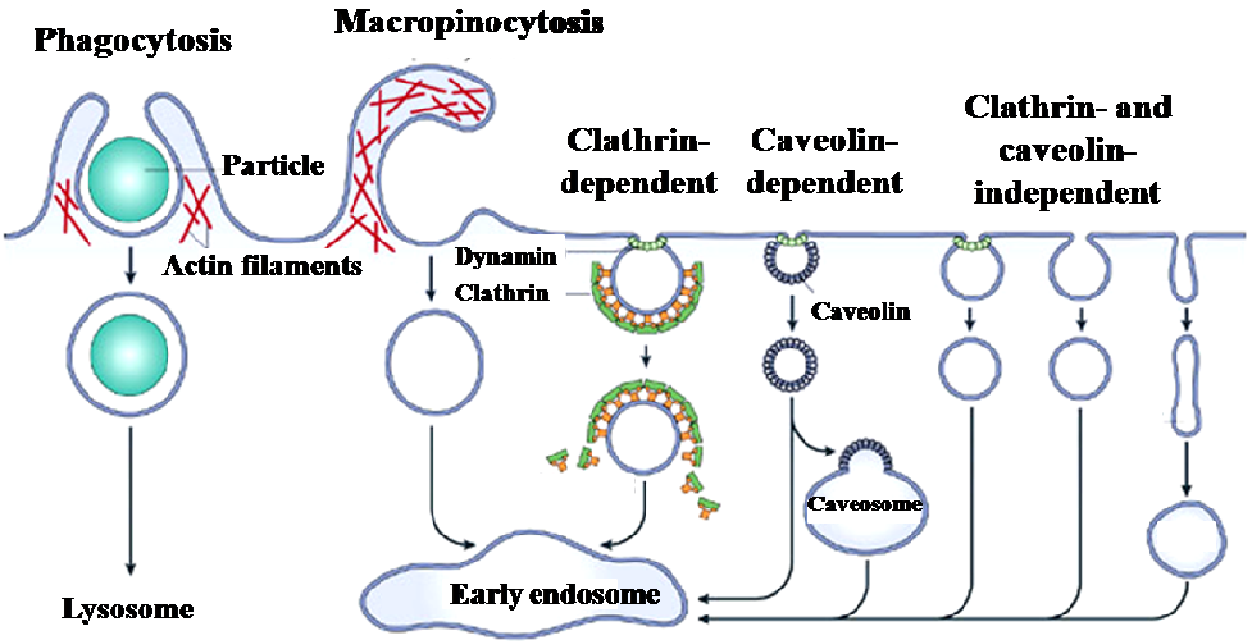

Figure 8: Endocytosis pathways. *Large particles are taken up by phagocytosis, whereas fluid uptake occurs by macropinocytosis. Both processes are triggered by actin-remodelling. Depending on various factors, particles can be taken up by many other pathways that are dependent on clathrin or caveolin or independent of both (Mayor and Pagano, 2007).*

3.2.1 Phagocytosis

Phagocytosis is a process in mammals that is driven by specialized cells, including macrophages, monocytes and neutrophils to clear large pathogens such as bacteria and cellular debris (Aderem and Underhill, 1999). This process is regulated by specific cell-surface receptors and signaling cascades. Particle internalization is initiated by the interaction of specific receptors on the surface of the phagocyte, leading to the polymerization of the actin and internalization of the particle (Hall and Nobes, 2000). Recent advances have highlighted the significance of phagocytic receptors, in particular the fibronectin receptor and other integrins (Blystone et al., 1994). The mechanism underlying actin assembly remains obscure. Recent advances suggest that

phosphatidylinositol 3-kinase and protein kinase C have a role in actin polymerization (Fallman et al., 1992; Panayotou and Waterfield, 1993; Zamudio et al., 1997). Further more, it is not clear if actin polymerization alone can drive particle internalization or if it requires molecular motors. Recently it has been shown that myosin II accumulates in macrophages and neutrophils during phagocytosis, implying that it might act as mechanical motor (Stendahl et al., 1980; Valerius et al., 1981). After internalization, the actin-based machinery is shed from the phagosome and the infectious agents are destroyed with the help of various acids, free oxygen radicals and acid hydrolases (Russell, 1995a; Russell, 1995b). There are different modes of phagocytosis which are basically determined by the particle to be ingested and the receptor that recognizes the particle.

3.2.2 Pinocytosis

Pinocytosis is a process of intracellular accumulation of molecules either by nonspecific binding of the solutes to the cell membrane or by binding to specific high-affinity receptors. During this process, there is invagination of the plasma membrane. This process is also referred to as cellular drinking, since the substances around the area of invagination are dissolved in water and ingested into the cell

3.2.2.1 Macropinocytosis

Macropinocytosis defines a series of events leading to extensive reorganization of plasma membrane. Unlike phagocytosis, macropinocytosis starts with the reorganization of actin, but here the protrusions do not climb up, but instead they collapse and fuse with the plasma membrane to generate large endocytic vesicles, called macropinosomes (Conner and Schmid, 2003). Macropinosomes are relatively large vesicles as compared to other pinocytotic vesicles and provide efficient route for non-selective endocytosis of solute macromolecules. Rab proteins are small GTPases that control multiple membrane trafficking events during the process of macropinocytosis. To date around twelve Rab members have been located around the endocytotic structures. Of these, Rab5 controls several processes including invagination, endosomal fusion, signaling and motility (Stenmark et al., 1994). ADP-ribosylation factors (ARFs) are also small GTPases that function in membrane traffic. One variant ARF6 in conjugation with actin cytoskeleton, exchange factors and activators, help in regulating macropinocytosis, cell adhesion

and migration (Donaldson, 2003; Sabe, 2003). Also possible involvement of rafts in macropinosome formation has been suggested (Watarai et al., 2002). However, the fate of the macropinosome is being debated since studies suggest either fusion with lysosomes (Racoosin and Swanson, 1993) or with each other (Hewlett et al., 1994) and this perhaps depends on the cell type used (Swanson and Watts, 1995).

3.2.2.2 Clathrin-mediated endocytosis (CAE)

Clathrin-mediated endocytosis was previously referred to as receptor mediated endocytosis but, nowadays it is well established that most pinocytic pathways also involve specific receptor-ligand interactions. The uptake of transferrin and its receptors is a classical example of CAE (Hanover et al., 1984; van Dam and Stoorvogel, 2002). CAE is important for intercellular communication during tissue and organ development and throughout the life of an organism as it modulates signal transduction (Di Fiore and De Camilli, 2001; Seto et al., 2002). CAE of membrane pumps that controls the transport of ions across the plasma membrane in neurons helps in controlling synaptic transmission and may have a role in learning and memory (Beattie et al., 2000). It is also involved in recycling vesicle proteins (Takei et al., 1996).

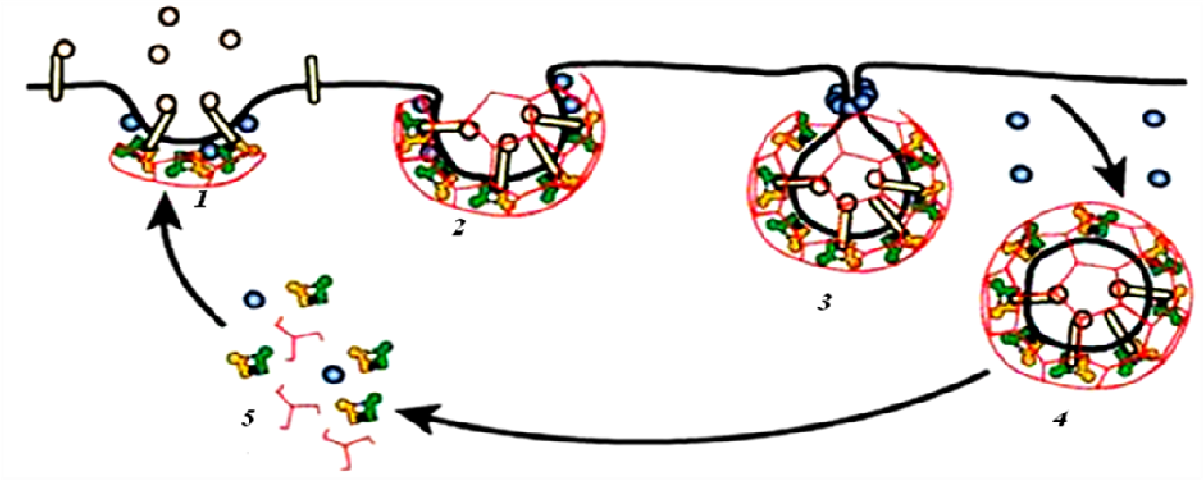

Figure 9: Clathrin-mediated endocytosis. *(1) Assembly of clathrin triskelions into polygonal lattice with the help of adaptor proteins; (2) Deformation of plasma membrane into coated pits; (3) Recruitment of dynamin to the neck of coated pits; (4) Pinching off of the coated pit; (5) Recycling of clathrin triskelions, adaptor proteins and dynamin (Conner and Schmid, 2003).*

CAE involves interaction of multi-functional adaptor proteins with plasma membrane, clathrin and several accessory proteins and phosphoinositides. It occurs at specialized structures called coated pits, which are formed by the assembly of cytosolic coat proteins, the main assembly unit being clathrin. Assembly unit of clathrin called triskelion, is a three-legged structure consisting of three heavy and three light chains (Greene et al., 2000; Schmid, 1997). Under non-physiological conditions, clathrin triskelions self-assemble into closed polygonal cages, however in physiological conditions, it requires adaptor proteins. Two classes of adaptor proteins have been identified based on their ability to assemble clathrin, namely monomeric assembly protein AP180 and heterotetrameric adaptor protein (AP1-4) (Kirchhausen, 1999; Robinson and Bonifacino, 2001). Complex formation between AP180 and AP2 gives greater clathrin assembly activity suggesting synergistic effects between them in clathrin assembly (Hao et al., 1999). AP2 basically consists of two domains namely, core and ear. The Core consists of two large structurally related subunits called α- and β2- adaptins, a medium subunit, μ2, and a small subunit, σ2. Ears are formed by the carboxy termini of α- and β2- adaptins, respectively (Collins et al., 2002). Together, the coat proteins, clathrin, AP2 and AP180 are involved to select the cargo and form coated pits. These coated pits are eventually pinched off from the plasma membrane, a process regulated by dynamin. Dynamin is a large-molecular-mass protein with GTPase activity. It has an N-terminal GTPase domain involved in binding and hydrolysis of GTP. The central region specifically binds to phosphatidylinositol-4, 5-bisphosphate and the C-terminal region is involved in dynamin oligomerization and self assembly (McNiven et al., 2000; Muhlberg et al., 1997; Schmid et al., 1998; Wigge and McMahon, 1998). After the endocytic vesicle is pinched off, clathrin is recycled back to the plasma membrane and reused, whereas the endocytic vesicle is targeted to the early endosome (Figure 9).

3.2.2.3 Caveolin-mediated uptake

Caveolae are flask-shaped invaginations of the plasma membrane and are characterized by the presence of caveolin in many cell types (Figure 10). Caveolin is a hairpin-like integral membrane protein of 21 kDa. Caveolins are palmitoylated in the C-terminal segment (Dietzen et al., 1995), phosphorylated on tyrosine residues (Glenney, 1989), bind to cholesterol (Murata et al., 1995) and they form dimmers and oligomers (Monier et al., 1995). Caveolins are essential for

the formation and stability of caveolae. In the absence of caveolins, no caveolae are seen and when expressed in cells lacking caveolae, they induce caveolar formation (Fra et al., 1995). Basically three isoforms of caveolins have been identified; Caveolin-1 and 2 are often seen in majority of differentiated cells, whereas caveolin 3 is localized in skeletal and cardiac muscles (Way and Parton, 1995).

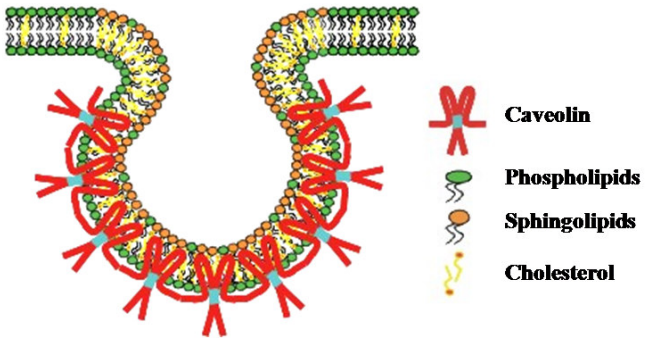

Figure 10: Caveolae. *Caveolae are generally considered to be "invaginated" lipid rafts formed primarily due to enrichment of proteins known as the caveolins. Lipid rafts are rich in cholesterol and sphingolipids (Galbiati et al., 2001).*

The lipid composition of the caveolae corresponds to that of lipid rafts rich in cholesterol and sphingolipids. They are essential for the formation and stability of caveolae (Brown and London, 1998; Simons and Toomre, 2000). Removal of cholesterol from the plasma membrane, leads to the disappearance of caveolae. Thus caveolae can also defined as caveolin-containing plasma membrane invaginations rich in lipid rafts (Rothberg et al., 1992). In addition caveolae also contains dynamin which is localized to the neck of flask-shaped caveolar vesicles (Henley et al., 1998; Oh et al., 1998). As in case of clathrin-mediated endocytosis, dynamin is involved in pinching off the caveolar vesicles from the plasma membrane (De Camilli et al., 1995; Sever et al., 2000).

Recent works have confirmed the caveolar entry of cholera toxin (Montesano et al., 1982), folic acid (Rothberg et al., 1990), serum albumin (Schnitzer et al., 1994) and alkaline phosphatase (Parton et al., 1994). Simian virus 40 (SV40) is one of the most exclusively studied ligands for caveolar endocytosis (Pelkmans et al., 2001; Roy et al., 1999). SV40 has several advantages as model ligand since the particle is well characterized in terms of composition and structure. SV40 after binding to the plasma membrane through the major histocompatibility

(MHC) class I antigen (Breau et al., 1992), diffuses laterally until it gets trapped in caveolae (Pelkmans et al., 2001). Lateron, virus containing caveolae, which are relatively smaller in diameter compared to virus-free caveolae (Stang et al., 1997), pinch off from the plasma membrane and move as caveolin-coated endocytic vesicles in the cytoplasm. Virus-free caveolae do not internalize. Some of the other events triggered during this process include tyrosine phosphorylation (Pelkmans et al., 2002), recruitment of actin and formation of actin tails (Chen and Norkin, 1999). But most of these events are transient; once SV40 is internalized, phosohotyrosines disappear and actin cytoskeleton returns to a normal pattern.

3.2.2.4 Clathrin- and caveolin- independent uptake

The mechanisms of endocytosis governed independent of caveolae and clathrin are very poorly understood. Each of these endocytosis processes fulfills unique functions in cell by the transport of various cargoes that include ligands, fluid, adhesion molecules and toxins. Depending on the type of cargo molecules to be transported, there are different types of processes involved in the formation of vesicles, pinching-off of the vesicle from the plasma membrane and in the regulation of entry of the cargo (Figure??). Again intracellular destiny in each case is not identical.

Rafts are small structures that diffuse freely on the surface of the cell (Edidin, 2001). They have unique lipid compositions that provide a physical basis for selectivity of membrane proteins and glycolipids (Anderson and Jacobson, 2002). Since rafts are small, they can be captured and internalized within an endocytic vesicle. Caveolae represents just one type of lipid rafts rich in cholesterol and sphingolipids. Based on ferro-fluid purification method, recently an endosomal protein, namely Flotillin-1 was identified. Flotillin-1 was found to reside in a specific population of endocytic intermediates and these intermediates accumulated both glycosylphosphatidylinositol (GPI)-linked proteins and cholera toxin B subunit. It was found that flotillin-1 small interfering RNA (siRNA) inhibited both clathrin-independent uptake of cholera toxin and endocytosis of a GPI-linked protein (Glebov et al., 2006). It has been reported that glycosylphosphatidylinositol-anchored proteins (GPI-Aps) have been endocytised to a recycling endosomal compartment but not to the Golgi through a clathrin- and caveolae- independent pathway (Sabharanjak and Mayor, 2004).

With ultrastructural and biochemical experiments, it was shown that clathrin-independent endocytosis of IL2 receptors exists constitutively in lymphocytes and is associated with detergent-resistant membrane domains (Lamaze et al., 2001). Thus recent identification of cargo molecule specific pathways helps in defining various mechanisms of endocytosis that have been broadly classified as independent of clathrin and caveolae uptake.

4. Cell-penetrating peptides

4.1 Introduction

Cell-penetrating peptides (CPPs) also known as protein transduction domains (PTDs) or membrane transduction peptides (MTPs) are usually 7 to 33 amino acid long peptides capable of translocating into cells. These peptides are classified either as cationic or amphipathic peptides based on their sequence. Cationic CPPs contain clusters of primarily arginine residues. Studies evolving in the field of CPPs have mainly focused on three important aspects, namely: i) Defining the structural properties of CPPs that afford the capability to translocate the cell membrane, ii) Elucidating the translocation mechanism of these peptides which remains a controversial topic and iii) Exploiting the ability of the CPPs to deliver a wide range of impermeable molecules across the cellular membrane.

In a non-exhaustive list of CPPs, one point to be noticed is the lack of sequence homology, but again they possess some common functional features. Structure based studies indicate an important role of basic amino acids in transduction (Mi et al., 2000; Mitchell et al., 2000). In addition, the spatial separation of hydrophobic and positively charged residues appears important for defining good transducers (Oehlke et al., 1998; Scheller et al., 1999). Generally, CPPs lack cell selectivity. They can enter into numerous cell types though the quantitative comparison of the efficacy of penetration in various cell types for different CPPs would reveal some differences. A recent systematic evaluation of transduction of fluorescent oligo-arginines has showed highly variable differences of penetration between D- and L- forms of peptides (Tunnemann et al., 2007).

Cell penetration of CPPs does not require any specific membrane receptor for their translocation but this does not mean that they do not interact with any membrane components. Two types of cell surface components have been shown to interact with CPPs, glycoaminoglycans (GAGs) and the negatively charged lipids (Console et al., 2003; Magzoub et al., 2002) and the basis of these interactions were shown to be electrostatic (Ziegler and Seelig, 2004). One more assumption which is being hotly debated is that CPPs do not require metabolic energy for cell entry (Thoren et al., 2000). Evidence for this comes from experiments in which

CPP cell entry was preserved even at 4°C (Esteve et al., 2005) or in the presence of metabolic inhibitors (Vives et al., 2003). However several mechanisms of penetration have been proposed (Patel et al., 2007). In one process, penetration involves a reorganization of the plasma membrane which allows the peptide to move from the extracellular face of the membrane to the intracellular one (Thoren et al., 2004). This mechanism allows for the delivery of the peptide freely into the cytoplasm (Vasir and Labhasetwar, 2007). In another process, CPPs may follow any endocytotic pathway, a process which requires energy (Ross and Murphy, 2004). The type of endocytosis namely macropinocytosis, clathrin- or caveolin-dependent, clathrin- and caveolin-independent endocytosis depends on the cell type, CPP sequence and nature of cargo. Various experimental strategies are therefore pursued to favor the leak of CPP and cargo from the endosomes to the cytoplasm like addition of the lysosomotropic reagent chloroquine (Turner et al., 2005b).

4.2 Classes of Cell penetrating peptides

4.2.1 Tat-related peptides

The HIV-1 Tat is a protein composed of 86 amino acids that binds to the trans-acting response element (TAR) of the viral RNA to transactivate the viral promoter (Frankel and Young, 1998). In the late 1980s, energy-independent translocation of the Tat protein was reported (Frankel and Pabo, 1988; Green and Loewenstein, 1988). In 1994, it was reported that chemical conjugation of the Tat protein (residues 1-72 and 37-72) to other proteins enabled the conjugates to be efficiently internalized into cells (Fawell et al., 1994). Further studies suggested that the arginine-rich segment in the Tat protein (residues 48-60) is a critical component of translocation (Vives et al., 1997). Genetically engineered fusion proteins of Tat fused with cargo proteins, were produced in *E. coli*, purified and purified fusion proteins were shown to be efficiently internalized into the cells (Wadia and Dowdy, 2002; Wadia and Dowdy, 2003). Successful *in vivo* delivery of Tat-β-galactosidae fusion protein to various organs in mice after intraperitoneal injection of fusion protein was reported (Schwarze et al., 1999). Tat fusion proteins have been used to treat mouse models of cancer and inflammation (Snyder and Dowdy, 2005; Wadia and Dowdy, 2005).

Tat has also been used to deliver phage encapsulated DNA to cells, and liposome encapsulated DNA for gene expression in mice (Eguchi et al., 2001; Glover et al., 2005). Efficiency of transduction of Tat depends on the cargoes being used and this principle is clearly demonstrated by difficulties in transducing large cargoes like nucleic acids (Fischer et al., 2005; Meade and Dowdy, 2007). An interesting finding based on the studies with Tat suggested that the cell fixation process has a considerable effect on the cellular localization of the internalized peptide. In unfixed cells, the internalized peptide was seen in punctuate structures within the cytosol, whereas in fixed cells, the punctuate structures were lost and the peptide was found diffused throughout the cytosol and in the nucleus (Richard et al., 2003).

Cell penetrating peptide	***Amino acid sequence***
Tat_{49-57}	RKKRRQRRR
Penetratin	RQIKIWFQNRRMKWKK
Transportan	GWTLNSAGYLLGKINLKALAALAKKIL
Pep-1	KETWWETWWTEWSQPKKKRKV
MPG	GALFLGFLGAAGSTMGAWSQPKKKRKV
Polyarginines (R_9)	RRRRRRRRR
Crotamine	YKQCHKKGGHCFPKEKICLPPSSDFGKMDCRWRWKCCKKGSG

Table 1: Amino acid sequence of CPPs.

4.2.2 Penetratins (Homeodomain-derived peptides)

Homeodomain proteins belong to the class of transcription factors that bind to DNA through specific sequence of 60 amino acids called the homeodomain. It consists of three α-helices, with one β turn between helices 2 and 3. It was first found that the 60 amino acid long polypeptide was able to cross the plasma membrane of the differentiated neurons (Joliot et al., 1991a). Several mutants of homeodomains were analysed for the cell penetration and it was found that with deletion of two hydrophobic residues at positions 48 and 49 within the third α-helix, the peptide lost its ability to cross the plasma membrane (Joliot et al., 1991b). Further more, a synthetic peptide of 16 residues corresponding to amino acids 43-58 of the homeodomain called as penetratin was confirmed to possess the translocation properties of the entire homeodomain (Derossi et al., 1994). Penetratin is claimed to be the first reported CPP. It is characterized by a high content in basic residues and hydrophobic residues mostly tryptophanes

(Derossi et al., 1994). Biophysical studies indicate that penetratin interacts with purely lipidic vesicles and that these interactions involve tryptophane residues (Christiaens et al., 2002).

Cellular internalization of penetratin occurs at 37°C as well as 4°C which suggest that internalization does not require receptor protein (Derossi et al., 1994), but recent studies also indicate the involvement of an endocytic uptake (Duchardt et al., 2007; Maiolo et al., 2005).

4.2.3 Transportans

Transportan is a 27 amino acids long chimeric peptide containing the first 12 amino acids from the amino-terminal part of neuropeptide galanin followed by the 14 amino acid long wasp venom peptide, mastoparan, both connected via a lysine residue (Pooga et al., 1998a; Pooga et al., 1998b; Pooga et al., 1998c; Pooga et al., 1998d). The N-terminal part of the neuropeptide, galanin is recognized by galanin receptors and the mastoparan part of the molecule shows an inhibitory effect on basal GTPase activity in Bowes melanoma cell membranes. This feature may represent a drawback for transportan as a carrier peptide. To eliminate any cellular activity, truncated and modified analogues were designed and tested for cellular penetration. One of the analogues namely transportan 10 retained the cell penetration ability but lacked the GTPase activity (Soomets et al., 2000).

4.2.4 VP22

VP22 is a structural protein from herpes simplex virus type 1 (HSV-1). It is highly basic and consists of 301 amino acids (Leifert and Whitton, 2003). VP22 has been reported as being able to exit the cell in which it is synthesised via an uncharacterized, golgi-independent secretory pathway, and subsequently enters surrounding cells by a non-endocytic mechanism. This remarkable property of intercellular trafficking of VP22 where it is disseminated to many surrounding cells is retained even when it is fused to another protein such as the green fluorescent protein (Elliott and Meredith, 1992). Some studies were not able to detect VP22 intercellular trafficking in live unfixed cells, but rather only after cell fixation (Aints et al., 1999; Elliott and O'Hare, 1999). Anyway, the potential intercellular trafficking of VP22 makes it a promising tool for overcoming low transduction efficiencies in gene therapy.

4.2.5 MPG and Pep families

MPG is a 27 amino acid peptide that contains two domains namely, the hydrophobic domain derived from the fusion sequence of HIV gp41 (glycoprotein 41) and a hydrophilic domain derived from the nuclear localization sequence of SV40 T-antigen. Pep differs from MPG mainly in the hydrophobic domain which contains a tryptophan-rich cluster. The hydrophobic and hydrophilic domains are required mainly for the interactions with nucleic acids, intracellular trafficking of the cargo and solubility of the peptide vector. In both peptides, the integrity and flexibility of both domains are improved by a linker domain (WSQP) (Morris et al., 1997; Simeoni et al., 2003). MPG and Pep are found to form stable complexes with several cargoes, that includes plasmid DNA, nucleic acids, siRNA, proteins, peptides and quantum dots without any chemical modification or cross-linking and are able to efficiently deliver them across the plasma membrane in a variety of cell lines (Morris et al., 2001; Morris et al., 2007; Simeoni et al., 2003; Simeoni et al., 2005).

4.2.6 Crotamine

Crotamine is a 42 amino acid cationic peptide from the venom of South American rattlesnake *Crotalus durissus terrificus.* This peptide is cross linked by three disulphide bonds. Its three dimensional structure as determined by ^{1}H-NMR is arranged as αβββ. Such folds are usually seen in scorpion toxins active on Na^{+} channels (Fadel et al., 2005). By using mouse embryonic stem cells, it was first demonstrated that crotamine can actively translocate across the plasma membrane (Kerkis et al., 2004). Recently, crotamine, at non-toxic concentrations, was shown to bind electrostatically to plasmid DNA leading to the formation of a stable DNA-peptide complexes, whose stabilities overcame the need for chemical conjugation for carrying nucleic acids into cells (Nascimento et al., 2007).

4.2.7 Maurocalcine (MCa)

MCa is a 33-amino acid residue peptide toxin initially isolated from the scorpion *Scorpio maurus palmatus*. Two pieces of evidence suggest that MCa should be able to cross the plasma membrane to reach its intracellular target. First, MCa has biological activity consistent with the

direct activation of RyR when added to the extracellular medium. Second, the structural and functional features show that it resembles many cell penetrating peptides.

4.2.7.1 Structural evidences

The 3-D structure of MCa, determined in solution by ^{1}H-NMR (Mosbah et al., 2000), shows an inhibitor cystine knot motif (Pallaghy et al., 1994) and three β-strands running from amino acid residues 9–11 (strand 1), 20–23 (strand 2) and 30–33 (strand 3), respectively. The β-strands 2 and 3 form an antiparallel sheet. This peptide is cross-linked by three disulfide bridges according to the pattern: Cys^{3}–Cys^{17}, Cys^{10}–Cys^{21} and Cys^{16}–Cys^{32} (Fajloun et al., 2000a). MCa is a highly basic peptide since 12 out of 33 residues are positively charged, including the amino terminal Gly residue, seven Lys residues and four Arg residues. In contrast, MCa contains only four negatively charged residues, meaning that the global net charge is positive. A representation of the electrostatic surface potential of MCa demonstrates that MCa presents a basic face in which the first Gly residue and all Lys residues are involved. Interestingly, none of the four Arg residues are involved in this basic face. The rest of the molecule is mainly hydrophobic, meaning that MCa is a strongly polarized molecule and possesses an important dipole moment.

4.2.7.2 Functional evidences

The very first proof that MCa could act as CPP came from the study in which a biotinylated derivative of MCa was coupled to fluorescent derivate of streptavidin and the complex was assayed for cell penetration in variety of cell lines (Esteve et al., 2005). According to these results, MCa-coupled fluorescent streptavidin was able to enter into all types of cells including HEK293, wild and glycosaminoglycan-deficient CHO cells, MCF7 cells, differentiated and non-differentiated L6 cells and primary neuronal cells (Boisseau et al., 2006; Esteve et al., 2005; Mabrouk et al., 2007). The cell penetration of MCa/streptavidin complexes is rapid since half-saturation in cytoplasm is produced within 20 minutes. Again it should be noted that the kinetics of penetration of MCa is dependent on the nature of the cargo attached used since extracellular application of free MCa to myotubes produce a rise in intracellular calcium within seconds. MCa penetration is observed at concentrations as low as 10 nM with half-effects observed at around 500 nM (Boisseau et al., 2006).

4.3 Internalization and intracellular processing of cell penetrating peptides

CPP internalization mechanism is the most challenging and hotly debated topic in recent past. The first and foremost step in most of the cases is the interaction of the CPP with the extracellular matrix, followed by translocation through the membrane either by endocytotic or non-endocytotic mechanism. These steps are followed by the trafficking and processing of CPPs within the cytoplasm.

4.3.1 Interaction with the extracellular matrix

Proteoglycans (PGs) are one of the most well studied components of the extracellular matrix that interact with CPPs during the process of penetration. They are a heterogenous group of proteins substituted with long, linear, polysulphated and negatively charged glycosaminoglyans (GAG) polysaccharides. The most prevalent GAGs in PGs are heparin, heparin sulphate, chondroitin sulphate or dermatan sulphate (Sandgren et al., 2002). Several methods that have been used to study the interaction and role of heparan sulphate proteoglycans (HSPGs) in CPP uptake include isothermal titration calorimetry (Ziegler and Seelig, 2004), affinity chromatography (Fuchs and Raines, 2004), surface plasma resonance (Article III), enzymatic degradation of extracellular HS chains and use of HSPG-deficient cell lines (Tyagi et al., 2001).

Initial studies with the full-length Tat protein suggested that cell-surface PGs are implicated in the internalization of CPPs (Rusnati et al., 1997). Later, it was demonstrated that incubation of Tat with HSPGs resulted in impaired cellular uptake (Suzuki et al., 2002). Internalization of Arg_9 was completely blocked in mutant CHO cell line that does not produce heparan sulphate (CHO-pgsD-677) (Fuchs and Raines, 2004). Dextran sulphate was found to inhibit the uptake of Tat complex but not of penetratin. MPG and Pep-1 were also found to interact with GAGs. These interactions were followed by a selective activation of the GTPase Rac1, leading to the rearrangement of actin network. GTPase activation and actin remodeling thus impact membrane fluidity to a greater extent and helps in the entry of MPG and Pep-1 alone or when coupled to cargoes (Gerbal-Chaloin et al., 2007). Interaction of arginine rich peptides with proteoglycans was crucial for induction of actin organization leading to macropinocytosis

(Nakase et al., 2007). Interaction of CPP with HSPGs follows either endocytosis or direct membrane penetration (Belting, 2003). Taking into account the ability of the guanidinium groups to form hydrogen bonds with sulphate and carboxylate groups, the interaction between Arg-rich CPPs and HSPGs was thought to occur through hydrogen bonds as compared to electrostatic interaction (Fernandez-Carneado et al., 2005). Internalization of penetratin was atleast four times more efficient in cells expressing the neuronal cell adhesion molecule, α-2, 8-polysialic acid (PSA) as compared to ones that do not express PSA (Joliot et al., 1991b; Perez et al., 1992). This initial step of interaction of CPPs with extracellular matrix, mainly HSPGs, is followed by the translocation of CPP through the cell membrane.

4.3.2 Translocation through the cell membrane

It was initially thought that CPPs were internalized via a rapid, receptor- and energy-independent mechanism (Derossi et al., 1996; Elliott and O'Hare, 1999; Futaki et al., 2001; Suzuki et al., 2002). Penetration of helix composed of D-enantiomers, at 4°C and 37°C strongly suggested that the third helix of the homeodomain, penetratin is internalized by a receptor-independent mechanism. Later, an inverted micelle model was proposed (Figure 11). According to this model, positively charged penetratin interacts with negatively charged components of the membrane and upon interaction, the tryptophane residues penetrate into the membrane. This leads to the formation of an inverted micelle which eventually collapses back to the planar bilayer. Depending on the direction of collapse, penetratin may be released into the cytoplasm (Derossi et al., 1994; Fischer et al., 2000). Another model was proposed for the direct penetration of Tat fusion protein. According to this finding, Tat fusion protein can interact electrostatically with cell surface in denatured, high energy form and penetrate directly into the cytosol with subsequent protein refolding with the help of chaperons (Nagahara et al., 1998; Schwarze et al., 1999). More recent hypothesis about the translocation of guanidinium-rich cationic CPPs is as follows: the presence of different counter anions (amphiphilic or hydrophilic anions) will either lead to charge neutralization or charge inversion, consequently, altering the lipophilicity and solubility of CPP. This alteration will enable the penetration of CPP into the lipid bilayer and release into the cytosol (Sakai and Matile, 2003; Takeuchi et al., 2006). Recently, yet another model was proposed for the penetration of MPG/Pep peptides (Figure 12). Here, the peptides,

along with the cargoes were initially found to interact with the cell surface components, namely proteoglycans and phospholipid head groups. This step was followed by the direct interaction of the peptide with the lipid phase of the cell membrane along with the Rac1-associated membrane dynamics, which allowed the insertion of the complex into the membrane and later the release of complexes into the cytoplasm. This insertion step was found to be associated with conformational changes of the peptides that induce membrane structure perturbations (Morris et al., 2008).

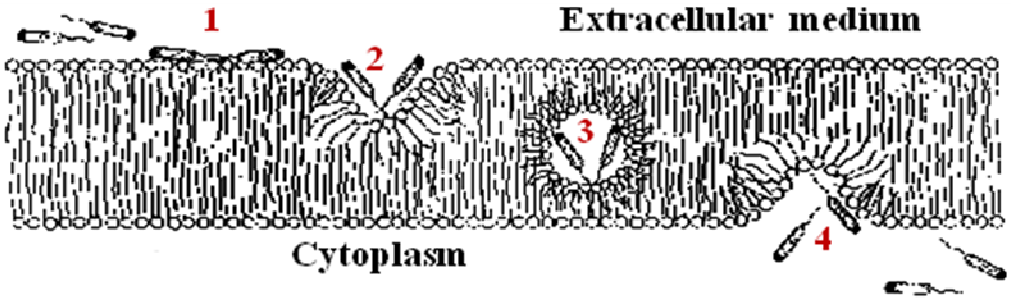

Figure 11: Cellular internalization of penetratin.*(1) Interaction of penetratin with charged phospholipids on the outer side of membrane; (2) Destabilization of the bilayer leading to formation of inverted micelles; (3) Inverted micelles traversing across the membrane; (4) Opening of micelles on its cytoplasmic side and release of penetratin into the cytoplasm(Derossi et al., 1998).*

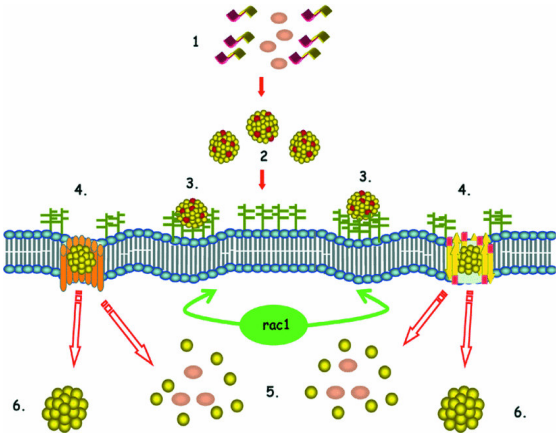

Figure 12: Cellular uptake of MPG- or Pep- cargo complexes. *(1)Formation of peptide-cargo complexes through electrostatic and hydrophobic interaction; (2)Electrostatic interaction with cell surface proteoglycans; (3) Followed by interaction with phospholipid head groups; (4) Direct interaction of the peptide with lipid phase together with Rac1-associated membrane dynamics, which allows insertion of the complex into membrane; (5) Release of complex into cytoplasm; (6) Targeted to nucleus or specific organelles (Morris et al., 2008).*

4.3.3 Endocytosis as a major route of entry of CPPs

Recent studies on the cellular internalization of CPPs have focused on endocytosis as major route of cell internalization. Since some studies suggested that cell fixation caused an artifical redistribution of CPPs, it lead to numerous studies in live cells, inorder to re-examine the internalization mechanism of CPPs (Richard et al., 2003). Moreover, it was observed that flow cytometry could not discriminate quantitatively between the membrane-bound and internalized peptide. In this case, trypsination of cells before analysis is a necessary step to avoid overestimation of the level of internalization of CPP (Boisseau et al., 2006). For Tat, two different mechanisms have beed described: caveolin mediated endocytosis and macropinoytosis. Internalization of GST-Tat-EGFP construct was found to co-localize with caveolin-1, cholera toxin and found to be sensitive to drugs (cyclodextrin or cytochalasin D) that reduce lipid raft formation, indicating that caveolae mediated endocytosis is responsible for the uptake of Tat (Binder and Lindblom, 2003; Zaro et al., 2006). On the other hand, the fusogenic Tat-Cre protein was found to internalize by lipid raft-dependent macropinocytosis since the internalization was not dynamin dependent but required cholesterol (Saalik et al., 2004). It was observed that liposomes modified with a high density of Arg_8 were preferably internalized by macropinocytosis, but liposomes modified with low density of Arg_8 resulted in clathrin-mediated uptake (Khalil et al., 2006). In HeLa cells, fluorescent labeled Arg_8 was found to internalize through macropinocytosis (Nakase et al., 2004), but co-incubation of [^{125}I]-Arg_8 with epidermal growth factor, a known stimulator of macropinocytosis did not increase cytosolic localization of the iodinated peptide (Zaro et al., 2006). Maurocalcine internalization was found be sensitive to amiloride (inhibitor of macropinocytosis) both in CHO wild-type and GAG-deficient cell lines indicating that both GAG-dependent and -independent penetrations rely similarly on the macropinocytosis pathway (Article III). Once the CPP enters into the cytoplasm, it takes up different compartments depending on the cell internalization mechanism.

Depending on the type of endocytosis, CPP alone or along with cargo end up in different organelles of the cytoplasm. In clathrin-mediated endocytosis, endosomes are routed from early endosomes to late endosomes and ultimately to lysosomes (Campbell et al., 1987; Conner and Schmid, 2003). The fate of macropinosomes is different in different cells. In HeLa cells, the

macropinosomes resulting from macropinocytosis show little interaction with endosomal compartments and mainly recycle their contents back to extracellular spaces (Swanson and Watts, 1995). In caveolin-mediated endocytosis, the endosomes are targeted to golgi apparatus or to the endoplasmic reticulum (Fischer et al., 2004). In general, the CPPs internalized by endocytosis are enclosed in vesicles from which they must escape to reach the target sites of their cargoes.

4.3.4 Endosomal escape

Since endocytosis is the major route of entry of CPPs alone or when attached to cargoes, there is a need for an efficient and feasible method for the disruption of the endosomes. The cargo needs to be released freely into the cytoplasm in order to reach its target. N-terminal domain hemagglutin-2 of influenza virus that can induce lysis of membranes has been utilized to promote the endosomal escape of Tat-Cre fusion protein (Wadia et al., 2004). Fluorescent labeled CPPs and peptide nucleic acid coupled CPP conjugate entrapped in endosomes were subjected to reactive oxygen spescies (ROS) generated by photosensitizers in order to release the endocystosed CPPs (Maiolo et al., 2004; Shiraishi and Nielsen, 2006). It is known that during endosomal trafficking, there is a decrease in the vesicular pH from approximately 7.4 to 5.0 (Langer et al., 2001). This suggests that acid-sensitive linkers can be used to release the cargo covalently linked to CPP.

In the recent past, most *in vitro* experiments produced endosomal disruption by chloroquine or sucrose. Chloroquine is a lysosomotropic agent thought to have a buffering capacity preventing endosomal acidification and in addition can lead to swelling and bursting of the endosomes. Addition of chloroquine was found to increase the nuclear delivery of functional Tat-Cre recombinase in NIH SSR fibroblasts suggesting the endosomal rupture. Adding sucrose to the cell culture medium produces intracellular cytoplasmic swelling within endosomes, thus helping in the rupture of endosomes (Caron et al., 2004). In yet another case, attachment of transducible fusogenic TAT-HA2 efficiently delivered magnetic nanoparticles into HeLa cells. But these particles ended up in the endosomes leading punctate distribution within the cytoplasm. However, co-incubation with chloroquine increased the concentration of nanoparticles outside the endosomes (Nudleman et al., 2005). Some studies showed that use of Ca^{2+} can effectively enhance *in vitro* cellular delivery of cationic peptide-conjugated PNA oligomers, and also

emphasize the significance of the endosomal escape route for such peptides (Shiraishi et al., 2005). Thus it is very important for the CPP-cargo to be free in the cytosol in order to reach its destiny.

4.3.5 Nuclear localization

Trafficking of macromolecules across the nuclear envelope is considered to be mediated by the nuclear pore complex (NPC). In general, the diffusion of CPP-Cargo from cytoplasm to nucleus depends on the size of CPP-cargo, metabolic stability and cytoplasmic concentration of the CPP-cargo and other cellular events that may block the nuclear entry. Nuclear accumulation of CPPs was shown in fixed cells, but later it was considered as an artifact due to the cell fixation process (Richard et al., 2003). Cargos with their biological activity targeted to the nucleus include plasmid or gene regulating -proteins, -peptides and -oligonucleotides. Since these cargos exceed the size limit for free diffusion to nucleus when coupled to CPPs, they need nuclear localization signal (NLS) along with the cargo that can bind to the nuclear import machinery and subsequently translocate across NPC (Lechardeur and Lukacs, 2006). Tat and penetratin are known to be derived from transcription factors and NLS are embedded within the sequence of the CPP (Gehring et al., 1994; Truant and Cullen, 1999).

4.3.6 Degradation of CPPs within the endosomes or cytoplasm

Studies haven't focused much on the degradation of CPPs within the endosomes or when released to the cytoplasm. Since endocytosis is the major route of CPP entry and with over 40 hydrolytic enzymes being characterized within the lysosome, there is a significant possibility that the CPPs may encounter the degradation pathways of the lysosome if they do not escape from the lumen. In cytosol, the major degradation pathway for proteins is the ubiquitin-proteasome pathway (Glickman and Ciechanover, 2002). Other than this, there are several cytosolic peptidases such as tripeptidylpeptidase II that could possibly digest the CPPs (Geier et al., 1999). Metabolic stability of three CPPs namely, Tat, penetratin, and hCT were studied in different epithelial cells. It was found that the CPPs were subjected to rapid cleavage by endopeptidases (Trehin et al., 2004). pVEC, a CPP derived from vascular endothelial cadherin was found to be rapidly degraded when incubated with human aorta endothelial or murine A9 fibroblasts

(Elmquist and Langel, 2003). Some of the strategies developed to overcome this problem were the addition of protease inhibitors *in vivo.* Thus it is important that there is no premature degradation of CPP-cargo before it reaches the target.

4.4 Inhibitors of endocytosis

Endocytosis is an energy driven process. At 4°C, all cellular processes, including ATP hydrolysis, are arrested, thereby blocking endocytosis itself. Again, at this temperature, membrane fluidity is also affected. Since transduction also depends on the interaction of the CPP with the cell membrane, it is conceivable that inhibition of membrane fluidity also inhibits non-endocytotic pathways of internalization. This has been tested for oligoarginine at 4, 16, and 37°C in CHO cells. Results clearly indicate that inhibition of membrane fluidity at 4°C can affect both endocytosis and direct membrane transduction (Zaro and Shen, 2003; Zaro and Shen, 2005). Thus, indicating that, analysis of cell penetration at 4°C is just not sufficient in understanding the mechanism of penetration of CPPs.

There are various drugs that inhibit the process of endocytosis (Table 2). Amiloride is known to block macropinocytosis, methyl-β-cyclodextrin to deplete membrane cholesterol and inhibit lipid raft-dependent pathways, nocodazole to inhibit microtubule formation, and cytochalasin D to inhibit F-actin elongation, required for macropinocytosis and clathrin-dependent endocytosis and chlorpromazine, an inhibitor of clathrin-mediated endocytosis (Mano et al., 2005). Another approach in studying the mechanism of uptake would be the use of a dominant negative mutant version of a cellular protein. This approach provides a more specific way to analyse the function of defined pathways within the cell. When expressed at high levels, dominant negative mutants act by overwhelming the wild-type protein and preventing its function. This type of approach has been used extensively in studying the function of GTPases within the cell, where a dominant negative protein can lead to sequestration of effectors and regulatory molecules and effectively shut down the function of the endogenous wild-type protein (Feig, 1999).

Pathway	Inhibitor
Clathrin	Anti-clathrin antibodies
	Low pH shock
	Potassium depletion
	Brefeldin A
	Chlorpromazine
	Dominant-negative dynamin mutant
	Dominant-negative Eps15 mutant
	Clathrin hub domain
	AP-2 μ2 Subunit
Caveolae	Sterol-binding drugs
	Dominant-negative caveolin mutant
Macropinocytosis	Cytochalasin D
	PI_3K inhibitors
	Toxin B
	Amiloride
	ARF_6 GTPase mutant
	Rho family GTPase mutants
	PAK_1autoinhibiltory domain
Endosomes	Rab GTPase mutants
	Rho family GTPase mutants
	PI_3 inhibitors
	PKC inhibitors

Table 2: Toolbox of reagents targeting the endocytic pathway *(Sieczkarski and Whittaker, 2002).*

By using a transducible Tat-Cre recombinase reporter assay on live cells, Tat-fusion proteins was found to be internalized by lipid raft-dependent macropinocytosis and ruled out the possibility of interleukin-2 receptor/raft-, caveolar- and clathrin-mediated endocytosis. Use of drugs like methyl-β-cyclodextrin, nystatin, cytochalasin D or amiloride and expression of a dominant-negative mutant of dynamin to block the endocytosis process were used inorder to derive the internalization pathway of Tat-fusion proteins (Wadia et al., 2004). Using potassium depletion and chlorpromazine as specific inhibitors of clathrin-meditaed endocytosis, Tat peptide uptake was inhibited by around 50% (Richard et al., 2005). Uptake of maurocalcine was found to be affected by amiloride, nocodazole and cytochalasin D to an extent of about 80, 60 and 20%, respectively, indicating macropinocytosis is involved in the entry of maurocalcine. But uptake was completely unaffected in presence of methyl-β-cyclodextrin or when dominant-negative

mutant of dynamin was expressed (Article III). The cellular uptake of CPP, S413-PV was analysed in presence of various endocytosis inhibitors. The results obtained by both confocal microscopy and flow cytometry demonstrated that, among all the tested drugs, only cytochalasin D had an inhibitory effect on the cellular uptake of the $S4_{13}$-PV peptide (Mano et al., 2005).

4.5 Toxicity of CPPs

The primary structure, net charge and pharmacological targets, if any, are the important factors influencing the toxicity of CPPs. Some of the methods used in assessing the cell toxicity of CPPs *in vitro* include iodide propidium cell incorporation (Boisseau et al., 2006), 3-(4, 5-dimethylthiazol-2-yl)-2, 5-diphenyl-tetrazolium bromide (MTT) assay (Article I)., WST-1 (water-soluble tetrazolium salt 1) assay and lactate dehyrogenase (LDH) release assay (El-Andaloussi et al., 2007). Full length Tat was found to exhibit toxic action on primary rat neuronal cultures (Lindgren et al., 2004). Further more it was demonstrated that the cysteine-rich and basic domain of Tat protein induced endothelial apoptosis (Jia et al., 2001). Toxic effects of penetratin on osteosarcoma cells were seen only at concentrations as high as 50 μM (Garcia-Echeverria et al., 2001). Poly-L-arginine was found to induce inflammatory responses in rat lungs *in vivo.* The lethality of poly-L-arginine was due to electrostatic interaction of the polycation with anionic surfaces present in the pulmonary epithelium (Santana et al., 1993). An important observation in case of MCa is that, though it had an intracellular target, RyR and is involved in the release of Ca^{2+} from the intracellular store, it still had no toxicity effects on various cell lines tested (Boisseau et al., 2006).

5. Applications of cell penetrating peptides

Since cellular membranes form major barriers for the movement of macromolecules into the cells, CPPs are being widely used for the delivery of various macromolecules across the cellular membrane both *in vitro* and *in vivo*. To use CPPs as delivery vehicles, one important aspect to be considered is that the CPPs should possibly be coupled to different cargoes without losing their translocation properties.

5.1 Cargo coupling methods

The coupling of cargo to the CPP depends on the nature of the cargo to be translocated. The link between the CPP and cargo is usually a covalent bond. Cargoes like peptides and proteins can be directly linked to the same polypeptide chain in synthesis or recombinant expression. Usually direct linkage of cargoes is not advisable since it might often lead to loss of biological activity of cargo molecule and also alter the translocation properties of the CPPs (Temsamani and Vidal, 2004). Alternatively, a suitable amino acid side-chain, thiol group, bifunctional crosslinkers or noncovalent interactions can be used to couple the cargoes to the CPPs. The disulphide bridge formed between the cargo and CPP due to the thiol groups of cysteine will readily be cleaved in the cytoplasm of the cell after translocation, resulting in the release of cargo from the CPP for its biological activity (Davidson et al., 2004). The tumor killing ability of free doxorubicin (anticancer drug) was compared to that of doxorubicin when coupled to Tat through a bifunctional crosslinker, namely succinimidyl-4-(*N*-maleimidomethyl) cyclohexane-1-carboxylate (SMCC) (Liang and Yang, 2005).

Noncovalent conjugation of cargoes to CPPs by biotin-avidin complexation seems to be a stable as compared to covalent conjugation. But in the recent past, coupling through charge-charge interactions between cargo and CPP is being used widely. Mixing of CPP and proteins (Morris et al., 2001), plasmids (Nascimento et al., 2007) and siRNAs (Simeoni et al., 2003) was shown to increase the uptake of these cargoes. The most important thing to be considered in case of charge-charge interactions is the ratio between the cargo and the CPP. Increasing the number of Tat molecules from one to 15 per nanoparticle, increased the uptake exponentially (Zhao et al., 2002) and a study showed that atleast 5-10 penetratin molecules were required for the uptake of

liposomes (Tseng et al., 2002). An overview of different modes of cargo attachment is represented in figure 13.

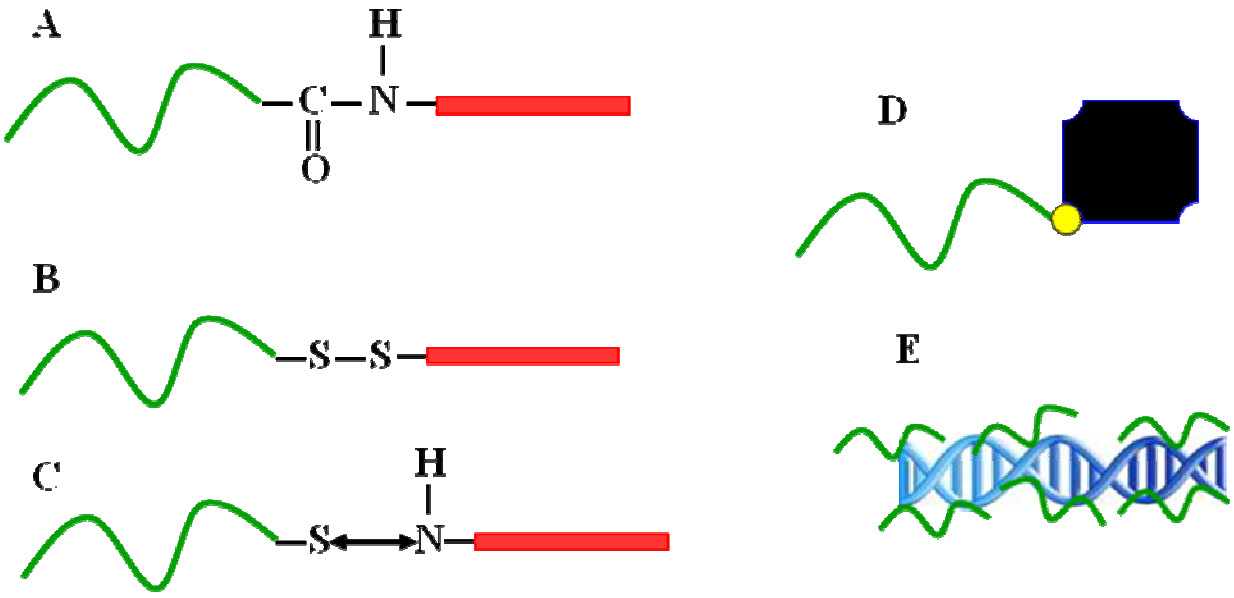

Figure 13: Cargo coupling to CPPs . *Coupling via a peptide bond (A), disulfide bridge (B), and bifunctional linker (C).The large cargo molecule, streptavidin is non-covalently bound to biotinylated CPP (D) and DNA coupled to CPP through charge interaction. Colour code: CPP (green), cargo (red), biotin (yellow), streptavidin (black) and DNA (blue).*

5.2 Intracellular delivery of different molecules

5.2.1 Delivery of peptides

Peptide-based drugs represent a class of therapeutics that exhibit improved activity when delivered with the help of CPPs. It is always an advantage to use peptide sequences that possess biological activity rather than using the full-length protein.

In order to understand the physiological importance of the caveolin-1 scaffolding domain *in vivo*, a chimeric peptide with a cellular internalization sequence was fused to the caveolin-1 scaffolding domain (amino acids 82−101) and the chimeric peptide was efficiently delivered into blood vessels and endothelial cells, leading to selective inhibition of acetylcholine (Ach)-induced vasodilation and nitric oxide (NO) production. These results suggest that caveolin-1 scaffolding

domain can selectively regulate signal transduction to endothelial nitric oxide synthase (eNOS) in endothelial cells and this domain may provide a new therapeutic approach (Bucci et al., 2000).

CPP used	***Cargo***	***Target***	***Reference***
Tat-p53C, Tat-RXL	DV3	Selective killing of tumor CXCR4-overexpressed cells	(Snyder et al., 2005)
Tat	P15	Reduction of tumor mass	(Perea et al., 2004)
Penetratin	Shepherdin	Induction of tumor cell death	(Plescia et al., 2005)
Polyarginine	polyanion	Tumor imaging with specific matrix metalloproteinase proteolytic activation of CPP.	(Jiang et al., 2004)
Penetratin	BH3 helix	Inhibition of pro-apoptotic Bcl-2 family members	(Dixon et al., 2007)
Polyarginine	ARF-derived peptide	Inhibition of foxm1-activated transcription	(Schwarze et al., 1999)
Penetratin, Tat	Apaf-1 peptoid inhibitor	Activation of apotosome	(Mader and Hoskin, 2006)
Penetratin	NEMO-derived peptide	NF-κB activation	(Javadpour et al., 1996)
Penetratin	$pG_{\alpha s}$	Inhibition of signal transduction from G_s-coupled receptors.	(D'Ursi et al., 2006)
Penetratin	p53p	Induction of apoptosis in pre-malignant and malignant cells	(Li et al., 2005)
Tat, penetratin	Mek1 N-terminus	*In vivo* inhibition of mitogen-activated protein kinase activation	(Kelemen et al., 2002)
TP10	PKC and cannabinoid receptor fragments	Beta-hexosaminidase secretion and phospholipase D activation	(Howl et al., 2003)
Tat	Cyclin dependent	Selective killing of transformed cells by cyclin/cyclin-dependent kinase 2	(Chen et al.,

	kinase inhibitors	antagonists	1999)
polyarginine	PKA inhibitor	Role of PKA in long-lasting long-term potentiation	(Matsushita et al., 2001)
polyarginine	Hemagglutinin epitope	Delivery of peptide to different tissues	(Robbins et al., 2002)
Tat	c-Jun kinase inhibitor	Protection against excitotoxicity and cerebral ischemia	(Borsello et al., 2003)

Table 3: Recent application of CPPs in peptide delivery.

Shepherdin, an anticancer agent that selectively kills tumor cells and spares normal tissues was conjugated to either penetratin or Tat for its delivery across the cell membrane both *in vitro* and *in vivo* (Plescia et al., 2005). Two functional peptide fragments from cyclin inhibitor, $p21^{WAF1}$, have been conjugated to penetratin and have been used to inhibit cancer cell growth through cell cycle inhibition. P16, peptide known to inhibit hypophosphorylation of the retinoblastoma, when coupled to Tat, causes an early G_1 cell cycle arrest in nearly 100% of human keratinocytes (Gius et al., 1999). Calpain is a calcium-dependent cysteine protease that regulates the function of several intracellular proteins that contributes to the pathogenesis of neuronal diseases. Generally calpain inhibitors, have the disadvantage to lack specificity or poor cellular permeability. Therefore, calpastatin peptide derived from the endogenous peptide calpastatin was linked to polyarginine and shown to significantly inhibit calpain activity in primary neuronal cells (Wu et al., 2003). KLA, an amphipathic antimicrobial peptide that induces apoptosis by disrupting the mitochondrial membrane was attached to heptarginine for its delivery across the cell membrane of several tumor cell lines as well as *in vivo*. Furthermore, to prevent rapid intracellular degradation, the D-isoform of KLA and heptaarginine was used (Law et al., 2006). Some of the other examples in which CPPs are used for the delivery of peptides are listed in table 3.

5.2.2 Delivery of proteins

Plasmid based genetic recombination technique for the delivery of proteins into the cells in order to elucidate their function has several disadvantages, like poor transfection efficiency and cellular toxicity. Thus, CPPs are being employed for the delivery of biologically active, full-length proteins both *in vivo* and *in vitro*. In order to assess the ability of the Tat peptide to carry various molecules across the cell membrane, several proteins, beta-galactosidase, horseradish peroxidase, RNase A and domain III of pseudomonas exotoxin A (PE) were chemically coupled to Tat and the uptake was monitored colorimetrically on several cell lines (Fawell et al., 1994).

CPP used	***Cargo***	***Target***	***Reference***
Tat	EGFP	Delivering protein into the neurons of brain slices	(Matsushita et al., 2001)
Pep1	Superoxide dismutase	Protection against ischemic insult.	(Eum et al., 2004)
Tat	Cre recombinase	Activation of EGFP expression	(Wadia et al., 2004)
Tat	Rho GTPase	To show that Rho-A is critical for osteoclast podosome organization, motility, and bone resorption	(Chellaiah et al., 2000)
Tat, penetratin	Avidin	Binding of CPPs to cell surface glycosaminoglycans.	(Console et al., 2003)
Tat	Dominant negative Ras	Blockade of focal clustering and active conformation in beta 2-integrin-mediated adhesion of eosinophils to intercellular adhesion molecule-1	(Myou et al., 2002)
Tat	Heat shock protein	Small heat shock-related protein HSP20 inhibits hyperplasia	(Tessier et al., 2004)
MCa	Streptavidin	Proof that MCa acts as CPP	(Boisseau et al., 2006)
Tat	Exonuclease III	Reduction of repair of mtDNA	(Shokolenko

			et al., 2005)
Tat	Herpes simplex virus type-1 thymidine kinase	Sustained cell killing activity	(Cao et al., 2006)
Penetratin	scFv antibody	Delivery and prolonged retention of scFv antibody into solid tumors	(Jain et al., 2005)
Tat	N-CoR fragments	Unblockage of differentiation in leukemia cells	(Racanicchi et al., 2005)
Tat	Anti-Tat scFv	Suppression of Tat-dependent transcription of HIV-1 reporter gene	(Theisen et al., 2006)
Tat	Glutamate dehydrogenase	GDH disorders	(Yoon et al., 2002)
VP22	GFP	Enhanced spread of adenovirally delivered GFP in retina and striatum	(Kretz et al., 2003)

Table 4: Recent application of CPPs in protein delivery.

Tat fused anti-apoptotic protein Bcl-X_L of the BCL2 family was able to prevent apoptosis in retinal ganglion cells (Diem et al., 2005). P53, the tumor suppressor gene, is usually mutated in cancers, leading to uncontrolled cell proliferation and tumor formation. A VP22-P53 fusion protein has been shown to induce apoptosis in P53 negative human osteosarcoma cells. VP22 or P53 alone did not have any biological effects (Phelan et al., 1998). Green fluorescence protein (GFP), a widely used biomarker for various biological studies, has been anchored to different CPPs, such as Penetratin (Han et al., 2000), Tat (Caron et al., 2001) and oligoarginine (Han et al., 2001) and these conjugates have been used to study trafficking, intracellular localization and protein interaction. To deliver exonuclease III, a mtDNA repair enzyme to its target, the mitochondrial matrix of breast cancer cells, a fusion protein that has a mitochondrial targeting signal (MTS) on the N-terminal and a Tat peptide on the C-terminal end was constructed. This study exemplifies a rational design that applies a combination of transduction properties of CPP and targeting signals, not only to deliver the protein intracellular but also to the intended target

(Shokolenko et al., 2005). Loss of cholinergic neurons in the basal forebrain being one of the hallmarks of Alzheimers disease (AD), acetyl transferase, the enzyme required for acetylcholine synthesis, was coupled to Tat to deliver the enzyme to the brain of AD model mice (Fu et al., 2004). Glial cell derived neurotrophic factor, also known as GDNF, is a small protein that potently promotes the survival of many types of neurons. However it does not readily cross the blood brain barrier (BBB), which complicates its use as a therapeutic molecule. GDNF was coupled to Tat and efficiently delivered across the BBB after intravenous injection (Kilic et al., 2003). Thus CPPs facilitate the delivery of various proteins and show great potential in therapy (Table 4)

5.2.3 Delivery of oligonucleotides

For controlling the gene expression or for silencing the activity of certain proteins, oligonucleotides (ONs) such as siRNAs, plasmids and their analogues such as peptide nucleic acids (PNAs) have been employed over the past (Table 5). Again, one of the drawback as in most of the cases is their delivery across the cell membrane. Conjugation of CPPs to various ONs has enabled their delivery into mammalian cells both *in vitro* and *in vivo*.

CPP used	***Cargo***	***Target***	***Reference***
Tat	12mer OMe/LNA	Observation of CPP-cargo uptake without biological activity of cargo owing to endosomal entrapment	(Turner et al., 2005a)
Penetratin, Transportan	SiRNA	Reduction of transient and stable expression of reporter transgenes	(Muratovska and Eccles, 2004)
TP10	Myc decoy DNA	Decreased proliferation activity	(El-Andaloussi et al., 2005)
Tat, Arginine	Splice correcting PNA	Restoring normal splicing with Ca^{2+} enhanced endosomal escape	(Shiraishi et al., 2005)
Penetratin	Superoxide dismutase antisense	Downregulation of Cu/Zn	(Troy et al.,

	oligodeoxynucleotide	superoxide	1996)
Penetratin	Prepro-oxytocin antisense PNA	Antisense activity depresses the target mRNA and protein in magnocellular oxytocin neurons	(Aldrian-Herrada et al., 1998)
MPG	Plasmid full-length antisense cDNA of human cdc25C	Reduced cdc25C expression levels and promoted a block to cell cycle progression	(Morris et al., 1999)
Tat	Plasmid encoding beta-galactosidase	To develop versatile gene delivery systems based on penetratin application for human disease therapy	(Ignatovich et al., 2003)
Penetratin, Transportan	GalR1 antisense PNA	Regulation of galanin receptor levels and modification of pain transmission *in vivo*	(Pooga et al., 1998d)
Transportan	Anti-HIV transactivation response element PNA	Inhibition of HIV-1 replication	(Kaushik et al., 2002)
MPG	18 and 36 mer fragments of HIV natural primer binding site	Proof that MPG electrostatically interacts with oligonucleotide and delivers into cells	(Morris et al., 1997)
Transportan	X-chromosome targeting PNA	PNA targeted against a particular region of Xist RNA caused the disruption of the Xi	(Beletskii et al., 2001)
Penetratin	PNA targeting telomerase RNA component	Inhibition of telomerase activity in human melanoma cells	(Villa et al., 2000)

Table 5: Recent application of CPPs in oligonucleotide delivery.

Penetratin conjugated oligonucleotide against Cu/Zn superoxide dismutase showed a 100-fold higher efficiency in culture as compared to oligonucleotide itself (Troy et al., 1996). Oligonucleotide against cell surface P-glycoprotein, covalently coupled to Tat and penetratin through disulfide bridge, showed significant inhibition of P-glycoprotein expression as compared to the ON alone (Astriab-Fisher et al., 2000). MPG containing the hydrophobic domain was non-covalently coupled to fluorescently labeled oligonucleotides and delivered into cells and localized to the nucleus through an non-endocytotic pathway (Morris et al., 1997). Monomeric form of Tat peptide was complexed with plasmid DNA through charge interaction and internalized through endocytotic pathway (Ignatovich et al., 2003). In some cases the transfection efficiency of plasmid DNA was improved through the use of CPPs along with the conventional transfection agents (Ross and Murphy, 2004). Another approach for improving gene delivery was coupling of polylysine peptides to CPP. Tat was linked to polylysine (Tat-pK), then coupled to plasmid DNA and delivered across the cell membrane via endocytotic pathway (Hashida et al., 2004).

The inability of naked siRNA to translocate to the intracellular environment has initiated the use of CPPs in siRNA delivery. Linking of synthetic siRNA to penetratin through disulfide bridge resulted in rapid, highly efficient uptake of siRNA by cultured primary mammalian hippocampal and sympathetic neurons. This treatment leads to specific knock-down of targeted proteins within hours without signs of toxicity (Davidson et al., 2004). Thiol containing siRNAs corresponding to luciferase or green fluorescent protein transgenes were synthesized and conjugated to penetratin or transportan and it was found that the CPPs-siRNAs efficiently reduced transient and stable expression of reporter transgenes in several cell types (Muratovska et al., 2003). MPG was non-covalent coupled to siRNA and delivered in various cell lines including adherent cell lines, cells in suspension, cancer and primary cell lines which cannot be transfected using other non-viral approaches. MPG has been used for the delivery of siRNA that targets an essential cell cycle regulator cyclin B1 *in vivo.* Intravenous injection of MPG/siRNA particles has been shown to efficiently block tumor growth (Deshayes et al., 2008).

Peptide nucleic acid (PNA) complementary to human galanin receptor type 1 mRNA was coupled to trasportan and penetratin, and was efficiently delivered into bowes cells where it blocked the expression of galanin receptors (Pooga et al., 1998d). In yet another study,

transportan conjugated to PNA was used to elucidate the interaction between RNA and RNA-binding proteins, which further facilitates the understanding of the role of RNA-binding proteins in regulation of gene expression (Zielinski et al., 2006).

5.2.4 Delivery of imaging agents

Imaging agents are being widely used for visualizing internal features, physiological structures and cellular functions of living organisms. Biomedical imaging techniques such as fluorescence imaging and magnetic resonance imaging (MRI) have been developed for *in vivo* application. However, the inability of these agents for cellular uptake and inadequate targeting brings in the need for the use of CPPs to deliver them across the cell membrane both *in vitro* and *in vivo*. Various fluorophores conjugated to CPPs have been developed as imaging agents. Supermagnetic iron oxide particles conjugated to Tat and fluorescein isothiocyanate (FITC) were efficiently delivered to T cells, B cells and macrophages (Kaufman et al., 2003). Paramagnetic particles were attached to Tat and intracellular concentrations were detected by (MRI) (Bhorade et al., 2000). FITC-doped monodisperse silica particles were modified with Tat for cellular delivery and were shown to efficiently cross the blood-brain barrier (Santra et al., 2004). Tat and an appropriate peptide-based motif (epsilon-KGC) that provides an N(3)S donor core for chelating technetium and rhenium were synthesized and were rapidly translocated in human Jurkat, KB 3-1 and KB 8-5 tumor cells for imaging and radiotherapy (Polyakov et al., 2000).

5.2.5 Delivery of nanoparticles

Nanoparticles are being extensively used as drug carriers and in various imaging applications. One of the limiting factors being their use across the cellular membrane. CPPs are being widely used to favor their intracellular delivery. Nanoparticles can be modified with a higher amount of CPP per particle. Biocompatible dextran coated superparamagnetic iron oxide particles were conjugated to Tat and internalized into lymphocytes 100-fold more efficiently than uncoupled particles. These particles were found to be localized in the cytoplasm and nuclei as determined by fluorescence microscopy and immunohistochemistry (Josephson et al., 1999). Tat coupled gold nanoparticles modified with nuclear localization peptides, were delivered into NIH-3T3 and HepG2 cells and the uptake was temperature dependent, suggesting an endosomal

uptake (Tkachenko et al., 2004). Ultra small paramagnetic iron oxide nanoparticles used as contrasting agents in MRI, were functionalized with Tat and efficiently used to label CD4+ T cells (Garden et al., 2006).

Luminescent semiconductor nanocrystals or quantum dots (Qdots) are relatively new classes of fluorescent probes with unique optical properties that make them superior to conventional organic dyes for many biological applications. Qdots are being widely used for labeling various biological targets on the cellular membrane, but the limitation in use of QDots lies in their inability to cross the plasma membrane. Of the various strategies being used to deliver QDots across the cell membrane, CPP driven delivery seems to be most efficient system. Polyarginine coupled Qdots were efficiently delivered to lysosomes in both HeLa and baby hamster kidney cells (Silver and Ou, 2005). Covalent coupling of Qdots to an 11-mer polyarginine facilitated rapid uptake and localization in the nucleus of vero cells (Hoshino et al., 2004). A bifunctional oligoarginine bearing a terminal polyhistidine tract was synthesized and used for the delivery of Qdots. The polyhistidine sequence allowed the self assembly of the peptide onto Qdot surface via metal-affinity interactions. Upon internalization, Qdots displayed a punctuate staining in which some but not all Qdots localized within endosomes (Delehanty et al., 2006). Multiple copies of two structurally diverse fluorescent proteins, the 27 kDa monomeric yellow fluorescent protein and the 240 kDa multichromophore beta-phycoerythrin complex, were attached to QDs using either metal-affinity driven self-assembly or biotin-streptavidin binding, respectively and these complexes were found to depend on the conjugation of CPPs for their intracellular delivery (Medintz et al., 2008). Tat conjugated Qdots were intra-arterially delivered to rat brain, and rapidly labeled the brain tissue. Qdots without Tat did not label the brain tissue confirming the fact that Tat peptide was necessary to overcome the BBB (Santra et al., 2005). These initial findings of using CPPs to deliver nanoparticles, sets a stage for more elegant *in vitro* and *in vivo* applications of nanoparticles.

III. RESULTS

1. Articles I and II

Critical amino acid residues of maurocalcine involved in pharmacology, lipid interaction and cell penetration.

Mabrouk K*, Ram N*, Boisseau S, Strappazzon F, Rehaim A, Darbon H, Ronjat M, De Waard M.

***Both authors contributed equally to this work**

Biochim Biophys Acta. 2007 Oct; 1768(10):2528-40. Epub 2007 Jul 10.

Design of a disulfide-less, pharmacologically-inert and chemically-competent analog of maurocalcine for the efficient transport of impermeant compounds into cells.

Ram N, Weiss N, Texier-Nogues I, Aroui S, Andreotti N, Pirollet F, Ronjat M, Sabatier JM, Darbon H, Jacquemond V, De Waard M.

J Biol Chem. 2008 Jul 21. [Epub ahead of print], PMID: 18621738 [PubMed - as supplied by publisher]

Introduction

Maurocalcine (MCa) is a 33 mer peptide toxin isolated from the venom of Tunisian scorpion. Since its initial isolation, it has been chemically synthesized, which allows the characterization of biological activity and the solution of its three dimensional structure. MCa possess three disulfide bridges and folds along an inhibitor cystine knot motif. In addition, it also contains three beta-strands (Mosbah et al., 2000). MCa has been shown to be a potent activator of skeletal muscle RyR, an intracellular calcium channel target. Initially, two pieces of evidences suggested that MCa should be able to cross the plasma membrane to reach its intracellular target. First, MCa has biological activity consistent with the direct activation of RyR when added to extracellular medium (Esteve et al., 2003). Second, structural analysis of MCa reveals a stretch of positively charged amino acids that is reminiscent of the protein transduction domains found in proteins (Esteve et al., 2005).

Greater interest in MCa has been triggered by the observation that it can efficiently cross the plasma membrane alone or when coupled to membrane impermeable protein such as streptavidin (Boisseau et al., 2006). Because of its potential to behave as CPP, it appeared essential to define a new analogue of MCa that lacks the pharmacological effects of wild-type MCa but preserve or enhance its cell penetration efficiencies. To achieve this, several mutated analogues were chemically synthesized and assessed for their effects on RyR, cell penetration efficiencies and also tested for their toxicity on primary neuronal cultures. Since it is expected that membrane lipids are implicated in the cell penetration of CPPs, MCa analogues were also tested for their ability to interact with membrane lipids. Later, from the study of mutated MCa analogues, it was learnt that MCa did possess many residues in common for the pharmacology and cell penetration. Thus, on the basis of sole amino acid substitutions, the task of functionally segregating the pharmacological and cell penetration properties of MCa was found to be more complex. So we used a new strategy for the design of a novel analogue of MCa in which all native cysteine residues engaged in disulfide bridges were replaced by isosteric 2-aminobutyric acid residues. The new analogue was analyzed for their pharmacology, cell penetration and toxicity

Available online at www.sciencedirect.com
ScienceDirect
Biochimica et Biophysica Acta 1768 (2007) 2528–2540
Biochimica et Biophysica Acta
BBA
www.elsevier.com/locate/bbamem

Critical amino acid residues of maurocalcine involved in pharmacology, lipid interaction and cell penetration

Kamel Mabrouk [a,1], Narendra Ram [b,1], Sylvie Boisseau [c], Flavie Strappazzon [c], Amel Rehaim [d], Rémy Sadoul [c], Hervé Darbon [e], Michel Ronjat [b], Michel De Waard [b,*]

[a] *Laboratoire Chimie Biologie et Radicaux Libre, Universite Aix-Marseille, Avenue Escadrille Normandie Niemen, 13397 Marseille, France*
[b] *Inserm U607, Canaux Calciques, Fonctions et Pathologies, CEA, Département Réponse et Dynamique Cellulaire, Bâtiment C3, 17 rue des Martyrs, 38054 Grenoble Cedex 09, France*
[c] *Equipe Inserm 108 / UJF, Pavillon de Neurologie, CHU de Grenoble, 38043 Grenoble, France*
[d] *Unité de Biochimie et Biologie Moléculaire, Faculté des Sciences de Tunis, Campus Universitaire, 2092 El Manar, Tunis, Tunisia*
[e] *CNRS, Laboratoire AFMB, 31 chemin Joseph-Aiguier, F-13402 Marseille cedex 20, France*

Received 24 November 2006; received in revised form 5 June 2007; accepted 7 June 2007
Available online 10 July 2007

Abstract

Maurocalcine (MCa) is a 33-amino acid residue peptide that was initially identified in the Tunisian scorpion *Scorpio maurus palmatus*. This peptide triggers interest for three main reasons. First, it helps unravelling the mechanistic basis of Ca^{2+} mobilization from the sarcoplasmic reticulum because of its sequence homology with a calcium channel domain involved in excitation–contraction coupling. Second, it shows potent pharmacological properties because of its ability to activate the ryanodine receptor. Finally, it is of technological value because of its ability to carry cell-impermeable compounds across the plasma membrane. Herein, we characterized the molecular determinants that underlie the pharmacological and cell-penetrating properties of maurocalcine. We identify several key amino acid residues of the peptide that will help the design of cell-penetrating analogues devoid of pharmacological activity and cell toxicity. Close examination of the determinants underlying cell penetration of maurocalcine reveals that basic amino acid residues are required for an interaction with negatively charged lipids of the plasma membrane. Maurocalcine analogues that penetrate better have also stronger interaction with negatively charged lipids. Conversely, less effective analogues present a diminished ability to interact with these lipids. These findings will also help the design of still more potent cell penetrating analogues of maurocalcine.

Keywords: Maurocalcine; Ryanodine receptor; Cell penetration; Cell penetrating peptide; Lipid interaction; Cell toxicity

1. Introduction

Maurocalcine (MCa) is a 33-amino acid residue peptide that originates from the venom of the chactid scorpion *Scorpio maurus palmatus* [1]. It can be produced by chemical synthesis without structural alteration [1]. The solution structure of MCa, as defined by ^{1}H-NMR, displays an inhibitor cystine knot motif [2] containing three β-strands (strand 1 from amino acid residues 9 to 11, strand 2 from 20 to 23, and strand 3 from 30 to 33). Both β-strands 2 and 3 form an antiparallel sheet. The folded/oxidized peptide contains three disulfide bridges arranged according to the pattern: Cys^3–Cys^{17}, Cys^{10}–Cys^{21} and Cys^{16}–Cys^{32} [1]. MCa now belongs to a family of scorpion toxins since it has

Abbreviations: BSA, bovine serum albumin; CGN, cerebellar granule neurons; CHO, chinese hamster ovary; CPP, cell penetrating peptide; DHE, dihydroethidium; DHP, dihydropyridine; DHPR, dihydropyridine receptor; DMEM, dulbecco's modified eagle's medium; DMSO, dimethyl sulfoxide; EDTA, ethylenediaminetetraacetic acid; FACS, fluorescence activated cell sorter; Fmoc, *N*-α-fluorenylmethyloxycarbonyl; HEK293, human embryonic kidney 293 cells; HEPES, 4-(2-hydroxyethyl)-1-piperazineethanesulfonic acid; HMP, 4-hydroxymethylphenyloxy; ^{1}H-NMR, proton nuclear magnetic resonance; HPLC, high pressure liquid chromatography; MCa, maurocalcine; MCa_b, biotinylated maurocalcine; MTT, 3-(4, 5-dimethylthiazol-2-yl)-2, 5-diphenyl-tetrazolium bromide; PC_{50}, half-maximal penetration concentration; PBS, phosphate buffered saline; PtdIns, phosphatidylinositol; RyR, ryanodine receptor; SR, sarcoplasmic reticulum; strep-Cy5 (Cy3), streptavidine-cyanine 5 (cyanine 3); TFA, trifluoroacetic acid

* Corresponding author. Tel.: +33 4 38 78 68 13; fax: +33 4 38 78 50 41.
E-mail address: mdewaard@cea.fr (M. De Waard).
[1] Both authors contributed equally to this work.

0005-2736/$ - see front matter © 2007 Elsevier B.V. All rights reserved.
doi:10.1016/j.bbamem.2007.06.030

strong sequence identity with imperatoxin A from the scorpion *Pandinus imperator* (82% identity; [3]) and with both opicalcine 1 and 2 from the scorpion *Opistophthalmus carinatus* (91 and 88% identities, respectively, [4]).

MCa and its structurally related analogues trigger interest for three main reasons. First, MCa is a powerful activator of the ryanodine receptor (RyR), thereby triggering calcium release from intracellular stores [5,6]. MCa binds with nanomolar affinity onto RyR, a calcium channel from the sarcoplasmic reticulum (SR), and generates greater channel opening probability interspersed with long-lasting openings in a mode of sub-conductance state [1]. Second, MCa has a unique sequence homology with a cytoplasmic domain (termed domain A) of the pore-forming subunit of the skeletal muscle dihydropyridine (DHP)-sensitive voltage-gated calcium channel (DHP receptor, DHPR). This homology implicates a DHPR region that is well known for its involvement in the mechanical coupling between the DHPR and RyR, a process whereby a modification in membrane potential is sensed by the DHPR, transmitted to RyR, and produces internal calcium release followed by muscle contraction. It is therefore expected that a close examination of the cellular effects of MCa on the process of excitation–contraction coupling may reveal intimate details of the mechanistic aspects linking the functioning of the DHPR to that of RyR. In that sense, a role of domain A in the termination of calcium release upon membrane repolarisation has been proposed through the use of MCa [7]. Third, MCa appears unique in the field of scorpion toxins for its ability to cross the plasma membrane. Application of MCa in the extracellular medium of cultured myocytes triggers a transient calcium release from the SR intracellular store within seconds suggesting a very fast passage across the membrane [5]. The identification of MCa's binding site on RyR and the cytoplasmic localization of this site indicate that MCa crosses the plasma membrane to reach the cytoplasm of the cell [8]. To demonstrate the ability of MCa to cross the plasma membrane, a biotinylated derivative of MCa (MCa_b) was synthesized, coupled to a fluorescent derivative of streptavidine, and the entire complex was shown to reach the cytoplasm of many cell types [9,10]. This cell penetration does not require metabolic energy but endocytosis cannot be ruled out. It is rapid, reaches saturation within minutes, is dependent on the transmembrane potential and occurs at concentrations as low as 10 nM [10]. Cell penetration of a large protein such as streptavidine indicates that MCa can be used as a vector for the cell penetration of cell impermeable compounds. This raises considerable technological interest in the peptide.

Considering its characteristics, it makes no doubt that it now belongs to the structurally unrelated family of cell-penetrating peptides (CPPs). Known CPPs include the HIV-encoded transactivator of transcription (Tat) [11], the insect transcription factor Antennapedia (Antp or penetratin) [12], the herpes virus protein VP22, a transcription regulator, the chimeric peptide transportan [13] made in part by the neuropeptide galanin and by the wasp venom peptide mastoparan, and polyarginine peptides [14]. The only structural feature that MCa has in common with these other CPPs is the presence of a large basic domain. Indeed, MCa carries a net positive charge of +8, 12 residues out of 33 are basic, and the electrostatic surface potential of MCa indicates that it presents a basic face involving the first amino terminal Gly residue and all Lys residues of the peptide. CPPs are efficient vectors for the cell penetration of oligonucleotides [15], plasmids [16], antisense peptide nucleic acids [17], peptides [18], proteins [19,20], liposomes [21] and nanoparticles [22]. As such, CPPs appear invaluable for numerous medical, technological and diagnostic applications.

Because of the potential of MCa to deliver membrane impermeable compounds without signs of cell toxicity, and considering its efficiency at low concentrations, it appears essential to define new analogues that lack the pharmacological effects of wild-type MCa but preserve or enhance its cell penetration efficiencies. Several new mutated analogues were chemically synthesized, and assessed for their effects on RyR and their penetration efficiencies, as well as compared for their toxicity on primary cultures of neurons. Finally, these analogues were also evaluated for their ability to interact with membrane lipids that are presumed to be implicated in the cell penetration of CPPs. The data obtained indicate that monosubstitution of amino acids can improve MCa's ability to penetrate within cells and further decrease the neuronal toxicity of the peptide. They confirm the contribution of the basic amino acid residues in cell penetration and provide new leads for the synthesis of peptide analogues devoid of pharmacological effects.

2. Materials and methods

2.1. Chemical synthesis of biotinylated maurocalcine and point-mutated analogues

N-α-fluorenylmethyloxycarbonyl (Fmoc) L-amino acids, 4-hydroxymethylphenyloxy (HMP) resin, and reagents used for peptide synthesis were obtained from Perkin-Elmer. *N*-α-Fmoc-L-Lys(Biotin)-OH was purchased from Neosystem group SNPE. Solvents were analytical grade products from Carlo Erba-SDS (Peypin, France). Biotinylated MCa (MCa_b) and its biotinylated point-mutated analogues were obtained by the solid-phase method [23] using an automated peptide synthesizer (Model 433A, Applied Biosystems Inc.). Sixteen different analogues were designed such that Ala replaced a native amino acid of MCa (Fig. 1). Peptide chains were assembled stepwise on 0.25 mEq of hydroxymethylphenyloxy resin (1% cross-linked; 0.77 mEq of amino group/g) using 1 mmol of *N*-α-Fmoc amino acid derivatives. The side chain-protecting groups were: trityl for Cys and Asn; *tert*-bytyl for Ser, Thr, Glu, and Asp; pentamethylchroman for Arg, and *tert*-butyloxycarbonyl or Biotin for Lys. *N*-α-amino groups were deprotected by treatment with 18% and 20% (v/v) piperidine/N-methylpyrrolidone for 3 and 8 min, respectively. The Fmoc-amino acid derivatives were coupled (20 min) as their hydroxybenzotriazole active esters in N-methylpyrrolidone (4 fold excess). After peptide chain assembly, the peptide resin was treated between 2 and 3 h at room temperature, in constant shaking, with a mixture of trifluoroacetic acid (TFA)/H_2O/thioanisol/ethanedithiol (88/5/5/2, v/v) in the presence of crystalline phenol (2.25 g). The peptide mixture was then filtered, and the filtrate was precipitated by adding cold *t*-butylmethyl ether. The crude peptide was pelleted by centrifugation (3000×*g*; 10 min) and the supernatant was discarded. The reduced peptide was then dissolved in 200 mM Tris–HCl buffer, pH 8.3, at a final concentration of 2.5 mM and stirred under air to allow oxidation/folding (between 50 and 72 h, room temperature). The target products, MCa_b and its analogues, were purified to homogeneity, first by reversed-phase high pressure liquid chromatography, HPLC, (Perkin-Elmer, C_{18} Aquapore ODS 20 μm, 250 × 10 mm) by means of a 60-min linear gradient of 0.08% (v/v) TFA/0-–30% acetonitrile in 0.1% (v/v) TFA/H_2O at a flow rate of 6 ml/min (λ = 230 nm). The homogeneity and identity of the peptides were assessed by: (i) analytical C_{18} reversed-phase HPLC (Merck, C_{18} Li-chrospher 5 μm, 4 × 200 mm) using a 60-min linear gradient of 0.08% (v/v) TFA/0–60% acetonitrile in 0.1% (v/v) TFA/H_2O at a flow rate of 1 ml/min;

		Net global charge
MCa	GDCLPHLKLCKENKDCCSKKCKRRGTNIEKRCR	+8
MCa_b	K(biot)-GDCLPHLKLCKENKDCCSKKCKRRGTNIEKRCR	+8
MCa_b D2A	K(biot)-G**A**CLPHLKLCKENKDCCSKKCKRRGTNIEKRCR	+9
MCa_b L4A	K(biot)-GDC**A**PHLKLCKENKDCCSKKCKRRGTNIEKRCR	+8
MCa_b P5A	K(biot)-GDCL**A**HLKLCKENKDCCSKKCKRRGTNIEKRCR	+8
MCa_b H6A	K(biot)-GDCLP**A**LKLCKENKDCCSKKCKRRGTNIEKRCR	+8
MCa_b L7A	K(biot)-GDCLPH**A**KLCKENKDCCSKKCKRRGTNIEKRCR	+8
MCa_b K8A	K(biot)-GDCLPHL**A**LCKENKDCCSKKCKRRGTNIEKRCR	+7
MCa_b L9A	K(biot)-GDCLPHLK**A**CKENKDCCSKKCKRRGTNIEKRCR	+8
MCa_b E12A	K(biot)-GDCLPHLKLCK**A**NKDCCSKKCKRRGTNIEKRCR	+9
MCa_b N13A	K(biot)-GDCLPHLKLCKE**A**KDCCSKKCKRRGTNIEKRCR	+8
MCa_b D15A	K(biot)-GDCLPHLKLCKENK**A**CCSKKCKRRGTNIEKRCR	+9
MCa_b K19A	K(biot)-GDCLPHLKLCKENKDCCS**A**KCKRRGTNIEKRCR	+7
MCa_b K20A	K(biot)-GDCLPHLKLCKENKDCCSK**A**CKRRGTNIEKRCR	+7
MCa_b K22A	K(biot)-GDCLPHLKLCKENKDCCSKKC**A**RRGTNIEKRCR	+7
MCa R23A	GDCLPHLKLCKENKDCCSKKCK**A**RGTNIEKRCR	+7
MCa_b R24A	K(biot)-GDCLPHLKLCKENKDCCSKKCKR**A**GTNIEKRCR	+7
MCa T26A	GDCLPHLKLCKENKDCCSKKCKRRG**A**NIEKRCR	+8

Fig. 1. Amino acid sequences of MCa and of its biotinylated analogues. Amino acid residues are described by single letter code. K_b=biotinylated version of lysine residue. The net global charge of the molecule is provided for each MCa analogue.

(ii) amino acid analysis after acidolysis (6N HCl / 2% (w/v) phenol, 20 h, 118 °C, N_2 atmosphere); and (iii) mass determination by matrix assisted laser desorption ionization–time of flight mass spectrometry.

2.2. Conformational analyses of MCa, MCa E12A, MCa K20A and MCa R24A by circular dichroism

Circular dichroism (CD) spectra were recorded on a Jasco 810 dichrograph using 1-mm-thick quartz cells. Spectra were recorded between 180 and 260 nm at 0.2 nm/min and were averaged from three independent acquisitions. The spectra were corrected for water signal and smoothed by using a third-order least squares polynomial fit.

2.3. Preparation of heavy SR vesicles

Heavy SR vesicles were prepared following the method of Kim et al. [24] modified as described previously [25]. Protein concentration was measured by the Biuret method.

2.4. [^{3}H]-ryanodine binding assay

Heavy SR vesicles (1 mg/ml) were incubated at 37 °C for 3 h in an assay buffer composed of 5 nM [^{3}H]-ryanodine, 150 mM NaCl, 2 mM EGTA, 2 mM $CaCl_2$ (pCa=5), and 20 mM HEPES, pH 7.4. Wild-type or mutant MCa_b was added to the assay buffer just prior the addition of heavy SR vesicles. [^{3}H]-ryanodine bound to heavy SR vesicles was measured by filtration through Whatmann GF/B glass filters followed by three washes with 5 ml of ice-cold washing buffer composed of 150 mM NaCl, 20 mM HEPES, pH 7.4. Filters were then soaked overnight in 10 ml scintillation cocktail (Cybscint, ICN) and bound radioactivity determined by scintillation spectrometry. Non-specific binding was measured in the presence of 20 μM cold ryanodine. Each experiment was performed in triplicate and repeated at least two times. All data are presented as mean±S.D.

2.5. Cell culture

Chinese hamster ovary (CHO) cell line (from ATCC) were maintained at 37 °C in 5% CO_2 in F-12K nutrient medium (InVitrogen) supplemented with 10% (v/v) heat-inactivated foetal bovine serum (InVitrogen) and 10,000 units/ml streptomycine and penicillin (InVitrogen).

2.6. Primary culture of cerebellar granule neurons

Media used for the culture of cerebellar granule neurons (CGN) was based on Dulbecco's modified Eagle's medium (DMEM, Invitrogen) containing 10 unit/ml penicillin, 10 μg/ml streptomycin, 2 mM L-glutamine, and 10 mM HEPES (K5 medium). KCl was added to a final concentration of 25 mM (K25 medium) and supplemented with 10% fetal bovine serum (K25+S medium). Primary cultures of CGN were prepared from 6-day-old S/IOPS NMRI mice (Charles River Laboratories), as described previously [26,27] with some modifications. The cerebella were removed, cleared of their meninges, and cut into 1-mm pieces. They were then incubated at 37 °C for 10 min in 0.25% trypsin-EDTA (Invitrogen) in DMEM. An equal volume of K25+S medium and 3000 units/ml DNase I (Sigma) were added before dissociation by triturating using flame-polished Pasteur pipettes. Next, an equal volume of DMEM containing trypsin inhibitor (Sigma) and 300 units/ml DNase I were added to the cells. Dissociated cells were centrifuged for 5 min at 500×*g*. The pellet was resuspended in fresh K25+S medium and cells were plated onto poly-D-lysine (10 μg/ml, Sigma) precoated 96-well plates at a density of 8×10^4 cells/well. The cerebellar granule neurons were grown in K25+S medium in a humidified incubator with 5% CO_2 / 95% air at 37°C. Cytosine-β-D-arabinoside (10 μM, Sigma) was added after 1 day *in vitro* to prevent the growth of non-neuronal cells.

2.7. MTT assay

Primary cultures of CGN were seeded into 96 well micro plates at a density of approximately 8×10^4 cells/well. After 4 days of culture, the cells were incubated for 24 h at 37 °C with MCa_b or its analogues at a concentration of 1 or 10 μM. Control wells containing cell culture medium alone or with cells, both without peptide addition, were included in each experiment. The cells were then incubated with 3-(4, 5-dimethylthiazol-2-yl)-2, 5-diphenyl-tetrazolium bromide (MTT) for 30 min. Conversion of MTT into purple colored MTT formazan by the living cells indicates the extent of cell viability. The crystals were dissolved with dimethyl sulfoxide (DMSO) and the optical density was measured at 540 nm using a microplate reader (Biotek ELx-800, Mandel Scientific Inc.) for quantification of cell viability. All assays were run in triplicates.

2.8. Membrane integrity LDH assay

A lactate dehydrogenase (LDH) assay was used to probe membrane integrity disturbance by MCa, MCa E12A and MCa K20A according to the protocol

provided by the manufacturer (CytoTox-ONE™, Promega). Briefly, CHO cells were incubated with 10 μM peptide for 24 h, then 30 min at 22 °C, a volume of CytoTox-ONE™ reagent was added, mixed and incubated at 22 °C for 10 min, 50 μl of STOP solution added, and the fluorescence was measured (excitation wavelength of 560 nm and emission at 590 nm). Control experiments were also performed to measure background LDH release in the absence of the peptide, and also maximal release of LDH after total cell lysis. Percentage of cell toxicity is measured as follows: 100 × (Experimental with peptide − cultured media background) / (maximal LDH release − cultured media background).

2.9. Formation of MCa_b (wild-type or mutant)/streptavidin–cyanine complex

Soluble streptavidine–cyanine 5 or streptavidine–cyanine 3 (Strep-Cy5 or Strep-Cy3, Amersham Biosciences) was mixed with four molar equivalents of wild-type or mutant MCa_b 2 h at 37 °C in the dark in PBS (phosphate-buffered saline) (in mM): NaCl 136, Na_2HPO_4 4.3, KH_2PO_4 1.47, KCl 2.6, $CaCl_2$ 1, $MgCl_2$ 0.5, pH 7.2.

2.10. Flow cytometry

Wild-type or mutant MCa_b–Strep-Cy5/Cy3 complexes were incubated for 2 h with live cells to allow cell penetration to occur. The cells were then washed twice with PBS to remove the excess extracellular complexes. Next the cells were treated with 1 mg/ml trypsin (InVitrogen) for 10 min at 37 °C to remove remaining membrane-associated extracellular cell surface-bound complexes. After trypsin incubation, the cell suspension was centrifuged at 500×*g* and suspended in PBS. Flow cytometry analyses were performed with live cells using a Becton Dickinson FACSCalibur flow cytometer (BD Biosciences). Data were obtained and analyzed using CellQuest software (BD Biosciences). Live cells were gated by forward/side scattering from a total of 10,000 events.

2.11. Confocal microscopy and immunocytochemistry

For analysis of the subcellular localization of wild-type or mutant MCa_b–Strep-Cy3/Cy5 complexes in living cells, cells were incubated with the complexes for 2 h, and then washed with DMEM alone. Immediately after washing, the nucleus was stained with 1 μg/ml dihydroethidium (DHE, Molecular probes, USA) for 20 min, and then washed again with DMEM. DHE shows a blue fluorescence (absorption/emission: 355/420 nm) in the cytoplasm of cells until oxidization to form ethidium which becomes red fluorescent (absorption/emission: 518/605 nm) upon DNA intercalation. Only the red fluorescence was measured in the nucleus. After this step, the plasma membrane was stained with 5 μg/ml FITC-conjugated Concanavalin A (Molecular Probes) for 3 min. Cells were washed once more, but with PBS. Live cells were then immediately analyzed by confocal laser scanning microscopy using a Leica TCS-SP2 operating system. Alexa-488 (FITC, 488 nm) and Cy3 (543 nm) or Cy5 (642 nm) were sequentially excited and emission fluorescence were collected in z-confocal planes of 10–15 nm steps. Images were merged in Adobe Photoshop 7.0.

2.12. Interaction of MCa_b and its mutants with different lipids

Strips of nitrocellulose membranes containing spots with different phospholipids and sphingolipids were obtained from Molecular probes. These membranes were first blocked with TBS-T (150 mM NaCl, 10 mM Tris–HCl, pH 8.0, 0.1% (v/v) Tween 20) supplemented with 0.1% free bovine serum albumin (BSA) for about 1 h at room temperature. Later, these membranes were incubated with 100 nM wild-type or mutant MCa_b along with TBS-T and 0.1% free BSA for 2 h at room temperature. Incubation with 100 nM biotin alone was used as a negative control condition. The membranes were then washed a first time with TBS-T 0.1% free BSA using gentle agitation for 10 min. Binding of wild-type or mutant MCa_b onto the lipid strips was detected by incubating 30 min the lipid strips with 1 μg/ml ready to use streptavidine horse radish peroxidase (Vector labs, SA-5704). The membranes were washed a second time with TBS-T 0.1% free BSA. Interaction was detected by incubating the membranes with horseradish peroxidase substrate (Western Lightning, Perkin-Elmer Life Science) for 1 min in each case followed by exposure to Biomax film (Kodak).

3. Results

3.1. Synthesis of MCa analogues

Fig. 1 illustrates the primary structure of the various analogues of MCa that were chemically synthesized. Most of the analogues were biotinylated at their amino-terminus to favor their coupling to streptavidine. All substitutions were made by alanine residues. The global net charge of each peptide is also indicated. Biotinylation does not alter the global net charge of MCa. Some of the mutated analogues of MCa were reported previously, but in their non-biotinylated version [5].

3.2. Effects of MCa analogues on [^{3}H]-ryanodine binding to RyR1

The purpose of this study is to compare the pharmacological efficacy of various MCa analogues to their efficiency of cell penetration. The ultimate aim is to help the design of new point mutated analogues of MCa that can serve as good cell penetration carriers without displaying an adverse pharmacological effect once penetrated inside cells. The pharmacological potential of MCa analogues can be assessed by their efficacy in stimulating [^{3}H]-ryanodine binding onto RyR1 oligomers from SR vesicles, an effect that appears linked to the promotion of opening modes of the channel. Since the analogues synthesized were biotinylated for the purpose of forming a complex with fluorescent derivatives of streptavidine, we first compared the efficacy of [^{3}H]-ryanodine binding stimulation between MCa and MCa_b (Table 1). Adding a biotin group to the N-terminus

Table 1
Effect of MCa_b and its analogues on the parameters of [^{3}H]-ryanodine binding onto SR vesicles

MCa analogue	EC_{50} (nM)	Binding stimulation (*x*-fold)
MCa	25.2±2.1	16.7
MCa_b	35.2±7.5	17.9
MCa_b D2A	10.3±0.7	17.6
MCa_b L4A	28.8±6.1	15.0
MCa_b P5A	9.0±1.2	17.5
MCa_b H6A	29.4±3.2	16.6
MCa_b L7A	74.9±3.6	7.1
MCa_b K8A	104.3±13.3	10.1
MCa_b L9A	17.3±1.2	18.2
MCa_b E12A	7.3±0.4	15.7
MCa_b N13A	13.8±1.4	14.6
MCa_b D15A	9.5±1.1	14.1
MCa_b K19A	71.0±8.1	12.2
MCa_b K20A	114.5±14.3	9.4
MCa_b K22A	162.6±18.7	5.1
MCa R23A	302.5±62.1	4.5
MCa_b R24A	>1000	1.1
MCa T26A	121.1±33.0	13.7

The EC_{50} values and stimulation factors are obtained from the fit of the data shown in Fig. 2.

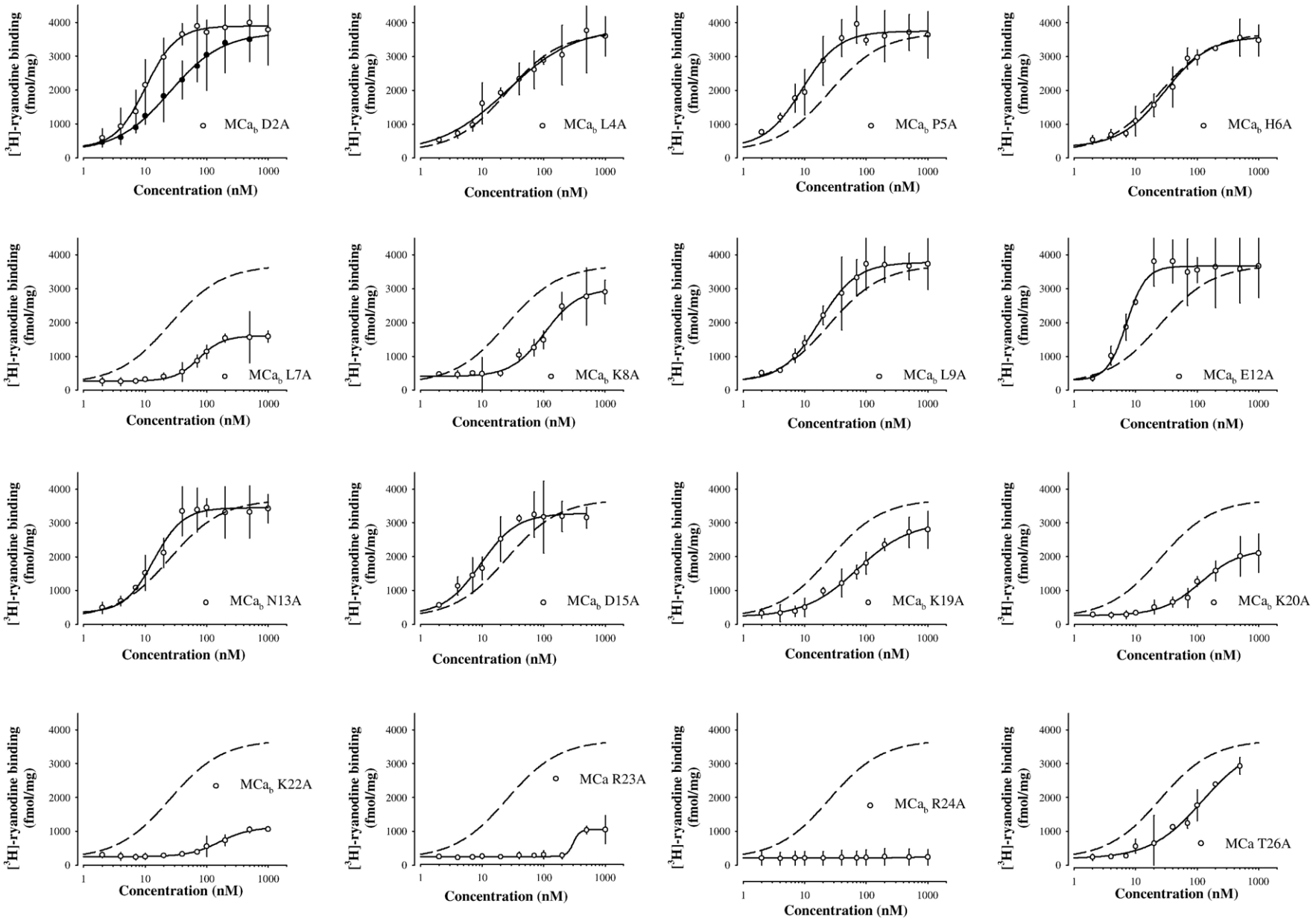

Fig. 2. Concentration-dependent effect of MCa analogues on [^{3}H]-ryanodine binding to heavy SR vesicles. [^{3}H]-ryanodine binding was measured at pCa 5 (free Ca^{2+} 10 μM) in the presence of 5 nM [^{3}H]-ryanodine for 3 h at 37 °C. Non specific binding was less than 5% of the total binding and was independent of the concentration of each MCa analogue. Data were fitted with a logistic function of the type $y=y_0+(a/(1+(x/EC_{50})^b))$ where y_0 is the basal [^{3}H]-ryanodine binding in the absence of MCa or its analogues, a the maximum achievable binding, b the slope coefficient and EC_{50} the concentration of half-binding stimulation. Experimental data for the effect of MCa is shown once (top left binding curve, filled circles) and the fit of these data shown each time as dashed line for the purpose of comparison with each MCa analogue. EC_{50} values and binding stimulation factors are provided in Table 1. Data are triplicates. Representative cases of $n=3$ experiments.

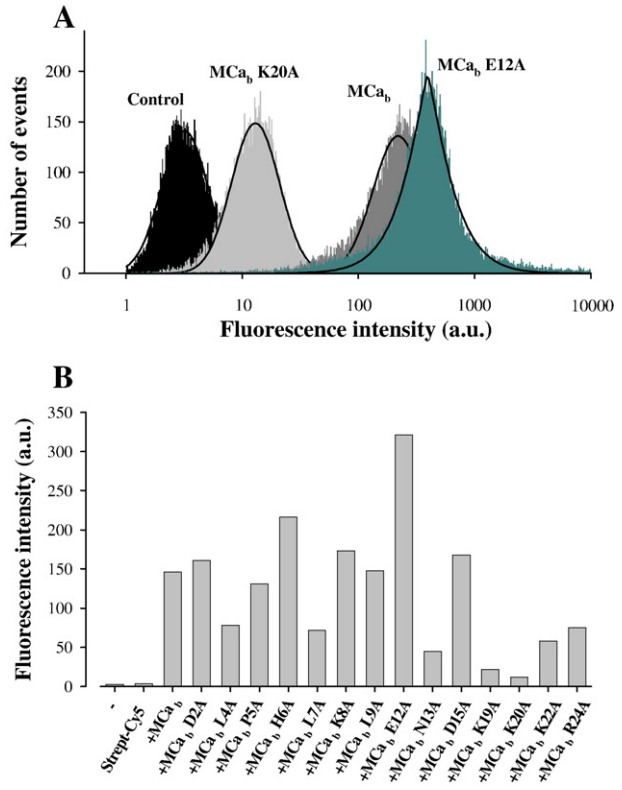

Fig. 3. Cell penetration of wild-type and mutated MCa$_b$ in complex with streptavidine–Cy5 in CHO cells as assessed quantitatively by FACS. The concentration used for all the analogues is 4 μM combined with 1 μM streptavidine–Cy5. Cells were incubated 2 h with the complex before being washed and treated for 10 min with 1 mg/ml trypsin. (A) Comparison of FACS data on CHO cells for streptavidine–Cy5 alone (control), for MCa$_b$ K20A, the least penetrating mutant, for MCa$_b$, and for MCa$_b$ E12A, the most penetrating analogue. (B) Comparison of mean fluorescence intensity for the cell penetration of all MCa$_b$ analogues in CHO cells. The dash represents the mean fluorescence of cells alone. All data were performed the same day with the same batch of cells. Representative case of $n=3$ experiments.

of MCa did not alter significantly the EC_{50} value for [^{3}H]-ryanodine binding stimulation or the stimulation factor (between 16- and 18-fold). The properties of all the point mutated analogues of MCa$_b$ (14 of the 16 mutants) should thus also be comparable to similar point mutated analogues of MCa (2 of the 16 mutants). Next, all the mutants were compared using a similar batch of SR preparation. We noticed that basal binding of [^{3}H]-ryanodine binding (in the absence of any analogues) varies greatly with the SR batch although saturation appears more or less similar. Hence, the stimulation efficacy of the binding (ratio between stimulated [^{3}H]-ryanodine binding and basal [^{3}H]-ryanodine binding) also varies with the SR batch (data not shown). Fig. 2 thus compares the effects of various point-mutated analogues of MCa$_b$ onto the [^{3}H]-ryanodine binding to SR vesicles from the same batch preparation. The main results are summarized in Table 1. Six analogues have greater affinity for RyR1 than MCa$_b$: MCa$_b$ D2A, MCa$_b$ P5A, MCa$_b$ L9A, MCa$_b$ E12A, MCa$_b$ N13A and MCa$_b$ D15A. It is of interest that a greater affinity for RyR1 can be triggered by mutating negatively charged amino acid residues that increase the net positive change of MCa from +8 to +9 (Fig. 1). Of note, none of these mutants affected the binding stimulation factor suggesting that these analogues behave similarly than MCa and MCa$_b$ at saturating concentrations. Alanine substitution of many of the positively charged amino acid residues of MCa that belong to the basic face of the molecule [10] reduce the affinity of MCa for RyR1. These residues comprise Lys^8, Lys^{19}, Lys^{20}, and Lys^{22}, which confirms previous findings with similar non-biotinylated MCa analogues [5]. Mutation of two other positively charged residues, Arg^{23} and Arg^{24}, induce similar effects. Besides these six analogues, MCa$_b$ L7A and MCa$_b$ T26A also display a significant reduction in the affinity of MCa$_b$ for RyR1. All MCa$_b$ analogues that were shown to have reduced affinity for RyR1 also present reduced potencies of [^{3}H]-ryanodine binding stimulation (Table 1). A form of correlation appears to occur between the reduction in affinity and stimulation efficacy, with the notable exception of MCa$_b$ T26A that kept a rather good stimulation efficacy despite a strong reduction in affinity. Finally, among the sixteen mutants that were tested, MCa$_b$ L4A and MCa$_b$ H6A did neither change the affinity nor the stimulation efficacy of MCa$_b$.

In conclusion, for the purpose of selecting mutated analogues of MCa defective in pharmacological effects, mutations at amino acid positions 7, 23, 24 and 26 appear particularly interesting since they do not contribute to the presentation of the basic face of MCa that is presumably required for cell penetration of MCa [10].

3.3. Effects of point mutations of MCa$_b$ on its cell penetration efficiency

To perform a quantitative comparison of the cell penetration efficacy of the various mutated analogues of MCa$_b$, FACS

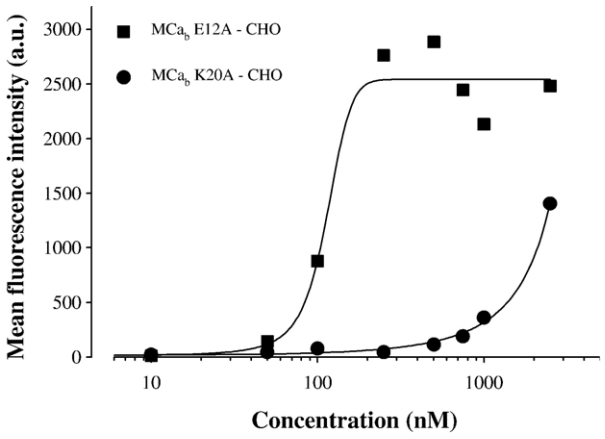

Fig. 4. Mean cell fluorescence intensity as a function of concentration of cell penetrating complexes. The indicated concentrations are for streptavidine–Cy5 (from 10 nM to 2.5 μM). Streptavidine concentrations higher than 2.5 μM are toxic to cells when allowed to penetrate and cannot be tested. MCa$_b$ K20A and MCa$_b$ E12A concentrations are fourfold greater than streptavidine–Cy5 concentrations (from 40 nM to 10 μM). The data for MCa$_b$ E12A could be fit by a sigmoid function of the type $y=a/(1+\exp(-(x-PC_{50})/b))$ where $a=2541\pm108$ a.u., the maximal fluorescence intensity, $PC_{50}=113\pm16$ nM, the half-maximal effective penetrating concentration, and $b=20.9\pm17.9$. Experiments were repeated three times.

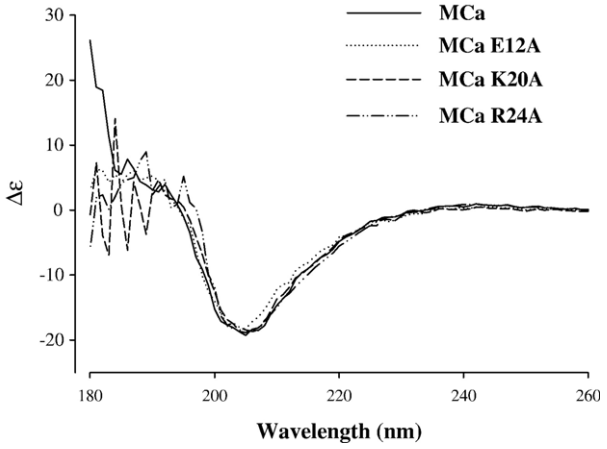

Fig. 5. Conformational analysis of maurocalcin analogues by circular dichroism. Far-UV CD spectra of MCa and three of its analogues at 50 μM in pure water recorded at 20 °C. Each spectrum is the mean of three independent acquisitions.

analyses were performed with living CHO cells (Fig. 3). Cells were incubated for 2 h with 1 μM of wild-type or mutant MCa_b/streptavidine–Cy5 complexes (4 μM of wild-type or mutant MCa_b for 1 μM of streptavidine–Cy5) before washing, 10 min treatment with 1 mg/ml of trypsin, and FACS analysis. Representative histograms indicating the intensity of cell fluorescence for wild-type and two mutants MCa_b/streptavidine–Cy5 complexes are shown in Fig. 3A. MCa_b K20A induced a mean cell penetration of streptavidine that was 12.5-fold less pronounced than wild-type MCa_b, whereas MCa_b E12A increased its cell penetration by a factor of 2.2-fold. A quantitative comparison of the cell penetration of the various MCa_b analogues was performed and is shown in Fig. 3B. Not all point mutated analogues of MCa_b behave similarly in terms of cell penetration, at least at the concentration tested (1 μM) and for the duration examined (2 h). Besides MCa_b E12A, two other mutants provide a better cell penetration than MCa_b itself (MCa_b H6A and MCa_b K8A). In contrast, two other mutants almost completely inhibit the cell penetration (MCa_b K19A and MCa_b K20A). Mild reduction in cell penetration efficacy is observed for MCa_b L4A, N13A, K22A and R24A (between 1.9- and 3.2-fold). These data thus indicate that the cell penetration properties of MCa_b can be greatly modulated by selective point mutation of it amino acid sequence. Improved analogues, as well as less potent derivatives, can be produced using simple amino acid substitutions.

To determine the reasons that may underlie these differences in cell penetration efficacies between the various analogues, a dose–response curve on CHO cells was performed for the most and the least penetrating analogues, MCa_b E12A and MCa_b K20A, respectively (Fig. 4). As shown, the two mutants differed in their half-effective concentration for cell penetration efficacy over a 2-h incubation period. MCa_b E12A penetrates with a half-effective concentration of $PC_{50} = 113 \pm 16$ nM. In contrast, MCa_b K20A penetrates with an estimated half-effective concentration of $PC_{50} = 1300–1400$ nM. For the MCa_b K20A mutant, concentrations higher than 2.5 μM could not be tested because of cell toxicity of streptavidine. In spite of this toxicity, it was observed that, at saturating concentrations, the same maximal amount of streptavidine–Cy5 could be carried into the cell as with MCa_b E12A. Therefore, it is possible that the differences in penetration efficacies, observed between the various mutated analogues in Fig. 3C, is more linked to differences in "cell affinity" for one or several membrane components than to an impairment of the mechanism of cell penetration. The observation that the cell penetration of MCa_b E12A/streptavidine–Cy5 can saturate is an indication that the process is halted once a form of concentration equilibrium is reached or that the plasma membrane constituents required for cell penetration of the complexes are present in finite amounts.

Finally, we also determined whether differences in pharmacological effects and cell penetration among various MCa analogues could be linked to adverse structural alterations introduced by the point mutations. This was performed by circular dichroism analyses of wild-type MCa, MCa E12A, MCa K20A and MCa R24A since these analogues represented some extreme cases (Fig. 5). As shown, the CD spectra of all these peptides are fully superimposed. One can thus deduce that the three analogues possess the same conformation as native MCa.

3.4. Altered cell penetration efficacies of the MCa_b analogues is not associated with differences in cell localization

To check the cell distribution of MCa_b/streptavidine–Cy5 complexes, it is recommended to work on living cells since cell fixation has been reported to alter the cell distribution of various CPPs [28]. As shown in Fig. 6, MCa_b/streptavidine–Cy5 complexes are present as punctuate dots in the cytoplasm of living CHO cells (2 h of incubation with the complex, wash, staining and immediate observation by confocal microscopy). The plasma membrane is labeled with concanavaline A, whereas the nucleus is stained with DHE. The distribution of the MCa_b/streptavidine–Cy5 complex is not different than the one observed in fixed HEK293 cells [10], suggesting that, contrary to other CPPs, cell fixation does not alter the distribution of this particular CPP. With mutated MCa_b analogues that penetrate better or less than wild-type MCa_b (MCa_b E12A and MCa_b K20A), a similar subcellular distribution of the complex is observed suggesting that the mechanism of cell penetration is not altered by point mutation of MCa_b. Corroborating the FACS experiments, a significant reduction of complex entry is observed with the MCa_b K20A

Fig. 6. Confocal immunofluorescence images of living CHO cells incubated for 2 h with 1 μM streptavidine–Cy5 in complex with 4 μM MCa_b, MCa_b E12A or MCa_b K20A. Streptavidine–Cy5 appears in blue, the nucleus in red and the plasma membrane in green. Note the lack of differences in cell distribution of streptavidine–Cy5 with the MCa_b analogues but the obvious differences in cell penetration efficiencies. Images are from a single confocal plane. Control images were also included for cells incubated with MCa_b alone to show that the blue fluorescence observed is only due to the presence of streptavidine and is not related to the ability of DHE to fluoresce in blue in the cytoplasm (top panel).

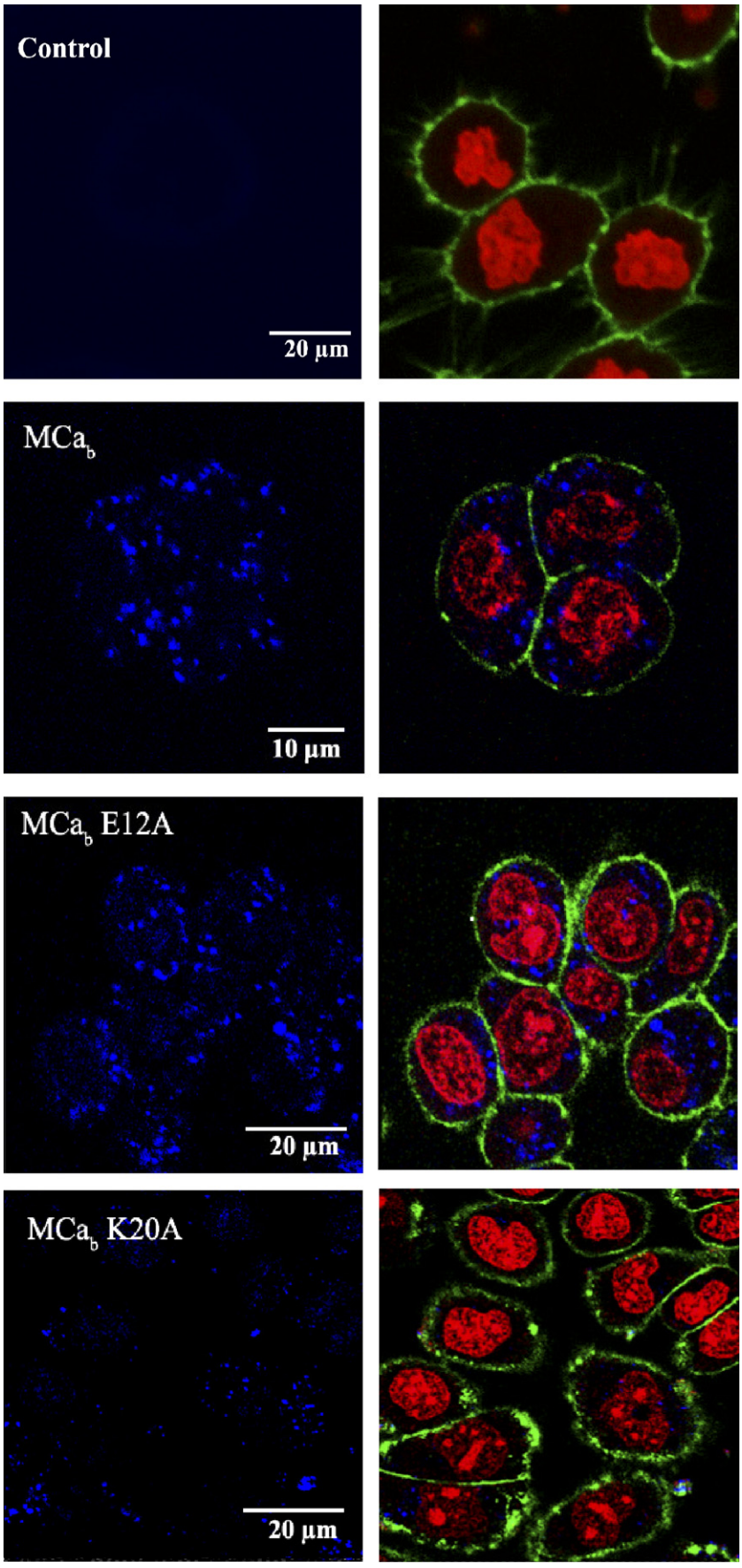
Control
20 µm
MCa$_b$
10 µm
MCa$_b$ E12A
20 µm
MCa$_b$ K20A
20 µm

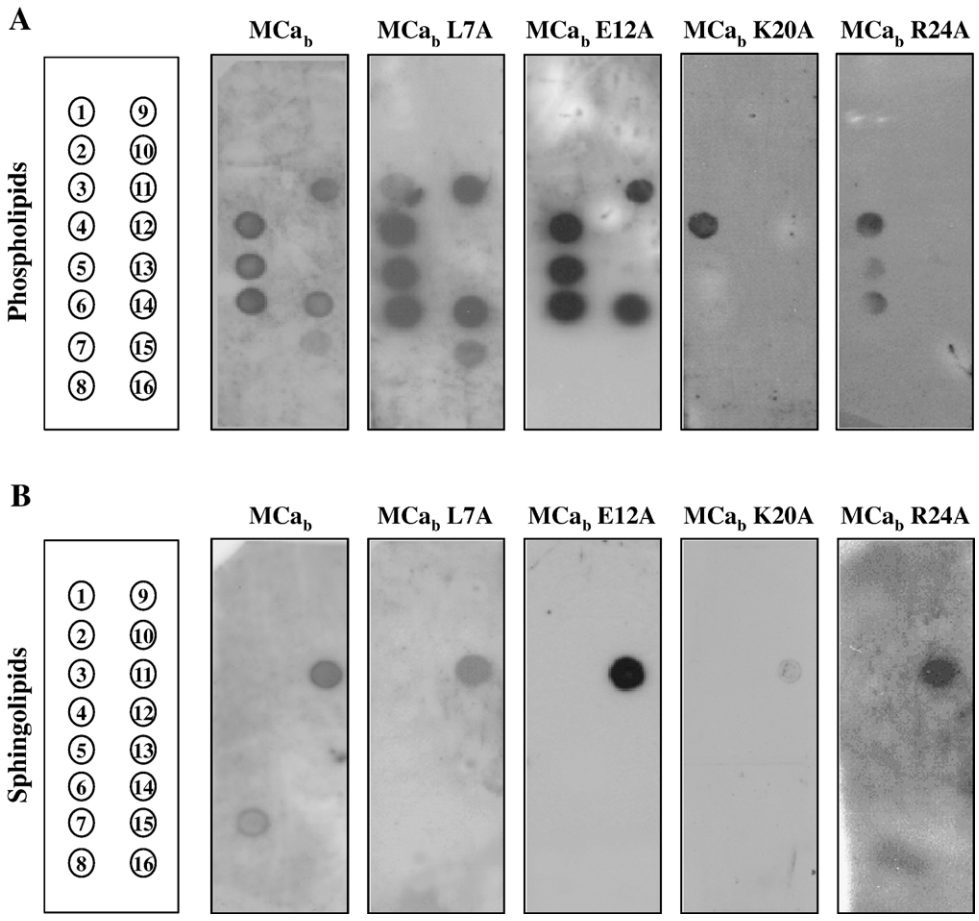

Fig. 7. Interaction of MCa_b or mutated analogues with membrane lipids. The MCa_b analogues were used at a concentration of 100 nM and incubated for 2 h with the lipid strips. Each dot possesses 100 pmol of lipid immobilized on the strip. Representative examples are shown for MCa_b, MCa_b L7A, MCa_b E12A, MCa_b K20A and MCa_b R24A. (A) Interaction with various phospholipids. The lipids are identified by their numbered positions on the strip (left panel). Numbers refer to: lysophosphatidic acid (1), lysophosphatidylcholine (2), phosphatidylinositol (PtdIns) (3), PtdIns(3)P (4), PtdIns(4)P (5), PtdIns(5)P (6), phosphatidylethanolamine (7), phosphatidylcholine (8), sphingosine 1-phosphate (9), PtdIns(3,4)P_2 (10), PtdIns(3,5)P_2 (11), PtdIns(4,5)P_2 (12), PtdIns(3,4,5)P3 (13), phosphatidic acid (14), phosphatidylserine (15), and no lipids (16). (B) Interactions of MCa_b and mutated analogues with sphingolipids. Numbers refer to: sphingosine (1), sphingosine 1-phosphate (2), phytosphingosine (3), ceramide (4), sphingomyelin (5), sphingosylphosphophocholine (6), lysophosphatidic acid (7), myriocin (8), monosialoganglioside (9), disialoganglioside (10), sulfatide (11), sphingosylgalactoside (12), cholesterol (13), lysophosphatidyl choline (14), phosphatidylcholine (15), and blank (16).

mutant, whereas a clear increase is observed with the MCa_b E12A mutant. Similar observations were made in HEK293 cells, 3T3 cells, hippocampal and DRG neurons (unpublished observations).

3.5. Differential interaction of MCa_b and its analogues with negatively charged lipids

For a direct membrane translocation of MCa into cells, a process whereby the peptide would flip from the outer face of the plasma membrane to the inner face, then released free into the cytoplasm, the peptide should interact with various lipids of the membrane, preferably negatively charged ones. These interactions were challenged by incubating 100 nM of MCa_b with lipid strips from Molecular Probes. The immobilized peptide was then revealed with streptavidine–horse radish peroxidase (HRP). MCa_b was found to strongly interact with phosphatidylinositol (PtdIns)(3)P, PtdIns(4)P, PtdIns(5)P, phosphatidic acid and sulfatide, and more weakly with lysophosphatidic acid, PtdIns(3,5)P_2 and phosphatidylserine (Fig. 7, Table 2). These are all negatively charged lipids. In contrast, at 100 nM, it does not interact with lysophosphatidylcholine, phosphatidylcholine, sphingosine, sphingosine 1-phosphate, phytosphingosine, ceramide, sphingomyelin, sphingosylphosphocholine, myriocin, monosialoganglioside, disialoganglioside, sphingosylgalactoside, cholesterol, lysophosphatidyl choline, or phosphatidylcholine (Fig. 7). As control experiment, 100 nM biotin was probed alone and no interaction was found with any of the lipids (data not shown). In comparison with wild-type MCa_b and of all the MCa_b mutants tested, two mutants displayed a new lipid interaction with PtdIns (MCa_b L4A and MCa_b L7A) and four mutants with PtdIns(4,5)P_2 (MCa_b D2A, MCa_b L4A, MCa_b H6A and MCa_b N13A). These new interactions were mostly weak, except for MCa_b L4A with PtdIns(4,5)P_2. In contrast, many of the weak lipid interactions of MCa_b were lost as a result of various mutations. This is the case for the interactions with lysophosphatidic acid, PtdIns(3,5)P_2 and phosphatidylserine, although it should be mentioned that

Table 2
Strength of lipid interactions for MCa_b and its analogues

MCa_b and analogues	Lysophosphatidic acid	Phosphatidylinositol (Ptdlns)	Ptdlns (3)P	Ptdlns (4)P	Ptdlns (5)P	Ptdlns $(3,5)P_2$	Ptdlns $(4,5)P_2$	Phosphatidic acid	Phosphatidylserine	Sulfatide
MCa_b	+		++	++	++	+		++	+	++
MCa_b D2A	+		++	++	++	++	+	++		++
MCa_b L4A		+	++	++	++		++	++	+	++
MCa_b P5A			++	+	++			++	+	++
MCa_b H6A	+		++	++	++		+	++	+	++
MCa_b L7A		+	++	++	++	++		++	+	++
MCa_b K8A	+		+	+	++			+	+	++
MCa_b L9A			+++	+++	+++	++		++		+++
MCa_b E12A			+++	+++	+++	++		+++		+++
MCa_b N13A			++	++	++		+	++	+	++
MCa_b D15A			++	++	++					++
MCa_b K19A			++		++					+
MCa_b K20A			++							+
MCa_b K22A			+	+	+	+		+		+
MCa_b R24A			++	+	+					++

Experimental conditions as described in the legend of Fig. 6.
■ (+++) very strong interaction ● (++) strong interaction ■ (+) weak interaction.

in the case of PtdIns(3,5)P_2 the interaction could be reinforced. Although it is difficult to correlate specific lipid interactions with the strength of cell penetration, some basic conclusions can be reached. The MCa_b E12A mutant displayed the strongest lipid interactions of all mutants, which is probably at the basis of its better cell penetration properties. In contrast, both MCa_b

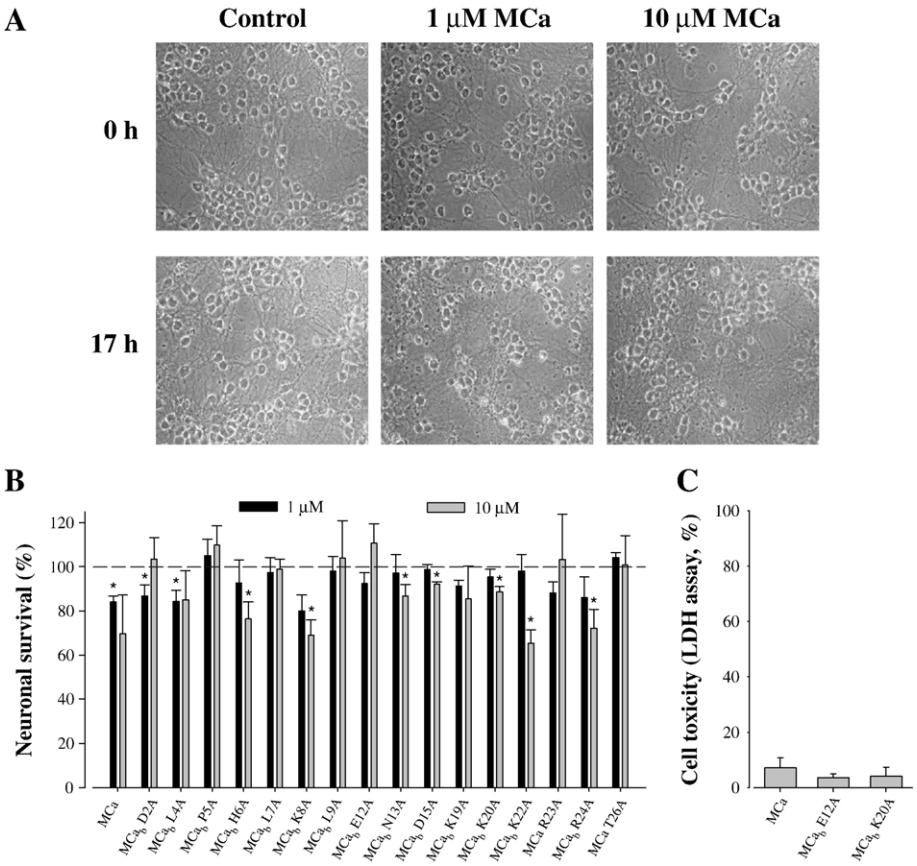

Fig. 8. Neuronal toxicity of MCa and mutated analogues. Peptides were tested alone without coupling to streptavidine. (A) Transmitted light images (differential interference contrast) illustrating cerebellar granule cells in primary culture before (0 h) and after (17 h) incubation with 1 or 10 μM MCa. (B) Neuronal survival after a 17h incubation period with either 1 or 10 μM MCa or one of its mutated biotinylated analogue as assessed by the MTT test. MCa and MCa_b produced similar results. These experiments were repeated three times, data shown as triplicates. Significance is provided as a deviation of three times the SD value from 100% (denoted as asterisks). (C) Cell toxicity effect of 10 μM MCa, MCa E12A or MCa K20A incubated 24 h with CHO cells as measured by LDH release.

K19A and MCa_b K20A, that had the weakest cell penetration properties, also displayed the poorest repertoire of lipid interaction and/or the weakest interactions. Further detailed lipid pharmacology combined with FACS analysis will be required to determine the identity of the lipid(s) that are essential for an efficient cell penetration of MCa.

3.6. Cell toxicity of MCa_b and mutated analogues

MCa was shown to be non-toxic to HEK293 cells for incubation periods of 24 h and at concentrations up to 5 μM [10]. Since HEK293 cells might be more resistant to toxic agents than cells from primary origin, the effect of MCa_b and mutated analogues were also tested on the survival rate of cerebellar granule cells maintained in primary culture (Fig. 8). As seen, no cell toxicity could be observed by transmitted light microscopy for a 17-h incubation period with 1 or 10 μM MCa (Fig. 8A). However, using the more sensitive MTT assay, MCa produced 16.0±2.8% cell toxicity at 1 μM. The biotinylated analogue of MCa, MCa_b, behaved similarly to MCa (not shown) suggesting that biotinylated and non-biotinylated analogues could be compared among each others. However, most MCa_b analogues showed either no neuronal toxicity or limited toxicity at a concentration of 1 μM (Fig. 8B). Incubation of neuronal cells with a higher concentration of MCa (10 μM) produced greater cell death (30.4±17.6%). Similar neuronal survival percentages were obtained for MCa_b H6A, MCa_b K8A, MCa_b K22A and MCa_b R24A. At 10 μM however, most other peptides remained non-toxic including many of the best cell-penetrating analogues such as MCa_b D2A, MCa_b P5A, MCa_b L7A, MCa_b L9A, MCa_b E12A and MCa_b D15A. In conclusion, most MCa_b analogues show almost no toxicity on neurons provided that they are used at 1 μM, a concentration range that displays a very significant extent of cell penetration for most mutants in complex with streptavidine. Higher concentrations can still be used without adverse effects for several analogues of MCa. Since the peptides interact with the cell membrane lipids, we determined whether some representative peptides could have any effect on cell membrane integrity by assessing LDH release from cells (Fig. 8C). As seen, no greater LDH release is produced by a 24-h incubation of 10 μM MCa, MCa E12A or MCa K20A with CHO cells than expected from limited cell toxicity at this concentration.

4. Discussion

4.1. Cell toxicity and pharmacological profile of MCa

MCa is a potent activator of RyR. As such, it has the potential to influence Ca^{2+} homeostasis in each cell type that expresses a RyR channel. In spite of its effect on Ca^{2+} mobilization from intracellular stores, MCa presents limited cell toxicity. No toxicity has been observed on CHO cells or on HEK293 cells, possibly because of the absence of expression of RyR [10]. Cell toxicity can be detected to a very limited extent on primary cultures of cerebellar granule cells, in which the presence of RyR is known, but it is difficult to correlate this toxicity to the pharmacological action of the peptide. Indeed, a similar limited toxicity is apparent at concentrations above 1 μM for the MCa R24A mutant that has not the ability to mobilize Ca^{2+} from SR [9], whereas, in contrast, the MCa E12A mutant, that stimulates [^{3}H]-ryanodine binding onto RyR1 at lower concentrations than MCa, does not display any sign of cell toxicity at 10 μM. It should be emphasized that neurons are more likely to express the RyR2 and RyR3 isoforms than the RyR1 isoform tested herein. Since neither the pharmacological action of MCa onto these two isoforms, nor the key residues responsible for this potential effect, have been determined, it remains difficult to make a precise correlation between a key amino acid residue of MCa and some adverse effect on neuronal survival. Nevertheless, several conclusions are within reach for the design of an efficient drug carrier based on MCa's sequence. First, it is highly desirable to develop a carrier that is devoid of effect on any of the RyR isoforms, particularly with regard to Ca^{2+} mobilization. The partial alanine scan we performed on the sequence of MCa reveals that this goal is largely accessible experimentally. Further mutations may be planned, and more extensive tests will be required on the two other RyR isoforms, but it is clear that many key residues already represent starting leads for the rationale design of pharmacologically inert analogues of MCa. The amino acid residues of interest include L7, K8, K19, K20, K22, R23, R24 and T26, which represents a sufficiently diverse array of workable opportunities. Second, developing a cell penetrating analogue of MCa that is devoid of cell toxicity is also clearly within reach. Most analogues were non-toxic to neurons, and many other appear as efficient protein carriers when used at concentrations well below the toxic concentration. For instance, the MCa E12A mutant is maximally effective in carrying streptavidine into cells when used at a concentration of 250 nM, whereas it is non-toxic even at 10 μM. Among the pharmacologically least active analogues devoid of cell toxicity, we can mention those that are mutated at position L7, K19, K20, R23 and T26. This still represents sufficient diversity for the design of numerous novel cell penetrating analogues lacking both pharmacological activity and signs of cell toxicity. Third, taking into account the two above-mentioned criteria, lack of pharmacological activity and lack of cell toxicity, any novel analogue designed should keep potent cell penetration efficiency. Among the residues of interest in terms of pharmacology (L7, K19, K20, R23 and T26), we tested three of them for their penetration efficiency (L7, K19 and K20). Only the L7 locus appears as an interesting lead position since the MCa L7A mutant displays an efficient cell penetration. The L7A being a rather conservative substitution, the strong impact it displays on the pharmacology of MCa is quite encouraging. It seems very likely that less conservative substitutions at this position should further impact the pharmacology without impairing cell penetration. It should be mentioned also that for the design of novel potent analogues, an alternative strategy to a mono substitution would be to perform several substitution at a time: one that impairs the pharmacological impact of MCa and shows a lack of toxicity, combined with another that has improved cell penetration efficiency. Obviously, this study illustrates that many leading strategies can

be developed in the future for the production of highly competent analogues of MCa. Further development of a potent MCa analogue will also be based on the chemical strategies for coupling MCa to cargoes. As such, the recent finding that a MCa analogue devoid of internal cysteine residues, required for the disulfide bridges formation, penetrates into cells, is of great interest if N-terminal cysteine chemistry is pursued as coupling strategy (data not shown).

4.2. The molecular determinants of MCa implicated in pharmacology and cell penetration overlap partially

A peptide that (i) has homology with a calcium channel sequence (domain A of the II–III loop of $Ca_v1.1$), (ii) acts as a pharmacological activator of RyR, and (iii) penetrates efficiently into cells by crossing the plasma membrane puts considerable stringency on its primary structure. Proof of this fact comes from a sequence comparison with MCa related peptide (IpTx A, opicalcine 1 and opicalcine 2) that demonstrates very little sequence variation. Amino acid residues of MCa analogous to domain A include K19, K20, K22, R23, R24, and T26. Absolutely all these residues are essential for the pharmacological effect of MCa, even though they are not solely implicated in the recognition of RyR. A similar residue profile appears to exist for the interaction of MCa with negatively charged lipids (Table 2) and for cell penetration (Fig. 3), although R23 and T26 mutants were not tested. Undoubtedly, the most prominent effects were observed for K19 and K20 mutations, with milder effects for K22 and R24 mutations, suggesting that cell penetration was less deeply hampered by single point mutations of MCa residues that are analogous to those of domain A. Proof that structural divergence exists between MCa and domain A is the observation that domain A is unable to penetrate into cells in spite of its homology by the presence of basic residues (data not shown). The structural requirements for the cell penetration efficiency of MCa are less stringent than those involved in the pharmacological effect of the peptide. This is in line with what is known on other CPPs, with the main structural requirement being the presence of a basic surface for an efficient cell penetration. This lower stringency is also in line with the considerations developed above on the fact that it should be feasible to uncouple both properties by developing peptide analogues devoid of pharmacological effects but keeping considerable cell penetration efficiencies. Nevertheless, a particular mention should be made to the fact that each mutation of MCa that increases the net positive charge of the peptide (D2A, D15A and E12A), all improve the EC_{50} effect on [^{3}H]-ryanodine binding. This may implicate that the nature of the interaction between MCa and its binding site on RyR is electrostatic. In the RyR sites identified for the binding of domain A or MCa, there is indeed a stretch of negatively charged amino acid residues within site F7.2 that look as promising candidates for the interaction [8]. Further experimental work will be required to test out this hypothesis. Only one of the mutations of the negatively charged residues of MCa (E12A and not D2A or D15A) contributes to an improved cell penetration when tested at a micromolar concentration. But since the E12A mutant also displays an improved dose–response curve for cell penetration, similar dose–responses will need to be performed in order to really efficiently compare the cell penetration potency of MCa D2A and MCa D15A. Conversely, the K8A mutation induces a slightly better cell penetration, also indicating that increasing the net global positive charges of the molecule is not a prerequisite for a better penetration. Since this mutation increases the dipole moment of the molecule, this may better explain the greater potential of this analogue.

4.3. A correlation appears to exist between the strength of lipid interaction and the potency of cell penetration of MCa's analogues

The mechanism of cell penetration of CPPs is not well dissected. Two modes of cell penetration have been proposed. One involves a direct interaction of CPPs with charged heparan sulfates present at the cell surface, followed by macropinocytosis. Delivery into the cytoplasm would be partial and would occur from late endosomes. A second one implies a direct interaction of the CPPs with negatively charged lipids, followed by a translocation mechanism that delivers the penetrating peptide and its cargo into the cytoplasm. Both modes are not contradictory and may well coexist in a variety of cell types. Also, the concept that one set of interactions directs the mode of penetration (lipids for translocation, and heparin sulfates for a form of endocytosis) is by itself unproven. Herein, we have further examined the interaction of MCa and mutated analogues with several lipids. The observations made are coherent with the presence of a basic surface on MCa. The peptides interact well with many negatively charged lipids which is a prerequisite for a mechanism of penetration that is based on membrane translocation. Among all the lipids identified, it is difficult to declare that a particular lipid is responsible for the penetration of MCa. Even for the least efficient MCa analogue, MCa K20A, that interacts only with PtdIns(3)P and sulfatide, there is still some degree of cell penetration. What seems to differ among all analogues is not whether these peptides penetrate or not, it is rather the effective concentration that is required for cell penetration. This was obvious when comparing the dose–response curve for cell penetration of the two extreme mutants, MCa E12A and MCa K20A. It is therefore tempting to conclude that cell penetration requires both a good affinity for many of the negatively charged lipids and a wide set of interactions. Further experimental work will be required to determine the affinity of MCa for each of the negatively charged lipid identified here in order to determine whether a particular correlation may exist between the half-effective concentration of MCa for penetration and its affinity for some lipids. Also, the evidence that the penetrated streptavidine appears as punctuate dots in the cytoplasm of cells may after all indicate a strong contribution of the interaction of MCa with lipids in a form of endocytosis. Clarification will be needed on this issue.

Our data indicate that many basic residues of MCa are involved in the interaction with lipids. The fact that a simple mutation of some chosen basic residues can so drastically alter the interaction with some lipids is surprising owing to the fact

that many other basic residues remain present within MCa. Nevertheless, these data indicate that amino acid substitution may thus represent a very interesting alternative to develop MCa analogues presenting greater affinity for these lipids or even wider selectivity. Ultimately, this should lead to the development of analogues of greater potential for cell penetration. Another surprising finding is that many of the residues that appear important for an interaction with negatively charged lipids are also those that are involved in sequence homology with domain A and in the pharmacological effect of MCa. This leads to the interesting and unexplored possibility that (i) domain A may itself interact with negatively lipids adding complexity to the role of the plasma membrane in the process of excitation–contraction, and (ii) lipids may competitively favor or suppress the interaction of MCa or domain A with its binding site on RyR. Obviously further work will be required to address these challenging issues.

Acknowledgements

We acknowledge financial support of Inserm, Université Joseph Fourier and CEA for this project. Narendra Ram is a fellow of the Région Rhône-Alpes and is supported by an Emergence grant. We acknowledge the technical support of Pascal Mansuelle in peptide analyses.

References

[1] Z. Fajloun, R. Kharrat, L. Chen, C. Lecomte, E. di Luccio, D. Bichet, M. El Ayeb, H. Rochat, P.D. Allen, I.N. Pessah, M. De Waard, J.M. Sabatier, Chemical synthesis and characterization of maurocalcine, a scorpion toxin that activates Ca^{2+} release channel/ryanodine receptors, FEBS Lett. 469 (2000) 179–785.

[2] A. Mosbah, R. Kharrat, Z. Fajloun, J.G. Renisio, E. Blanc, J.M. Sabatier, M. El Ayeb, H. Darbon, A new fold in the scorpion toxin family, associated with an activity on a ryanodine-sensitive calcium channel, Proteins 40 (2000) 436–442.

[3] R. El Hayek, A.J. Lokuta, C. Arevalo, H.H. Valdivia, Peptide probe of ryanodine receptor function. Imperatoxin A, a peptide from the venom of the scorpion *Pandinus imperator*, selectively activates skeletal-type ryanodine receptor isoforms, J. Biol. Chem. 270 (1995) 28696–28704.

[4] S. Zhu, H. Darbon, K. Dyason, F. Verdock, J. Tytgat, Evolutionary origin of inhibitor cystine knot peptides, FASEB J. 17 (2003) 1765–1767.

[5] E. Estève, S. Smida-Rezgui, S. Sarkozi, C. Szegedi, I. Regaya, L. Chen, X. Altafaj, H. Rochat, P. Allen, I.N. Pessah, I. Marty, J.M. Sabatier, I. Jona, M. De Waard, M. Ronjat, Critical amino acid residues determine the binding affinity and the Ca^{2+} release efficacy of maurocalcine in skeletal muscle cells, J. Biol. Chem. 278 (2003) 37822–37831.

[6] L. Chen, E. Estève, J.M. Sabatier, M. Ronjat, M. De Waard, P.D. Allen, I.N. Isaac, Maurocalcine and peptide A stabilize distinct subconductance states of ryanodine receptor type 1, revealing a proportional gating mechanism, J. Biol. Chem. 278 (2003) 16095–16106.

[7] S. Pouvreau, L. Csernoch, B. Allard, J.M. Sabatier, M. De Waard, M. Ronjat, V. Jacquemond, Transient loss of voltage control of Ca2+ release in the presence of maurocalcine in mouse skeletal muscle, Biophys. J. 91 (2006) 2206–2215.

[8] X. Altafaj, E. Cheng, E. Esteve, J. Urbani, D. Grunwald, J.M. Sabatier, R. Coronado, M. De Waard, M. Ronjat, Maurocalcine and domain A of the II–III loop of the dihydroprydine receptor $Ca_v1.1$ subunit share common binding sites on the skeletal ryanodine receptor, J. Biol. Chem. 280 (2005) 4013–4016.

[9] E. Esteve, K. Mabrouk, A. Dupuis, S. Smida-Rezgui, X. Altafaj, D. Grunwald, J.C. Platel, N. Andreotti, I. Marty, J.M. Sabatier, M. Ronjat, M. De Waard, Transduction of the scorpion toxin maurocalcine into cells. Evidence that the toxin crosses the plasma membrane, J. Biol. Chem. 280 (2005) 12833–12839.

[10] S. Boisseau, K. Mabrouk, N. Ram, N. Garmy, V. Collin, A. Tadmouri, M. Mikati, J.M. Sabatier, M. Ronjat, J. Fantini, M. De Waard, Cell penetration properties of maurocalcine, a natural venom peptide active on the intracellular ryanodine receptor, Biochim. Biophys. Acta 1758 (2006) 308–319.

[11] A.D. Frankel, C.O. Pabo, Cellular uptake of the Tat protein from human immunodeficiency virus, Cell 55 (1988) 1189–1193.

[12] D. Derossi, S. Calvet, A. Trembleau, A. Brunissen, G. Chassaing, A. Prochiantz, Cell internalization of the third helix of the Antennapedia homeodomain is receptor-independent, J. Biol. Chem. 271 (1996) 18188–18193.

[13] M. Pooga, M. Hällbrink, M. Zorko, Ü. Langel, Cell penetration of transportan, FASEB J. 12 (1998) 67–77.

[14] S.M. Fuchs, R.T. Raines, Pathway for polyarginine entry into mammalian cells, Biochemistry 43 (2004) 2438–2444.

[15] A. Astriab-Fischer, D. Sergueev, M. Fiscjer, B.R. Shaw, R.L. Juliano, Conjugates of antisense oligonucleotides with the Tat and antennapedia cell-penetrating peptides: effects on cellular uptake, binding to target sequences, and biologic actions, Pharm. Res. (N.Y.) 19 (2002) 744–754.

[16] I.A. Ignatovich, E.B. Dizhe, A.V. Pavlotskaya, B.N. Akifiev, S.V. Burov, S.V. Orlov, A.P. Perevozchikov, Complexes of plasmid DNA with basic domain 47–57 of the HIV-1 tat protein are transferred to mammalian cells by endocytosis-mediated pathways, J. Biol. Chem. 278 (2003) 42625–42636.

[17] M. Pooga, U. Soomets, M. Hällbrink, A. Valkna, K. Saar, K. Rezaei, U. Kahl, J.X. Hao, X.J. Xu, Z. Wiesenfeld-Hallin, T. Hökfelt, T. Bartfai, Ü. Langel, Cell penetrating PNA constructs regulate galanin receptor levels and modify pain transmission in vivo, Nat. Biotech. 16 (1998) 857–861.

[18] N. Shibagaki, M.C. Udey, Dendritic cells transduced with protein antigens induce cytotoxic lymphocytes and elicit antitumor immunity, J. Immunol. 168 (2002) 2393–2401.

[19] M. Rojas, J.P. Donahue, Z. Tan, Y.Z. Lin, Genetic engineering of proteins with cell membrane permeability, Nat. Biotech. 16 (1998) 370–375.

[20] M. Pooga, C. Kut, M. Kihlmark, M. Hällbrink, S. Fernaeus, R. Raid, T. Land, E. Hallberg, T. Bartfai, Ü. Langel, Cellular translocation of proteins by transportan, FASEB J. 15 (2001) 1451–1453.

[21] V.P. Torchilin, R. Rammohan, V. Weissig, T.S. Levchenko, TAT peptide on the surface of liposomes affords their efficient intracellular delivery even at low temperature and in the presence of metabolic inhibitors, Proc. Natl. Acad. Sci. U. S. A. 98 (2001) 8786–8791.

[22] M. Lewin, N. Carlesso, C.H. Tung, X.W. Tang, D. Cory, D.T. Scadden, R. Weissleder, Tat peptide-derivatized magnetic nanoparticles allow in vivo tracking and recovery of progenitor cells, Nat. Biotech. 18 (2000) 410–414.

[23] B. Merrifield, Solid phase synthesis, Science 232 (1986) 341–347.

[24] D.H. Kim, S.T. Ohnishi, N. Ikemoto, Kinetic studies of calcium release from sarcoplasmic reticulum in vitro, J. Biol. Chem. 258 (1983) 9662–9668.

[25] I. Marty, D. Thevenon, C. Scotto, S. Groh, S. Sainnier, M. Robert, D. Grunwald, M. Villaz, Cloning and characterization of a new isoform of skeletal muscle triadin, J. Biol. Chem. 275 (2000) 8206–8212.

[26] V. Gallo, A. Kingsbury, R. Balazs, O.S. Jorgensen, The role of depolarization in the survival and differentiation of cerebellar granule cells in culture, J. Neurosci. 7 (1987) 2203–2213.

[27] T.M. Miller, E.M. Johnson Jr., Metabolic and genetic analyses of apoptosis in potassium/serum-deprived rat cerebellar granule cells, J. Neurosci. 16 (1996) 7487–7495.

[28] J.P. Richard, K. Melikov, E. Vives, C. Ramos, B. Verbeure, M.J. Gait, L.V. Chernomordik, B. Lebleu, Cell-penetrating peptides. A reevaluation of the mechanism of cellular uptake, J. Biol. Chem. 278 (2003) 585–590.

THE JOURNAL OF BIOLOGICAL CHEMISTRY VOL. 283, NO. 40, pp. 27048–27056, October 3, 2008

Design of a Disulfide-less, Pharmacologically Inert, and Chemically Competent Analog of Maurocalcine for the Efficient Transport of Impermeant Compounds into Cells*

Received for publication, June 20, 2008, and in revised form, July 8, 2008 Published, JBC Papers in Press, July 11, 2008, DOI 10.1074/jbc.M804727200

Narendra Ram[‡1], Norbert Weiss[§], Isabelle Texier-Nogues[¶], Sonia Aroui[‡], Nicolas Andreotti[‖], Fabienne Pirollet[‡], Michel Ronjat[‡], Jean-Marc Sabatier[‖], Hervé Darbon[**], Vincent Jacquemond[§], and Michel De Waard[‡2]

*From the [‡]Research Group 3 Calcium Channels, Functions, and Pathologies, Unité Inserm 836, Grenoble Institute of Neuroscience, Université Joseph Fourier, Site Santé, BP 170, 38042 Grenoble Cedex 09, France, the [§]Physiologie Intégrative Cellulaire et Moléculaire, Université Claude Bernard Lyon 1, UMR CNRS 5123, 69622 Villeurbanne, France, the [¶]CEA Grenoble/LETI-DTBS, 17 rue des Martyrs, 38054 Grenoble Cedex, France, the [‖]Faculté de Médecine Nord ERT62, Université de la Méditérannée-Ambrillia Biopharma, Marseille Cedex 20, France, and the **AFMB CNRS-UMR 6098, Aix-Marseille Universités, Campus de Luminy, 163 Avenue de Luminy, F-13288 Marseille Cedex 09, France*

Maurocalcine is a 33-mer peptide initially isolated from the venom of a Tunisian scorpion. It has proved itself valuable as a pharmacological activator of the ryanodine receptor and has helped the understanding of the molecular basis underlying excitation-contraction coupling in skeletal muscles. Because of its positively charged nature, it is also an innovative vector for the cell penetration of various compounds. We report a novel maurocalcine analog with improved properties: (i) the complete loss of pharmacological activity, (ii) preservation of the potent ability to carry cargo molecules into cells, and (iii) coupling chemistries not affected by the presence of internal cysteine residues of maurocalcine. We did this by replacing the six internal cysteine residues of maurocalcine by isosteric 2-aminobutyric acid residues and by adding an additional N-terminal biotinylated lysine (for a proof of concept analog) or an N-terminal cysteine residue (for a chemically competent coupling analogue). Additional replacement of a glutamate residue by alanyl at position 12 further improves the potency of these analogues. Coupling to several cargo molecules or nanoparticles are presented to illustrate the cell penetration potency and usefulness of these pharmacologically inactive analogs.

Maurocalcine (MCa)[3] is a highly basic 33-mer peptide isolated from the venom of the scorpion *Scorpio maurus palmatus*. It efficiently binds to the ryanodine receptor of skeletal muscles (RyR1 isoform) (1) and promotes channel opening to promote calcium release from the sarcoplasmic reticulum (SR). This pharmacological effect of MCa can be indirectly monitored through the stimulation it exerts on [^{3}H]ryanodine binding (2). In muscle fibers, MCa produces a transient loss of voltage control of Ca^{2+} release from RyR1 channels. This effect is due to an alteration of repolarization-induced closure of RyR1 channels, a process normally under the control of voltage-dependent dihydropyridine (DHP)-sensitive calcium channels (3). This function of MCa is due to a partial sequence homology between MCa and a cytoplasmic loop of the DHP-sensitive channel (2). These observations explain why MCa, along with other members of the same family of toxins such as imperatoxin 1A (4), hemicalcin (5), and opicalcin 1 and 2 (6) are useful both for their pharmacological properties and for deciphering fine molecular details of the excitation-contraction coupling process.

Recently, MCa has also proven of interest for its property of efficiently crossing the plasma membrane, either alone or when coupled to a membrane-impermeant cargo protein (2, 7). MCa is a highly charged peptide with 12 basic residues out of 33, and a net global positive charge of +8. Most of these residues are on one face of the molecule, the opposite face being mostly hydrophobic in nature. The rich content of basic amino acid residues of MCa is reminiscent of that of all cell-penetrating peptides (CPPs) characterized so far (Tat, penetratin, and poly-R). Hence, MCa can be classified within an emerging family of toxin CPPs that have no structural homologies apart from their content in basic residues. Recently, a new toxin, crotamin, has been purified from the venom of a South American snake. It also behaves as a CPP but apparently with a preference for dividing cells (8). The great diversity in CPP sequences observed so far suggests that designing new MCa CPP analogues should be easy. This tolerance in sequence variation is possibly due to the diverse nature of membrane receptors implicated in CPP cell translocation. These receptors nevertheless possess a single point in common: they all appear to interact with CPPs on the basis of electrostatic interactions. In contrast, the structural characteristics of the interaction between MCa

* This work was supported in part by INSERM and the Fonds de Valorisation of the CEA. The costs of publication of this article were defrayed in part by the payment of page charges. This article must therefore be hereby marked "*advertisement*" in accordance with 18 U.S.C. Section 1734 solely to indicate this fact.

[1] Fellow of the Région Rhône-Alpes and supported by an Emergence grant (to M. D. W.).

[2] To whom correspondence should be addressed: Inserm U836, GIN, UJF, BP 170, 38042 Grenoble Cedex 09, France. Tel.: 33-4-56-52-05-63; E-mail: michel.dewaard@ujf-grenoble.fr.

[3] The abbreviations used are: MCa, maurocalcine; CD, circular dichroism; CHO, Chinese Hamster Ovary cells; CPP, cell-penetrating peptide; DHE, dihydroethidium; DHP, dihydropyridine; DMSO, dimethylsulfoxide; FITC, fluorescein isothiocyanate; MTT, 3-(4, 5-dimethylthiazol-2-yl)-2, 5-diphenyl-tetrazolium bromide; FACS, fluorescence-activated cell sorter; FDB, *flexor digitorum brevis*; PBS, phosphate-buffered saline; QD, quantum dot; RyR1, ryanodine receptor type I; SR, sarcoplasmic reticulum; Strep-Cy5, streptavidin-cyanine5; Abu, 2-aminobutyric acid.

and RyR1 appear far more constrained. A single mutation within MCa, the replacement of an Arg residue by an alanyl, abolishes the pharmacological effect of MCa but has only a mild effect on its cell penetration efficacy (9). Nevertheless, segregating the pharmacological properties from the cell-penetrating properties proved more complex than expected on the sole basis of amino acid substitutions of MCa (9). This appears to be due to structural imperatives of the molecule because it has four functions to fulfill: first, possess the attributes of a CPP; second, conserve sequence homology with the DHP-sensitive calcium channel; third, bind to RyR1; and fourth, activate this latter channel. Many residues contribute both to the pharmacological effects and the cell penetration properties, namely some basic residues that make the functional segregation difficult with simple amino acid substitutions.

To both circumvent these difficulties and take advantage of the flexibility in structural constraints required for MCa cell penetration, we sought a novel strategy for the design of an MCa analogue that would lose its pharmacological activity while retaining most of its cell penetration efficacy. As determined by ^{1}H NMR, MCa folds along an inhibitor cystine knot motif with a disulfide bridge pattern of Cys^3–Cys^{17}, Cys^{10}–Cys^{21}, and Cys^{16}–Cys^{32}. It contains three β-strands that run from amino acid residues 9–11 (strand 1), 20–23 (strand 2), and 30–33 (strand 3), with β-strands 2 and 3 forming an antiparallel β-sheet (10). In earlier studies on another toxin, maurotoxin (MTX), active on voltage-gated potassium channels, it was found that the disulfide bridges of the peptide play an essential role in the three-dimensional structure of the toxin and thus on its activity (11). We therefore adopted a similar strategy for the design of a novel analogue of MCa in which we replaced all native cysteine residues, engaged in the three disulfide bridges, by isosteric 2-aminobutyric acid residues. The goal was to obtain a structurally altered analogue displaying a complete loss of pharmacological activity but preserving the positively charged nature of the peptide, a property required for the efficient cell penetration of a CPP. To further validate this analogue, three derivatives were produced that comprise either an N-terminal biotinylated lysine residue with or without an alanyl substitution of Glu^{12}, previously shown to favor cell penetration (9), or an N-terminal cysteine residue for coupling chemistries to various cargoes. This chemical synthesis was accompanied by pharmacological assays, toxicity experiments, and proof of concept that cargo penetration is fully conserved. The data indicate that cysteine replacement within MCa can produce potent cell-penetrating analogues of MCa devoid of pharmacological activity.

EXPERIMENTAL PROCEDURES

Reagents—Streptavidin-Cy5 (Strep-Cy5) was from Amersham Biosciences, dihydroethidium (DHE) from Molecular Probes, and rhodamine- and FITC-conjugated concanavalin A were from AbCys and Sigma, respectively. Doxorubicin was from Alexis Biochemicals. The TK705-amino-(polyethyleneglycol) quantum dots (QD) with surface-activated amine groups were purchased from Invitrogen. [^{3}H]Ryanodine was from PerkinElmer Life Sciences.

Peptide Synthesis—MCa_b was synthesized as previously described (7). MCa_b-Abu, MCa_b-Abu E12A, and FITC-Gpep-Cys were purchased from the Department of Pharmaceutical Sciences, University of Ferrara (Italy). Cys-MCa-Abu was synthesized by NeoMPS. MTX_b-Abu was assembled by the group of Dr. J. M. Sabatier.

Formation of MCa_b/, MCa_b-Abu/, MCa_b-Abu E12A/, or MTX_b-Abu/Strep-Cy5 Complexes—Soluble Strep-Cy5 was mixed with four molar equivalents of MCa_b, MCa_b-Abu, MCa_b-Abu E12A, or MTX_b-Abu for 2 h at 37 °C in the dark in phosphate-buffered saline (PBS, in mM: NaCl 136, Na_2HPO_4 4.3, KH_2PO_4 1.47, KCl 2.6, $CaCl_2$ 1, $MgCl_2$ 0.5, pH 7.2).

Conjugation of Cys-MCa-Abu to Various Cargoes—Cys-MCa-Abu was conjugated to a FITC-Gpep-Cys molecule (sequence derived from Gβ_1: FITC-β-AGITSVAFSRSGRLL-LAGYDDFN-Abu-NIWDAMKGDRAC-OH) according to the method used by Davidson *et al.* (12). Briefly, an equimolar mixture of Cys-MCa-Abu and FITC-Gpep-Cys was heated to 65 °C for 15 min and then incubated at 37 °C for 1 h. The complex was purified by fast protein liquid chromatography.

Cys-MCa-Abu was also conjugated to doxorubicin. Briefly, doxorubicin.HCl (1 mg/ml) was suspended in PBS, pH 8.0, and conjugated to Cys-MCa-Abu using succinimidyl-4-(*N*-maleimidomethyl) cyclohexane-1-carboxylate (Pierce) according to the protocol of Liang and Yang (13). Successful coupling was followed by a 16.5% SDS-PAGE and UV detection of the resulting conjugated doxorubicin-linker-Cys-MCa-Abu peptide.

QD were also conjugated to Cys-MCa-Abu. The amino groups of the QD (≈100–120 functions per particle) were first converted into a maleimide coating as described (14), thereby yielding QD_M. Briefly, QD (1 nmol) were incubated for 4 h in the dark at room temperature in PBS in the presence of 4-maleimidobutyric acid *N*-hydrosuccinimide ester (1.8 μmol, in anhydrous dimethyl sulfoxide (DMSO)), then purified using NAP-5 columns (Amersham Biosciences). 20 μl of Tris-(2-carboxyethyl)phosphine hydrochloride solution 0.5 M was added to 100 nmol of the Cys-MCa-Abu in 80 μl of water for 30 min, and then incubated overnight at room temperature with QD_M in the presence of 1 mM EDTA, pH 7.4. Non-reacted maleimide groups were quenched for 20 min by adding 2-mercapthoethanol in excess (500 nmol). The QD_M-Cys-MCa-Abu conjugates were purified using NAP-5 columns. Surface modifications of QD were detected by 1% agarose gel electrophoresis in a TAE buffer pH 8, and imaged by fluorescence using a 633-nm excitation wavelength and collecting emitted light above 700 nm. The hydrodynamic diameter of the QD_M-Cys-MCa-Abu nanoparticles measured using a Zetasizer Nano (Malvern Instruments) were 25 nm in PBS (20.5 nm for non-modified QD). The QD_M-Cys-MCa-Abu concentration was calculated using 532 nm absorbance measurements (QD molar extinction coefficient $\epsilon = 2.1 \times 10^6\ M^{-1}\ cm^{-1}$ at 532 nm).

Cell Culture—Wild-type Chinese Hamster Ovary (CHO-K1) cells (from ATCC) were maintained at 37 °C in 5% CO_2 in F-12K nutrient medium (Invitrogen) supplemented with 10% (v/v) heat-inactivated fetal bovine serum (Invitrogen) and 10,000 units/ml streptomycin and penicillin (Invitrogen). MDA-MB-231 cells from ATCC were grown in Leibovitz L15 medium supplemented with 10% (v/v) heat-inactivated fetal

bovine serum and 10,000 units/ml streptomycin and penicillin. Media used for the culture of cerebellar granule neurons was based on Dulbecco's modified Eagle's medium (Invitrogen) containing 10 unit/ml penicillin, 10 μg/ml streptomycin, 2 mM L-glutamine, and 10 mM HEPES, 25 mM KCl, and 10% fetal bovine serum. Primary cultures were prepared from 6-day-old S/IOPS NMRI mice (Charles River Laboratories), as described previously (15).

Preparation of Heavy SR Vesicles—Heavy SR vesicles were prepared following the method of Kim *et al.* (16). Protein concentration was measured by the Biuret method.

Isolation and Preparation of Flexor Digitorum Brevis Muscle Fibers—Experiments were performed on single skeletal fibers isolated from the *flexor digitorum brevis* (FDB) muscles from 4–8-week-old OF1 mice (Charles River Laboratories) in accordance with the guidelines of the French Ministry of Agriculture (87/848) and of the European Community (86/609/EEC). Procedures for enzymatic isolation of single fibers and partial insulation of the fibers with silicone grease were as previously described (17, 18). In brief, mice were killed by cervical dislocation after halothane (Sigma-Aldrich) inhalation before removal of the muscles. Muscles were treated with 2 mg/ml collagenase type I (Sigma-Aldrich) in Tyrode solution for 60 min at 37 °C. Single fibers were then isolated by triturating the muscles in the experimental chamber. The major part of a single fiber was electrically insulated with silicone grease (Rhodia Siliconi Italia, Treviolo, Italia) so that whole-cell voltage-clamp could be achieved on a short portion of the fiber extremity. All experiments were performed at room temperature (20–22 °C).

Structural Analyses of MCa_b, MCa_b-Abu, and MCa_b-Abu E12A by Circular Dichroism—Circular dichroism (CD) spectra were recorded on a Jasco 810 dichrograph using 1-mm thick quartz cells. Spectra were recorded between 180 and 260 nm at 0.2 nm/min and were averaged from three independent acquisitions. The spectra were corrected for water signal and smoothed using a third-order least squares polynomial fit.

[^{3}H]Ryanodine Binding Assay—Heavy SR vesicles (1 mg/ml) were incubated at 37 °C for 3 h in an assay buffer composed of 5 nM [^{3}H]ryanodine, 150 mM NaCl, 2 mM EGTA, 2 mM $CaCl_2$ (pCa = 5), and 20 mM HEPES, pH 7.4. 1 μM MCa_b, MCa_b-Abu, or MCa_b-Abu E12A was added to the assay buffer just prior to the addition of heavy SR vesicles. [^{3}H]Ryanodine bound to heavy SR vesicles was measured by filtration through Whatman GF/B glass filters followed by three washes with 5 ml of ice-cold washing buffer composed of 150 mM NaCl, 20 mM HEPES, pH 7.4. Filters were then soaked overnight in 10 ml of scintillation mixture (Cybscint, ICN) and bound radioactivity determined by scintillation spectrometry. Nonspecific binding was measured in the presence of 20 μM cold ryanodine. Each experiment was performed in triplicate and repeated three times. All data are presented as mean ± S.D.

Fluorescent Measurements under Voltage-Clamp Conditions—An RK400 patch-clamp amplifier (BioLogic) was used in whole-cell configuration as previously described (18). Voltage-clamp was performed with a microelectrode filled with the intracellular-like solution (in mM: 120 K glutamate, 5 Na_2-ATP, 5 Na_2-phosphocreatine, 5.5 $MgCl_2$, 5 D-glucose, 5 HEPES adjusted to pH 7.2 with KOH). Indo-1 (Molecular Probes) was present in this solution at 0.2 mM for fluorescence measurements under voltage-clamp conditions. The extracellular solution contained (in mM): 140 TEA-methanesulphonate, 2.5 $CaCl_2$, 2 $MgCl_2$, 0.002 tetrodotoxin, 10 HEPES, pH 7.2. The tip of the microelectrode was inserted through the silicon, within the insulated part of the fiber. Membrane depolarizations were applied every 30 s from a holding command potential of −80 mV. For the present set of measurements, the cytoplasm was dialyzed with the microelectrode solution, which contained the calcium dye Indo-1 and a given peptide to be tested (200 μM for MCa_b-Abu and MCa_b-Abu E12A, and 100 μM for MCa_b). To facilitate intracellular dialysis, the electrode tip was broken within the silicon-insulated portion of the fiber by pushing it back and forth a few times toward the bottom of the chamber. Under these conditions, intracellular equilibration of the solution was awaited for 30 min. Equilibration was followed from the time course of increase of indo-1 fluorescence in the tested portion of the fiber. Indo-1 fluorescence was measured on an inverted Nikon Diaphot epifluorescence microscope equipped with a commercial optical system allowing the simultaneous detection of fluorescence at 405 nm (F_{405}) and 485 nm (F_{485}) by two photomultipliers (IonOptix, Milton, MA) upon 360-nm excitation. Background fluorescence at both emission wavelengths was measured next to each fiber tested and was then subtracted from all measurements. In an earlier study, we showed that 10–100 μM levels of MCa were necessary to affect voltage-activated Ca^{2+} release in intact mammalian skeletal muscle fibers (3). For this reason, and despite the cell penetration properties of MCa and of its derivatives, it is easier and less costly to apply these compounds intracellularly through the voltage-clamp electrode rather than in the extracellular medium.

Calibration of the Indo-1 Response and $[Ca^{2+}]_{intra}$ Calculation—The standard ratio method was used with the parameters: $r = F_{405}/F_{485}$, with R_{min}, R_{max}, K_D, and β having their usual definitions. Results were either expressed in terms of Indo-1% saturation or in actual free calcium concentration (18, 19). *In vivo* values for R_{min}, R_{max}, and β were measured using procedures previously described (17). No correction was made for Indo-1 Ca^{2+} binding and dissociation kinetics.

MTT Assay—Primary cultures of cerebellar granule neurons were seeded into 96-well microplates at a density of ~8×10^4 cells/well. After 4 days of culture, the cells were incubated for 24 h at 37 °C with 10 μM MCa_b, MCa_b-Abu, Cys-MCa-Abu, or MCa_b E12A-Abu. Control wells containing cell culture medium alone or with cells, both without peptide addition, were included in each experiment. The cells were then incubated with 3-(4, 5-dimethylthiazol-2-yl)-2, 5-diphenyl-tetrazolium bromide (MTT) for 30 min. Conversion of MTT into purple-colored MTT formazan by the living cells indicates the degree of cell viability. The crystals were dissolved in DMSO, and the optical density was measured at 540 nm using a microplate reader (Biotek ELx-800, Mandel Scientific Inc.) for quantification of cell viability. All assays were run in triplicate.

Flow Cytometry—MCa_b/, MCa_b-Abu/, MCa_b-Abu E12A, or MTX_b-Abu/Strep-Cy5 complexes were incubated for 2 h with CHO cells to allow cell penetration. Control condition was represented by an incubation of cells with Strep-Cy5 alone. The

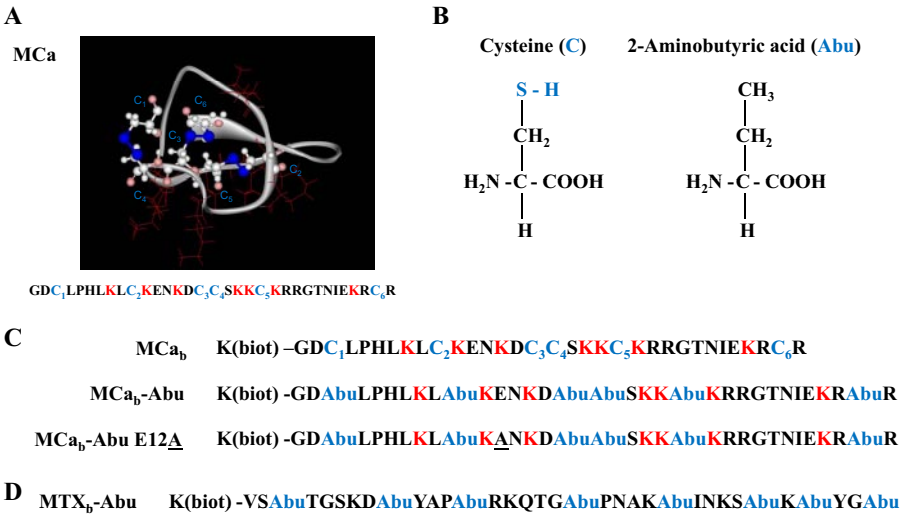

FIGURE 1. **MCa analogues, MCa_b-Abu and MCa_b-Abu E12A.** *A*, *ribbon representation* of the three-dimensional solution structure of MCa illustrating the positions of the three disulfide bridges C_1-C_4, C_2-C_5, and C_3-C_6. S-S bonds are shown in *blue*. The positions of positively charged lysines, essential for cell penetration, are shown in *red*. *B*, differences in side chain between cysteine residues and 2-aminobutyric acid (*Abu*) used for substitution of all cysteine residues in MCa amino acid sequence. *C*, amino acid sequences of three different MCa analogs used in this study. A fourth analog is shown in Fig. 7*A*. *D*, amino acid sequence of MTX_b-Abu, an analog of MTX in which all cysteine residues are replaced by Abu, and an extra biotinylated lysine residue added at the N terminus. Note that MTX contains six basic amino acid residues in its sequence.

cells were then washed twice with PBS to remove the excess extracellular complexes. Next, the cells were treated with 1 mg/ml trypsin (Invitrogen) for 10 min at 37 °C to remove remaining membrane-associated extracellular cell surface-bound complexes. The cell suspension was centrifuged at 500 × *g* and resuspended in PBS. Flow cytometry analyses were performed with live cells using a Becton Dickinson FACSCalibur flow cytometer (BD Biosciences). Data were obtained and analyzed using CellQuest software (BD Biosciences). Live cells were gated by forward/side scattering from a total of 10,000 events. Mean fluorescence values were determined from Gaussian fits of the resulting histograms and plotted as a function of complex concentration. Mean values of intracellular fluorescence for Strep-Cy5 alone incubation (less than 1% of the fluorescence observed for the lowest concentration of any of the various MCa/Strep-Cy5 complexes) were also subtracted.

Analysis of the Subcellular Localization of Various MCa/or MTX/Cargo Complexes by Confocal Microscopy—For Strep-Cy5 complexes, 4 μM MCa_b, MCa_b-Abu, MCa_b-Abu E12A, or MTX_b-Abu were coupled to 1 μM Strep-Cy5 as described above. CHO cells were incubated with the resulting complexes for 2 h, and then washed with Dulbecco's modified Eagle's medium alone. Immediately after washing, the nucleus was stained with 1 μg/ml DHE for 20 min, and then washed again with DMEM. After this step, the plasma membrane was stained with 5 μg/ml of FITC-conjugated concanavalin A for 3 min. Cells were washed once more, but with PBS. For the FITC-Gpep-Cys-Cys-MCa-Abu complex, 1 μM conjugate was incubated with CHO cells for 2 h, the plasma membrane stained with 5 μg/ml of rhodamine-conjugated concanavalin A. For the QD_M-Cys-MCa-Abu complex, 50 nM of the complex was incubated with CHO cells for 2 h, and the nuclei stained with 1 μg/ml DHE for 20 min. For the doxorubicin-linker-Cys-MCa-Abu complex, 3 μM of the conjugate was incubated with MDA-MB-231 for 2 h, followed by staining of the plasma membrane with 5 μg/ml of FITC-conjugated concanavalin A for 3 min. In all experiments, live cells were immediately analyzed by confocal laser scanning microscopy using a Leica TCS-SP2. Alexafluor-488 (excitation at 488 nm), rhodamine and doxorubicin (excitation at 543 nm), or Cy5 and QD_M (excitation at 642 nm) were sequentially excited and emission fluorescence collected in z-confocal planes of 10–15-nm steps. Images were merged in Adobe Photoshop 7.0.

RESULTS

Synthesis of Disulfide-less Analogs of MCa—Fig. 1*A* illustrates the three-dimensional solution structure of MCa with three disulfide bridges. The aim of this study was to design a MCa analog for which convenient chemical coupling could be performed by using an N-terminal additional cysteine residue. As shown, MCa already contains six cysteine residues that contribute to the folding of the peptide to form an inhibitor cysteine knot motif. Adding an additional cysteine residue at the N terminus may significantly change the normal folding of the peptide and the classical disulfide bridge arrangement (C_1-C_4, C_2-C_5, and C_3-C_6) in an unpredicted manner. In turn, this could significantly affect the pharmacological activity and cell-penetration properties of the resulting molecule(s). To facilitate chemical coupling strategies of MCa to cargo molecules, we investigated the requirement of disulfide bridges on MCa pharmacology and cell penetration properties. Several analogs were synthesized, each with an N-terminal biotinylated lysine for easy binding to fluorescent streptavidin molecules (our reporter cargo for this study): MCa_b, intact with the native disulfide bridges, MCa_b-Abu in which we replaced all internal cysteine residues by isosteric 2-aminobutyric acid (*Abu*, Fig. 1*B*), and MCa_b-Abu E12A, an analog of MCa_b-Abu in which Glu^{12} was replaced by alanyl, a substitution known to improve cell penetration efficacy of MCa_b (9) (Fig. 1*C*). We would expect that removing the disulfide bridges of MCa might affect its pharmacology more than its cell penetration properties for two reasons. First, disulfide bridge patterns are known to contribute to the pharmacological activity of toxins (20, 21). Second, the structural requirements for the pharmacological activity of MCa were shown to be more stringent than those required for cell penetration as probed by alanine scanning of MCa (9). Finally, we synthesized MTX_b-Abu, a biotinylated version of MTX that has no cell-penetrating properties on its own and that acts on voltage-dependent potassium channels (Fig. 1*D*). This peptide, in which we also replaced six internal cysteine residues by Abu derivatives, as for the MCa_b-Abu peptide, was used as a negative control in cell penetration experiments.

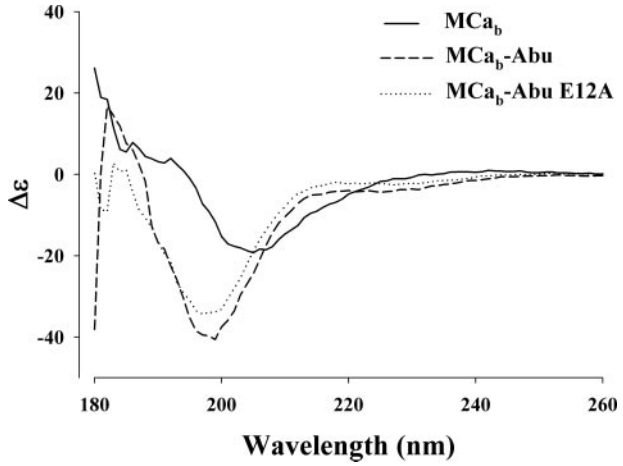

FIGURE 2. **Determination of the secondary structures of MCa$_b$, MCa$_b$-Abu, and MCa$_b$-Abu E12A by circular dichroism.** Each spectrum presented is the mean of three independent acquisitions taken at a concentration of 50 μM in pure water at 20 °C.

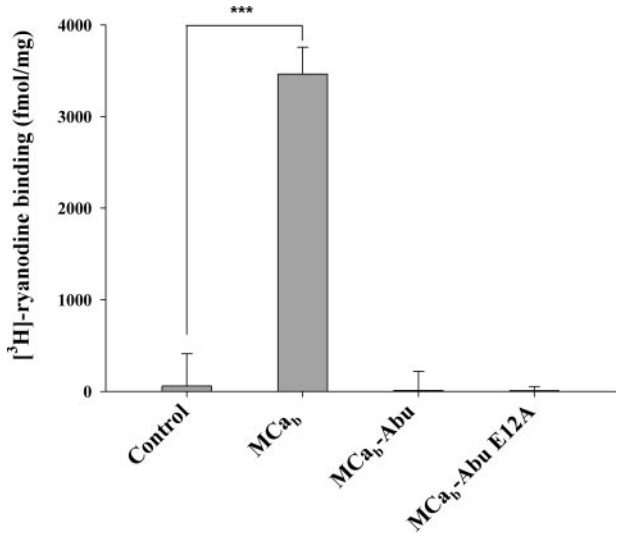

FIGURE 3. **Effect of 1 μM MCa$_b$, MCa$_b$-Abu, or MCa$_b$-Abu E12A on [^{3}H]ryanodine binding onto heavy SR vesicles.** Specific [^{3}H]ryanodine binding was measured as described under "Experimental Procedures." Control binding has been performed in the absence of the MCa analog. ***, $p \leq 0.01$. Note the loss of effect upon cysteine replacement by Abu derivatives. The experiment was repeated three times with similar results.

Removing Disulfide Bridges in MCa Disrupts the Secondary Structure of the Peptide—Circular dichroism analyses were performed for MCa$_b$, MCa$_b$-Abu, and MCa$_b$-Abu E12A (Fig. 2). As shown, the spectra for MCa$_b$-Abu and MCa$_b$-Abu E12A differed significantly from MCa$_b$ indicating the alteration of secondary structures of the peptides. These observations are coherent with the role of disulfide brides in the acquisition/stabilization of secondary structures of toxins (11). These data clearly indicate that blocking disulfide bridge formation in MCa is a successful strategy to alter the structure of MCa.

Cysteine Replacement by Abu Derivatives Produces Pharmacologically Inert MCa Analogues—MCa is known to bind to RyR1 from skeletal muscles (2). Upon binding, it modifies the conformation of this intracellular calcium channel in such a way that it favors binding of [^{3}H]ryanodine to its receptor, probably by converting low affinity binding sites to high affinity ones. The effect of 1 μM MCa$_b$ on [^{3}H]ryanodine binding to SR containing RyR1 was confirmed in this study (Fig. 3). An average stimulation in binding of 59.7-fold was measured ($n = 3$). The value of this stimulation depends upon the basal level of binding and can occasionally be lower, down to 7-fold (not shown). Importantly, the two analogs in which the cysteine residues were replaced by Abu derivatives, MCa$_b$-Abu and MCa$_b$-Abu E12A, had no significant effect on [^{3}H]ryanodine binding, indicating that the structural impact of these substitutions fully blocked the effect of MCa on RyR1. Slight reductions in [^{3}H]ryanodine binding were observed, although these effects were not significant. Higher concentrations of these two analogs were also without effect (not shown). The E12A-substituted analogue thus proved no better than MCa$_b$-Abu, despite the fact that a similar mutation in the folded MCa has higher affinity for RyR1 (9).

We also investigated the effect of these analogs on Ca^{2+} homeostasis in muscles fibers. The effects of the three peptides MCa$_b$, MCa$_b$-Abu and MCa$_b$-Abu E12A were tested on the free Ca^{2+} transients elicited by voltage-clamp depolarizations in single skeletal muscle fibers from mouse. Fig. 4*A* shows representative Indo-1 saturation traces obtained in response to pulses from −80 mV to +10 mV of 5-, 10-, 20-, and 50-ms

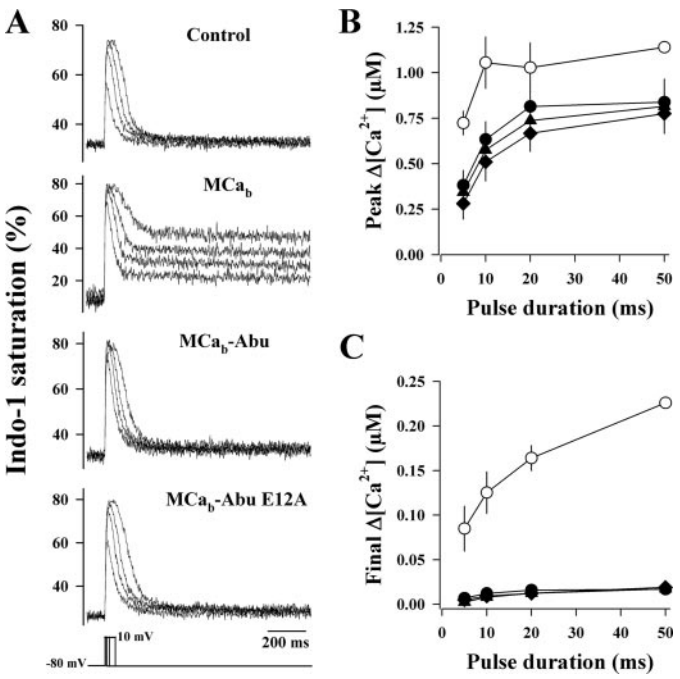

FIGURE 4. **Effects of MCa$_b$, MCa$_b$-Abu, and MCa$_b$-Abu E12A on voltage-activated sarcoplasmic reticulum Ca^{2+} release.** *A*, Indo-1 Ca^{2+} records in response to membrane depolarizations of increasing duration in a control fiber (●) and in fibers dialyzed, respectively, with MCa$_b$ (○, 100 μM), MCa$_b$-Abu (◆, 200 μM), and MCa$_b$-Abu E12A (▲, 200 μM). *B* and *C*, corresponding mean values for peak Δ[Ca^{2+}], and final Δ[Ca^{2+}] at the end of the record in control fibers ($n = 11$) and in fibers dialyzed with either MCa$_b$ ($n = 3$), MCa$_b$-Abu ($n = 10$), or MCa$_b$-Abu E12A ($n = 3$). Note the loss of pharmacological consequences of replacing cysteine by Abu derivatives.

duration in (from top to bottom) a control fiber, a fiber dialyzed with 100 μM MCa$_b$, a fiber dialyzed with 200 μM MCa$_b$-Abu, or a fiber dialyzed with 200 μM MCa$_b$-Abu E12A, respectively. These high concentrations of peptides were chosen to ensure that effective intracellular levels could be reached after equilibration (see "Experimental Procedures"). As previously

described (3), MCa_b produced a remarkable change in the time course of the Ca^{2+} transients: it prevented membrane repolarization-induced complete turn off of SR Ca^{2+} release, resulting in a prolonged elevation of the cytoplasmic [Ca^{2+}] after the end of the pulses. This was obviously not the case in the two fibers treated, respectively, with MCa_b-Abu and MCa_b-Abu E12A, for which the Ca^{2+} transients yielded properties very similar to the ones of the control fiber. Corresponding mean values for the peak $\Delta[Ca^{2+}]$ during the pulse, and the final $\Delta[Ca^{2+}]$ at the time of the end of the record, are presented in Fig. 4, *B* and *C*. For instance, MCa_b produced a mean final $\Delta[Ca^{2+}]$ value of 0.164 ± 0.032 ($n = 4$) following a pulse of 20 ms, whereas MCa_b-Abu and MCa_b-Abu E12A produced only values of 0.019 ± 0.009 ($n = 9$) and 0.016 ± 0.008 ($n = 11$), respectively, compared with 0.017 ± 0.007 ($n = 10$) for the control condition. There was thus no significant difference in the values for the peak $\Delta[Ca^{2+}]$, and the final $\Delta[Ca^{2+}]$ between control fibers and fibers treated with either MCa_b-Abu or MCa_b-Abu E12A clearly demonstrating a complete loss of MCa-induced activity on SR Ca^{2+} release for these two compounds. The effect of MCa likely results from competition with a physiological interaction between the DHP receptors and RyR1 (3) explaining why such high concentrations are required. We conclude that replacement of the cysteine in MCa by Abu derivatives produces non-folded and pharmacologically inert analogs.

Conserved Cell Penetration Properties of Disulfide-less MCa Analogues—Biotinylated MCa, MCa_b, favors the efficient penetration of fluorescently labeled streptavidin (Strep) (7, 9, 22), through macropinocytosis (23). The cell penetration of MCa_b/Strep complexes involves one or multiple steps of attachment to the membrane through binding to cell surface glycosaminoglycans and negatively charged lipids. The complex can be found predominantly in endosomes, leading to a punctate cytoplasmic distribution, a pattern that is supposedly linked to the nature of the cargo rather than the vector itself. Here, we investigated whether the disulfide-less analogues of MCa_b were capable of carrying Strep-Cy5 into CHO cells (Fig. 5*A*). As shown, 1 μM Strep-Cy5 alone is unable to enter CHO cells. This was true for 100% of the cells examined by confocal microscopy ($n = 200$). However, when coupled to either MCa_b, MCa_b-Abu, or MCa_b-Abu E12A in a 4:1 ratio and incubated for 2 h with living CHO cells, the resulting complexes gave punctate staining. Here again, 100% of the cells were positively stained by Strep-Cy5 ($n = 200$ for each condition). This punctate staining is an indication of endosomal distribution further confirming that it may be linked to the nature of the cargo rather than the vector, since similar distributions are observed for the MCa analogs despite the structural changes in the vector. In contrast, no cell penetration of Strep-Cy5 was observed in CHO cells using a biotinylated analogue of MTX, MTX_b-Abu, a voltage-gated K^+ channel blocker (Fig. 5*B*; 0% of $n = 200$ cells examined by confocal microscopy). This indicates that MCa_b-Abu is unlikely to penetrate into cells only because of its amphipathic nature.

To obtain half-maximal Penetration Concentration values (PC_{50}) and the extent of total penetration of the complex, quantification of cell penetration by fluorescence-activated cell sorting (FACS) was performed. Quantification is a way to distinguish the cell penetration efficacies of various MCa analogs (9) or of various cell lines (23). As shown in Fig. 6, after 2 h of incubation, both MCa_b-Abu and MCa_b-Abu E12A analogs were less effective than MCa_b because the total Strep-Cy5 fluorescence entering CHO cells at maximally effective concentration of the peptides (10 μM) was reduced on average by 28 and 59% for MCa_b-Abu E12A and MCa_b-Abu, respectively (Fig. 6). It is of interest that the E12A mutant was more effective than the analog without mutation. A similar observation was made with the folded version of this mutation (9). This effect is most likely due to an increase in the basic content of the molecule. With regard to PC_{50} values, only slight reductions in the efficacies of the analogs were observed. In these experiments, we measured PC_{50} values of 669 $\pm$ 27 nM for MCa_b/Strep-Cy5 ($n =$

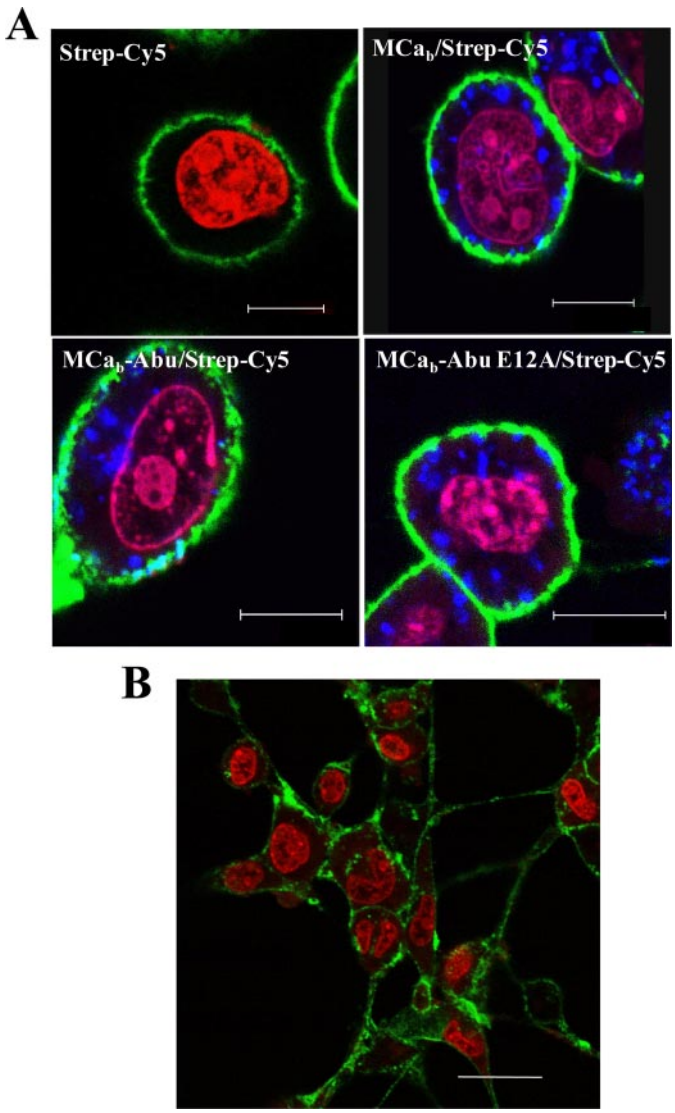

FIGURE 5. **Distribution of MCa_b/, MCa_b-Abu/, and MCa_b-Abu E12A/Strep-Cy5 in CHO cells.** *A*, confocal images showing the cell penetration of Strep-Cy5 (2 h of incubation) in the absence or presence of 4 μM MCa_b, MCa_b-Abu, or MCa_b-Abu E12A in CHO cells. Colors: *blue* (Strep-Cy5), *red* (nuclei, DHE), and *green* (plasma membrane, concanavalin A). Note the lack of differences in cell distribution between the various MCa analogue complexes. The punctate distribution is linked to the use of streptavidin as cargo. *Scale bars*: 10 μm. *B*, confocal image of CHO cells showing that 4 μM MTX_b-Abu is unable to deliver Strep-Cy5 inside cells (2 h of incubation). Color code is as in *A*. *Scale bar*: 15 μm.

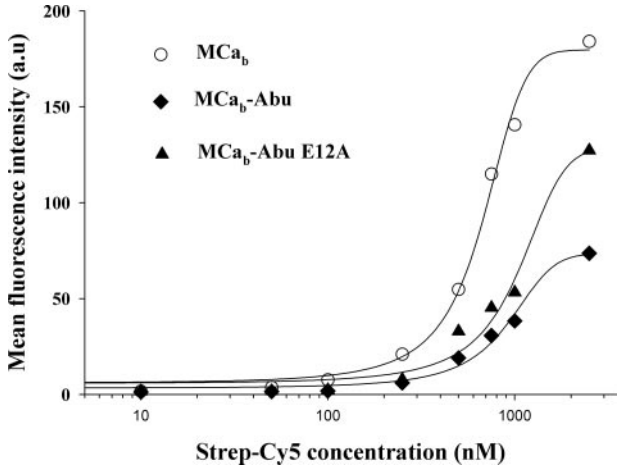

FIGURE 6. **Mean cell fluorescence intensities (*MFI*) as a function of the concentration of cell-penetrating complexes for each MCa analog.** Indicated concentrations are for Strep-Cy5 (10 nM to 2.5 μM). The ratio MCa analog/Strep-Cy5 was 4:1. Data were fitted by a sigmoid equation of the type $MFI = MFI_{max}/(1 + \exp(-(\times - PC_{50})/b))$ where $MFI_{max} = 180 \pm 6$ a.u. (MCa$_b$), 73 ± 4 a.u. (MCa$_b$-Abu), and 129 ± 8 a.u. (MCa$_b$-Abu E12A), $b = 200 \pm 18$ (MCa$_b$), 301 ± 38 (MCa$_b$-Abu) and 344 ± 64 (MCa$_b$-Abu E12A), and half-penetration concentration values $PC_{50} = 669 \pm 27$ nM (MCa$_b$), 910 ± 51 nM (MCa$_b$-Abu), and 1042 ± 89 nM (MCa$_b$-Abu E12A). *a.u.*: arbitrary units. The MFI values are obtained from a fit of the FACS histograms ($n = 10{,}000$ events in each case). Representative example of $n = 3$ experiments. Experiments could not be averaged because the different photomultiplier settings were not calibrated.

3), 910 ± 51 nM for MCa$_b$-Abu/Strep-Cy5 ($n = 3$) and 1042 ± 89 nM for MCa$_b$-Abu E12A/Strep-Cy5 ($n = 3$). Therefore, in the case of disulfide-less analogs, maximal cell penetration of Strep-Cy5 could be obtained using only slightly increased peptide concentrations.

Adding an N-terminal Cysteine Residue to a Disulfide-less MCa Analog Produces a Chemically Competent Peptide for the Cell Penetration of Various Cargoes—Although the use of Strep-Cy5 brings proof of concept, it remains a useless cargo for many biological applications, especially if it concentrates into endosomes. We therefore produced a novel disulfide-less analogue of MCa in which we simply replaced the N-terminal biotinylated lysine by a cysteine residue to make various chemical coupling strategies possible (Cys-MCa-Abu whose sequence is shown in Fig. 7*A*). Next, this peptide was coupled to various cargoes using several chemistries and investigated for its ability to enter cells (Fig. 7, *B–D*). Cys-MCa-Abu was first coupled to a FITC fluorescent peptide containing a C-terminal cysteine residue. The coupling consisted in favoring the formation of a disulfide bridge among the two peptides. At 1 μM, this complex entered CHO cells (100% of the cells by confocal microscopy, $n = 200$) whereas incubation of CHO cells with 1 μM FITC-labeled peptide alone resulted in no cell penetration (Fig. 7*B*; 0% of $n = 200$ cells observed). The FITC-peptide complex stained diffusely the cells, indicating that it reached both the cytoplasm and the nucleus either through direct plasma membrane translocation or through endosomal escape. Because the Strep and FITC complexes distribute differently in the cell, it appears that the cargo rather than the vector determines the cell distribution. Cys-MCa-Abu was also coupled to doxorubicin, an antitumor drug, which penetrates into MDA-MB-231 cells by itself, and concentrates in nuclei where it acts on DNA replication.

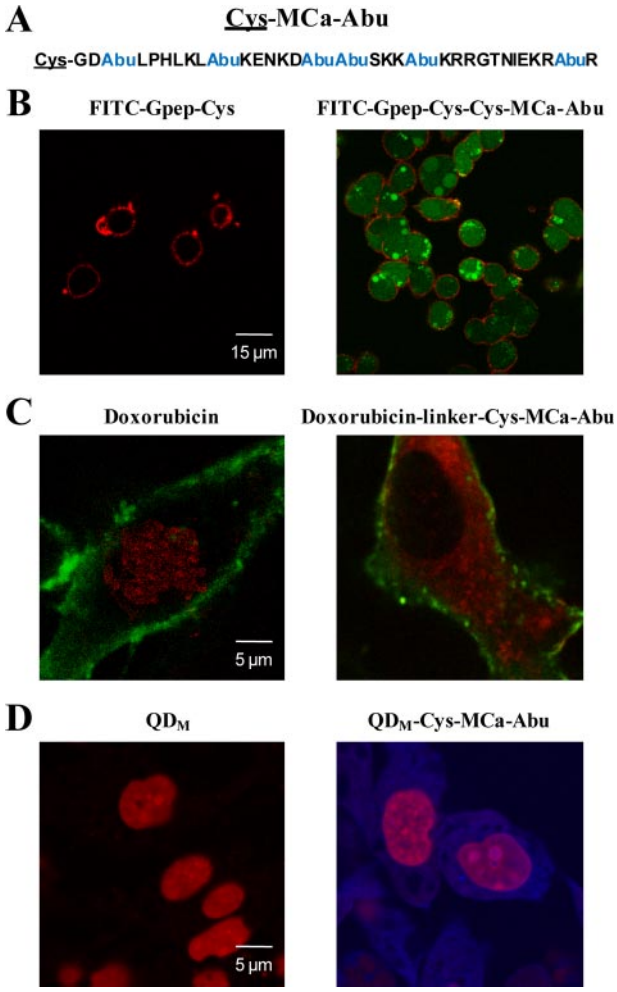

FIGURE 7. **Design of a cell-penetrating analog for the efficient coupling and delivery of a variety of cargoes.** *A*, primary amino acid sequence of the Cys-MCa-Abu analog. This analogue is identical to MCa$_b$-Abu except that the N-terminal K(biot) has been replaced by an N-terminal cysteine residue. *B*, cell penetration of FITC-Gpep-Cys when covalently linked to Cys-MCa-Abu (*right panel*, 1 μM concentration, 2 h incubation with CHO cells). No penetration is observed for 1 μM FITC-Gpep-Cys alone (*left panel*). Code colors: *red*, concanavalin-A-rhodamine, and *green*, FITC label. *C*, cell penetration of 3 μM doxorubicin or the covalently linked complex, doxorubicin-linker-Cys-MCa-Abu, in MDA-MB-231 cells. Note that doxorubicin alone goes to the nucleus (*red*, *left panel*), whereas coupled to Cys-MCa-Abu it concentrates in the cytoplasm. *Green*: concanavalin-A-FITC for plasma membrane staining. *D*, cell penetration of 50 nM QD alone (*left panel*) or coupled after maleimide modification of QDs to Cys-MCa-Abu in CHO cells (*right panel*). Code colors: *red*, nuclei (DHE) and *blue*, QDs. From *B* to *D*, note the diffuse cytoplasmic staining of the cargoes when coupled to Cys-MCa-Abu.

The chemical coupling was performed using a cross-linker, allowing a directional coupling with the unique amino group of doxorubicin and the SH function of the cysteine residue of Cys-MCa-Abu. As shown, incubation of MDA-MB-231 cells with either 3 μM doxorubicin or doxorubicin-linker-Cys-MCa-Abu resulted in significantly different cell distributions (Fig. 7*C*). Covalent linkage of doxorubicin with Cys-MCa-Abu produced a marked cytoplasmic localization, also diffuse, in marked contrast to the predominantly nuclear distribution of doxorubicin. In 96% of the cells examined ($n = 200$), the coupling to Cys-MCa-Abu resulted in a cytoplasmic distribution of doxorubicin. Finally, near-infrared emitting quantum dots from Invitrogen, with amine surfaces, were linked to Cys-MCa-Abu using

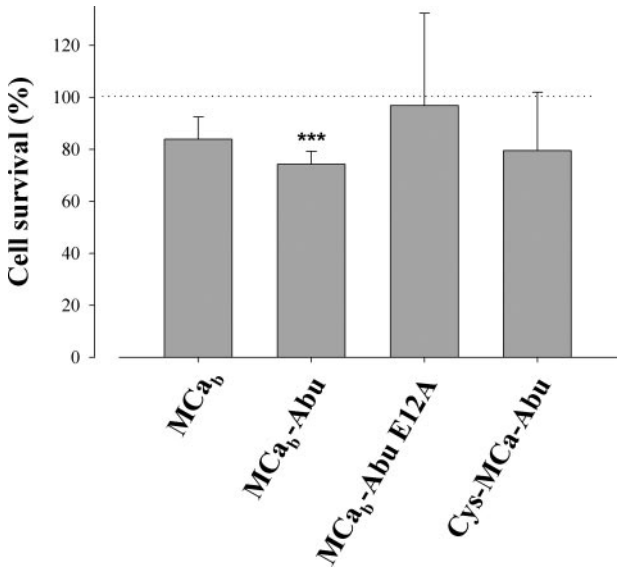

FIGURE 8. **Neuronal toxicity of MCa analogues.** Neuronal survival after 24 h of incubation with 10 μM of each MCa analogue was assessed with the MTT assay. No significant differences in neuronal survival were observed between the analogues. ***, survival affected with mean + 3 S.D. < 100%. The average of six data points is shown.

maleimide chemistry. Maleimide was added to QD yielding QD_M, that could further be linked to the SH function of the Cys residue of Cys-MCa-Abu. Incubation of 50 nM QD_M-Cys-MCa-Abu with CHO cells resulted in cell penetration with a diffuse distribution in both the cytoplasm and the nucleus (Fig. 7*D*; 100% of cells observed; $n = 200$). No penetration was observed with QD_M incubation alone (0% of cells, $n = 200$). The rather efficient penetration observed with such a low concentration of QD_M-Cys-MCa-Abu might be explained by the high potential of Cys-MCa-Abu grafting at the surface of QD_M (about 100–120 maleimide converted functions at the surface of a single QD).

Cell Toxicity of MCa Analogues—To be considered as good cell-penetrating vectors, peptides must have limited cell toxicity. We investigated cerebellar granule cell survival after incubation with 10 μM of free vector peptide for 24 h (Fig. 8). This cell system is generally used for the evaluation of neuronal survival. It is more stringent than the use of cell lines that are more resistant to toxic agents. The conditions used in this study were deliberately extreme, considering the conditions required for the cell penetration of our vectors. First, incubation times in the range of an hour are largely sufficient; second, cell penetration is observed at lower concentrations than 10 μM; and third, we have evidence suggesting that intracellular concentrations of cell-penetrating peptides increase markedly when cells are incubated with the vector alone rather than in complex with the cargo. Nevertheless, the experimental conditions used here indicate that only one of the analog had a significant effect on neuronal survival (MCa$_b$-Abu, mean survival of 74.3 ± 4.9%, $n = 6$), whereas all other analogs were without significant effect, despite the conditions used here ($n = 6$ for each condition).

Concluding Remarks—By simple substitution of the six cysteine residues of MCa, we have produced a series of analogs that are devoid of secondary structure and therefore of pharmacological activity. These analogs nevertheless possess cell-penetrating properties that are closely related to those established for native MCa. This finding indicates that the proper folding of MCa is not essential for the membrane translocation. Similarly, the spatial separation of a basic face and a hydrophobic face of MCa seems of little importance for cell penetration. It cannot be excluded however that during the translocation process itself, when the peptide interacts with negatively charged lipids, it may adopt a conformation close to that of native MCa. The observation that MTX$_b$-Abu, used as a negative control, does not penetrate cells indicates that MCa-Abu does not act as a detergent by means of its amphipathic nature. A slight increase in effective concentrations or reductions in total transport capacities of these analogs barely counterbalance the benefits of the loss of pharmacological effects or the ability to graft an extra N-terminal cysteine residue to the sequence for versatile cargo coupling strategies. Our results further indicate that the Cys-MCa-Abu vector is valuable for the cell delivery of a variety of cargoes. The cytoplasmic localization of the delivered cargoes using this vector should be invaluable for many biological applications for which targeting to this compartment are an absolute requirement. For future applications, it might be recommended to assess the cell toxicity of the vector/cargo complexes of interest in the conditions of the application. The benefits of all cell-penetrating peptides undoubtedly lie in the value of penetration/toxicity concentration ratio of the formed complexes, a value that needs to be determined for each application.

Acknowledgments—We thank the team of Pr. Rémy Sadoul for help with cerebellar granule cell cultures. We also thank Dr. Jonathan Coles for critical reading of the manuscript.

REFERENCES

1. Altafaj, X., Cheng, W., Esteve, E., Urbani, J., Grunwald, D., Sabatier, J. M., Coronado, R., De Waard, M., and Ronjat, M. (2005) *J. Biol. Chem.* **280,** 4013–4016
2. Esteve, E., Smida-Rezgui, S., Sarkozi, S., Szegedi, C., Regaya, I., Chen, L., Altafaj, X., Rochat, H., Allen, P., Pessah, I. N., Marty, I., Sabatier, J. M., Jona, I., De Waard, M., and Ronjat, M. (2003) *J. Biol. Chem.* **278,** 37822–37831
3. Pouvreau, S., Csernoch, L., Allard, B., Sabatier, J. M., De Waard, M., Ronjat, M., and Jacquemond, V. (2006) *Biophys. J.* **91,** 2206–2215
4. el-Hayek, R., Lokuta, A. J., Arevalo, C., and Valdivia, H. H. (1995) *J. Biol. Chem.* **270,** 28696–28704
5. Shahbazzadeh, D., Srairi-Abid, N., Feng, W., Ram, N., Borchani, L., Ronjat, M., Akbari, A., Pessah, I. N., De Waard, M., and El Ayeb, M. (2007) *Biochem. J.* **404,** 89–96
6. Zhu, S., Darbon, H., Dyason, K., Verdonck, F., and Tytgat, J. (2003) *Faseb. J.* **17,** 1765–1767
7. Boisseau, S., Mabrouk, K., Ram, N., Garmy, N., Collin, V., Tadmouri, A., Mikati, M., Sabatier, J. M., Ronjat, M., Fantini, J., and De Waard, M. (2006) *Biochim. Biophys. Acta* **1758,** 308–319
8. Nascimento, F. D., Hayashi, M. A., Kerkis, A., Oliveira, V., Oliveira, E. B., Radis-Baptista, G., Nader, H. B., Yamane, T., Tersariol, I. L., and Kerkis, I. (2007) *J. Biol. Chem.* **282,** 21349–21360
9. Mabrouk, K., Ram, N., Boisseau, S., Strappazzon, F., Rehaim, A., Sadoul, R., Darbon, H., Ronjat, M., and De Waard, M. (2007) *Biochim. Biophys. Acta* **1768,** 2528–2540
10. Mosbah, A., Kharrat, R., Fajloun, Z., Renisio, J. G., Blanc, E., Sabatier, J. M., El Ayeb, M., and Darbon, H. (2000) *Proteins* **40,** 436–442
11. di Luccio, E., Matavel, A., Opi, S., Regaya, I., Sandoz, G., M'Barek, S.,

Carlier, E., Esteve, E., Carrega, L., Fajloun, Z., Rochat, H., Loret, E., de Waard, M., and Sabatier, J. M. (2002) *Biochem. J.* **361,** 409–416
12. Davidson, T. J., Harel, S., Arboleda, V. A., Prunell, G. F., Shelanski, M. L., Greene, L. A., and Troy, C. M. (2004) *J. Neurosci.* **24,** 10040–10046
13. Liang, J. F., and Yang, V. C. (2005) *Bioorg. Med. Chem. Lett.* **15,** 5071–5075
14. Cai, W., Shin, D. W., Chen, K., Gheysens, O., Cao, Q., Wang, S. X., Gambhir, S. S., and Chen, X. (2006) *Nano. Lett.* **6,** 669–676
15. Gallo, V., Kingsbury, A., Balazs, R., and Jorgensen, O. S. (1987) *J. Neurosci.* **7,** 2203–2213
16. Kim, D. H., Ohnishi, S. T., and Ikemoto, N. (1983) *J. Biol. Chem.* **258,** 9662–9668
17. Collet, C., Allard, B., Tourneur, Y., and Jacquemond, V. (1999) *J. Physiol.* **520,** 417–429
18. Jacquemond, V. (1997) *Biophys. J.* **73,** 920–928
19. Csernoch, L., Bernengo, J. C., Szentesi, P., and Jacquemond, V. (1998) *Biophys. J.* **75,** 957–967
20. Fajloun, Z., Ferrat, G., Carlier, E., Fathallah, M., Lecomte, C., Sandoz, G., di Luccio, E., Mabrouk, K., Legros, C., Darbon, H., Rochat, H., Sabatier, J. M., and De Waard, M. (2000) *J. Biol. Chem.* **275,** 13605–13612
21. Fajloun, Z., Mosbah, A., Carlier, E., Mansuelle, P., Sandoz, G., Fathallah, M., di Luccio, E., Devaux, C., Rochat, H., Darbon, H., De Waard, M., and Sabatier, J. M. (2000) *J. Biol. Chem.* **275,** 39394–39402
22. Esteve, E., Mabrouk, K., Dupuis, A., Smida-Rezgui, S., Altafaj, X., Grunwald, D., Platel, J. C., Andreotti, N., Marty, I., Sabatier, J. M., Ronjat, M., and De Waard, M. (2005) *J. Biol. Chem.* **280,** 12833–12839
23. Ram, N., Aroui, S., Jaumain, E., Bichraoui, H., Mabrouk, K., Ronjat, M., Lortat-Jacob, H., and De Waard, M. (2008) *J. Biol. Chem.* **283,** 24274–24284

Conclusion

MCa is a potent activator of RyR and has the potential to influence Ca^{2+} homeostasis in all cell types that express a RyR channel. MCa's technological value lies in the fact that it can cross the plasma membrane also when coupled to cargo. It thus becomes very important to derive an analogue of MCa that lacks pharmacological activity. Several mutated analogues of MCa were derived through an alanine scan on the sequence of MCa and they were first analyzed for their activity on purified RyR. Of all the analogues tested, two mutants were found to be interesting: MCa R24A that did not stimulate [^{3}H]-ryanodine binding onto RyR, and also MCa E12A that did stimulate [^{3}H]-ryanodine binding onto RyR at much lower concentrations than wild-type MCa. But the interesting observation is that in spite of the fact that MCa E12A had greater affinity for RyR, it showed no signs of toxicity on primary neuronal cells as compared to MCa R24A or to the wild-type MCa. Other mutants showed very limited extent of toxicity, but it is difficult to correlate this toxicity to the pharmacological action of the peptide.

In addition to the lack of pharmacological activity or cell toxicity, any novel analogue should keep potent cell penetration efficiency. MCa E12A was maximally effective in carrying streptavidin into cells when used at a concentration of 250 nM, far better than the MCa R24A. Also, the MCa L7A mutant appeared as an interesting lead analogue since it displayed an efficient cell penetration. From this study, we also learned mutations of some basic residues can drastically alter the interaction with lipids, indicating that some specific basic residues of MCa are involved in the interaction with lipids. Also, we found that there is a form of correlation between the strength of lipid interaction and the potency of cell penetration of MCa's analogues. MCa E12A mutant displayed the strongest lipid interactions of all mutants, which is probably at the basis of its better cell penetration properties. In contrast, less penetrating mutants, MCa K19A and MCa K20A, showed the weakest lipid interaction. Taken together, it appears that MCa E12A mutant may be used as a basis for the development of new competent analogues of MCa.

Finally, in addition to lacking a pharmacological effect, being safe and possessing good cell penetration efficiency, a novel analogue should also be chemically competent for the coupling of various cargoes. To develop chemically competent analogues of MCa, a novel strategy, wherein all native cysteine residues of wild-type MCa and MCa E12A mutant were

replaced by isosteric 2-aminobutyric acid (Abu) residues and were analyzed for pharmacology, toxicity and cell penetration. Cysteine substitutions by Abu derivatives produced MCa analogues (MCa-Abu and MCa-Abu E12A) that were devoid of secondary structure, pharmacological activity and had limited cell toxicity. Allthough there was a slight reduction in the cell penetration efficiencies of these analogues as compared to wild-type MCa, other advantages over wild-type MCa, such as lack of pharmacological impact and the ability to graft an extra-N-terminal cysteine residue to the sequence for cargo coupling largely counterbalance the reduced cell penetration efficiencies of the analogues.

2. Article III

Direct peptide interaction with surface glycosaminoglycans contribute to the cell penetration of maurocalcine.

Ram N, Aroui S, Jaumain E, Bichraoui H, Sadoul R, Mabrouk K, Ronjat M, Lortat-Jacob H, De Waard M.

J Biol Chem. 2008 Aug 29; 283 (35):24274-24284. Epub 2008 Jul 3.

Introduction

Use of CPPs for the intracellular delivery of a range of bioactive and membrane-impermeable molecules is opening up new avenues in the areas of drug delivery. However, the mechanism of translocation of these CPPs alone or when coupled to cargoes is being hotly debated. Attempts to unravel the cell translocation mechanism of a growing number of CPPs have revealed molecular determinants essential for internalization. The peptide sequence, charge and nature of cargo have been proposed to be the major factors in determining the mode of cell entry and subsequent internalization pathway. However, studies argue both in favor of direct translocation as well endocytic uptake. Also plasma membrane-associated heparan sulfate proteoglycan (HSPG) and lipids are reported to play a crucial role in the cellular uptake of these CPPs. MCa is a new member of the CPP family and few studies have been made to understand the mechanism of cell translocation. Thus, it became necessary to understand the mechanism of translocation and also the nature of cell membrane components with whom MCa interacts.

Interaction of wild-type MCa and MCa K20A, a mutant analogue presenting reduced cell-penetration efficiency, with heparin (HP) and heparan sulfates (HS) was analyzed through surface plasma resonance (SPR). Later on the cell penetration efficiencies and distribution of MCa coupled to streptavidin was analyzed in wild-type and GAG-deficient CHO cells, to determine if GAGs play any role in cell penetration and distribution. To further identify the route of entry of MCa and analyze the impact of GAG depletion on this entry, several endocytotic inhibitors were tested on the entry of MCa in wild-type and GAG-deficient CHO cells.

THE JOURNAL OF BIOLOGICAL CHEMISTRY VOL. 283, NO. 35, pp. 24274–24284, August 29, 2008

Direct Peptide Interaction with Surface Glycosaminoglycans Contributes to the Cell Penetration of Maurocalcine*

Received for publication, December 6, 2007, and in revised form, April 25, 2008 Published, JBC Papers in Press, July 3, 2008, DOI 10.1074/jbc.M709971200

Narendra Ram[‡1], Sonia Aroui[‡], Emilie Jaumain[‡], Hicham Bichraoui[‡2], Kamel Mabrouk[§2], Michel Ronjat[‡], Hugues Lortat-Jacob[¶], and Michel De Waard[‡3]

From the [‡]INSERM U836, Grenoble Institute of Neurosciences, Research Group 3, Calcium Channels, Functions, and Pathologies Laboratory, Université Joseph Fourier, 38042 Grenoble Cedex 9, France, [§]Université Aix-Marseille 1, 2, and 3, CNRS-UMR 6517, Chimie, Biologie et Radicaux Libres, 15521 Avenue Esc. Normandie Niemen, 13397 Marseille Cedex 20, France, and [¶]Institut de Biologie Structurale, UMR 5075 CEA/CNRS/Université Joseph Fourier, 41 rue Jules Horowitz, 38027 Grenoble Cedex 1, France

Maurocalcine (MCa), initially identified from a tunisian scorpion venom, defines a new member of the family of cell penetrating peptides by its ability to efficiently cross the plasma membrane. The initiating mechanistic step required for the cell translocation of a cell penetrating peptide implicates its binding onto cell surface components such as membrane lipids and/or heparan sulfate proteoglycans. Here we characterized the interaction of wild-type MCa and MCa K20A, a mutant analogue with reduced cell-penetration efficiency, with heparin (HP) and heparan sulfates (HS) through surface plasma resonance. HP and HS bind both to MCa, indicating that heparan sulfate proteoglycans may represent an important entry route of the peptide. This is confirmed by the fact that (i) both compounds bind with reduced affinity to MCa K20A and (ii) the cell penetration of wild-type or mutant MCa coupled to fluorescent streptavidin is reduced by about 50% in mutant Chinese hamster ovary cell lines lacking either all glycosaminoglycans (GAGs) or just HS. Incubating MCa with soluble HS, HP, or chondroitin sulfates also inhibits the cell penetration of MCa-streptavidin complexes. Analyses of the cell distributions of MCa/streptavidin in several Chinese hamster ovary cell lines show that the distribution of the complex coincides with the endosomal marker Lyso-Tracker red and is not affected by the absence of GAGs. The distribution of MCa/streptavidin is not coincident with that of transferrin receptors nor affected by a dominant-negative dynamin 2 K44A mutant, an inhibitor of clathrin-mediated endocytosis. However, entry of the complex is greatly diminished by amiloride, indicating the importance of macropinocytosis in MCa/streptavidin entry. It is concluded that (i) interaction of MCa with GAGs quantitatively improves the cell penetration of MCa, and (ii) GAG-dependent and -independent MCa penetration rely similarly on the macropinocytosis pathway.

Maurocalcine (MCa)[4] is a 33-mer peptide isolated from the venom of the scorpion *Scorpio maurus palmatus.* MCa is a highly basic peptide, as 12 of 33 residues are positively charged including the amino-terminal Gly residue, seven Lys residues, and four Arg residues. Because it contains only four negatively charged residues, the net global charge of the peptide is also positive. MCa possesses three disulfide bridges connected according to the pattern Cys^3-Cys^{17}, Cys^{10}-Cys^{21}, and Cys^{16}-Cys^{32}. ^{1}H NMR analysis further indicates that MCa folds along an inhibitor cystine knot motif (1). MCa contains three β-strands running from amino acid residues 9 to 11 (strand 1), 20 to 23 (strand 2), and 30 to 33 (strand 3), respectively, with β-strands 2 and 3 forming an antiparallel β-sheet. MCa has proven to be a highly potent modulator of the skeletal muscle ryanodine receptor type 1 (RyR1), an intracellular calcium channel. The addition of MCa to the extracellular medium of cultured myotubes induces Ca^{2+} release from the sarcoplasmic reticulum into the cytoplasm within seconds, as shown using a calcium-imaging approach (2, 3). These observations suggested that MCa is able to cross the plasma membrane to reach its pharmacological target. This was first demonstrated when a biotinylated analogue of MCa was coupled to a fluorescent derivative of streptavidin, and the complex was shown to cross the plasma membrane (4). Cell penetration of this MCa-based complex is rapid, reaches saturation within minutes, and occurs at concentrations as low as 10 nM (5). Furthermore, an alanine scan of MCa indicates the importance of basic amino acid residues in the cell penetration mechanism. Reducing the net positive charge of the molecule appears to decrease its cell penetration efficiency. In parallel, MCa analogues exhibiting decreased penetration efficiency were also found to present reduced affinity for negatively charged lipids of the plasma membrane (6).

Over the past years several peptides have been characterized for their ability to cross the plasma membrane (7–11). Cell penetration of peptides obeys three fundamental steps; (i) binding

* This work was supported by INSERM, Université Joseph Fourier, and Commissariat à l'Energie Atomique (Saclay, France). The costs of publication of this article were defrayed in part by the payment of page charges. This article must therefore be hereby marked "*advertisement*" in accordance with 18 U.S.C. Section 1734 solely to indicate this fact.

[1] A fellow of the Région Rhône-Alpes and supported by an Emergence grant.

[2] A fellow of l'Agence Française contre les Myopathies

[3] Supported by the "Techno pour la Santé" program of the Commissariat à l'Énergie Atomique. To whom correspondence should be addressed. Tel.: 33-4-56-52-05-63; E-mail: michel.dewaard@ujf-grenoble.fr.

[4] A fellow of 1'Agence Francaise contre les Myopathies. The abbreviations used are: MCa, maurocalcine; MCa_b, biotinylated MCa; CHO, Chinese hamster ovary; CPP, cell penetrating peptide; CS, chondroitin sulfate; dp, degree of polymerization; FACS, fluorescence-activated cell sorter; HEK293, human embryonic kidney 293 cells; HS, heparan sulfate; HSPG, HS proteoglycans; HP, heparin; PC_{50}, half-maximal penetration concentration; PBS, phosphate-buffered saline; PtdIns, phosphatidylinositol; Strep-Cy5 (Cy3), streptavidin-cyanine 5 (cyanine 3); RU, response units.

to some components of the plasma membrane, (ii) the cell entry process *per se*, and (iii) the subsequent release into the cytoplasm. Obviously, none of these steps are well understood, and conflicting reports have emerged that may well arise from differences in the nature of the cell-penetrating peptide (CPP) considered, cell preparations, experimental conditions, type of linkage to cargoes, or even cargo nature. Two non-competing mechanisms have been proposed for the cell entry of CPP. One is direct translocation through the plasma membrane by the CPP-induced reorganization of the membrane after several possible structural alterations (7–11). According to some investigators, this mechanism implies a direct CPP interaction with negatively charged lipids of the plasma membrane. This mechanism of penetration would be independent of both cell metabolic energy and membrane receptor presence. For instance, it was proposed that penetratin binds to the polar heads of lipids leading to the formation of inverted micelles followed by a subsequent opening of these micelles inside the cell, and the release of the peptide into the cytoplasm (12). A second mechanism involves a form of endocytosis by which the CPP gets localized into late endosomes from where it may eventually leak out partially toward the cytoplasm. Endocytosis can be initiated by binding of CPPs to HS along with binding to negatively charged moieties on the cell surface, such as lipids (13). Lipid-raft dependent macropinocytosis has been evidenced as one endocytosis pathway for the cell entry of CPPs (14, 15). For instance, cellular uptake of a recombinant glutathione *S*-transferase-TAT-green fluorescent protein fusion protein depends on the presence of HS proteoglycans (HSPG) at the cell surface (16). Nevertheless, the role of GAGs in the cell penetration of CPPs remains debated. Stereochemistry, chain length, patterns of sulfation, and negative charge distribution of GAGs lead to a great variety of protein binding motifs. Furthermore, the CPP structure also appears to determine its specificity for HSPG (17).

In the present study we show that MCa interacts with GAGs such as HS and HP with apparent affinities in the micromolar range. A less penetrating analogue of MCa (MCa K20A) also shows a reduced apparent affinity for these GAGs, suggesting a direct link between GAG interaction and cell penetration. Cell penetration of MCa_b-streptavidin complex is strongly inhibited by an inhibitor of macropinocytosis indicating that this route of entry is responsible for MCa penetration. However, use of GAG-deficient cell lines indicates that half of the cell penetration of the complex is conserved and still relies on macropinocytosis. We conclude that GAG-dependent and -independent entries of MCa use similar pathways. Cell surface GAGs appear important to specify a higher cell penetration level, but penetration still can occur in their absence presumably because binding onto lipids can also activate macropinocytosis.

EXPERIMENTAL PROCEDURES

Equipment and Reagents—The Biacore 3000 apparatus, CM4 sensor chips, amine coupling kit, and HBS-P buffer (10 mM HEPES, 150 mM NaCl, 3 mM EDTA, 0.005% surfactant P20, pH 7.4) were from Biacore AB. Biotin-LC-hydrazide was from Pierce. Streptavidin, 6-kDa HP, and 35–45-kDa chondroitin 4 sulfate (CS-A, here abbreviated CS) were from Sigma, streptavidin-Cy5 or -Cy3 was from Amersham Biosciences, and 9-kDa HS was from Celsus. Concerning the 6-kDa HP, smaller molecular species that this material may contain were removed through a filtration column. This material was routinely used for Biacore analysis (18). This material was preferred to unfractionated heparin because it is less polydisperse. CS-A contains on average one sulfate group by disaccharide. The molecular weight of the HS used in this study was 9000 g/mol as determined by sedimentation-diffusion analysis. Its sulfur and nitrogen contents, determined by elemental analysis, were 6.96 and 2.15%, respectively.[5] LysoTracker red DND-99 and Alexa Fluor® 488- or 594-conjugated transferrin were from Invitrogen. Size-defined HP-derived oligosaccharides (dp6 (hexa)-, dp12 (dodeca)-, and dp18 octadecasaccharide) were prepared from porcine mucosal HP as described (19). These HP-derived oligosaccharides were obtained by size fractionation. Because the starting material was HP and HS, these samples were relatively homogenous and highly sulfated. Strong anion exchange high performance liquid chromatography analysis of the HP-derived octasaccharide gave rise to three major peaks.

MCa, MCa_b, MCa K20A, and MCa_b K20A Peptide Syntheses—Chemical syntheses of MCa and MCa K20A or biotinylated MCa_b and MCa_b K20A were performed as previously described (2, 6). The molecular weights of the peptides are 3858.62 (MCa) and 3801.52 (MCa K20A). Their pI values are 9.46 (MCa) and 9.30 (MCa K20A), indicating that they are basic at physiological pH 7.4. Primary structures of MCa and MCa K20A are shown in Fig. 1*A*. The position of biotin in MCa_b and MCa_b K20A is on an extra amino-terminal lysine residue.

Formation of MCa_b- or MCa_b K20A-Strep-Cy5/3 Complexes—Soluble streptavidin-Cy5 or -Cy3 (Amersham Biosciences) was mixed with 4 mol eq of MCa_b or MCa_b K20A for 2 h at 37 °C in the dark in phosphate-buffered saline (PBS): 136 mM NaCl, 4.3 mM Na_2HPO_4, 1.47 mM KH_2PO_4, 2.6 mM KCl, 1 mM $CaCl_2$, 0.5 mM $MgCl_2$, pH 7.2. In some experiments, where indicated, various molar ratios of MCa_b and streptavidin-Cy3 were used to prepare the MCa_b-Strep complex, the concentration of streptavidin-Cy3 being kept constant (1 μM).

Surface Plasmon Resonance Binding Experiments—6-kDa HP and HS were biotinylated at their reducing end with biotin-LC-hydrazide. The biotinylation procedure was checked by streptavidin-peroxidase labeling after blotting of the material onto zetaprobe membrane. These molecules have been widely used to study HP or HS binding onto several other proteins, such as RANTES (regulated on activation normal T cell expressed and secreted), gp120, or CXCL12 (18, 20–22). For the purpose of immobilization of biotinylated HP and HS on a Biacore sensorchip, flow cells of a CM4 sensorchip were activated with 50 μl of 0.2 M *N*-ethyl-*N*′-(diethylaminopropyl)-carbodiimide and 0.05 M *N*-hydroxysuccinimide before injection of 50 μl of streptavidin (0.2 mg/ml in 10 mM acetate buffer, pH 4.2). The remaining activated groups were blocked with 50 μl of ethanolamine 1 M, pH 8.5. Typically, this procedure permitted coupling of ~3.000–3.500 resonance units (RU) of streptavidin. Biotinylated HP (5 μg/ml) or HS (10 μg/ml) in HBS-P

[5] G. Pavlov and C. Ebel, personal communication.

buffer was then injected over a one-surface flow cell to obtain an immobilization level of ~50 RU. Flow cells were then conditioned with several injections of 2 M NaCl. One-flow cells were left untreated and served as negative control. For binding assays, different MCa concentrations in HBS-P and at 25 °C were simultaneously injected at 20 μl/min onto the control, HP, and HS surfaces for 5 min, after which the formed complexes were washed with running buffer. The sensorchip surfaces were regenerated with a 5-min pulse of 2 M NaCl in HBS-P buffer. For competition assays, MCa at 2 μM was preincubated for at least 45 min with various molar excesses of HP-derived oligosaccharides (dp6, dp12, and dp18) and then injected over the HP surface as described above.

Cell Culture and Transfection—The wild-type Chinese hamster ovary (CHO-K1) cell line and mutant CHO cell lines lacking all GAGs (pgsB-618) or HS (pgsD-677) (ATCC) were maintained at 37 °C in 5% CO_2 in F-12K nutrient medium (Invitrogen) supplemented with 10% (v/v) heat-inactivated fetal bovine serum (Invitrogen) and 10,000 units/ml streptomycin and penicillin (Invitrogen). For transfection experiments with FuGENE® HD (Roche Applied Science), wild-type and mutant pgsB-618 CHO cells were transfected with a plasmid that encodes a dominant-negative form of dynamin 2 (dynamin 2 K44A) in fusion with enhanced green fluorescent protein (pEGFP-N1 vector from Clontech). 24 h after transfection, cells were incubated with 1 μM MCa_b-Strep-Cy3 or transferrin-conjugated to Alexa Fluor-594 (25 μg/ml).

Flow Cytometry—MCa_b/MCa_b K20A-Strep-Cy5 complexes were incubated for 2 h in phosphate-buffered saline with CHO and mutant cells to allow cell penetration. The cells were then washed twice with PBS to remove the excess extracellular complexes. Next, the cells were treated with 1 mg/ml trypsin (Invitrogen) for 10 min at 37 °C to remove remaining membrane-associated extracellular cell surface-bound complexes. After trypsin incubation, the cell suspension was centrifuged at 500 × *g* and suspended in PBS. For inhibition studies, MCa_b-Strep-Cy5 complexes were preincubated with PBS containing variable concentrations (as indicated) of CS-A, HP, or HS for 45 min, and the mixture was incubated with cells for 2 h to investigate cell penetration. Washing and trypsination steps were also applied in these conditions. For experiments concerning endocytosis inhibitors, wild-type and mutant CHO cells were initially washed with F12K and preincubated for 30 min at 37 °C with different inhibitors of endocytosis: (i) 5 mM amiloride, (ii) 5 μM cytochalasin D, (iii) 5 mM nocodazole, or (iv) 5 mM methyl-β-cyclodextrin (all from Sigma). The cells were then incubated for 2 h at 37 °C with 1 μM MCa_b-Strep-Cy5 or with 25 μg/ml transferrin-Alexa Fluor 488 in the presence of each drug. For all these experimental conditions, flow cytometry analyses were performed with live cells using a BD Biosciences FACSCalibur flow cytometer. Data were obtained and analyzed using CellQuest software (BD Biosciences). Live cells were gated by forward/side scattering from a total of 10,000 events.

Confocal Microscopy—For analysis of the subcellular localization of MCa_b-Strep-Cy5 complexes in living cells, CHO and mutant cells were incubated with the complexes for 2 h and then washed with Dulbecco's modified Eagle's medium alone. Immediately after washing, the nucleus was stained with 1 μg/ml dihydroethidium (Molecular Probes) for 20 min and then washed again with Dulbecco's modified Eagle's medium. After this step the plasma membrane was stained with 5 μg/ml fluorescein isothiocyanate-conjugated concanavalin A (Sigma) for 3 min. Cells were washed once more, but with PBS. Live cells were then immediately analyzed by confocal laser scanning microscopy using a Leica TCS-SP2 operating system. Fluorescein isothiocyanate (E_x = 488 nm), Cy5 (E_x = 642 nm), or Cy3 (E_x = 543 nm) fluorescence emission were collected in z-confocal planes of 10–15 nm. Images were merged in Adobe Photoshop 7.0. For studies on endocytosis, wild-type and mutant CHO cells were incubated with 1 μM MCa_b-Strep-Cy5 along with 25 μg/ml transferrin conjugated to Alexa Fluor 488 (a marker of clathrin-mediated endocytosis) for 2 h, and the distribution was analyzed through confocal microscopy. In parallel studies cells were first incubated for 2 h with 1 μM MCa_b-Strep-Cy5, washed with PBS, and incubated with 50 nM LysoTracker red DND-99 for 20 min at 37 °C. Cells were then washed again with PBS and visualized alive by confocal microscopy.

Effect of HP on the Interaction of MCa_b with Lipids—Strips of nitrocellulose membranes containing spots with different phospholipids and sphingolipids were obtained from Molecular Probes. These membranes were first blocked with TBS-T (150 mM NaCl, 10 mM Tris-HCL, pH 8.0, 0.1% (v/v) Tween 20) supplemented with 0.1% free bovine serum albumin (BSA) for about 1 h at room temperature and then incubated for 2 h at room temperature in TBS-T, 0.1% free BSA with either 100 nM MCa_b alone or a MCa_b·HP complex, resulting from a 45-min preincubation of 100 nM MCa_b with 10 μg/ml HP. Incubation of the membranes with 100 nM biotin alone was used as a negative control condition. The membranes were then washed a first time with TBS-T, 0.1% free bovine serum albumin using a gentle agitation for 10 min. In all conditions MCa_b or biotin binding onto the lipid spots was detected by a 30-min incubation with 1 μg/ml streptavidin horseradish peroxidase (Vector labs, SA-5704) followed by a second wash with TBS-T 0.1% free bovine serum albumin and an incubation with horseradish peroxidase substrate (Western Lightning, PerkinElmer Life Science) for 1 min. Lipid membranes were then exposed to a Biomax film (Kodak). The intensity of interaction with the lipids was analyzed with Image J (National Institutes of Health).

RESULTS

MCa Interacts with HS and HP—Preincubation of MCa_b with HP was found to partially inhibit its penetration in HEK293 cells (5). To evaluate the binding of MCa to HSPGs, HP or HS was coupled to a Biacore sensorchip, and the MCa binding was monitored by SPR (Fig. 1). Injection of a range of MCa concentrations (up to 5 μM) over HP- or HS-coupled sensorchips gave rise to increasing binding amplitudes as shown in Fig. 1*B*. A mutated analogue of MCa (MCa K20A) showed impaired binding activity, indicating the importance of residue Lys-20 for glycosaminoglycan recognition. This finding is in agreement with the role of HSPGs in the cell entry of CPPs and with the observation that the MCa K20A has impaired cell penetration (6). The data could not be fitted to a binding model, presumably because all binding curves had a "square" shape

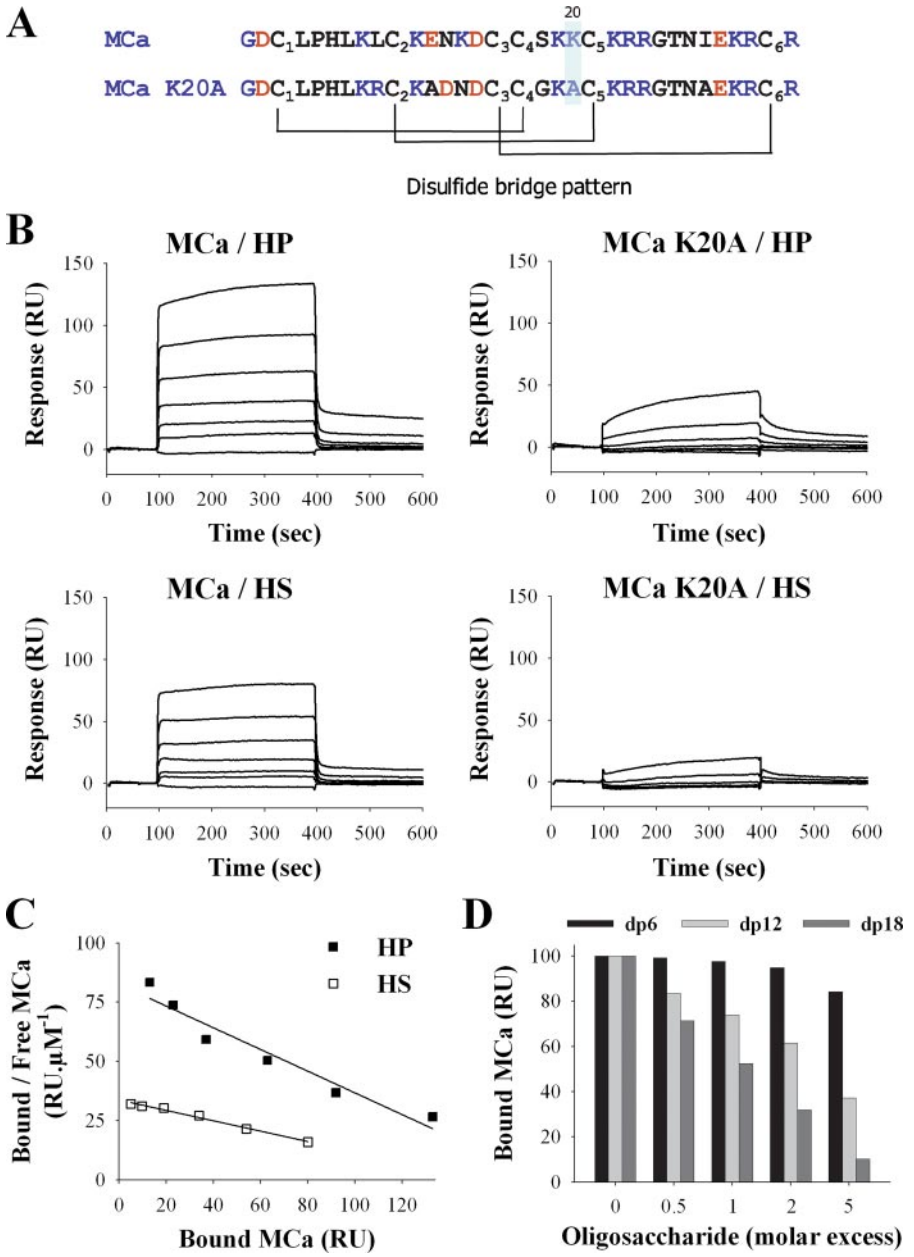

FIGURE 1. **Binding of wild-type MCa and MCa K20A to HP or HS immobilized on SPR sensorchip.** *A*, primary structure of MCa and MCa K20A. Basic and acidic residues are in *blue* and *red*, respectively. The disulfide bridge patterns of both molecules are shown. *B*, sensorgrams of the interactions. Various concentrations of MCa or MCa K20A were injected over a HP- or HS-activated surface at a flow rate of 20 µl/min during 5 min. After this peptide injection time, running buffer was injected to monitor the wash off reaction. All responses were recorded and subtracted from the control surface online as a function of time (in RUs). Each set of sensorgrams was obtained with MCa at (from *top to bottom*) 5, 2.5, 1.25, 0.62, 0.31, 0.15, and 0 µM. *C*, Scatchard plots of the equilibrium binding data measured on the sensorgrams corresponding to the injection of MCa over HP or HS SPR surfaces. Data were fitted with a linear equation of the type $y = a \times x + b$, where $a = -0.46$ (HP) or -0.22 (HS), and $b = 82.5$ (HP) or 33.7 (HS). Calculated binding affinities are $K_d = 2.1$ µM (HP) and $K_d = 4.6$ µM (HS). *D*, inhibition of the MCa/HP binding by HP-derived oligosaccharides. MCa (1 µM) was coincubated with increasing molar excess of dp6, dp12, or dp18 for 45 min, then injected over a HP-activated sensorchip for 5 min. Responses (in RU) were recorded and plotted as the percentage of maximum responses obtained without preincubation (70–80 RU).

with sharp edges, suggesting high association and dissociation rates. We were, thus, not able to extract reliable kinetic values from curve-fitting. Equilibrium data, plotted according to the Scatchard representation, were used to determine affinity (Fig. 1*C*). The straight lines obtained show that MCa recognizes a single class of binding site, characterized by an affinity constant of $K_d = 2.1$ µM (HP) or 4.6 µM (HS). Because HP (6 kDa) and HS (9 kDa), immobilized at a level of 55 and 45 RU, respectively, both permitted a maximum binding of 155 RU of MCa (3859 Da), we calculated that each HP molecule bound an average of 4.4 MCa, and each HS molecule bound an average of 8 MCa. These two molecules contain, respectively, an average of 20 and 36 saccharidic units (using an approximate M_r of 600 for the HP-derived disaccharides and 500 for the HS-derived disaccharides); thus, it can be estimated conversely that each MCa should occupy in both cases an average of 4.5 monosaccharide units (20/4.4 or 36/8) along the GAG chain.

HP is formed by the polymerization of a various number of disaccharide units. To study the effect of the size of the polymer on its interaction with MCa, we performed competition experiments using HP-derived oligosaccharides of a defined degree of polymerization (dp) (Fig. 1*D*). For this purpose wild-type MCa was preincubated with different HP-derived oligosaccharides (dp6, dp12, or dp18), as mentioned under "Experimental Procedures" and then injected over the HP-conjugated sensorchip. As shown, the oligosaccharides caused a dose-dependent inhibition of the interaction of MCa with HP. dp18 was the most active oligosaccharide with an IC_{50} close to 1 µM. In contrast, dp6 had almost no effect at 5 µM.

Dose-dependent Penetration of MCa_b-Strep-Cy5 in Wild-type and Mutant CHO Cell Lines—Results presented in Fig. 1 indicate that MCa interacts with negatively charged HP and HS. To challenge the implication of HP and HS in the cell penetration of MCa, the cell penetration efficacy of MCa_b-Strep-Cy5 was assessed using wild-type CHO cells (*CHO wild-type*) and mutant CHO cells lacking either HS (*CHO pgsD-677*) or all GAGs (*CHO pgsB-618*). Each CHO cell line was incubated for 2 h in the presence of variable concentrations of MCa_b-Strep-Cy5 complexes, and the amount of internalized complex was measured by FACS. Fig. 2*A* represents the dose-response curves for MCa_b-Strep penetration in

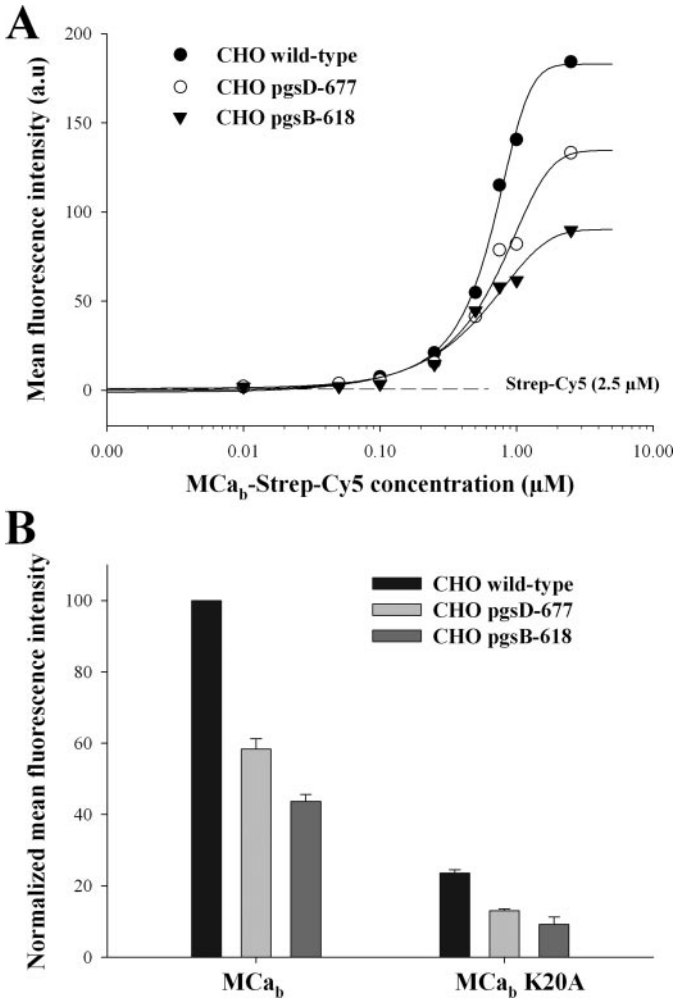

FIGURE 2. **Cell penetration of MCa$_b$-Strep-Cy5 and MCa$_b$ K20A-Strep-Cy5 in wild-type and HSPG mutant CHO cells.** *A*, dose-dependent cell penetration of wild-type MCa$_b$-Strep-Cy5 in wild-type and mutant CHO cells, as assessed quantitatively by FACS. Results are from a representative experiment. The indicated concentrations are for streptavidin-Cy5 (from 10 nM to 2.5 µM). Data were fitted by a sigmoid equation providing the following half effective concentrations: PC_{50} = 0.46 ± 0.01 µM (wild-type CHO), 0.56 ± 0.01 µM (pgsD-677), and 0.71 ± 0.01 µM (pgsB-618). *a.u.*, absorbance units. *B*, comparative cell penetration of 1 µM MCa$_b$-Strep-Cy5 and MCa$_b$ K20A-Strep-Cy5 in CHO and CHO mutant cell lines. Results are from a representative experiment of n = 3. Values are normalized with mean fluorescence intensity of wild-type CHO cells.

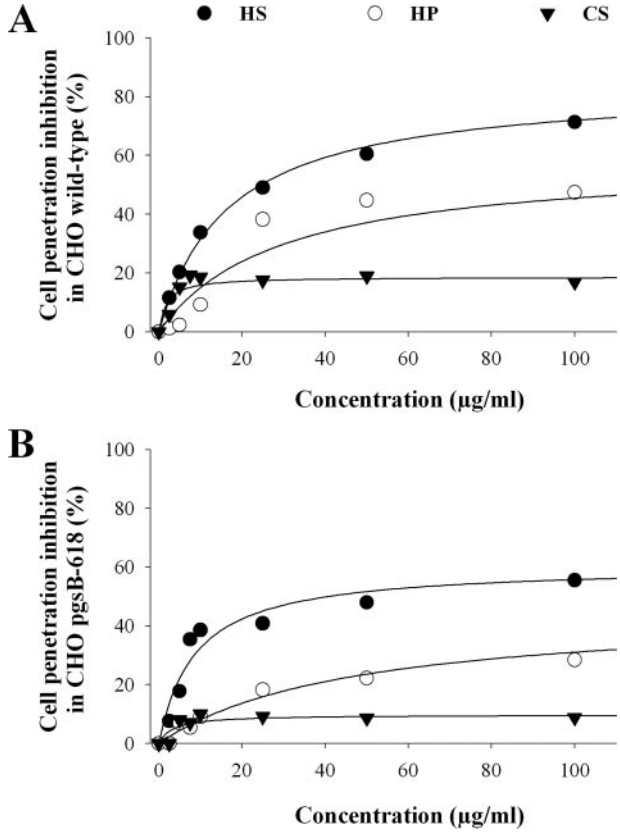

FIGURE 3. **Inhibition of MCa$_b$-Strep-Cy5 cell penetration by soluble GAGs in wild-type and GAG-deficient CHO cell lines.** *A*, dose-dependent inhibition of MCa$_b$-Strep-Cy5 cell penetration by soluble GAGs in wild-type CHO cells. Results are from a representative experiment of n = 3. Data were fitted by an hyperbola equation of the type $y = (a \times x)/(b + x)$, where a = 83.9 ± 1.7% (HS), 58.7 ± 9.8% (HP), and 18.7 ± 1.7% (CS) and b = 16.6 ± 1.2 µg/ml (HS), 29.1 ± 14.5 µg/ml (HP), and 1.8 ± 1.0 µg/ml (CS). *B*, dose-dependent inhibition of MCa$_b$-Strep-Cy5 cell penetration by soluble GAGs in GAG-deficient CHO cells. Results are from a representative experiment of n = 3. Fitting values are a = 60.6 ± 8.6% (HS), 45.4 ± 3.5% (HP), and 9.8 ± 1.3% (CS) and b = 8.6 ± 2.0 µg/ml (HS), 46.2 ± 8.9 µg/ml (HP), and 3.3 ± 2.1 µg/ml (CS).

the three CHO cell lines. Half saturation of MCa penetration (PC_{50}) was only slightly modified by the absence of GAG, with PC_{50} values of 0.46, 0.56, and 0.71 µM in CHO wild-type, CHO pgsD-677, and CHO pgsB-618, respectively. In contrast, the maximum amount of incorporated MCa$_b$-Strep-Cy5, measured in the presence of 1 µM of complex, was strongly reduced in both the pgsD-677 and pgsB-618 CHO lines compared with the wild-type CHO, 43.0 ± 3.0% (n = 3) and 57.0 ± 2.5% (n = 3) reduction in pgsD-677 and pgsB-618 CHO, respectively (Fig. 2*B*). Similar experiments were done using the mutant MCa$_b$ K20A that was previously shown to exhibit reduced penetration compared with the wild-type MCa (6). Results presented on Fig. 2*B* show that although already strongly reduced in wild-type CHO, the penetration of this mutant was further reduced in the HS- or GAGs-deficient CHO, resulting in similar reductions in cell entry; 45 ± 2% (n = 3) and 60 ± 4% (n = 3) reduction in pgsD-677 and pgsB-618 CHO, respectively. This result indicates that the mechanism of cell penetration of the K20A mutant is identical to that of wild-type MCa despite the reduction in cell entry induced by the mutation. Therefore, MCa$_b$ K20A also relies on GAG-dependent and GAG-independent mechanisms for cell penetration. This observation is consistent with the fact that the K20A mutation in MCa only reduces the PC_{50} value (6). In addition, the significant amount of MCa$_b$-Strep-Cy5 taken up by GAG-deficient cells indicates that a significant fraction of MCa$_b$-Strep-Cy5 penetration is GAG-independent, likely relying on the contribution of plasma membrane lipids.

Inhibition of Cell Penetration of MCa$_b$-Strep-Cy5 by Soluble HSPGs—According to the two observations described above, (i) interaction of MCa with HSPGs and (ii) reduction in MCa cell penetration in GAG-deficient cells, one would expect that incubation of MCa with soluble GAGs also reduces the penetration of MCa$_b$-Strep-Cy5. To challenge this point, MCa$_b$-Strep-Cy5 was preincubated with various concentrations of HS, HP, or CS for 45 min before incubation with wild-type or GAG-deficient CHO cells for 2 h. The total amount of MCa$_b$-Strep-Cy5 inside the cell was then measured by flow cytometry (Fig. 3). In wild-type CHO cells, HS (250 µg/ml) produced the most

potent inhibition of cell penetration (84 ± 2%, $n = 3$, Fig. 3*A*). HP and CS were less efficient than HS with a mean inhibition of 59 ± 10% ($n = 3$) and 19 ± 2% ($n = 3$) for HP and CS, respectively (at 250 μg/ml). Linking inhibition with the global negative charge of the GAG tested remains hazardous because charge relationship follows the rule HP > CS > HS, and here we observe HS > HP > CS. Interestingly, all three GAGs also reduced the cell penetration of MCa_b-Strep-Cy5 in GAG-deficient cells with the same rank as observed for wild-type CHO cells (Fig. 3*B*). Incubation of MCa_b-Strep-Cy5 with HS, HP, or CS induced a significant inhibition in GAG-deficient cells (61 ± 9% ($n = 3$), 45 ± 4% ($n = 3$), and 10 ± 1% ($n = 3$) in the presence, respectively, of 250 μg/ml HS, HP, and CS) although lower than in wild-type CHO cells. Therefore, these data indicate that binding of soluble GAGs to MCa inhibits the cell penetration of MCa_b-Strep-Cy5 not only by preventing its interaction with CHO cell surface GAGs but also with non-GAG cell surface components.

To check whether GAGs could inhibit the interaction of MCa with membrane lipids, we investigated the effect of HP on MCa_b interaction with lipids immobilized on strips (Fig. 4*A*). MCa_b (100 nM) was incubated for 45 min in the presence or absence of HP (10 μg/ml) before incubation with lipid strips, as described under "Experimental Procedures." As shown in Fig. 4, HP significantly decreased the interaction of MCa_b with phosphatidic acid (66%), sulfatide (30%), phosphatidylinositol (Ptdlns) (4)P (31%), Ptdlns(3,4)P_2 (26%), and Ptdlns(3,4,5)P_3 (72%) but not with lipids such as Ptdlns(3)P, Ptdlns(5)P, or Ptdlns(3,4,5)P_2. These results provide a clear explanation of the fact that the interaction of MCa_b with soluble GAGs may also lead to an inhibition of the GAG-independent MCa_b cell penetration.

Effect of HSPGs on the Cell Distribution of MCa_b-Strep-Cy5—To examine the contribution of cell surface GAGs to the cell distribution of MCa_b-Strep-Cy5, MCa_b-Strep-Cy5 localization within the cell was defined using confocal microscopy and compared between wild-type and GAG-deficient CHO cell lines. For these experiments the plasma membrane, the nucleus, and MCa_b-Strep were labeled with concanavalin A (green), dihydroethidium (red), and Cy5 (blue), respectively. Images presented on Fig. 5 were obtained 2 h after the start of the cell incubation. Living cells were used to avoid possible cell distribution artifacts that may occur during the fixation procedure (5, 9, 23). As shown, MCa_b coupling to Strep-Cy5 is required for the cell penetration of Strep-Cy5 into CHO cells (Fig. 5*A*). The MCa_b-Strep-Cy5 complex is exclusively present as punctuate dots in the cytoplasm of living CHO cells. A similar cell distribution is observed in living CHO cell mutants lacking just HS (pgsD-677) or all GAGs (pgsB-618), suggesting that GAG-dependent and GAG-independent cell entries produce similar cell distributions (Fig. 5*B*). A Strep-Cy5 complex made with the MCa_b K20A analogue produces a similar subcellular distribution than MCa_b-Strep-Cy5 in wild-type and HS-deficient CHO cells, suggesting that the mechanism of cell penetration is not altered by point mutation of MCa_b (data not shown). Punctuate staining of MCa_b-Strep-Cy5 is indicative of a form of endosomal localization. This point was further investigated.

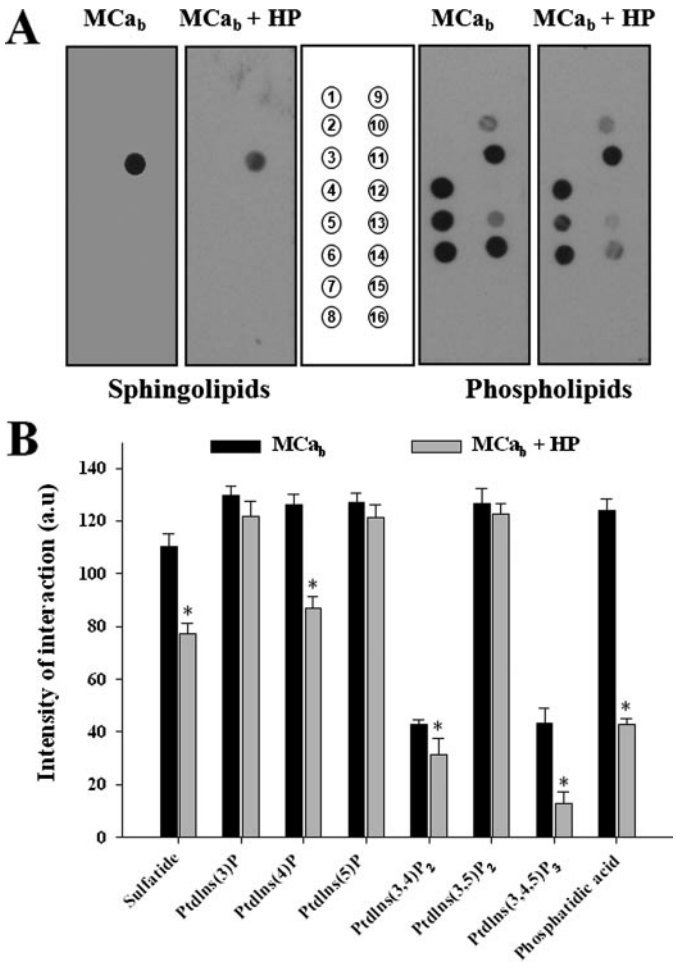

FIGURE 4. **Effect of HP on the interaction of MCa_b with membrane lipids.** *A*, 100 nM MCa_b alone or MCa_b preincubated for 45 min with 10 μg/ml of HP was incubated for 2 h with lipid strips. Each dot corresponds to 100 pmol of lipid immobilized on the strip. *Left panel*, interaction with various sphingolipids. *1*, sphingosine; *2*, sphingosine 1-phosphate; *3*, phytosphingosine; *4*, ceramide; *5*, sphingomyelin; *6*, sphingosylphosphophocholine; *7*, lysophosphatidic acid; *8*, myriocin; *9*, monosialoganglioside; *10*, disialoganglioside; *11*, sulfatide; *12*, sphingosylgalactoside; *13*, cholesterol; *14*, lysophosphatidyl choline; *15*, phosphatidylcholine; *16*, blank). *Right panel*, interaction with various phospholipids. The lipids are identified by their numbered positions on the strip (*middle panel*). *1*, lysophosphatidic acid; *2*, lysophosphatidylcholine; *3*, Ptdlns; *4*, Ptdlns(3)P; *5*, Ptdlns(4)P; *6*, Ptdlns(5)P; *7*, phosphatidylethanolamine; *8*, phosphatidylcholine; *9*, sphingosine 1-phosphate; *10*, Ptdlns(3,4)P_2; *11*, Ptdlns(3,5)P_2; 12, Ptdlns(4,5)P_2; *13*, Ptdlns(3,4,5)P_3; *14*, phosphatidic acid; *15*, phosphatidylserine; *16*, blank. *B*, Intensity of the interaction of MCa_b or MCa_b + HP with various lipids as analyzed by Image J (NIH). The data are quantified in arbitrary units, and the results are presented as histograms. These experiments were repeated three times; data shown as triplicates. Significance is provided as a deviation of three times the S.D. value from 100% (denoted as *asterisks*). *a.u.*, arbitrary units.

MCa_b-Strep-Cy5 Localizes to Endosomal Structures That Do Not Originate from Clathrin-mediated Endocytosis—Using confocal microscopy, the cell distribution of MCa_b-Strep-Cy5 was compared with that of endosomal structures as revealed by LysoTracker red staining. As shown on Fig. 6*A*, there is a very good co-localization between MCa_b-Strep-Cy5 and LysoTracker red fluorescence in all cell lines used (CHO wild-type, CHO pgsB-618, and CHO pgsD-677). These data clearly indicate that the lack of GAGs does not alter the subcellular localization of MCa_b-Strep-Cy5, suggesting that both GAG-dependent and GAG-independent cell penetration rely on

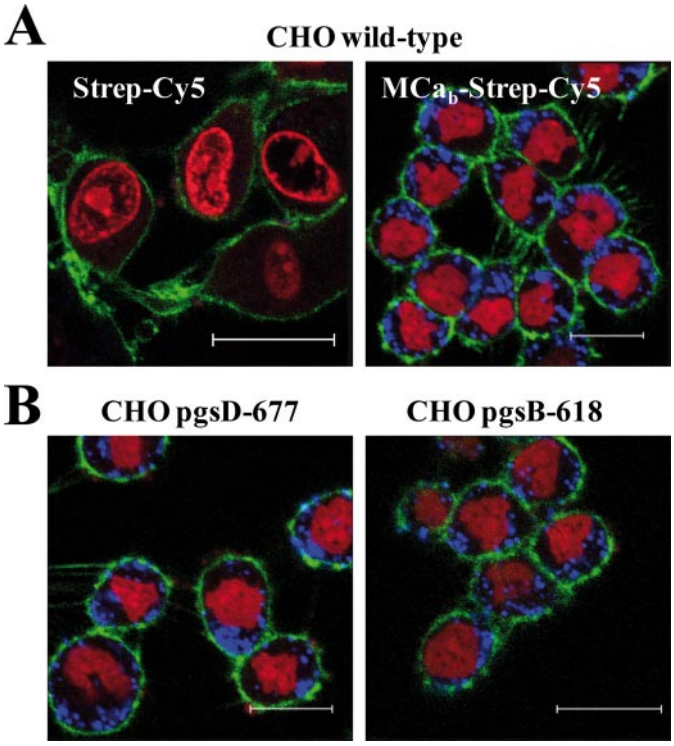

FIGURE 5. **Cell distribution of MCa$_b$-Strep-Cy5 in living wild-type or mutant CHO cells.** *A*, confocal images showing the cell penetration of Strep-Cy5 (2 h of incubation) in the absence (*left panel*) or presence (*right panel*) of MCa$_b$ (4 μM) in wild-type CHO cells. *Scale bars*, 25 μm (*left*) and 15 μm (*right bar*). *B*, cell distribution of MCa$_b$-Strep-Cy5 in mutant CHO cells. *Scale bars*, 15 μm (*left*) and 20 μm (*right bar*). *Blue*, Strep-Cy5; *red*, dihydroethidium, nuclei; *green*, concanavalin A, plasma membrane.

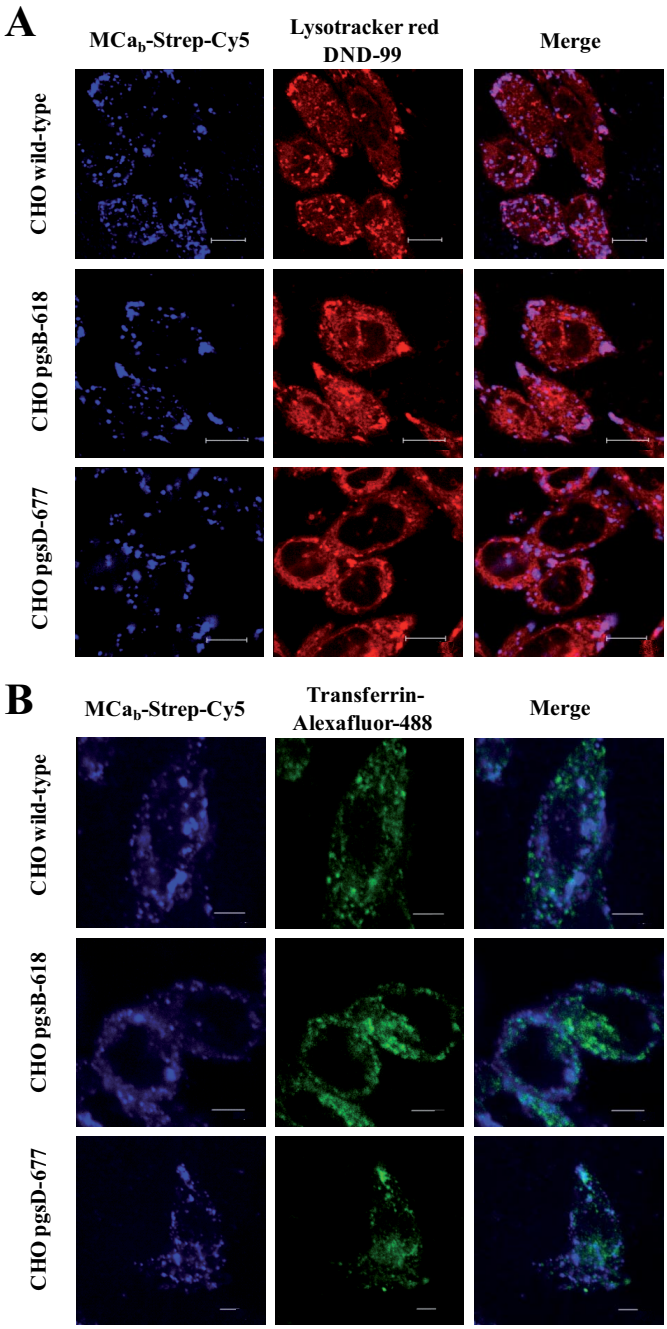

FIGURE 6. **MCa$_b$-Strep-Cy5 entry and endocytosis.** *A*, endocytic route of entry of MCa$_b$-Strep-Cy5. Various CHO cell lines (*upper panels*, wild type; *middle panels*, pgsB-618; *lower panels*, pgsD-677,) were incubated 2 h with 1 μM of MCa$_b$-Strep-Cy5, washed, and incubated with 50 nM LysoTracker red DND-99 for 20 min right before confocal acquisition. *Scale bars*, 10 μm (*upper panels*) and 11 μm (*middle* and *lower panels*). *B*, different endocytic entry pathways for transferrin-Alexa Fluor 488 and MCa$_b$-Strep-Cy5. Confocal immunofluorescence images of living wild-type or mutant CHO cells to compare the cell distribution of transferrin-Alexa Fluor 488 and MCa$_b$-Strep-Cy5. Cells were incubated 2 h with 1 μM MCa$_b$-Strep-Cy5 (*blue*) along with 25 μg/ml transferrin-Alexa Fluor 488 (*green*), washed, and immediately analyzed by confocal microscopy. *Scale bars*, 5 μm.

endocytosis. To determine whether the type of endocytosis involved in MCa$_b$-Strep-Cy5 entry could be altered in GAG-deficient cells, we first analyzed whether it had common features with clathrin-mediated endocytosis. Transferrin is known to enter cells via transferrin receptors through clathrin-mediated endocytosis (24, 25). As shown here, there was an almost complete absence of co-localization between MCa$_b$-Strep-Cy5 and transferrin-labeled with Alexa Fluor 488 in wild-type as well as in mutant CHO cells (Fig. 6*B*). These data indicate that the route of entry of Strep-Cy5 when coupled to MCa$_b$ is not through clathrin-mediated endocytosis. It also indicates that the absence of GAGs at the cell surface does not favor clathrin-dependent endocytosis for the cell entry of MCa$_b$-Strep-Cy5 over other mechanisms of endocytosis. Expression of a dominant-negative mutant of dynamin 2, dynamin 2 K44A, is known to prevent normal clathrin-mediated endocytosis (26). As shown in Fig. 7*A*, expression of dynamin 2 K44A prevents the entry of transferrin-Alexa Fluor-594 in both wild-type and GAG-deficient CHO cells, confirming that transferrin receptors get internalized by clathrin-mediated endocytosis. In contrast, MCa$_b$-Strep-Cy3 entry was not prevented by the expression of dynamin 2 K44A (Fig. 7*B*), clearly indicating that clathrin-mediated endocytosis was not required for the entry of MCa$_b$ when coupled to streptavidin.

Lack of Alteration of the Main Endocytosis Entry Pathway in GAG-depleted Cells—To further identify the route of entry of MCa$_b$-Strep-Cy5 and analyze the impact of GAG depletion on this process, several inhibitors were tested by FACS on the entry of MCa$_b$-Strep-Cy5 in wild-type (Fig. 8*A*) and pgsB-618 CHO cells (Fig. 8*B*). These inhibitors were also tested on the entry of transferrin-Alexa Fluor 488 for comparison. Amiloride was tested to block macropinocytosis, methyl-β-cyclodextrin to deplete membrane cholesterol and inhibit lipid raft-depend-

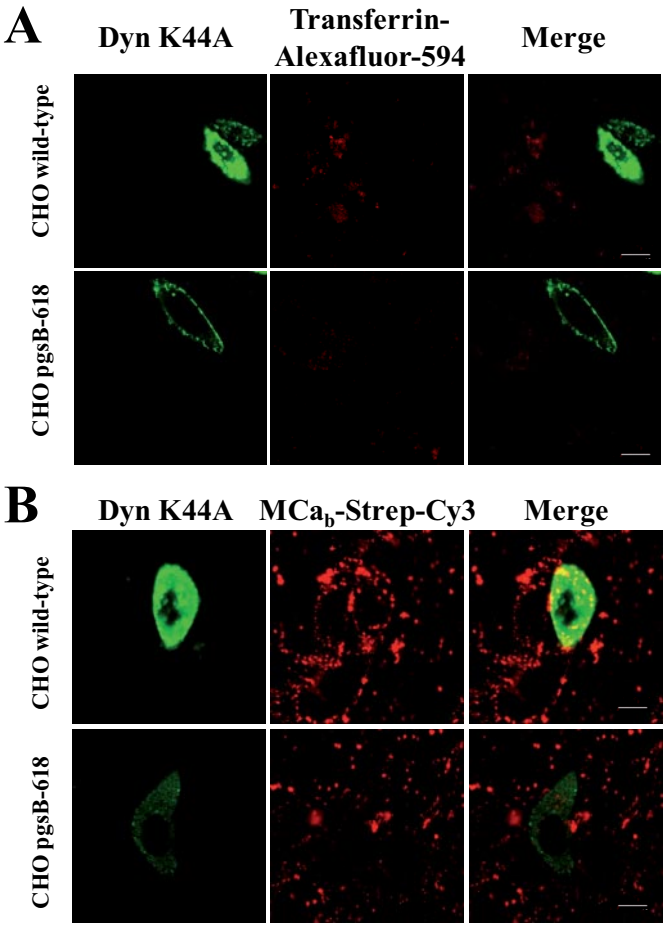

FIGURE 7. **Expression of the dominant-negative dynamin 2 K44A mutant blocks clathrin-mediated endocytosis and transferring entry but spares MCa$_b$-Strep-Cy3 entry.** *A*, transferrin entry is inhibited in dynamin 2 K44A transfected wild-type and pgsB-618 mutant CHO cells. *B*, MCa$_b$-Strep-Cy3 entry is preserved in dynamin 2 K44A-transfected wild-type and pgsB-618 mutant CHO cells. *Scale bars*, 10 μM. Note that expression of dynamin 2 K44A mutant was always less in pgsB-618 mutant CHO cells than in wild-type CHO cells, possibly due to a role of GAGs in plasmid entry.

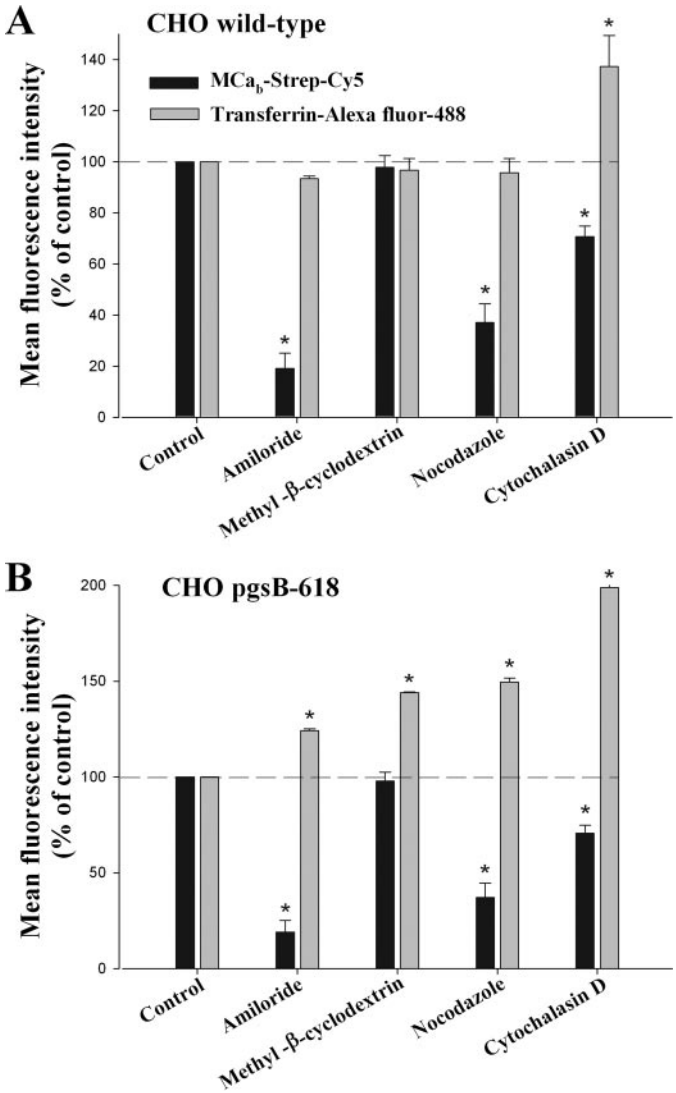

FIGURE 8. **Effect of endocytic inhibitors on the entry of transferrin-Alexa Fluor 488 and MCa$_b$-Strep-Cy5.** Data are expressed in percentage of mean control fluorescence as assessed by FACS. Average data are from three experiments. *A*, data for wild-type CHO cells. *B*, data for pgsB-618 CHO cells. Significance is provided as a deviation of three times the S.D. value from 100% (denoted as *asterisks*).

ent pathways, nocodazole to inhibit microtubule formation, and cytochalasin D to inhibit F-actin elongation, required for macropinocytosis and clathrin-dependent endocytosis (27). Chlorpromazine, an inhibitor of clathrin-mediated endocytosis, could not be tested because it produced cell dissociation from the plastic dish surface (data not shown). In wild-type CHO cells, transferrin-Alexa Fluor 488 endocytosis was not affected by amiloride, methyl-β-cyclodextrin, or nocodazole, as expected for clathrin-mediated endocytosis. Cytochalasin D was found to produce a curious 37% increase in the cell entry of transferrin, indicating an alteration in clathrin-dependent endocytosis. In contrast, with the exception of methyl-β-cyclodextrin, all drugs tested were found to inhibit partially the entry of MCa$_b$-Strep-Cy5 in wild-type CHO cells (Fig. 8*A*). The lack of effect of methyl-β-cyclodextrin indicates that caveolae-mediated endocytosis is not involved in the entry of MCa$_b$-Strep-Cy5. The fact that both amiloride and cytochalasin D inhibit MCa$_b$-Strep-Cy5 cell entry by 80 and 30%, respectively, indicates a significant contribution of macropinocytosis pathway. Cytochalasin D probably acts exclusively on macropinocytosis for the cell entry of MCa$_b$-Strep-Cy5 as the involvement of the other major endocytic pathway affected by this drug, clathrin-mediated endocytosis, can be ruled out. Nocodazole, which has a wide range of effects on various endocytosis pathways, also had a great effect, inducing a 63% reduction of MCa$_b$-Strep-Cy5 cell entry. Thus, the rather segregated effects of endocytosis inhibitors on cell penetration of transferrin and MCa$_b$-Strep-Cy5 is coherent with their lack of colocalization inside cells (Fig. 6*B*). These data stress the importance of macropinocytosis as the main entry pathway of Strep-Cy5 when coupled to MCa$_b$. The same set of drugs was then tested for the cell entry of both transferrin and MCa$_b$-Strep-Cy5 in GAG-deficient pgsB-618 CHO cells (Fig. 8*B*). Interestingly, in the absence of GAGs, the effects of the endocytosis inhibitors on MCa$_b$-Strep-Cy5 entry were not altered, indicating that in the absence of cell surface GAGs, macropinocytosis is still the main route of entry of the complex. This is in perfect agreement with the data shown in Figs. 5 and 6, suggesting similar cell distribution of the complex,

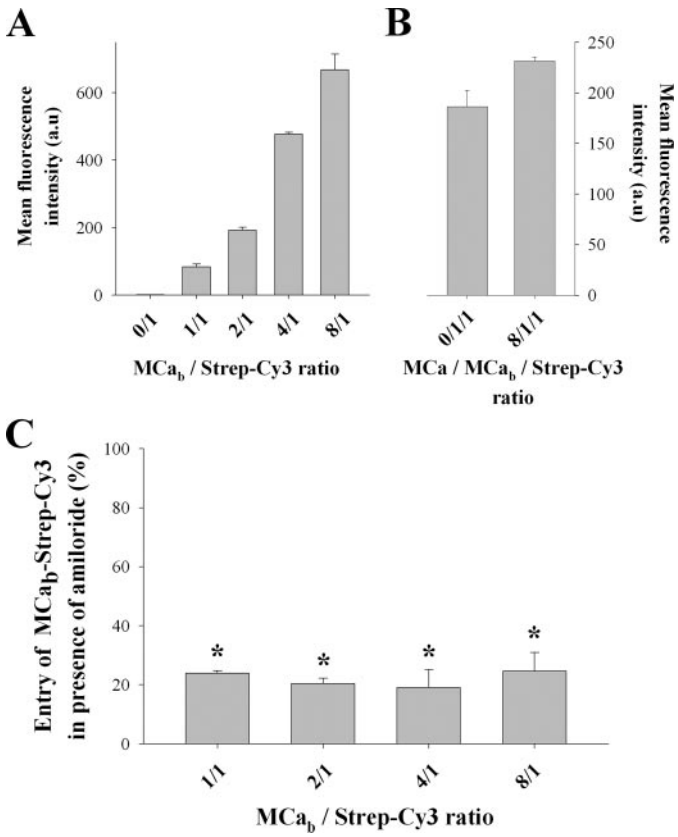

FIGURE 9. **Effect of MCa$_b$/strep ratio on the cell penetration of strep.** *A*, effect of MCa$_b$/Strep-Cy3 ratio on the total entry of Strep-Cy3 in wild-type CHO cells. *B*, effect of an 8-fold molar excess of non-biotinylated MCa on the penetration of MCa$_b$-Strep-Cy3 at a 1:1 molar ratio. *C*, effect of 5 mM amiloride on Strep-Cy3 entry into wild-type CHO cells as a function of MCa$_b$/Strep-Cy3 ratio. Significance is provided as a deviation of 3× the S.D. value from 100% (denoted as *asterisks*). Strep-Cy3 concentration was kept constant at 1 μM in all experiments. *a.u.*, arbitrary units.

colocalization with LysoTracker red, and identical effects of dynamin 2 K44A expression. Surprisingly, the absence of GAGs had an impact on the effects of the drugs on transferrin entry (Fig. 8*B*). Although no clear explanation can be provided for this observation, it may suggest that in the absence of GAGs inhibition of alternative endocytosis pathways favors somehow clathrin-mediated endocytosis. These effects remain, however, outside the focus of this study, namely the entry pathways of MCa, but are clear indications of the potential importance of GAGs in endocytosis.

The Molar Ratio MCa$_b$/Strep-Cy3 Does Not Influence the Type of Endocytosis—Streptavidin molecules are tetramers that can bind up to four MCa$_b$ peptides. It is, therefore, possible that the number of bound peptides may somehow affect the residency time of the complex at the cell surface and thereby influence the mode of cell penetration. To test this hypothesis, various molar ratios of MCa$_b$ and Strep-Cy3 were mixed together to prepare complexes with increased numbers of MCa$_b$ immobilized on Strep-Cy3. The exact molar ratio between MCa$_b$ and Strep-Cy3 can, however, not be warranted by simply mixing various molar ratios of the two molecules. Once these complexes were prepared, their cell entry along with the effect of amiloride was quantified by FACS (Fig. 9). Increasing the molar ratio of MCa$_b$ over Strep-Cy3 from 1:1 to 8:1 dramatically increased the amount of Strep-Cy3 that penetrates into wild-type CHO cells (Fig. 9*A*). These data indicate that immobilizing an increasing number of MCa$_b$ onto streptavidin greatly favors the entry of the complex, possibly by multiplying the number of contacts with cell surface components and/or increasing the residency time at the cell surface. In contrast, using increased amounts of non-biotinylated MCa, unable to bind Strep-Cy3, in place of MCa$_b$ did not produce any increase in Strep-Cy3 penetration, indicating that coupling of MCa to Strep-Cy3 was required (Fig. 9*B*). This result also shows that the association of MCa to cell surface components does not trigger a generalized increase in cell endocytosis that would indirectly favor the penetration of MCa$_b$-Strep-Cy3 complexes. Finally, Fig. 9*C* indicates that coupling several MCa$_b$ peptides to streptavidin does not quantitatively alter the effect of 5 mM amiloride, indicating that macropinocytosis remains the predominant mode of entry of the complex regardless of the MCa$_b$/Strep-Cy3 molar ratio used.

DISCUSSION

HSPGs Are New Cell Surface Targets of MCa That Are Involved in Cell Penetration of This Peptide—Using a Biacore system, we have demonstrated that MCa, a member of a new family of CPPs, directly interacts with HP and HS with affinities in the low micromolar range (between 2 and 5 μM). These values are more or less well correlated to the PC$_{50}$ values of MCa$_b$-Strep-Cy5 in CHO cells (around 0.5 μM), suggesting a contribution of HSPGs to the cell penetration of this complex. This slight difference could be related to the fact that each streptavidin molecule has the ability to bind four MCa molecules, thereby increasing the local concentration of the CPP in the vicinity of the cell surface receptors. Indeed, we show here that increasing the molar ratio of MCa$_b$ over streptavidin during complex formation produces an increase in cell penetration efficiency. Alternatively, differences may also be related to the exact nature of the cell surface HSPG involved in MCa interaction. By using HS- and GAG-deficient CHO cell lines, we conclusively demonstrate that HSPGs quantitatively contribute to more than 57% of the cell entry of Strep-Cy5 when coupled to MCa. HS represents the most important GAG since it is responsible for 75% of the GAG contribution. However, because a significant fraction of the total cell entry is conserved in GAG-deficient cells, the entry of MCa$_b$-Strep-Cy5 does not solely rely on GAGs but also on other cell surface components, with apparent affinities closely related to that of MCa for HSPGs since the PC$_{50}$ values varied only mildly in GAG-deficient CHO cells. Data presented here and in previous manuscripts (5, 6) indicate that membrane lipids are also cell surface receptors for MCa. For instance, MCa was found to interact with the ganglioside GD3 with a closely related apparent affinity of 0.49 μM. Another important conclusion that can be made from these data is that the increase or the decrease of the penetration efficiency observed with specific mutants of MCa, such as MCa K20A tested herein, results from a modification of the apparent affinity of these MCa mutants for the cell surface components with which they interact. For instance, MCa K20A was found to have reduced apparent affinity for both HS and HP (present data) but also for membrane lipids (6). There is, thus,

an interesting parallel to pursue on the structural determinants of CPP interaction with HSPGs and negatively charged lipids that may ultimately result in the design of better CPP analogues. This observation appears particularly pertinent since the cell entry process of MCa-Strep-Cy5 or MCa-Strep-Cy3 complex, *i.e.* macropinocytosis, seems independent of the type of membrane receptor involved in MCa binding (HSPGs *versus* lipids).

HP Inhibition of the Cell Penetration of MCa-Strep Complex Is Not Limited to the Interaction of This CPP to Cell Surface HSPGs—HP-induced inhibition of CPPs cell entry is generally interpreted as being due to an inhibition of CPP interaction with cell surface HSPGs (28). However, an alternative possibility is that, by neutralizing the basic face of MCa, the interaction of HP with MCa also inhibits the subsequent interaction of MCa with negatively charged lipids of the cells, another surface component for the route of entry of MCa. Three sets of evidence indicate that this interpretation is likely to be correct. First, both soluble HS and HP inhibit the cell entry of MCa_b-Strep-Cy5 to levels beyond that measured for MCa_b-Strep-Cy5 entry in HS- and GAG-deficient CHO cells. Second, soluble HS and HP still produce significant reductions of MCa_b-Strep-Cy5 entry in GAG-deficient CHO cells, clearly indicating an inhibition through an alternate mode of inhibition. Third, incubation of HS with MCa_b produces a reduction in the interaction of MCa_b with several negatively charged lipids, the most dramatic effects being observed for PtdIns(3,4,5)P_3 and phosphatidic acid. These observations indicate that interpretation of the involvement of cell surface HSPGs in the penetration of CPPs based on soluble HP inhibition should be performed carefully. They also confirm the importance of the basic face of CPPs in the mechanism of cell penetration. Finally, the presence of a residual MCa-Strep complex penetration in GAG-deficient CHO cells in the presence of HS or HP might indicate that either the interaction between HSPGs is rapidly reversible or that this interaction does not fully cover the entire molecular surface of MCa required for cell penetration. Further detailed biochemical experiments will be needed to sort out the molecular determinants of MCa involved in HP or HS interaction. Such an investigation will determine to what extent the basic surface of MCa is involved in an interaction with HSPGs.

Macropinocytosis Is the Main Endocytic Pathway Used by MCa When Coupled to Streptavidin in GAG-positive and GAG-deficient CHO Cells—In previous work, we reported that MCa-Strep complex penetration in HEK293 cells was also observed in the presence of amiloride or nystatin, suggesting that a non-endocytic pathway was involved in the penetration process (4). Here, we provide a quantitative analysis of the effects of endocytosis inhibitors on the entry of MCa_b-Strep-Cy5 in CHO cells using a FACS method and show that endocytosis represents the major route of penetration, whereas only 20% of MCa_b-Strep-Cy5 penetration is still observed in the presence of endocytosis inhibitors (amiloride). Interestingly, the amount of MCa_b-Strep-Cy5 taken up in the presence of amiloride is close to the amount of complex taken up in GAG-deficient CHO cells in the presence of HS or HP. The apparent discrepancy between the two studies is likely due to the fact that confocal analysis used in the previous work was not quantitative enough to allow the calculation of the relative importance of each mechanism. Moreover, we cannot rule out the possibility that some endocytosis pathway, insensitive to amiloride or nystatin, may be present in the previously studied HEK293 cell line. This indicates that one needs to be cautious with regard to confocal images that are unfortunately not quantitative enough to rule out one or several cellular mechanisms for cell entry. Use of a marker of endosomes demonstrates that MCa_b-Strep-Cy5 is distributed within endosomes after cell entry, supporting the fact that endocytosis is a predominant route of entry of the cargo when coupled to MCa_b. The total lack of co-localization between transferrin-Alexa Fluor 488 and MCa_b-Strep-Cy5 clearly indicates that clathrin-mediated endocytosis is not at play in the entry of MCa_b-Strep-Cy5. This was further proven by (i) the lack of effect of expression of dynamin 2 K44A, a dominant negative construct that inhibits clathrin-mediated endocytosis but does not prevent MCa_b-Strep-Cy3 entry and (ii) the differential effects of various endocytosis blockers on transferrin-Alexa Fluor 488 and MCa_b-Strep-Cy5 cell entries. The effects of cytochalasin D and of amiloride indicate that macropinocytosis is predominantly involved in the cell entry of MCa_b-Strep-Cy5. This observation is consistent with many other reports that indicate a role of macropinocytosis in cell entry of other CPPs (14, 29). However, the lack of effect of methyl-β-cyclodextrin appears to indicate that endocytosis of MCa_b-Strep-Cy5 is not dependent on lipid rafts or at least on cholesterol availability. Because macropinocytosis appears to be responsible for the uptake of MCa_b-Strep-Cy5/3 in wild-type and GAG-deficient CHO cells alike, it seems that all surface components able to bind MCa, negatively charged HSPGs, and lipids are involved in macropinocytosis. Because of the nature of macropinosomes, which do not fuse with lysosomes and are leaky, it is likely that release of CPPs in the cytosol may occur very slowly. In the case of the Strep-Cy5 cargo, this leakage was, however, not observed when coupled to MCa_b.

Cargo Dependence of MCa Mode of Penetration and/or Release in the Cytosol?—The mechanism of cell penetration of CPPs remains highly debated. There are pro and con arguments in favor of membrane translocation, a process whereby the peptide would flip from the outer face of the plasma membrane to the inner face then be released free into the cytoplasm. Here we do not provide compelling evidence for a translocation mechanism for Strep-Cy5 entry when coupled to MCa_b. On the contrary, the data strongly emphasize the importance of endocytosis in the penetration of the vector/cargo complex. Nevertheless, the issue of the mode of penetration of MCa itself remains open to a large extent. First, there is compelling evidence that MCa has a near-complete pharmacological effect when applied at the extracellular face of cells. Second, the pharmacological site of MCa on the ryanodine receptor has been localized to the cytosol face of the calcium channel. Taken together, these results suggest that MCa must reach the cytosol within seconds or minutes. Two possibilities can be envisioned; (i) MCa may be released within the cytosol from leaky macropinosomes immediately after uptake, but the time scale seems inappropriate, or (ii) when "free", *i.e.* not coupled to a cargo, MCa may indeed simply translocate through the membrane. This raises immediately the question of the contribution of the

cargo to the mode of entry of MCa. Streptavidin is a cargo that can bind four different MCa_b molecules. Linking multiple vectors to a single cargo molecule could theoretically complicate the mode of entry of MCa. Intuitively, one could imagine that multiple attachment points to cell surface components might hamper the translocation of the peptide through the plasma membrane, increase the residency time at the cell surface, and thereby strongly promote macropinocytosis over direct translocation. Experimentally, this is, however, not observed. The fact that amiloride inhibits penetration of MCa_b-Strep-Cy5 complex, prepared with 1 MCa_b for 1 Strep-Cy5, as efficiently as the penetration of MCa_b-Strep-Cy5 complex, prepared with 8 MCa_b for 1 Strep-Cy5, indicates that macropinocytosis is not influenced by the presence of multiple MCa_b molecules. Therefore, the putative difference between free MCa_b and MCa_b-cargo complex might be due to the nature of the cargo rather than its specific properties of MCa_b binding. In addition, the size of the cargo may itself represent a problem for simple diffusion of the complex from "leaky" macropinosomes to the cytosol. Further studies will be required to investigate the contribution of cargo size and nature in the mode of entry and cell distribution (cytosol *versus* endosomes) of the vector. Nevertheless, these data are coherent with many other studies on CPPs, and macropinocytosis is likely to be the main entry route of many other cargoes that will be attached to maurocalcine. Although streptavidin is used as a reporter cargo here (fluorescence property), it is worth mentioning that its ability to bind to several different biotinylated molecules at a time should be considered as a significant advantage for the cell delivery of multiple cargoes with a single MCa vector.

Acknowledgments—We thank Rabia Sadir for the kind preparation of oligosaccharides. We also thank Dr. McNiven MA for providing the cDNA encoding dynamin 2 K44A mutant.

REFERENCES

1. Mosbah, A., Kharrat, R., Fajloun, Z., Renisio, J. G., Blanc, E., Sabatier, J. M., El Ayeb, M., and Darbon, H. (2000) *Proteins* **40,** 436–442
2. Esteve, E., Smida-Rezgui, S., Sarkozi, S., Szegedi, C., Regaya, I., Chen, L., Altafaj, X., Rochat, H., Allen, P., Pessah, I. N., Marty, I., Sabatier, J. M., Jona, I., De Waard, M., and Ronjat, M. (2003) *J. Biol. Chem.* **278,** 37822–37831
3. Chen, L., Esteve, E., Sabatier, J. M., Ronjat, M., De Waard, M., Allen, P. D., and Pessah, I. N. (2003) *J. Biol. Chem.* **278,** 16095–16106
4. Esteve, E., Mabrouk, K., Dupuis, A., Smida-Rezgui, S., Altafaj, X., Grunwald, D., Platel, J. C., Andreotti, N., Marty, I., Sabatier, J. M., Ronjat, M., and De Waard, M. (2005) *J. Biol. Chem.* **280,** 12833–12839
5. Boisseau, S., Mabrouk, K., Ram, N., Garmy, N., Collin, V., Tadmouri, A., Mikati, M., Sabatier, J. M., Ronjat, M., Fantini, J., and De Waard, M. (2006) *Biochim. Biophys. Acta* **1758,** 308–319
6. Mabrouk, K., Ram, N., Boisseau, S., Strappazzon, F., Rehaim, A., Sadoul, R., Darbon, H., Ronjat, M., and De Waard, M. (2007) *Biochim. Biophys. Acta* **1768,** 2528–2540
7. Derossi, D., Calvet, S., Trembleau, A., Brunissen, A., Chassaing, G., and Prochiantz, A. (1996) *J. Biol. Chem.* **271,** 18188–18193
8. Suzuki, T., Futaki, S., Niwa, M., Tanaka, S., Ueda, K., and Sugiura, Y. (2002) *J. Biol. Chem.* **277,** 2437–2443
9. Vives, E., Richard, J. P., Rispal, C., and Lebleu, B. (2003) *Curr. Protein Pept. Sci.* **4,** 125–132
10. Vives, E., Brodin, P., and Lebleu, B. (1997) *J. Biol. Chem.* **272,** 16010–16017
11. Terrone, D., Sang, S. L., Roudaia, L., and Silvius, J. R. (2003) *Biochemistry* **42,** 13787–13799
12. Berlose, J. P., Convert, O., Derossi, D., Brunissen, A., and Chassaing, G. (1996) *Eur. J. Biochem.* **242,** 372–386
13. Magzoub, M., and Graslund, A. (2004) *Q. Rev. Biophys.* **37,** 147–195
14. Wadia, J. S., Stan, R. V., and Dowdy, S. F. (2004) *Nat. Med.* **10,** 310–315
15. Foerg, C., Ziegler, U., Fernandez-Carneado, J., Giralt, E., Rennert, R., Beck-Sickinger, A. G., and Merkle, H. P. (2005) *Biochemistry* **44,** 72–81
16. Sandgren, S., Cheng, F., and Belting, M. (2002) *J. Biol. Chem.* **277,** 38877–38883
17. Nakase, I., Tadokoro, A., Kawabata, N., Takeuchi, T., Katoh, H., Hiramoto, K., Negishi, M., Nomizu, M., Sugiura, Y., and Futaki, S. (2007) *Biochemistry* **46,** 492–501
18. Laguri, C., Sadir, R., Rueda, P., Baleux, F., Gans, P., Arenzana-Seisdedos, F., and Lortat-Jacob, H. (2007) *PLoS ONE* **2,** e1110
19. Sadir, R., Baleux, F., Grosdidier, A., Imberty, A., and Lortat-Jacob, H. (2001) *J. Biol. Chem.* **276,** 8288–8296
20. Vives, R. R., Imberty, A., Sattentau, Q. J., and Lortat-Jacob, H. (2005) *J. Biol. Chem.* **280,** 21353–21357
21. Vives, R. R., Sadir, R., Imberty, A., Rencurosi, A., and Lortat-Jacob, H. (2002) *Biochemistry* **41,** 14779–14789
22. Sarrazin, S., Bonnaffe, D., Lubineau, A., and Lortat-Jacob, H. (2005) *J. Biol. Chem.* **280,** 37558–37564
23. Richard, J. P., Melikov, K., Vives, E., Ramos, C., Verbeure, B., Gait, M. J., Chernomordik, L. V., and Lebleu, B. (2003) *J. Biol. Chem.* **278,** 585–590
24. Kurten, R. C. (2003) *Adv. Drug Delivery Rev.* **55,** 1405–1419
25. Conner, S. D., and Schmid, S. L. (2003) *Nature* **422,** 37–44
26. Sun, T. X., Van Hoek, A., Huang, Y., Bouley, R., McLaughlin, M., and Brown, D. (2002) *Am. J. Physiol. Renal Physiol.* **282,** 998–1011
27. Mano, M., Teodosio, C., Paiva, A., Simoes, S., and Pedroso de Lima, M. C. (2005) *Biochem. J.* **390,** 603–612
28. Nascimento, F. D., Hayashi, M. A., Kerkis, A., Oliveira, V., Oliveira, E. B., Radis-Baptista, G., Nader, H. B., Yamane, T., Tersariol, I. L., and Kerkis, I. (2007) *J. Biol. Chem.* **282,** 21349–21360
29. Rinne, J., Albarran, B., Jylhava, J., Ihalainen, T. O., Kankaanpaa, P., Hytonen, V. P., Stayton, P. S., Kulomaa, M. S., and Vihinen-Ranta, M. (2007) *BMC Biotechnol.* **7,** 1

Conclusion

Cell surface components, such as HSPGs and negatively charged lipids, are major gateways for the translocation of CPPs across the cell membrane. They facilitate the accumulation of CPPs on the plasma membrane through charge interaction and this interaction can either lead to direct translocation (Morris et al., 2008) or endocytotic uptake (Article III) of the CPP. The mechanism of internalization of CPPs has not been resolved yet. Allthough there are some common features among these CPPs, the transduction mechanism is not the same in each case.

MCa was found to directly interact with HP and HS with affinities in the micromolar range. Another important observation is that MCa K20A mutant, which is known to have lower penetration ability, has also reduced affinity for HS and HP (Article III) and for membrane lipids (Article I). Thus, there seems to be an interesting parallel between the affinity of interaction of MCa with cell surface components and its penetration efficiencies. Use of GAG-deficient CHO cell lines confirm that the cell penetration of MCa partly relies on GAGs, however there was no effect on the distribution. Use an endosomal marker demonstrates that MCa is distributed within endosomes after cell entry, suggesting that endocytosis is a predominant route of entry of the MCa. Lack of co-localization between transferin and MCa, together with the penetration of MCa in dynamin 2 K44A (a dominant negative construct that inhibits clathrin-mediated endocytosis) expressed cells, clearly indicates that clathrin-mediated endocytosis is not involved in the entry of MCa. This was further validated by the differential effects of various endocytosis blockers on the penetration of MCa. Based on these results, it can be concluded that macropinocytosis is involved in the entry of MCa, at least when coupled to streptavidin. However, the molar ratio between MCa and streptavidin did not affect the type of endocytosis.

IV. GENERAL CONCLUSION, DISCUSSION AND FUTURE PROSPECTS

Toxins are usually associated with pharmacological activity and this remains a major drawback in using venomous toxins as vectors for biological applications. Hence, a complete structure-function analysis is required to develop analogues devoid of pharmacological activity but preserve or enhance the cell penetration properties of the original molecule. For most CPPs this type of study was not required because many of them have no biological activity on their own. One such CPP, transportan, contains the N-terminal part of the bioactive neuropeptide galanin and is therefore recognized by galanin receptors. Moreover, it also shows an inhibitory effect on basal GTPase activity in Bowes melanoma cell membranes, which is probably caused by the mastoparan part of the molecule. Though the inhibitory effect of transportan is detectable at higher concentrations than commonly used in delivery experiments, this feature could be a drawback for this carrier peptide. Therefore, several shorter analogues of transportan were synthesized and analyzed for GTPase activity and cell penetration (Soomets et al., 2000).

RyR being the pharmacological target of MCa, several mutated analogues of MCa were produced, mostly by alanine substitution of positively charged amino acids. These analogues were compared to the wild-type for their structure, RyR activity, cell penetration, interaction with lipids and cell toxicity. Various analogues were thus isolated that are of interest either for direct use as vector or that can lead to better vectors. Mutant MCa R24A is of interest despite its lower cell penetration because it has fully knocked out the pharmacological potential of the peptide. Also MCa E12A turns out as a great lead molecule for the design of novel analogue since it is the best mutant of MCa in terms of cell penetration efficiencies in spite of its greater pharmacological activity. But interestingly, this mutant had no toxic effects on primary neuronal cultures up to 10 μM and for an incubation period of 24 hrs, much higher than normally used for delivery experiments. Usually the first step in the translocation of CPPs is their interaction with the cell surface components. MCa and its mutants were found to interact with negatively charged lipids and there was some kind of correlation on the extent of penetration and interaction with the negatively charged lipids. This was also true with the other cell surface component, namely the HSPGs. Mutant MCa K20A had less affinity to HP and HS as compared to the wild-type MCa.

These results probably suggest that cell surface components play an important role in the cell penetration efficiencies of CPPs. This was found to be true, when the cell penetration efficiencies of MCa were compared in wild-type and GAG-deficient CHO cell lines.It was found however that a significant fraction of the total cell entry was conserved in GAG-deficient cells. Penetration of MCa in GAG-deficient cells thus suggests that the cell penetration of MCa does not solely rely on GAGs, but also on other cell surface components. However, GAGs did not play a role in the distribution of the peptide and was found to co-localize with the endosomal marker in both wild-type and GAG-deficient CHO cell lines suggesting an endocytotic uptake of MCa when coupled with streptavidin. To further understand the type of endocytosis involved in the translocation of MCa, cell penetration of MCa was analyzed in presence of several inhibitors of endocytosis. Lack of co-localization of MCa with transferin together with the cell penetration of MCa in dynamin 2K44A expressing cells, ruled out the possibility of Clathrin-mediated endocytosis. Of the several endocytosis inhibitors tested, amiloride and cytochalasin D contributed to nearly 80% and 30% inhibition of cell penetration respectively, indicating that macropinocytosis is the major pathway of MCa entry. However, negligible amounts of MCa taking up other routes of endocytosis or even direct translocation cannot be ruled out. Increasing the molar ratio of MCa over streptavidin dramatically increased the amount of peptide entry but the route of entry, macropinocytosis, remained the predominant mode of entry of MCa. These data suggested that the molar ratio between MCa and streptavidin had no effect on the type of cell entry or endocytosis.

Coupling of cargoes to CPPs through thiol groups has advantages. The presence of internal cysteine residues within the sequence of MCa may hinder easy chemical coupling of cargo molecules. Thus, a novel strategy was adopted for the design of an analogue of MCa. This included the replacement of all the six internal cysteine residues of MCa and MCa E12A mutant (mutant of MCa known to have better cell penetration efficiencies than wild type-MCa) by isosteric 2-aminobutyric acid (Abu) residues. These analogues were analyzed for their structure, pharmacological activity and ability to carry cargo molecules into cells. This strategy seemed to work out very well. In this sense, the analogues produced in this way were totally inactive on RyR, had limited cell toxicity and the addition of a cysteine at the N-terminal end allowed for the efficient coupling of cargoes. Though cell penetration efficiencies of these analogues were

reduced to some extent, other advantages over the wild-type MCa counterbalance the reduced cell penetration efficiencies. Interestingly, the distribution of wild-type MCa or Abu analogues remained punctuate when coupled to streptavidin, whereas when coupled to other cargoes like a peptide, Qdot or doxorubicin, either by formation of disulfide bridge or through a bifunctional linker, the distribution was more uniform within the cytoplasm. This suggests that the type of cell entry into cells leading to different cell distributions heavily relies on the nature of cargo attached as well as on the coupling strategy.

Considering that there are several CPPs on the market with proven biological applications, the question naturally arises about the add-on value of MCa. Among the disadvantages of the peptide, one could cite the fact that MCa is of greater backbone length than other CPPs making it more expensive to synthesize. Beside cost considerations, it is also more difficult to produce considering that it has to fold properly and organize with three well defined disulfide bridges. One another strategy that can be taught off to develop a novel analogue and reducing the length of MCa would be to have truncated analogues of MCa and then analyze their ability for cell penetration, cell toxicity and pharmacological activity. This would help in reducing the production costs, which is an important aspect to be considered when used for various biological applications.

The presence of these disulfide bridges makes covalent cargo coupling more hazardous than if no cysteine residues are present in the peptide. Now with the development of an Abu analogue of MCa, this issue can be taken care off. However as for as the saying goes, “for every advantage, there is also a disadvantage”, the presence of disulfide bridges is of greater advantage in stabilizing the 3D structure of the peptide but the disadvantage lies in the cargo coupling chemistry. Disulfide bridges also contribute to greater peptide stability, which may turn into a significant advantage for *in vivo* applications. For instance Tat, that lacks disulfide bridges, was found to rapidly degrade in the extracellular medium of epithelial cells (Trehin et al., 2004). CPPs have in common the property of cell penetration, but might be well different in their mechanism of cell penetration. Depending on the type of cell penetration, the applications that can be envisioned are drastically different. MCa produces a rapid raise of intracellular calcium in myotubes, implicating that MCa originally a free vector, in its non-complexed form, should enter

cells through translocation. Cargo nature and size might induce a shift in the entry pathway, from translocation to macropinocytosis pathway, which is true in case of Tat as well (Richard et al., 2005), but this point needs to be further clarified with appropriate studies. Cell toxicity of CPPs is an essential parameter to be considered in any given application. We found that MCa and its analogues have limited toxicity and the toxicity was observed at much higher concentration than normally used for the delivery experiments. Further, thorough comparisons between CPPs need to be performed on several essential issues like *in vivo* distribution, intracellular concentrations and *in vivo* toxicity.

One question appears to be crucially important for the development of novel vector-based applications: what kind of intracellular concentrations does MCa reach within cell? Extracellular application of 100 nM MCa on myotubes produces calcium release within seconds through activation of RyR. Since the K_d of MCa for RyR is in 10-20 nM range, these data suggest that MCa very rapidly reaches these concentrations inside the cell (Esteve et al., 2003). Such rapid rise may indicate that the final concentration of MCa in cells might get close to 100 nM or even higher.

The number of applications that can be developed with CPPs are simply astonishing and endless. Now that MCa is a proven and efficient CPP, many original applications can now be envisioned for MCa analogues. For instance, the peptide may help liposomal-induced drug delivery into cells, as observed for Tat and penetratin (Tseng et al., 2002). Owing to the heparin binding affinity of MCa, its purification becomes as easy as fusion protein, which is true for other CPPs as well. It also holds great potential for many *in vivo* applications.

Quantum dots (Qdots) hold great potential for *in vitro* and *in vivo* applications due to their excellent photo stability and large surface to volume ratio. However, major limitations for the use of quantum dots in biological applications lie in their inability to access the cell interior. This issue is being addressed by coupling MCa to streptavidin-coated Qdots to efficiently deliver Qdots into living and primary neuronal cells. With these prospects, it can envisioned that MCa is on the many track for many biological, diagnostic and technological applications.

V. REFERENCES

Aderem, A., and D.M. Underhill. 1999. Mechanisms of phagocytosis in macrophages. *Annu Rev Immunol*. 17:593-623.

Ahern, G.P., P.R. Junankar, and A.F. Dulhunty. 1994. Single channel activity of the ryanodine receptor calcium release channel is modulated by FK-506. *FEBS Lett*. 352:369-74.

Aints, A., M.S. Dilber, and C.I. Smith. 1999. Intercellular spread of GFP-VP22. *J Gene Med*. 1:275-9.

Airey, J.A., M.M. Grinsell, L.R. Jones, J.L. Sutko, and D. Witcher. 1993. Three ryanodine receptor isoforms exist in avian striated muscles. *Biochemistry*. 32:5739-45.

Aldrian-Herrada, G., M.G. Desarmenien, H. Orcel, L. Boissin-Agasse, J. Mery, J. Brugidou, and A. Rabie. 1998. A peptide nucleic acid (PNA) is more rapidly internalized in cultured neurons when coupled to a retro-inverso delivery peptide. The antisense activity depresses the target mRNA and protein in magnocellular oxytocin neurons. *Nucleic Acids Res*. 26:4910-6.

Altafaj, X., W. Cheng, E. Esteve, J. Urbani, D. Grunwald, J.M. Sabatier, R. Coronado, M. De Waard, and M. Ronjat. 2005. Maurocalcine and domain A of the II-III loop of the dihydropyridine receptor Cav 1.1 subunit share common binding sites on the skeletal ryanodine receptor. *J Biol Chem*. 280:4013-6.

Altafaj, X., J. France, J. Almassy, I. Jona, D. Rossi, V. Sorrentino, K. Mabrouk, M. De Waard, and M. Ronjat. 2007. Maurocalcine interacts with the cardiac ryanodine receptor without inducing channel modification. *Biochem J*. 406:309-15.

Anderson, R.G., and K. Jacobson. 2002. A role for lipid shells in targeting proteins to caveolae, rafts, and other lipid domains. *Science*. 296:1821-5.

Astriab-Fisher, A., D.S. Sergueev, M. Fisher, B.R. Shaw, and R.L. Juliano. 2000. Antisense inhibition of P-glycoprotein expression using peptide-oligonucleotide conjugates. *Biochem Pharmacol*. 60:83-90.

Barg, S., J.A. Copello, and S. Fleischer. 1997. Different interactions of cardiac and skeletal muscle ryanodine receptors with FK-506 binding protein isoforms. *Am J Physiol*. 272:C1726-33.

Beard, N.A., M.M. Sakowska, A.F. Dulhunty, and D.R. Laver. 2002. Calsequestrin is an inhibitor of skeletal muscle ryanodine receptor calcium release channels. *Biophys J*. 82:310-20.

Beattie, E.C., R.C. Carroll, X. Yu, W. Morishita, H. Yasuda, M. von Zastrow, and R.C. Malenka. 2000. Regulation of AMPA receptor endocytosis by a signaling mechanism shared with LTD. *Nat Neurosci*. 3:1291-300.

Beletskii, A., Y.K. Hong, J. Pehrson, M. Egholm, and W.M. Strauss. 2001. PNA interference mapping demonstrates functional domains in the noncoding RNA Xist. *Proc Natl Acad Sci U S A*. 98:9215-20.

Bell, W.R., Jr. 1997. Defibrinogenating enzymes. *Drugs*. 54 Suppl 3:18-30; discussion 30-1.

Belting, M. 2003. Heparan sulfate proteoglycan as a plasma membrane carrier. *Trends Biochem Sci*. 28:145-51.

Berridge, M.J., M.D. Bootman, and H.L. Roderick. 2003. Calcium signalling: dynamics, homeostasis and remodelling. *Nat Rev Mol Cell Biol*. 4:517-29.

Bhorade, R., R. Weissleder, T. Nakakoshi, A. Moore, and C.H. Tung. 2000. Macrocyclic chelators with paramagnetic cations are internalized into mammalian cells via a HIV-tat derived membrane translocation peptide. *Bioconjug Chem*. 11:301-5.

Binder, H., and G. Lindblom. 2003. Charge-dependent translocation of the Trojan peptide penetratin across lipid membranes. *Biophys J*. 85:982-95.

Blazev, R., M. Hussain, A.J. Bakker, S.I. Head, and G.D. Lamb. 2001. Effects of the PKA inhibitor H-89 on excitation-contraction coupling in skinned and intact skeletal muscle fibres. *J Muscle Res Cell Motil*. 22:277-86.

Blystone, S.D., I.L. Graham, F.P. Lindberg, and E.J. Brown. 1994. Integrin alpha v beta 3 differentially regulates adhesive and phagocytic functions of the fibronectin receptor alpha 5 beta 1. *J Cell Biol*. 127:1129-37.

Boisseau, S., K. Mabrouk, N. Ram, N. Garmy, V. Collin, A. Tadmouri, M. Mikati, J.M. Sabatier, M. Ronjat, J. Fantini, and M. De Waard. 2006. Cell penetration properties of maurocalcine, a natural venom peptide active on the intracellular ryanodine receptor. *Biochim Biophys Acta*. 1758:308-19.

Borsello, T., P.G. Clarke, L. Hirt, A. Vercelli, M. Repici, D.F. Schorderet, J. Bogousslavsky, and C. Bonny. 2003. A peptide inhibitor of c-Jun N-terminal kinase protects against excitotoxicity and cerebral ischemia. *Nat Med*. 9:1180-6.

Breau, W.C., W.J. Atwood, and L.C. Norkin. 1992. Class I major histocompatibility proteins are an essential component of the simian virus 40 receptor. *J Virol*. 66:2037-45.

Brown, D.A., and E. London. 1998. Functions of lipid rafts in biological membranes. *Annu Rev Cell Dev Biol*. 14:111-36.

Bucci, M., J.P. Gratton, R.D. Rudic, L. Acevedo, F. Roviezzo, G. Cirino, and W.C. Sessa. 2000. In vivo delivery of the caveolin-1 scaffolding domain inhibits nitric oxide synthesis and reduces inflammation. *Nat Med*. 6:1362-7.

Bull, R., and J.J. Marengo. 1993. Sarcoplasmic reticulum release channels from frog skeletal muscle display two types of calcium dependence. *FEBS Lett*. 331:223-7.

Bultynck, G., D. Rossi, G. Callewaert, L. Missiaen, V. Sorrentino, J.B. Parys, and H. De Smedt. 2001. The conserved sites for the FK506-binding proteins in ryanodine receptors and inositol 1,4,5-trisphosphate receptors are structurally and functionally different. *J Biol Chem*. 276:47715-24.

Campbell, K.P., C.M. Knudson, T. Imagawa, A.T. Leung, J.L. Sutko, S.D. Kahl, C.R. Raab, and L. Madson. 1987. Identification and characterization of the high affinity [3H]ryanodine receptor of the junctional sarcoplasmic reticulum Ca2+ release channel. *J Biol Chem*. 262:6460-3.

Cao, L., J. Si, W. Wang, X. Zhao, X. Yuan, H. Zhu, X. Wu, J. Zhu, and G. Shen. 2006. Intracellular localization and sustained prodrug cell killing activity of TAT-HSVTK fusion protein in hepatocelullar carcinoma cells. *Mol Cells*. 21:104-11.

Carbone, E., E. Wanke, G. Prestipino, L.D. Possani, and A. Maelicke. 1982. Selective blockage of voltage-dependent K+ channels by a novel scorpion toxin. *Nature*. 296:90-1.

Carlier, E., V. Avdonin, S. Geib, Z. Fajloun, R. Kharrat, H. Rochat, J.M. Sabatier, T. Hoshi, and M. De Waard. 2000. Effect of maurotoxin, a four disulfide-bridged toxin from the chactoid scorpion Scorpio maurus, on Shaker K+ channels. *J Pept Res*. 55:419-27.

Caron, N.J., S.P. Quenneville, and J.P. Tremblay. 2004. Endosome disruption enhances the functional nuclear delivery of Tat-fusion proteins. *Biochem Biophys Res Commun*. 319:12-20.

Caron, N.J., Y. Torrente, G. Camirand, M. Bujold, P. Chapdelaine, K. Leriche, N. Bresolin, and J.P. Tremblay. 2001. Intracellular delivery of a Tat-eGFP fusion protein into muscle cells. *Mol Ther*. 3:310-8.

Castle, N.A., D.O. London, C. Creech, Z. Fajloun, J.W. Stocker, and J.M. Sabatier. 2003. Maurotoxin: a potent inhibitor of intermediate conductance Ca2+-activated potassium channels. *Mol Pharmacol*. 63:409-18.

Catterall, W.A. 1980. Neurotoxins that act on voltage-sensitive sodium channels in excitable membranes. *Annu Rev Pharmacol Toxicol*. 20:15-43.

Chagot, B., C. Pimentel, L. Dai, J. Pil, J. Tytgat, T. Nakajima, G. Corzo, H. Darbon, and G. Ferrat. 2005. An unusual fold for potassium channel blockers: NMR structure of three toxins from the scorpion Opisthacanthus madagascariensis. *Biochem J*. 388:263-71.

Chellaiah, M.A., N. Soga, S. Swanson, S. McAllister, U. Alvarez, D. Wang, S.F. Dowdy, and K.A. Hruska. 2000. Rho-A is critical for osteoclast podosome organization, motility, and bone resorption. *J Biol Chem*. 275:11993-2002.

Chen, L., E. Esteve, J.M. Sabatier, M. Ronjat, M. De Waard, P.D. Allen, and I.N. Pessah. 2003. Maurocalcine and peptide A stabilize distinct subconductance states of ryanodine receptor type 1, revealing a proportional gating mechanism. *J Biol Chem*. 278:16095-106.

Chen, S.R., K. Ebisawa, X. Li, and L. Zhang. 1998. Molecular identification of the ryanodine receptor Ca2+ sensor. *J Biol Chem*. 273:14675-8.

Chen, Y., and L.C. Norkin. 1999. Extracellular simian virus 40 transmits a signal that promotes virus enclosure within caveolae. *Exp Cell Res*. 246:83-90.

Chen, Y.N., S.K. Sharma, T.M. Ramsey, L. Jiang, M.S. Martin, K. Baker, P.D. Adams, K.W. Bair, and W.G. Kaelin, Jr. 1999. Selective killing of transformed cells by cyclin/cyclin-dependent kinase 2 antagonists. *Proc Natl Acad Sci U S A*. 96:4325-9.

Christiaens, B., S. Symoens, S. Verheyden, Y. Engelborghs, A. Joliot, A. Prochiantz, J. Vandekerckhove, M. Rosseneu, and B. Vanloo. 2002. Tryptophan fluorescence study of the interaction of penetratin peptides with model membranes. *Eur J Biochem*. 269:2918-26.

Chu, A., M. Fill, E. Stefani, and M.L. Entman. 1993. Cytoplasmic Ca2+ does not inhibit the cardiac muscle sarcoplasmic reticulum ryanodine receptor Ca2+ channel, although Ca(2+)-induced Ca2+ inactivation of Ca2+ release is observed in native vesicles. *J Membr Biol*. 135:49-59.

Collins, B.M., A.J. McCoy, H.M. Kent, P.R. Evans, and D.J. Owen. 2002. Molecular architecture and functional model of the endocytic AP2 complex. *Cell*. 109:523-35.

Conner, S.D., and S.L. Schmid. 2003. Regulated portals of entry into the cell. *Nature*. 422:37-44.

Console, S., C. Marty, C. Garcia-Echeverria, R. Schwendener, and K. Ballmer-Hofer. 2003. Antennapedia and HIV transactivator of transcription (TAT) "protein transduction domains" promote endocytosis of high molecular weight cargo upon binding to cell surface glycosaminoglycans. *J Biol Chem*. 278:35109-14.

Copello, J.A., S. Barg, H. Onoue, and S. Fleischer. 1997. Heterogeneity of Ca2+ gating of skeletal muscle and cardiac ryanodine receptors. *Biophys J*. 73:141-56.

Copello, J.A., S. Barg, A. Sonnleitner, M. Porta, P. Diaz-Sylvester, M. Fill, H. Schindler, and S. Fleischer. 2002. Differential activation by Ca2+, ATP and caffeine of cardiac and skeletal muscle ryanodine receptors after block by Mg2+. *J Membr Biol*. 187:51-64.

Coronado, R., J. Morrissette, M. Sukhareva, and D.M. Vaughan. 1994. Structure and function of ryanodine receptors. *Am J Physiol*. 266:C1485-504.

Cruz, L.J., W.R. Gray, B.M. Olivera, R.D. Zeikus, L. Kerr, D. Yoshikami, and E. Moczydlowski. 1985. Conus geographus toxins that discriminate between neuronal and muscle sodium channels. *J Biol Chem*. 260:9280-8.

D'Ursi, A.M., L. Giusti, S. Albrizio, F. Porchia, C. Esposito, G. Caliendo, C. Gargini, E. Novellino, A. Lucacchini, P. Rovero, and M.R. Mazzoni. 2006. A membrane-permeable peptide containing the last 21 residues of the G alpha(s) carboxyl terminus inhibits G(s)-coupled receptor signaling in intact cells: correlations between peptide structure and biological activity. *Mol Pharmacol*. 69:727-36.

Davidson, T.J., S. Harel, V.A. Arboleda, G.F. Prunell, M.L. Shelanski, L.A. Greene, and C.M. Troy. 2004. Highly efficient small interfering RNA delivery to primary mammalian neurons induces MicroRNA-like effects before mRNA degradation. *J Neurosci*. 24:10040-6.

De Camilli, P., K. Takei, and P.S. McPherson. 1995. The function of dynamin in endocytosis. *Curr Opin Neurobiol*. 5:559-65.

de Weille, J.R., H. Schweitz, P. Maes, A. Tartar, and M. Lazdunski. 1991. Calciseptine, a peptide isolated from black mamba venom, is a specific blocker of the L-type calcium channel. *Proc Natl Acad Sci U S A*. 88:2437-40.

DeBin, J.A., J.E. Maggio, and G.R. Strichartz. 1993. Purification and characterization of chlorotoxin, a chloride channel ligand from the venom of the scorpion. *Am J Physiol*. 264:C361-9.

Debont, T., A. Swerts, J.J. Van der Walt, G.J. Muller, F. Verdonck, P. Daenens, and J. Tytgat. 1998. Comparison and characterization of the venoms of three Parabuthus scorpion species occurring in southern Africa. *Toxicon*. 36:341-52.

Dei Cas, L., M. Metra, S. Nodari, A. Dei Cas, and M. Gheorghiade. 2003. Prevention and management of chronic heart failure in patients at risk. *Am J Cardiol*. 91:10F-17F.

Delehanty, J.B., I.L. Medintz, T. Pons, F.M. Brunel, P.E. Dawson, and H. Mattoussi. 2006. Self-assembled quantum dot-peptide bioconjugates for selective intracellular delivery. *Bioconjug Chem*. 17:920-7.

Derossi, D., S. Calvet, A. Trembleau, A. Brunissen, G. Chassaing, and A. Prochiantz. 1996. Cell internalization of the third helix of the Antennapedia homeodomain is receptor-independent. *J Biol Chem*. 271:18188-93.

Derossi, D., G. Chassaing, and A. Prochiantz. 1998. Trojan peptides: the penetratin system for intracellular delivery. *Trends Cell Biol*. 8:84-7.

Derossi, D., A.H. Joliot, G. Chassaing, and A. Prochiantz. 1994. The third helix of the Antennapedia homeodomain translocates through biological membranes. *J Biol Chem*. 269:10444-50.

Deshayes, S., M. Morris, F. Heitz, and G. Divita. 2008. Delivery of proteins and nucleic acids using a non-covalent peptide-based strategy. *Adv Drug Deliv Rev*. 60:537-47.

Di Fiore, P.P., and P. De Camilli. 2001. Endocytosis and signaling. an inseparable partnership. *Cell*. 106:1-4.

Diem, R., N. Taheri, G.P. Dietz, A. Kuhnert, K. Maier, M.B. Sattler, I. Gadjanski, D. Merkler, and M. Bahr. 2005. HIV-Tat-mediated Bcl-XL delivery protects retinal ganglion cells during experimental autoimmune optic neuritis. *Neurobiol Dis*. 20:218-26.

Dietzen, D.J., W.R. Hastings, and D.M. Lublin. 1995. Caveolin is palmitoylated on multiple cysteine residues. Palmitoylation is not necessary for localization of caveolin to caveolae. *J Biol Chem*. 270:6838-42.

Dixon, M.J., L. Bourre, A.J. MacRobert, and I.M. Eggleston. 2007. Novel prodrug approach to photodynamic therapy: Fmoc solid-phase synthesis of a cell permeable peptide incorporating 5-aminolaevulinic acid. *Bioorg Med Chem Lett*. 17:4518-22.

Donaldson, J.G. 2003. Multiple roles for Arf6: sorting, structuring, and signaling at the plasma membrane. *J Biol Chem*. 278:41573-6.

Duchardt, F., M. Fotin-Mleczek, H. Schwarz, R. Fischer, and R. Brock. 2007. A comprehensive model for the cellular uptake of cationic cell-penetrating peptides. *Traffic*. 8:848-66.

Dulhunty, A.F., D.R. Laver, E.M. Gallant, M.G. Casarotto, S.M. Pace, and S. Curtis. 1999. Activation and inhibition of skeletal RyR channels by a part of the skeletal DHPR II-III loop: effects of DHPR Ser687 and FKBP12. *Biophys J*. 77:189-203.

Edidin, M. 2001. Shrinking patches and slippery rafts: scales of domains in the plasma membrane. *Trends Cell Biol*. 11:492-6.

Eguchi, A., T. Akuta, H. Okuyama, T. Senda, H. Yokoi, H. Inokuchi, S. Fujita, T. Hayakawa, K. Takeda, M. Hasegawa, and M. Nakanishi. 2001. Protein transduction domain of HIV-1 Tat protein promotes efficient delivery of DNA into mammalian cells. *J Biol Chem*. 276:26204-10.

El-Andaloussi, S., P. Jarver, H.J. Johansson, and U. Langel. 2007. Cargo-dependent cytotoxicity and delivery efficacy of cell-penetrating peptides: a comparative study. *Biochem J*. 407:285-92.

El-Andaloussi, S., H. Johansson, A. Magnusdottir, P. Jarver, P. Lundberg, and U. Langel. 2005. TP10, a delivery vector for decoy oligonucleotides targeting the Myc protein. *J Control Release*. 110:189-201.

El-Hayek, R., and N. Ikemoto. 1998. Identification of the minimum essential region in the II-III loop of the dihydropyridine receptor alpha 1 subunit required for activation of skeletal muscle-type excitation-contraction coupling. *Biochemistry*. 37:7015-20.

Elison, C., and D.J. Jenden. 1967. The effects of ryanodine on model systems derived from muscle. 3. Reconstituted actomyosin. *Biochem Pharmacol*. 16:1355-63.

Elliott, G., and P. O'Hare. 1999. Intercellular trafficking of VP22-GFP fusion proteins. *Gene Ther*. 6:149-51.

Elliott, G.D., and D.M. Meredith. 1992. The herpes simplex virus type 1 tegument protein VP22 is encoded by gene UL49. *J Gen Virol*. 73 (Pt 3):723-6.

Elmquist, A., and U. Langel. 2003. In vitro uptake and stability study of pVEC and its all-D analog. *Biol Chem*. 384:387-93.

Eng, J., W.A. Kleinman, L. Singh, G. Singh, and J.P. Raufman. 1992. Isolation and characterization of exendin-4, an exendin-3 analogue, from Heloderma suspectum venom. Further evidence for an exendin receptor on dispersed acini from guinea pig pancreas. *J Biol Chem*. 267:7402-5.

Escoubas, P., J.R. De Weille, A. Lecoq, S. Diochot, R. Waldmann, G. Champigny, D. Moinier, A. Menez, and M. Lazdunski. 2000. Isolation of a tarantula toxin specific for a class of proton-gated Na+ channels. *J Biol Chem*. 275:25116-21.

Esteve, E., K. Mabrouk, A. Dupuis, S. Smida-Rezgui, X. Altafaj, D. Grunwald, J.C. Platel, N. Andreotti, I. Marty, J.M. Sabatier, M. Ronjat, and M. De Waard. 2005. Transduction of the scorpion toxin maurocalcine into cells. Evidence that the toxin crosses the plasma membrane. *J Biol Chem*. 280:12833-9.

Esteve, E., S. Smida-Rezgui, S. Sarkozi, C. Szegedi, I. Regaya, L. Chen, X. Altafaj, H. Rochat, P. Allen, I.N. Pessah, I. Marty, J.M. Sabatier, I. Jona, M. De Waard, and M. Ronjat. 2003. Critical amino acid residues determine the binding affinity and the Ca2+ release efficacy of maurocalcine in skeletal muscle cells. *J Biol Chem*. 278:37822-31.

Eum, W.S., D.W. Kim, I.K. Hwang, K.Y. Yoo, T.C. Kang, S.H. Jang, H.S. Choi, S.H. Choi, Y.H. Kim, S.Y. Kim, H.Y. Kwon, J.H. Kang, O.S. Kwon, S.W. Cho, K.S. Lee, J. Park, M.H.

Won, and S.Y. Choi. 2004. In vivo protein transduction: biologically active intact pep-1-superoxide dismutase fusion protein efficiently protects against ischemic insult. *Free Radic Biol Med*. 37:1656-69.

Fabiato, A. 1985. Effects of ryanodine in skinned cardiac cells. *Fed Proc*. 44:2970-6.

Fadel, V., P. Bettendorff, T. Herrmann, W.F. de Azevedo, Jr., E.B. Oliveira, T. Yamane, and K. Wuthrich. 2005. Automated NMR structure determination and disulfide bond identification of the myotoxin crotamine from Crotalus durissus terrificus. *Toxicon*. 46:759-67.

Fainzilber, M., O. Kofman, E. Zlotkin, and D. Gordon. 1994. A new neurotoxin receptor site on sodium channels is identified by a conotoxin that affects sodium channel inactivation in molluscs and acts as an antagonist in rat brain. *J Biol Chem*. 269:2574-80.

Fajloun, Z., R. Kharrat, L. Chen, C. Lecomte, E. Di Luccio, D. Bichet, M. El Ayeb, H. Rochat, P.D. Allen, I.N. Pessah, M. De Waard, and J.M. Sabatier. 2000a. Chemical synthesis and characterization of maurocalcine, a scorpion toxin that activates Ca(2+) release channel/ryanodine receptors. *FEBS Lett*. 469:179-85.

Fajloun, Z., A. Mosbah, E. Carlier, P. Mansuelle, G. Sandoz, M. Fathallah, E. di Luccio, C. Devaux, H. Rochat, H. Darbon, M. De Waard, and J.M. Sabatier. 2000b. Maurotoxin versus Pi1/HsTx1 scorpion toxins. Toward new insights in the understanding of their distinct disulfide bridge patterns. *J Biol Chem*. 275:39394-402.

Fallman, M., M. Gullberg, C. Hellberg, and T. Andersson. 1992. Complement receptor-mediated phagocytosis is associated with accumulation of phosphatidylcholine-derived diglyceride in human neutrophils. Involvement of phospholipase D and direct evidence for a positive feedback signal of protein kinase. *J Biol Chem*. 267:2656-63.

Favreau, P., L. Menin, S. Michalet, F. Perret, O. Cheneval, M. Stocklin, P. Bulet, and R. Stocklin. 2006. Mass spectrometry strategies for venom mapping and peptide sequencing from crude venoms: case applications with single arthropod specimen. *Toxicon*. 47:676-87.

Fawell, S., J. Seery, Y. Daikh, C. Moore, L.L. Chen, B. Pepinsky, and J. Barsoum. 1994. Tat-mediated delivery of heterologous proteins into cells. *Proc Natl Acad Sci U S A*. 91:664-8.

Feig, L.A. 1999. Tools of the trade: use of dominant-inhibitory mutants of Ras-family GTPases. *Nat Cell Biol*. 1:E25-7.

Fernandez-Carneado, J., M. Van Gool, V. Martos, S. Castel, P. Prados, J. de Mendoza, and E. Giralt. 2005. Highly efficient, nonpeptidic oligoguanidinium vectors that selectively internalize into mitochondria. *J Am Chem Soc*. 127:869-74.

Filippovich, I., N. Sorokina, P.P. Masci, J. de Jersey, A.N. Whitaker, D.J. Winzor, P.J. Gaffney, and M.F. Lavin. 2002. A family of textilinin genes, two of which encode proteins with antihaemorrhagic properties. *Br J Haematol*. 119:376-84.

Fill, M., and R. Coronado. 1988. Ryanodine receptor channel of sarcoplasmic reticulum. *Trends Neurosci*. 11:453-7.

Fischer, P.M., N.Z. Zhelev, S. Wang, J.E. Melville, R. Fahraeus, and D.P. Lane. 2000. Structure-activity relationship of truncated and substituted analogues of the intracellular delivery vector Penetratin. *J Pept Res*. 55:163-72.

Fischer, R., M. Fotin-Mleczek, H. Hufnagel, and R. Brock. 2005. Break on through to the other side-biophysics and cell biology shed light on cell-penetrating peptides. *Chembiochem*. 6:2126-42.

Fischer, R., K. Kohler, M. Fotin-Mleczek, and R. Brock. 2004. A stepwise dissection of the intracellular fate of cationic cell-penetrating peptides. *J Biol Chem*. 279:12625-35.

Fleischer, S. 2008. Personal recollections on the discovery of the ryanodine receptors of muscle. *Biochem Biophys Res Commun*. 369:195-207.

Fleischer, S., and M. Inui. 1989. Biochemistry and biophysics of excitation-contraction coupling. *Annu Rev Biophys Biophys Chem*. 18:333-64.

Fleischer, S., E.M. Ogunbunmi, M.C. Dixon, and E.A. Fleer. 1985. Localization of Ca2+ release channels with ryanodine in junctional terminal cisternae of sarcoplasmic reticulum of fast skeletal muscle. *Proc Natl Acad Sci U S A*. 82:7256-9.

Fra, A.M., E. Williamson, K. Simons, and R.G. Parton. 1995. De novo formation of caveolae in lymphocytes by expression of VIP21-caveolin. *Proc Natl Acad Sci U S A*. 92:8655-9.

Frank, M., and W.W. Sleator. 1975. Effects of ryanodine on a myocardial membrane vesicular fraction. *Res Commun Chem Pathol Pharmacol*. 11:65-72.

Frankel, A.D., and C.O. Pabo. 1988. Cellular uptake of the tat protein from human immunodeficiency virus. *Cell*. 55:1189-93.

Frankel, A.D., and J.A. Young. 1998. HIV-1: fifteen proteins and an RNA. *Annu Rev Biochem*. 67:1-25.

Franzini-Armstrong, C., L.J. Kenney, and E. Varriano-Marston. 1987. The structure of calsequestrin in triads of vertebrate skeletal muscle: a deep-etch study. *J Cell Biol*. 105:49-56.

Froemming, G.R., B.E. Murray, S. Harmon, D. Pette, and K. Ohlendieck. 2000. Comparative analysis of the isoform expression pattern of Ca(2+)-regulatory membrane proteins in

fast-twitch, slow-twitch, cardiac, neonatal and chronic low-frequency stimulated muscle fibers. *Biochim Biophys Acta*. 1466:151-68.

Fruen, B.R., J.R. Mickelson, N.H. Shomer, P. Velez, and C.F. Louis. 1994. Cyclic ADP-ribose does not affect cardiac or skeletal muscle ryanodine receptors. *FEBS Lett*. 352:123-6.

Fu, A.L., Q. Li, Z.H. Dong, S.J. Huang, Y.X. Wang, and M.J. Sun. 2004. Alternative therapy of Alzheimer's disease via supplementation with choline acetyltransferase. *Neurosci Lett*. 368:258-62.

Fuchs, S.M., and R.T. Raines. 2004. Pathway for polyarginine entry into mammalian cells. *Biochemistry*. 43:2438-44.

Furuichi, T., D. Furutama, Y. Hakamata, J. Nakai, H. Takeshima, and K. Mikoshiba. 1994. Multiple types of ryanodine receptor/Ca2+ release channels are differentially expressed in rabbit brain. *J Neurosci*. 14:4794-805.

Futaki, S., T. Suzuki, W. Ohashi, T. Yagami, S. Tanaka, K. Ueda, and Y. Sugiura. 2001. Arginine-rich peptides. An abundant source of membrane-permeable peptides having potential as carriers for intracellular protein delivery. *J Biol Chem*. 276:5836-40.

Gaburjakova, M., J. Gaburjakova, S. Reiken, F. Huang, S.O. Marx, N. Rosemblit, and A.R. Marks. 2001. FKBP12 binding modulates ryanodine receptor channel gating. *J Biol Chem*. 276:16931-5.

Galbiati, F., B. Razani, and M.P. Lisanti. 2001. Emerging themes in lipid rafts and caveolae. *Cell*. 106:403-11.

Galvan, D.L., E. Borrego-Diaz, P.J. Perez, and G.A. Mignery. 1999. Subunit oligomerization, and topology of the inositol 1,4, 5-trisphosphate receptor. *J Biol Chem*. 274:29483-92.

Garcia-Echeverria, C., L. Jiang, T.M. Ramsey, S.K. Sharma, and Y.P. Chen. 2001. A new Antennapedia-derived vector for intracellular delivery of exogenous compounds. *Bioorg Med Chem Lett*. 11:1363-6.

Garcia, M.L., M. Hanner, H.G. Knaus, R. Koch, W. Schmalhofer, R.S. Slaughter, and G.J. Kaczorowski. 1997. Pharmacology of potassium channels. *Adv Pharmacol*. 39:425-71.

Garden, O.A., P.R. Reynolds, J. Yates, D.J. Larkman, F.M. Marelli-Berg, D.O. Haskard, A.D. Edwards, and A.J. George. 2006. A rapid method for labelling CD4+ T cells with ultrasmall paramagnetic iron oxide nanoparticles for magnetic resonance imaging that preserves proliferative, regulatory and migratory behaviour in vitro. *J Immunol Methods*. 314:123-33.

Gehring, W.J., Y.Q. Qian, M. Billeter, K. Furukubo-Tokunaga, A.F. Schier, D. Resendez-Perez, M. Affolter, G. Otting, and K. Wuthrich. 1994. Homeodomain-DNA recognition. *Cell*. 78:211-23.

Geier, E., G. Pfeifer, M. Wilm, M. Lucchiari-Hartz, W. Baumeister, K. Eichmann, and G. Niedermann. 1999. A giant protease with potential to substitute for some functions of the proteasome. *Science*. 283:978-81.

Gerbal-Chaloin, S., C. Gondeau, G. Aldrian-Herrada, F. Heitz, C. Gauthier-Rouviere, and G. Divita. 2007. First step of the cell-penetrating peptide mechanism involves Rac1 GTPase-dependent actin-network remodelling. *Biol Cell*. 99:223-38.

Gius, D.R., S.A. Ezhevsky, M. Becker-Hapak, H. Nagahara, M.C. Wei, and S.F. Dowdy. 1999. Transduced p16INK4a peptides inhibit hypophosphorylation of the retinoblastoma protein and cell cycle progression prior to activation of Cdk2 complexes in late G1. *Cancer Res*. 59:2577-80.

Glebov, O.O., N.A. Bright, and B.J. Nichols. 2006. Flotillin-1 defines a clathrin-independent endocytic pathway in mammalian cells. *Nat Cell Biol*. 8:46-54.

Glenney, J.R., Jr. 1989. Tyrosine phosphorylation of a 22-kDa protein is correlated with transformation by Rous sarcoma virus. *J Biol Chem*. 264:20163-6.

Glickman, M.H., and A. Ciechanover. 2002. The ubiquitin-proteasome proteolytic pathway: destruction for the sake of construction. *Physiol Rev*. 82:373-428.

Glover, D.J., H.J. Lipps, and D.A. Jans. 2005. Towards safe, non-viral therapeutic gene expression in humans. *Nat Rev Genet*. 6:299-310.

Gonoi, T., K. Ashida, D. Feller, J. Schmidt, M. Fujiwara, and W.A. Catterall. 1986. Mechanism of action of a polypeptide neurotoxin from the coral Goniopora on sodium channels in mouse neuroblastoma cells. *Mol Pharmacol*. 29:347-54.

Grabner, M., R.T. Dirksen, N. Suda, and K.G. Beam. 1999. The II-III loop of the skeletal muscle dihydropyridine receptor is responsible for the Bi-directional coupling with the ryanodine receptor. *J Biol Chem*. 274:21913-9.

Green, M., and P.M. Loewenstein. 1988. Autonomous functional domains of chemically synthesized human immunodeficiency virus tat trans-activator protein. *Cell*. 55:1179-88.

Greene, B., S.H. Liu, A. Wilde, and F.M. Brodsky. 2000. Complete reconstitution of clathrin basket formation with recombinant protein fragments: adaptor control of clathrin self-assembly. *Traffic*. 1:69-75.

Gurrola, G.B., C. Arevalo, R. Sreekumar, A.J. Lokuta, J.W. Walker, and H.H. Valdivia. 1999. Activation of ryanodine receptors by imperatoxin A and a peptide segment of the II-III loop of the dihydropyridine receptor. *J Biol Chem*. 274:7879-86.

Hain, J., H. Onoue, M. Mayrleitner, S. Fleischer, and H. Schindler. 1995. Phosphorylation modulates the function of the calcium release channel of sarcoplasmic reticulum from cardiac muscle. *J Biol Chem*. 270:2074-81.

Hakamata, Y., J. Nakai, H. Takeshima, and K. Imoto. 1992. Primary structure and distribution of a novel ryanodine receptor/calcium release channel from rabbit brain. *FEBS Lett*. 312:229-35.

Hall, A., and C.D. Nobes. 2000. Rho GTPases: molecular switches that control the organization and dynamics of the actin cytoskeleton. *Philos Trans R Soc Lond B Biol Sci*. 355:965-70.

Hamilton, S.L., I. Serysheva, and G.M. Strasburg. 2000. Calmodulin and Excitation-Contraction Coupling. *News Physiol Sci*. 15:281-284.

Han, K., M.J. Jeon, K.A. Kim, J. Park, and S.Y. Choi. 2000. Efficient intracellular delivery of GFP by homeodomains of Drosophila Fushi-tarazu and Engrailed proteins. *Mol Cells*. 10:728-32.

Han, K., M.J. Jeon, S.H. Kim, D. Ki, J.H. Bahn, K.S. Lee, J. Park, and S.Y. Choi. 2001. Efficient intracellular delivery of an exogenous protein GFP with genetically fused basic oligopeptides. *Mol Cells*. 12:267-71.

Hancock, R.E. 2001. Cationic peptides: effectors in innate immunity and novel antimicrobials. *Lancet Infect Dis*. 1:156-64.

Hanover, J.A., M.C. Willingham, and I. Pastan. 1984. Kinetics of transit of transferrin and epidermal growth factor through clathrin-coated membranes. *Cell*. 39:283-93.

Hao, W., Z. Luo, L. Zheng, K. Prasad, and E.M. Lafer. 1999. AP180 and AP-2 interact directly in a complex that cooperatively assembles clathrin. *J Biol Chem*. 274:22785-94.

Hashida, H., M. Miyamoto, Y. Cho, Y. Hida, K. Kato, T. Kurokawa, S. Okushiba, S. Kondo, H. Dosaka-Akita, and H. Katoh. 2004. Fusion of HIV-1 Tat protein transduction domain to poly-lysine as a new DNA delivery tool. *Br J Cancer*. 90:1252-8.

Henley, J.R., E.W. Krueger, B.J. Oswald, and M.A. McNiven. 1998. Dynamin-mediated internalization of caveolae. *J Cell Biol*. 141:85-99.

Hewlett, L.J., A.R. Prescott, and C. Watts. 1994. The coated pit and macropinocytic pathways serve distinct endosome populations. *J Cell Biol*. 124:689-703.

Hidalgo, C., P. Donoso, and P.H. Rodriguez. 1996. Protons induce calsequestrin conformational changes. *Biophys J*. 71:2130-7.

Hoshino, A., K. Fujioka, T. Oku, S. Nakamura, M. Suga, Y. Yamaguchi, K. Suzuki, M. Yasuhara, and K. Yamamoto. 2004. Quantum dots targeted to the assigned organelle in living cells. *Microbiol Immunol*. 48:985-94.

Howl, J., S. Jones, and M. Farquhar. 2003. Intracellular delivery of bioactive peptides to RBL-2H3 cells induces beta-hexosaminidase secretion and phospholipase D activation. *Chembiochem*. 4:1312-6.

Hymel, L., M. Inui, S. Fleischer, and H. Schindler. 1988. Purified ryanodine receptor of skeletal muscle sarcoplasmic reticulum forms Ca2+-activated oligomeric Ca2+ channels in planar bilayers. *Proc Natl Acad Sci U S A*. 85:441-5.

Igami, K., N. Yamaguchi, and M. Kasai. 1999. Regulation of depolarization-induced calcium release from skeletal muscle triads by cyclic AMP-dependent protein kinase. *Jpn J Physiol*. 49:81-7.

Ignatovich, I.A., E.B. Dizhe, A.V. Pavlotskaya, B.N. Akifiev, S.V. Burov, S.V. Orlov, and A.P. Perevozchikov. 2003. Complexes of plasmid DNA with basic domain 47-57 of the HIV-1 Tat protein are transferred to mammalian cells by endocytosis-mediated pathways. *J Biol Chem*. 278:42625-36.

Imagawa, T., J.S. Smith, R. Coronado, and K.P. Campbell. 1987. Purified ryanodine receptor from skeletal muscle sarcoplasmic reticulum is the Ca2+-permeable pore of the calcium release channel. *J Biol Chem*. 262:16636-43.

Inagaki, K., Y. Kihara, T. Izumi, and S. Sasayama. 2000. The cardioprotective effects of a new 1,4-benzothiazepine derivative, JTV519, on ischemia/reperfusion-induced Ca2+ overload in isolated rat hearts. *Cardiovasc Drugs Ther*. 14:489-95.

Inui, M., A. Saito, and S. Fleischer. 1987. Purification of the ryanodine receptor and identity with feet structures of junctional terminal cisternae of sarcoplasmic reticulum from fast skeletal muscle. *J Biol Chem*. 262:1740-7.

Jain, M., S.C. Chauhan, A.P. Singh, G. Venkatraman, D. Colcher, and S.K. Batra. 2005. Penetratin improves tumor retention of single-chain antibodies: a novel step toward optimization of radioimmunotherapy of solid tumors. *Cancer Res*. 65:7840-6.

Javadpour, M.M., M.M. Juban, W.C. Lo, S.M. Bishop, J.B. Alberty, S.M. Cowell, C.L. Becker, and M.L. McLaughlin. 1996. De novo antimicrobial peptides with low mammalian cell toxicity. *J Med Chem*. 39:3107-13.

Jenden, D.J., and A.S. Fairhurst. 1969. The pharmacology of ryanodine. *Pharmacol Rev*. 21:1-25.

Jeyakumar, L.H., J.A. Copello, A.M. O'Malley, G.M. Wu, R. Grassucci, T. Wagenknecht, and S. Fleischer. 1998. Purification and characterization of ryanodine receptor 3 from mammalian tissue. *J Biol Chem*. 273:16011-20.

Jia, H., M. Lohr, S. Jezequel, D. Davis, S. Shaikh, D. Selwood, and I. Zachary. 2001. Cysteine-rich and basic domain HIV-1 Tat peptides inhibit angiogenesis and induce endothelial cell apoptosis. *Biochem Biophys Res Commun*. 283:469-79.

Jiang, T., E.S. Olson, Q.T. Nguyen, M. Roy, P.A. Jennings, and R.Y. Tsien. 2004. Tumor imaging by means of proteolytic activation of cell-penetrating peptides. *Proc Natl Acad Sci U S A*. 101:17867-72.

Joliot, A., C. Pernelle, H. Deagostini-Bazin, and A. Prochiantz. 1991a. Antennapedia homeobox peptide regulates neural morphogenesis. *Proc Natl Acad Sci U S A*. 88:1864-8.

Joliot, A.H., A. Triller, M. Volovitch, C. Pernelle, and A. Prochiantz. 1991b. alpha-2,8-Polysialic acid is the neuronal surface receptor of antennapedia homeobox peptide. *New Biol*. 3:1121-34.

Josephson, L., C.H. Tung, A. Moore, and R. Weissleder. 1999. High-efficiency intracellular magnetic labeling with novel superparamagnetic-Tat peptide conjugates. *Bioconjug Chem*. 10:186-91.

Kaufman, C.L., M. Williams, L.M. Ryle, T.L. Smith, M. Tanner, and C. Ho. 2003. Superparamagnetic iron oxide particles transactivator protein-fluorescein isothiocyanate particle labeling for in vivo magnetic resonance imaging detection of cell migration: uptake and durability. *Transplantation*. 76:1043-6.

Kaushik, N., A. Basu, and V.N. Pandey. 2002. Inhibition of HIV-1 replication by anti-trans-activation responsive polyamide nucleotide analog. *Antiviral Res*. 56:13-27.

Kawasaki, T., and M. Kasai. 1994. Regulation of calcium channel in sarcoplasmic reticulum by calsequestrin. *Biochem Biophys Res Commun*. 199:1120-7.

Kelemen, B.R., K. Hsiao, and S.A. Goueli. 2002. Selective in vivo inhibition of mitogen-activated protein kinase activation using cell-permeable peptides. *J Biol Chem*. 277:8741-8.

Kerkis, A., I. Kerkis, G. Radis-Baptista, E.B. Oliveira, A.M. Vianna-Morgante, L.V. Pereira, and T. Yamane. 2004. Crotamine is a novel cell-penetrating protein from the venom of rattlesnake Crotalus durissus terrificus. *FASEB J*. 18:1407-9.

Khalil, I.A., K. Kogure, S. Futaki, and H. Harashima. 2006. High density of octaarginine stimulates macropinocytosis leading to efficient intracellular trafficking for gene expression. *J Biol Chem*. 281:3544-51.

Kharrat, R., K. Mabrouk, M. Crest, H. Darbon, R. Oughideni, M.F. Martin-Eauclaire, G. Jacquet, M. el Ayeb, J. Van Rietschoten, H. Rochat, and J.M. Sabatier. 1996. Chemical synthesis and characterization of maurotoxin, a short scorpion toxin with four disulfide bridges that acts on K+ channels. *Eur J Biochem*. 242:491-8.

Kharrat, R., P. Mansuelle, F. Sampieri, M. Crest, R. Oughideni, J. Van Rietschoten, M.F. Martin-Eauclaire, H. Rochat, and M. El Ayeb. 1997. Maurotoxin, a four disulfide bridge toxin from Scorpio maurus venom: purification, structure and action on potassium channels. *FEBS Lett*. 406:284-90.

Kilic, U., E. Kilic, G.P. Dietz, and M. Bahr. 2003. Intravenous TAT-GDNF is protective after focal cerebral ischemia in mice. *Stroke*. 34:1304-10.

Kirchhausen, T. 1999. Adaptors for clathrin-mediated traffic. *Annu Rev Cell Dev Biol*. 15:705-32.

Kohno, M., M. Yano, S. Kobayashi, M. Doi, T. Oda, T. Tokuhisa, S. Okuda, T. Ohkusa, and M. Matsuzaki. 2003. A new cardioprotective agent, JTV519, improves defective channel gating of ryanodine receptor in heart failure. *Am J Physiol Heart Circ Physiol*. 284:H1035-42.

Kretz, A., W.A. Wybranietz, S. Hermening, U.M. Lauer, and S. Isenmann. 2003. HSV-1 VP22 augments adenoviral gene transfer to CNS neurons in the retina and striatum in vivo. *Mol Ther*. 7:659-69.

Kuniyasu, A., S. Kawano, Y. Hirayama, Y.H. Ji, K. Xu, M. Ohkura, K. Furukawa, Y. Ohizumi, M. Hiraoka, and H. Nakayama. 1999. A new scorpion toxin (BmK-PL) stimulates Ca2+-release channel activity of the skeletal-muscle ryanodine receptor by an indirect mechanism. *Biochem J*. 339 (Pt 2):343-50.

Lai, F.A., H.P. Erickson, E. Rousseau, Q.Y. Liu, and G. Meissner. 1988. Purification and reconstitution of the calcium release channel from skeletal muscle. *Nature*. 331:315-9.

Lai, F.A., Q.Y. Liu, L. Xu, A. el-Hashem, N.R. Kramarcy, R. Sealock, and G. Meissner. 1992. Amphibian ryanodine receptor isoforms are related to those of mammalian skeletal or cardiac muscle. *Am J Physiol*. 263:C365-72.

Lamaze, C., A. Dujeancourt, T. Baba, C.G. Lo, A. Benmerah, and A. Dautry-Varsat. 2001. Interleukin 2 receptors and detergent-resistant membrane domains define a clathrin-independent endocytic pathway. *Mol Cell*. 7:661-71.

Lamb, G.D., and D.G. Stephenson. 1996. Effects of FK506 and rapamycin on excitation-contraction coupling in skeletal muscle fibres of the rat. *J Physiol*. 494 (Pt 2):569-76.

Langer, M., F. Kratz, B. Rothen-Rutishauser, H. Wunderli-Allenspach, and A.G. Beck-Sickinger. 2001. Novel peptide conjugates for tumor-specific chemotherapy. *J Med Chem*. 44:1341-8.

Laver, D.R., T.M. Baynes, and A.F. Dulhunty. 1997. Magnesium inhibition of ryanodine-receptor calcium channels: evidence for two independent mechanisms. *J Membr Biol*. 156:213-29.

Laver, D.R., L.D. Roden, G.P. Ahern, K.R. Eager, P.R. Junankar, and A.F. Dulhunty. 1995. Cytoplasmic Ca2+ inhibits the ryanodine receptor from cardiac muscle. *J Membr Biol*. 147:7-22.

Law, B., L. Quinti, Y. Choi, R. Weissleder, and C.H. Tung. 2006. A mitochondrial targeted fusion peptide exhibits remarkable cytotoxicity. *Mol Cancer Ther*. 5:1944-9.

Lechardeur, D., and G.L. Lukacs. 2006. Nucleocytoplasmic transport of plasmid DNA: a perilous journey from the cytoplasm to the nucleus. *Hum Gene Ther*. 17:882-9.

Ledbetter, M.W., J.K. Preiner, C.F. Louis, and J.R. Mickelson. 1994. Tissue distribution of ryanodine receptor isoforms and alleles determined by reverse transcription polymerase chain reaction. *J Biol Chem*. 269:31544-51.

Lee, H.C. 1997. Mechanisms of calcium signaling by cyclic ADP-ribose and NAADP. *Physiol Rev*. 77:1133-64.

Lehnart, S.E., X.H. Wehrens, and A.R. Marks. 2004. Calstabin deficiency, ryanodine receptors, and sudden cardiac death. *Biochem Biophys Res Commun*. 322:1267-79.

Leifert, J.A., and J.L. Whitton. 2003. "Translocatory proteins" and "protein transduction domains": a critical analysis of their biological effects and the underlying mechanisms. *Mol Ther*. 8:13-20.

Lewis, R.J. 2000. Ion channel toxins and therapeutics: from cone snail venoms to ciguatera. *Ther Drug Monit*. 22:61-4.

Lewis, R.J., and M.L. Garcia. 2003. Therapeutic potential of venom peptides. *Nat Rev Drug Discov*. 2:790-802.

Lewis, R.J., K.J. Nielsen, D.J. Craik, M.L. Loughnan, D.A. Adams, I.A. Sharpe, T. Luchian, D.J. Adams, T. Bond, L. Thomas, A. Jones, J.L. Matheson, R. Drinkwater, P.R. Andrews, and P.F. Alewood. 2000. Novel omega-conotoxins from Conus catus discriminate among neuronal calcium channel subtypes. *J Biol Chem*. 275:35335-44.

Li, Y., Y. Mao, R.V. Rosal, R.D. Dinnen, A.C. Williams, P.W. Brandt-Rauf, and R.L. Fine. 2005. Selective induction of apoptosis through the FADD/caspase-8 pathway by a p53 c-terminal peptide in human pre-malignant and malignant cells. *Int J Cancer*. 115:55-64.

Liang, J.F., and V.C. Yang. 2005. Synthesis of doxorubicin-peptide conjugate with multidrug resistant tumor cell killing activity. *Bioorg Med Chem Lett*. 15:5071-5.

Lindgren, M.E., M.M. Hallbrink, A.M. Elmquist, and U. Langel. 2004. Passage of cell-penetrating peptides across a human epithelial cell layer in vitro. *Biochem J*. 377:69-76.

Lokuta, A.J., T.B. Rogers, W.J. Lederer, and H.H. Valdivia. 1995. Modulation of cardiac ryanodine receptors of swine and rabbit by a phosphorylation-dephosphorylation mechanism. *J Physiol*. 487 (Pt 3):609-22.

Lopez-Gonzalez, I., T. Olamendi-Portugal, J.L. De la Vega-Beltran, J. Van der Walt, K. Dyason, L.D. Possani, R. Felix, and A. Darszon. 2003. Scorpion toxins that block T-type Ca2+ channels in spermatogenic cells inhibit the sperm acrosome reaction. *Biochem Biophys Res Commun*. 300:408-14.

Lu, X., L. Xu, and G. Meissner. 1994. Activation of the skeletal muscle calcium release channel by a cytoplasmic loop of the dihydropyridine receptor. *J Biol Chem*. 269:6511-6.

Lukyanenko, V., I. Gyorke, T.F. Wiesner, and S. Gyorke. 2001. Potentiation of Ca(2+) release by cADP-ribose in the heart is mediated by enhanced SR Ca(2+) uptake into the sarcoplasmic reticulum. *Circ Res*. 89:614-22.

Mabrouk, K., N. Ram, S. Boisseau, F. Strappazzon, A. Rehaim, R. Sadoul, H. Darbon, M. Ronjat, and M. De Waard. 2007. Critical amino acid residues of maurocalcine involved in pharmacology, lipid interaction and cell penetration. *Biochim Biophys Acta*. 1768:2528-40.

Mader, J.S., and D.W. Hoskin. 2006. Cationic antimicrobial peptides as novel cytotoxic agents for cancer treatment. *Expert Opin Investig Drugs*. 15:933-46.

Magzoub, M., L.E. Eriksson, and A. Graslund. 2002. Conformational states of the cell-penetrating peptide penetratin when interacting with phospholipid vesicles: effects of surface charge and peptide concentration. *Biochim Biophys Acta*. 1563:53-63.

Maiolo, J.R., 3rd, E.A. Ottinger, and M. Ferrer. 2004. Specific redistribution of cell-penetrating peptides from endosomes to the cytoplasm and nucleus upon laser illumination. *J Am Chem Soc*. 126:15376-7.

Maiolo, J.R., M. Ferrer, and E.A. Ottinger. 2005. Effects of cargo molecules on the cellular uptake of arginine-rich cell-penetrating peptides. *Biochim Biophys Acta*. 1712:161-72.

Mano, M., C. Teodosio, A. Paiva, S. Simoes, and M.C. Pedroso de Lima. 2005. On the mechanisms of the internalization of S4(13)-PV cell-penetrating peptide. *Biochem J*. 390:603-12.

Marks, A.R. 1996. Cellular functions of immunophilins. *Physiol Rev*. 76:631-49.

Marks, A.R., P. Tempst, K.S. Hwang, M.B. Taubman, M. Inui, C. Chadwick, S. Fleischer, and B. Nadal-Ginard. 1989. Molecular cloning and characterization of the ryanodine receptor/junctional channel complex cDNA from skeletal muscle sarcoplasmic reticulum. *Proc Natl Acad Sci U S A*. 86:8683-7.

Martin, C., K.E. Chapman, J.R. Seckl, and R.H. Ashley. 1998. Partial cloning and differential expression of ryanodine receptor/calcium-release channel genes in human tissues including the hippocampus and cerebellum. *Neuroscience*. 85:205-16.

Marx, S.O., S. Reiken, Y. Hisamatsu, T. Jayaraman, D. Burkhoff, N. Rosemblit, and A.R. Marks. 2000. PKA phosphorylation dissociates FKBP12.6 from the calcium release channel (ryanodine receptor): defective regulation in failing hearts. *Cell*. 101:365-76.

Matsushita, M., K. Tomizawa, A. Moriwaki, S.T. Li, H. Terada, and H. Matsui. 2001. A high-efficiency protein transduction system demonstrating the role of PKA in long-lasting long-term potentiation. *J Neurosci*. 21:6000-7.

Mayor, S., and R.E. Pagano. 2007. Pathways of clathrin-independent endocytosis. *Nat Rev Mol Cell Biol*. 8:603-12.

McIntosh, J.M., A.D. Santos, and B.M. Olivera. 1999. Conus peptides targeted to specific nicotinic acetylcholine receptor subtypes. *Annu Rev Biochem*. 68:59-88.

McNiven, M.A., L. Kim, E.W. Krueger, J.D. Orth, H. Cao, and T.W. Wong. 2000. Regulated interactions between dynamin and the actin-binding protein cortactin modulate cell shape. *J Cell Biol*. 151:187-98.

McPherson, P.S., and K.P. Campbell. 1993. The ryanodine receptor/Ca2+ release channel. *J Biol Chem*. 268:13765-8.

Meade, B.R., and S.F. Dowdy. 2007. Exogenous siRNA delivery using peptide transduction domains/cell penetrating peptides. *Adv Drug Deliv Rev*. 59:134-40.

Medintz, I.L., T. Pons, J.B. Delehanty, K. Susumu, F.M. Brunel, P.E. Dawson, and H. Mattoussi. 2008. Intracellular Delivery of Quantum Dot-Protein Cargos Mediated by Cell Penetrating Peptides. *Bioconjug Chem*.

Meszaros, L.G., J. Bak, and A. Chu. 1993. Cyclic ADP-ribose as an endogenous regulator of the non-skeletal type ryanodine receptor Ca2+ channel. *Nature*. 364:76-9.

Mi, Z., J. Mai, X. Lu, and P.D. Robbins. 2000. Characterization of a class of cationic peptides able to facilitate efficient protein transduction in vitro and in vivo. *Mol Ther*. 2:339-47.

Mikami, A., K. Imoto, T. Tanabe, T. Niidome, Y. Mori, H. Takeshima, S. Narumiya, and S. Numa. 1989. Primary structure and functional expression of the cardiac dihydropyridine-sensitive calcium channel. *Nature*. 340:230-3.

Miller, C., E. Moczydlowski, R. Latorre, and M. Phillips. 1985. Charybdotoxin, a protein inhibitor of single Ca2+-activated K+ channels from mammalian skeletal muscle. *Nature*. 313:316-8.

Mintz, I.M., V.J. Venema, M.E. Adams, and B.P. Bean. 1991. Inhibition of N- and L-type Ca2+ channels by the spider venom toxin omega-Aga-IIIA. *Proc Natl Acad Sci U S A*. 88:6628-31.

Mitchell, D.J., D.T. Kim, L. Steinman, C.G. Fathman, and J.B. Rothbard. 2000. Polyarginine enters cells more efficiently than other polycationic homopolymers. *J Pept Res*. 56:318-25.

Monier, S., R.G. Parton, F. Vogel, J. Behlke, A. Henske, and T.V. Kurzchalia. 1995. VIP21-caveolin, a membrane protein constituent of the caveolar coat, oligomerizes in vivo and in vitro. *Mol Biol Cell*. 6:911-27.

Montesano, R., J. Roth, A. Robert, and L. Orci. 1982. Non-coated membrane invaginations are involved in binding and internalization of cholera and tetanus toxins. *Nature*. 296:651-3.

Morris, M.C., L. Chaloin, J. Mery, F. Heitz, and G. Divita. 1999. A novel potent strategy for gene delivery using a single peptide vector as a carrier. *Nucleic Acids Res*. 27:3510-7.

Morris, M.C., J. Depollier, J. Mery, F. Heitz, and G. Divita. 2001. A peptide carrier for the delivery of biologically active proteins into mammalian cells. *Nat Biotechnol*. 19:1173-6.

Morris, M.C., S. Deshayes, F. Heitz, and G. Divita. 2008. Cell-penetrating peptides: from molecular mechanisms to therapeutics. *Biol Cell*. 100:201-17.

Morris, M.C., E. Gros, G. Aldrian-Herrada, M. Choob, J. Archdeacon, F. Heitz, and G. Divita. 2007. A non-covalent peptide-based carrier for in vivo delivery of DNA mimics. *Nucleic Acids Res*. 35:e49.

Morris, M.C., P. Vidal, L. Chaloin, F. Heitz, and G. Divita. 1997. A new peptide vector for efficient delivery of oligonucleotides into mammalian cells. *Nucleic Acids Res*. 25:2730-6.

Morrissette, J., M. Beurg, M. Sukhareva, and R. Coronado. 1996. Purification and characterization of ryanotoxin, a peptide with actions similar to those of ryanodine. *Biophys J*. 71:707-21.

Mosbah, A., R. Kharrat, Z. Fajloun, J.G. Renisio, E. Blanc, J.M. Sabatier, M. El Ayeb, and H. Darbon. 2000. A new fold in the scorpion toxin family, associated with an activity on a ryanodine-sensitive calcium channel. *Proteins*. 40:436-42.

Muhlberg, A.B., D.E. Warnock, and S.L. Schmid. 1997. Domain structure and intramolecular regulation of dynamin GTPase. *EMBO J*. 16:6676-83.

Murata, M., J. Peranen, R. Schreiner, F. Wieland, T.V. Kurzchalia, and K. Simons. 1995. VIP21/caveolin is a cholesterol-binding protein. *Proc Natl Acad Sci U S A*. 92:10339-43.

Muratovska, A., and M.R. Eccles. 2004. Conjugate for efficient delivery of short interfering RNA (siRNA) into mammalian cells. *FEBS Lett*. 558:63-8.

Muratovska, A., C. Zhou, S. He, P. Goodyer, and M.R. Eccles. 2003. Paired-Box genes are frequently expressed in cancer and often required for cancer cell survival. *Oncogene*. 22:7989-97.

Murayama, T., T. Oba, E. Katayama, H. Oyamada, K. Oguchi, M. Kobayashi, K. Otsuka, and Y. Ogawa. 1999. Further characterization of the type 3 ryanodine receptor (RyR3) purified from rabbit diaphragm. *J Biol Chem*. 274:17297-308.

Murayama, T., and Y. Ogawa. 1992. Purification and characterization of two ryanodine-binding protein isoforms from sarcoplasmic reticulum of bullfrog skeletal muscle. *J Biochem*. 112:514-22.

Myou, S., X. Zhu, E. Boetticher, S. Myo, A. Meliton, A. Lambertino, N.M. Munoz, and A.R. Leff. 2002. Blockade of focal clustering and active conformation in beta 2-integrin-mediated adhesion of eosinophils to intercellular adhesion molecule-1 caused by transduction of HIV TAT-dominant negative Ras. *J Immunol*. 169:2670-6.

Nagahara, H., A.M. Vocero-Akbani, E.L. Snyder, A. Ho, D.G. Latham, N.A. Lissy, M. Becker-Hapak, S.A. Ezhevsky, and S.F. Dowdy. 1998. Transduction of full-length TAT fusion proteins into mammalian cells: TAT-p27Kip1 induces cell migration. *Nat Med*. 4:1449-52.

Nakai, J., T. Imagawa, Y. Hakamat, M. Shigekawa, H. Takeshima, and S. Numa. 1990. Primary structure and functional expression from cDNA of the cardiac ryanodine receptor/calcium release channel. *FEBS Lett*. 271:169-77.

Nakase, I., M. Niwa, T. Takeuchi, K. Sonomura, N. Kawabata, Y. Koike, M. Takehashi, S. Tanaka, K. Ueda, J.C. Simpson, A.T. Jones, Y. Sugiura, and S. Futaki. 2004. Cellular uptake of arginine-rich peptides: roles for macropinocytosis and actin rearrangement. *Mol Ther*. 10:1011-22.

Nakase, I., A. Tadokoro, N. Kawabata, T. Takeuchi, H. Katoh, K. Hiramoto, M. Negishi, M. Nomizu, Y. Sugiura, and S. Futaki. 2007. Interaction of arginine-rich peptides with membrane-associated proteoglycans is crucial for induction of actin organization and macropinocytosis. *Biochemistry*. 46:492-501.

Nascimento, F.D., M.A. Hayashi, A. Kerkis, V. Oliveira, E.B. Oliveira, G. Radis-Baptista, H.B. Nader, T. Yamane, I.L. Tersariol, and I. Kerkis. 2007. Crotamine mediates gene delivery into cells through the binding to heparan sulfate proteoglycans. *J Biol Chem*. 282:21349-60.

Newcomb, R., B. Szoke, A. Palma, G. Wang, X. Chen, W. Hopkins, R. Cong, J. Miller, L. Urge, K. Tarczy-Hornoch, J.A. Loo, D.J. Dooley, L. Nadasdi, R.W. Tsien, J. Lemos, and G. Miljanich. 1998. Selective peptide antagonist of the class E calcium channel from the venom of the tarantula Hysterocrates gigas. *Biochemistry*. 37:15353-62.

Nicholson, G.M., M. Willow, M.E. Howden, and T. Narahashi. 1994. Modification of sodium channel gating and kinetics by versutoxin from the Australian funnel-web spider Hadronyche versuta. *Pflugers Arch*. 428:400-9.

Nudleman, E., D. Wall, and D. Kaiser. 2005. Cell-to-cell transfer of bacterial outer membrane lipoproteins. *Science*. 309:125-7.

Oehlke, J., A. Scheller, B. Wiesner, E. Krause, M. Beyermann, E. Klauschenz, M. Melzig, and M. Bienert. 1998. Cellular uptake of an alpha-helical amphipathic model peptide with the potential to deliver polar compounds into the cell interior non-endocytically. *Biochim Biophys Acta*. 1414:127-39.

Ogawa, Y. 1994. Role of ryanodine receptors. *Crit Rev Biochem Mol Biol*. 29:229-74.

Oh, P., D.P. McIntosh, and J.E. Schnitzer. 1998. Dynamin at the neck of caveolae mediates their budding to form transport vesicles by GTP-driven fission from the plasma membrane of endothelium. *J Cell Biol*. 141:101-14.

Olivera, B.M., L.J. Cruz, V. de Santos, G.W. LeCheminant, D. Griffin, R. Zeikus, J.M. McIntosh, R. Galyean, J. Varga, W.R. Gray, and et al. 1987. Neuronal calcium channel antagonists. Discrimination between calcium channel subtypes using omega-conotoxin from Conus magus venom. *Biochemistry*. 26:2086-90.

Olivera, B.M., J.M. McIntosh, L.J. Cruz, F.A. Luque, and W.R. Gray. 1984. Purification and sequence of a presynaptic peptide toxin from Conus geographus venom. *Biochemistry*. 23:5087-90.

Omecinsky, D.O., K.E. Holub, M.E. Adams, and M.D. Reily. 1996. Three-dimensional structure analysis of mu-agatoxins: further evidence for common motifs among neurotoxins with diverse ion channel specificities. *Biochemistry*. 35:2836-44.

Pallaghy, P.K., K.J. Nielsen, D.J. Craik, and R.S. Norton. 1994. A common structural motif incorporating a cystine knot and a triple-stranded beta-sheet in toxic and inhibitory polypeptides. *Protein Sci*. 3:1833-9.

Panayotou, G., and M.D. Waterfield. 1993. The assembly of signalling complexes by receptor tyrosine kinases. *Bioessays*. 15:171-7.

Parton, R.G., B. Joggerst, and K. Simons. 1994. Regulated internalization of caveolae. *J Cell Biol*. 127:1199-215.

Patel, L.N., J.L. Zaro, and W.C. Shen. 2007. Cell penetrating peptides: intracellular pathways and pharmaceutical perspectives. *Pharm Res*. 24:1977-92.

Pelkmans, L., J. Kartenbeck, and A. Helenius. 2001. Caveolar endocytosis of simian virus 40 reveals a new two-step vesicular-transport pathway to the ER. *Nat Cell Biol*. 3:473-83.

Pelkmans, L., D. Puntener, and A. Helenius. 2002. Local actin polymerization and dynamin recruitment in SV40-induced internalization of caveolae. *Science*. 296:535-9.

Perea, S.E., O. Reyes, Y. Puchades, O. Mendoza, N.S. Vispo, I. Torrens, A. Santos, R. Silva, B. Acevedo, E. Lopez, V. Falcon, and D.F. Alonso. 2004. Antitumor effect of a novel proapoptotic peptide that impairs the phosphorylation by the protein kinase 2 (casein kinase 2). *Cancer Res*. 64:7127-9.

Perez, F., A. Joliot, E. Bloch-Gallego, A. Zahraoui, A. Triller, and A. Prochiantz. 1992. Antennapedia homeobox as a signal for the cellular internalization and nuclear addressing of a small exogenous peptide. *J Cell Sci*. 102 (Pt 4):717-22.

Perry, T., and N.H. Greig. 2002. The glucagon-like peptides: a new genre in therapeutic targets for intervention in Alzheimer's disease. *J Alzheimers Dis*. 4:487-96.

Phelan, A., G. Elliott, and P. O'Hare. 1998. Intercellular delivery of functional p53 by the herpesvirus protein VP22. *Nat Biotechnol*. 16:440-3.

Plescia, J., W. Salz, F. Xia, M. Pennati, N. Zaffaroni, M.G. Daidone, M. Meli, T. Dohi, P. Fortugno, Y. Nefedova, D.I. Gabrilovich, G. Colombo, and D.C. Altieri. 2005. Rational design of shepherdin, a novel anticancer agent. *Cancer Cell*. 7:457-68.

Polyakov, V., V. Sharma, J.L. Dahlheimer, C.M. Pica, G.D. Luker, and D. Piwnica-Worms. 2000. Novel Tat-peptide chelates for direct transduction of technetium-99m and rhenium into human cells for imaging and radiotherapy. *Bioconjug Chem*. 11:762-71.

Pooga, M., M. Hallbrink, M. Zorko, and U. Langel. 1998a. Cell penetration by transportan. *FASEB J*. 12:67-77.

Pooga, M., A. Jureus, K. Razaei, H. Hasanvan, K. Saar, K. Kask, P. Kjellen, T. Land, J. Halonen, U. Maeorg, A. Uri, S. Solyom, T. Bartfai, and U. Langel. 1998b. Novel galanin receptor ligands. *J Pept Res*. 51:65-74.

Pooga, M., M. Lindgren, M. Hallbrink, E. Brakenhielm, and U. Langel. 1998c. Galanin-based peptides, galparan and transportan, with receptor-dependent and independent activities. *Ann N Y Acad Sci*. 863:450-3.

Pooga, M., U. Soomets, M. Hallbrink, A. Valkna, K. Saar, K. Rezaei, U. Kahl, J.X. Hao, X.J. Xu, Z. Wiesenfeld-Hallin, T. Hokfelt, T. Bartfai, and U. Langel. 1998d. Cell penetrating PNA constructs regulate galanin receptor levels and modify pain transmission in vivo. *Nat Biotechnol*. 16:857-61.

Possani, L.D., B. Becerril, M. Delepierre, and J. Tytgat. 1999. Scorpion toxins specific for Na+-channels. *Eur J Biochem*. 264:287-300.

Pouvreau, S., L. Csernoch, B. Allard, J.M. Sabatier, M. De Waard, M. Ronjat, and V. Jacquemond. 2006. Transient loss of voltage control of Ca2+ release in the presence of maurocalcine in skeletal muscle. *Biophys J*. 91:2206-15.

Proenza, C., J. O'Brien, J. Nakai, S. Mukherjee, P.D. Allen, and K.G. Beam. 2002. Identification of a region of RyR1 that participates in allosteric coupling with the alpha(1S) (Ca(V)1.1) II-III loop. *J Biol Chem*. 277:6530-5.

Protasi, F., C. Paolini, J. Nakai, K.G. Beam, C. Franzini-Armstrong, and P.D. Allen. 2002. Multiple regions of RyR1 mediate functional and structural interactions with alpha(1S)-dihydropyridine receptors in skeletal muscle. *Biophys J*. 83:3230-44.

Racanicchi, S., C. Maccherani, C. Liberatore, M. Billi, V. Gelmetti, M. Panigada, G. Rizzo, C. Nervi, and F. Grignani. 2005. Targeting fusion protein/corepressor contact restores differentiation response in leukemia cells. *EMBO J*. 24:1232-42.

Racoosin, E.L., and J.A. Swanson. 1993. Macropinosome maturation and fusion with tubular lysosomes in macrophages. *J Cell Biol*. 121:1011-20.

Radmanesh, M. 1990. Clinical study of Hemiscorpion lepturus in Iran. *J Trop Med Hyg*. 93:327-32.

Richard, J.P., K. Melikov, H. Brooks, P. Prevot, B. Lebleu, and L.V. Chernomordik. 2005. Cellular uptake of unconjugated TAT peptide involves clathrin-dependent endocytosis and heparan sulfate receptors. *J Biol Chem*. 280:15300-6.

Richard, J.P., K. Melikov, E. Vives, C. Ramos, B. Verbeure, M.J. Gait, L.V. Chernomordik, and B. Lebleu. 2003. Cell-penetrating peptides. A reevaluation of the mechanism of cellular uptake. *J Biol Chem*. 278:585-90.

Robbins, P.B., S.F. Oliver, S.M. Sheu, J.B. Goodnough, P. Wender, and P.A. Khavari. 2002. Peptide delivery to tissues via reversibly linked protein transduction sequences. *Biotechniques*. 33:190-2, 194.

Robinson, M.S., and J.S. Bonifacino. 2001. Adaptor-related proteins. *Curr Opin Cell Biol*. 13:444-53.

Ross, M.F., and M.P. Murphy. 2004. Cell-penetrating peptides are excluded from the mitochondrial matrix. *Biochem Soc Trans*. 32:1072-4.

Rothberg, K.G., J.E. Heuser, W.C. Donzell, Y.S. Ying, J.R. Glenney, and R.G. Anderson. 1992. Caveolin, a protein component of caveolae membrane coats. *Cell*. 68:673-82.

Rothberg, K.G., Y.S. Ying, J.F. Kolhouse, B.A. Kamen, and R.G. Anderson. 1990. The glycophospholipid-linked folate receptor internalizes folate without entering the clathrin-coated pit endocytic pathway. *J Cell Biol*. 110:637-49.

Rousseau, E., J. Ladine, Q.Y. Liu, and G. Meissner. 1988. Activation of the Ca2+ release channel of skeletal muscle sarcoplasmic reticulum by caffeine and related compounds. *Arch Biochem Biophys*. 267:75-86.

Roy, S., R. Luetterforst, A. Harding, A. Apolloni, M. Etheridge, E. Stang, B. Rolls, J.F. Hancock, and R.G. Parton. 1999. Dominant-negative caveolin inhibits H-Ras function by disrupting cholesterol-rich plasma membrane domains. *Nat Cell Biol*. 1:98-105.

Rusnati, M., D. Coltrini, P. Oreste, G. Zoppetti, A. Albini, D. Noonan, F. d'Adda di Fagagna, M. Giacca, and M. Presta. 1997. Interaction of HIV-1 Tat protein with heparin. Role of the backbone structure, sulfation, and size. *J Biol Chem*. 272:11313-20.

Russell, D.G. 1995a. Mycobacterium and Leishmania: stowaways in the endosomal network. *Trends Cell Biol*. 5:125-8.

Russell, D.G. 1995b. Of microbes and macrophages: entry, survival and persistence. *Curr Opin Immunol*. 7:479-84.

Saalik, P., A. Elmquist, M. Hansen, K. Padari, K. Saar, K. Viht, U. Langel, and M. Pooga. 2004. Protein cargo delivery properties of cell-penetrating peptides. A comparative study. *Bioconjug Chem*. 15:1246-53.

Sabe, H. 2003. Requirement for Arf6 in cell adhesion, migration, and cancer cell invasion. *J Biochem*. 134:485-9.

Sabharanjak, S., and S. Mayor. 2004. Folate receptor endocytosis and trafficking. *Adv Drug Deliv Rev*. 56:1099-109.

Sakai, N., and S. Matile. 2003. Anion-mediated transfer of polyarginine across liquid and bilayer membranes. *J Am Chem Soc*. 125:14348-56.

Samsa, G.P., D.B. Matchar, G.R. Williams, and D.E. Levy. 2002. Cost-effectiveness of ancrod treatment of acute ischaemic stroke: results from the Stroke Treatment with Ancrod Trial (STAT). *J Eval Clin Pract*. 8:61-70.

Samso, M., R. Trujillo, G.B. Gurrola, H.H. Valdivia, and T. Wagenknecht. 1999. Three-dimensional location of the imperatoxin A binding site on the ryanodine receptor. *J Cell Biol*. 146:493-9.

Sandall, D.W., N. Satkunanathan, D.A. Keays, M.A. Polidano, X. Liping, V. Pham, J.G. Down, Z. Khalil, B.G. Livett, and K.R. Gayler. 2003. A novel alpha-conotoxin identified by gene sequencing is active in suppressing the vascular response to selective stimulation of sensory nerves in vivo. *Biochemistry*. 42:6904-11.

Sandgren, S., F. Cheng, and M. Belting. 2002. Nuclear targeting of macromolecular polyanions by an HIV-Tat derived peptide. Role for cell-surface proteoglycans. *J Biol Chem*. 277:38877-83.

Santana, A., S. Hyslop, E. Antunes, M. Mariano, Y.S. Bakhle, and G. de Nucci. 1993. Inflammatory responses induced by poly-L-arginine in rat lungs in vivo. *Agents Actions*. 39:104-10.

Santra, S., H. Yang, D. Dutta, J.T. Stanley, P.H. Holloway, W. Tan, B.M. Moudgil, and R.A. Mericle. 2004. TAT conjugated, FITC doped silica nanoparticles for bioimaging applications. *Chem Commun (Camb)*:2810-1.

Santra, S., H. Yang, J.T. Stanley, P.H. Holloway, B.M. Moudgil, G. Walter, and R.A. Mericle. 2005. Rapid and effective labeling of brain tissue using TAT-conjugated CdS:Mn/ZnS quantum dots. *Chem Commun (Camb)*:3144-6.

Scheller, A., J. Oehlke, B. Wiesner, M. Dathe, E. Krause, M. Beyermann, M. Melzig, and M. Bienert. 1999. Structural requirements for cellular uptake of alpha-helical amphipathic peptides. *J Pept Sci*. 5:185-94.

Schmid, S.L. 1997. Clathrin-coated vesicle formation and protein sorting: an integrated process. *Annu Rev Biochem*. 66:511-48.

Schmid, S.L., M.A. McNiven, and P. De Camilli. 1998. Dynamin and its partners: a progress report. *Curr Opin Cell Biol*. 10:504-12.

Schnitzer, J.E., P. Oh, E. Pinney, and J. Allard. 1994. Filipin-sensitive caveolae-mediated transport in endothelium: reduced transcytosis, scavenger endocytosis, and capillary permeability of select macromolecules. *J Cell Biol*. 127:1217-32.

Schwarze, S.R., A. Ho, A. Vocero-Akbani, and S.F. Dowdy. 1999. In vivo protein transduction: delivery of a biologically active protein into the mouse. *Science*. 285:1569-72.

Seto, E.S., H.J. Bellen, and T.E. Lloyd. 2002. When cell biology meets development: endocytic regulation of signaling pathways. *Genes Dev*. 16:1314-36.

Sever, S., H. Damke, and S.L. Schmid. 2000. Garrotes, springs, ratchets, and whips: putting dynamin models to the test. *Traffic*. 1:385-92.

Shachak, M., and S. Brand. 1983. The relationship between sit and wait foraging strategy and dispersal in the desert scorpion, Scorpio maurus palmatus. . *Oecologia*. 60:371-377.

Shahbazzadeh, D., N. Srairi-Abid, W. Feng, N. Ram, L. Borchani, M. Ronjat, A. Akbari, I.N. Pessah, M. De Waard, and M. El Ayeb. 2007. Hemicalcin, a new toxin from the Iranian scorpion Hemiscorpius lepturus which is active on ryanodine-sensitive Ca2+ channels. *Biochem J*. 404:89-96.

Shiraishi, T., and P.E. Nielsen. 2006. Photochemically enhanced cellular delivery of cell penetrating peptide-PNA conjugates. *FEBS Lett*. 580:1451-6.

Shiraishi, T., S. Pankratova, and P.E. Nielsen. 2005. Calcium ions effectively enhance the effect of antisense peptide nucleic acids conjugated to cationic tat and oligoarginine peptides. *Chem Biol*. 12:923-9.

Shokolenko, I.N., M.F. Alexeyev, S.P. LeDoux, and G.L. Wilson. 2005. TAT-mediated protein transduction and targeted delivery of fusion proteins into mitochondria of breast cancer cells. *DNA Repair (Amst)*. 4:511-8.

Sieczkarski, S.B., and G.R. Whittaker. 2002. Dissecting virus entry via endocytosis. *J Gen Virol*. 83:1535-45.

Silver, J., and W. Ou. 2005. Photoactivation of quantum dot fluorescence following endocytosis. *Nano Lett*. 5:1445-9.

Simeoni, F., M.C. Morris, F. Heitz, and G. Divita. 2003. Insight into the mechanism of the peptide-based gene delivery system MPG: implications for delivery of siRNA into mammalian cells. *Nucleic Acids Res*. 31:2717-24.

Simeoni, F., M.C. Morris, F. Heitz, and G. Divita. 2005. Peptide-based strategy for siRNA delivery into mammalian cells. *Methods Mol Biol*. 309:251-60.

Simons, K., and D. Toomre. 2000. Lipid rafts and signal transduction. *Nat Rev Mol Cell Biol*. 1:31-9.

Sitsapesan, R., and A.J. Williams. 1995. Cyclic ADP-ribose and related compounds activate sheep skeletal sarcoplasmic reticulum Ca2+ release channel. *Am J Physiol*. 268:C1235-40.

Smith, J.S., R. Coronado, and G. Meissner. 1985. Sarcoplasmic reticulum contains adenine nucleotide-activated calcium channels. *Nature*. 316:446-9.

Smith, J.S., E. Rousseau, and G. Meissner. 1989. Calmodulin modulation of single sarcoplasmic reticulum Ca2+-release channels from cardiac and skeletal muscle. *Circ Res*. 64:352-9.

Snyder, E.L., and S.F. Dowdy. 2005. Recent advances in the use of protein transduction domains for the delivery of peptides, proteins and nucleic acids in vivo. *Expert Opin Drug Deliv*. 2:43-51.

Snyder, E.L., C.C. Saenz, C. Denicourt, B.R. Meade, X.S. Cui, I.M. Kaplan, and S.F. Dowdy. 2005. Enhanced targeting and killing of tumor cells expressing the CXC chemokine receptor 4 by transducible anticancer peptides. *Cancer Res*. 65:10646-50.

Sonnleitner, A., S. Fleischer, and H. Schindler. 1997. Gating of the skeletal calcium release channel by ATP is inhibited by protein phosphatase 1 but not by Mg2+. *Cell Calcium*. 21:283-90.

Soomets, U., M. Lindgren, X. Gallet, M. Hallbrink, A. Elmquist, L. Balaspiri, M. Zorko, M. Pooga, R. Brasseur, and U. Langel. 2000. Deletion analogues of transportan. *Biochim Biophys Acta*. 1467:165-76.

Srinivasan, K.N., P. Gopalakrishnakone, P.T. Tan, K.C. Chew, B. Cheng, R.M. Kini, J.L. Koh, S.H. Seah, and V. Brusic. 2002. SCORPION, a molecular database of scorpion toxins. *Toxicon*. 40:23-31.

Stang, E., J. Kartenbeck, and R.G. Parton. 1997. Major histocompatibility complex class I molecules mediate association of SV40 with caveolae. *Mol Biol Cell*. 8:47-57.

Stendahl, O.I., J.H. Hartwig, E.A. Brotschi, and T.P. Stossel. 1980. Distribution of actin-binding protein and myosin in macrophages during spreading and phagocytosis. *J Cell Biol*. 84:215-24.

Stenmark, H., R.G. Parton, O. Steele-Mortimer, A. Lutcke, J. Gruenberg, and M. Zerial. 1994. Inhibition of rab5 GTPase activity stimulates membrane fusion in endocytosis. *EMBO J*. 13:1287-96.

Suarez-Kurtz, G., R. Vianna-Jorge, B.F. Pereira, M.L. Garcia, and G.J. Kaczorowski. 1999. Peptidyl inhibitors of shaker-type Kv1 channels elicit twitches in guinea pig ileum by

blocking kv1.1 at enteric nervous system and enhancing acetylcholine release. *J Pharmacol Exp Ther*. 289:1517-22.

Sutko, J.L., J.A. Airey, K. Murakami, M. Takeda, C. Beck, T. Deerinck, and M.H. Ellisman. 1991. Foot protein isoforms are expressed at different times during embryonic chick skeletal muscle development. *J Cell Biol*. 113:793-803.

Sutko, J.L., J.A. Airey, W. Welch, and L. Ruest. 1997. The pharmacology of ryanodine and related compounds. *Pharmacol Rev*. 49:53-98.

Suzuki, T., S. Futaki, M. Niwa, S. Tanaka, K. Ueda, and Y. Sugiura. 2002. Possible existence of common internalization mechanisms among arginine-rich peptides. *J Biol Chem*. 277:2437-43.

Swanson, J.A., and C. Watts. 1995. Macropinocytosis. *Trends Cell Biol*. 5:424-8.

Takei, K., O. Mundigl, L. Daniell, and P. De Camilli. 1996. The synaptic vesicle cycle: a single vesicle budding step involving clathrin and dynamin. *J Cell Biol*. 133:1237-50.

Takeshima, H. 1993. Primary structure and expression from cDNAs of the ryanodine receptor. *Ann N Y Acad Sci*. 707:165-77.

Takeshima, H., S. Komazaki, K. Hirose, M. Nishi, T. Noda, and M. Iino. 1998. Embryonic lethality and abnormal cardiac myocytes in mice lacking ryanodine receptor type 2. *EMBO J*. 17:3309-16.

Takeshima, H., S. Nishimura, T. Matsumoto, H. Ishida, K. Kangawa, N. Minamino, H. Matsuo, M. Ueda, M. Hanaoka, T. Hirose, and et al. 1989. Primary structure and expression from complementary DNA of skeletal muscle ryanodine receptor. *Nature*. 339:439-45.

Takeuchi, T., M. Kosuge, A. Tadokoro, Y. Sugiura, M. Nishi, M. Kawata, N. Sakai, S. Matile, and S. Futaki. 2006. Direct and rapid cytosolic delivery using cell-penetrating peptides mediated by pyrenebutyrate. *ACS Chem Biol*. 1:299-303.

Tanabe, T., K.G. Beam, B.A. Adams, T. Niidome, and S. Numa. 1990a. Regions of the skeletal muscle dihydropyridine receptor critical for excitation-contraction coupling. *Nature*. 346:567-9.

Tanabe, T., A. Mikami, T. Niidome, S. Numa, B.A. Adams, and K.G. Beam. 1993. Structure and function of voltage-dependent calcium channels from muscle. *Ann N Y Acad Sci*. 707:81-6.

Tanabe, T., A. Mikami, S. Numa, and K.G. Beam. 1990b. Cardiac-type excitation-contraction coupling in dysgenic skeletal muscle injected with cardiac dihydropyridine receptor cDNA. *Nature*. 344:451-3.

Temsamani, J., and P. Vidal. 2004. The use of cell-penetrating peptides for drug delivery. *Drug Discov Today*. 9:1012-9.

Tessier, D.J., P. Komalavilas, B. Liu, C.K. Kent, J.S. Thresher, C.M. Dreiza, A. Panitch, L. Joshi, E. Furnish, W. Stone, R. Fowl, and C.M. Brophy. 2004. Transduction of peptide analogs of the small heat shock-related protein HSP20 inhibits intimal hyperplasia. *J Vasc Surg*. 40:106-14.

Theisen, D.M., C. Pongratz, K. Wiegmann, F. Rivero, O. Krut, and M. Kronke. 2006. Targeting of HIV-1 Tat traffic and function by transduction-competent single chain antibodies. *Vaccine*. 24:3127-36.

Thoren, P.E., D. Persson, E.K. Esbjorner, M. Goksor, P. Lincoln, and B. Norden. 2004. Membrane binding and translocation of cell-penetrating peptides. *Biochemistry*. 43:3471-89.

Thoren, P.E., D. Persson, M. Karlsson, and B. Norden. 2000. The antennapedia peptide penetratin translocates across lipid bilayers - the first direct observation. *FEBS Lett*. 482:265-8.

Timerman, A.P., E. Ogunbumni, E. Freund, G. Wiederrecht, A.R. Marks, and S. Fleischer. 1993. The calcium release channel of sarcoplasmic reticulum is modulated by FK-506-binding protein. Dissociation and reconstitution of FKBP-12 to the calcium release channel of skeletal muscle sarcoplasmic reticulum. *J Biol Chem*. 268:22992-9.

Timerman, A.P., H. Onoue, H.B. Xin, S. Barg, J. Copello, G. Wiederrecht, and S. Fleischer. 1996. Selective binding of FKBP12.6 by the cardiac ryanodine receptor. *J Biol Chem*. 271:20385-91.

Tkachenko, A.G., H. Xie, Y. Liu, D. Coleman, J. Ryan, W.R. Glomm, M.K. Shipton, S. Franzen, and D.L. Feldheim. 2004. Cellular trajectories of peptide-modified gold particle complexes: comparison of nuclear localization signals and peptide transduction domains. *Bioconjug Chem*. 15:482-90.

Trehin, R., H.M. Nielsen, H.G. Jahnke, U. Krauss, A.G. Beck-Sickinger, and H.P. Merkle. 2004. Metabolic cleavage of cell-penetrating peptides in contact with epithelial models: human calcitonin (hCT)-derived peptides, Tat(47-57) and penetratin(43-58). *Biochem J*. 382:945-56.

Tripathy, A., W. Resch, L. Xu, H.H. Valdivia, and G. Meissner. 1998. Imperatoxin A induces subconductance states in Ca2+ release channels (ryanodine receptors) of cardiac and skeletal muscle. *J Gen Physiol*. 111:679-90.

Tripathy, A., L. Xu, G. Mann, and G. Meissner. 1995. Calmodulin activation and inhibition of skeletal muscle Ca2+ release channel (ryanodine receptor). *Biophys J*. 69:106-19.

Troy, C.M., D. Derossi, A. Prochiantz, L.A. Greene, and M.L. Shelanski. 1996. Downregulation of Cu/Zn superoxide dismutase leads to cell death via the nitric oxide-peroxynitrite pathway. *J Neurosci*. 16:253-61.

Truant, R., and B.R. Cullen. 1999. The arginine-rich domains present in human immunodeficiency virus type 1 Tat and Rev function as direct importin beta-dependent nuclear localization signals. *Mol Cell Biol*. 19:1210-7.

Tse, L.L., I. Chan, and J.K. Chan. 2001. Capsular intravascular endothelial hyperplasia: a peculiar form of vasoproliferative lesion associated with thyroid carcinoma. *Histopathology*. 39:463-8.

Tseng, Y.L., J.J. Liu, and R.L. Hong. 2002. Translocation of liposomes into cancer cells by cell-penetrating peptides penetratin and tat: a kinetic and efficacy study. *Mol Pharmacol*. 62:864-72.

Tunnemann, G., P. Karczewski, H. Haase, M.C. Cardoso, and I. Morano. 2007. Modulation of muscle contraction by a cell-permeable peptide. *J Mol Med*. 85:1405-12.

Turner, J.J., A.A. Arzumanov, and M.J. Gait. 2005a. Synthesis, cellular uptake and HIV-1 Tat-dependent trans-activation inhibition activity of oligonucleotide analogues disulphide-conjugated to cell-penetrating peptides. *Nucleic Acids Res*. 33:27-42.

Turner, J.J., G.D. Ivanova, B. Verbeure, D. Williams, A.A. Arzumanov, S. Abes, B. Lebleu, and M.J. Gait. 2005b. Cell-penetrating peptide conjugates of peptide nucleic acids (PNA) as inhibitors of HIV-1 Tat-dependent trans-activation in cells. *Nucleic Acids Res*. 33:6837-49.

Tyagi, M., M. Rusnati, M. Presta, and M. Giacca. 2001. Internalization of HIV-1 tat requires cell surface heparan sulfate proteoglycans. *J Biol Chem*. 276:3254-61.

Tytgat, J., K.G. Chandy, M.L. Garcia, G.A. Gutman, M.F. Martin-Eauclaire, J.J. van der Walt, and L.D. Possani. 1999. A unified nomenclature for short-chain peptides isolated from scorpion venoms: alpha-KTx molecular subfamilies. *Trends Pharmacol Sci*. 20:444-7.

Valdivia, H.H., M.S. Kirby, W.J. Lederer, and R. Coronado. 1992. Scorpion toxins targeted against the sarcoplasmic reticulum Ca(2+)-release channel of skeletal and cardiac muscle. *Proc Natl Acad Sci U S A*. 89:12185-9.

Valerius, N.H., O. Stendahl, J.H. Hartwig, and T.P. Stossel. 1981. Distribution of actin-binding protein and myosin in polymorphonuclear leukocytes during locomotion and phagocytosis. *Cell*. 24:195-202.

van Dam, E.M., and W. Stoorvogel. 2002. Dynamin-dependent transferrin receptor recycling by endosome-derived clathrin-coated vesicles. *Mol Biol Cell*. 13:169-82.

Vasir, J.K., and V. Labhasetwar. 2007. Biodegradable nanoparticles for cytosolic delivery of therapeutics. *Adv Drug Deliv Rev*. 59:718-28.

Villa, R., M. Folini, S. Lualdi, S. Veronese, M.G. Daidone, and N. Zaffaroni. 2000. Inhibition of telomerase activity by a cell-penetrating peptide nucleic acid construct in human melanoma cells. *FEBS Lett*. 473:241-8.

Vincent, J.P., M. Balerna, J. Barhanin, M. Fosset, and M. Lazdunski. 1980. Binding of sea anemone toxin to receptor sites associated with gating system of sodium channel in synaptic nerve endings in vitro. *Proc Natl Acad Sci U S A*. 77:1646-50.

Vives, E., P. Brodin, and B. Lebleu. 1997. A truncated HIV-1 Tat protein basic domain rapidly translocates through the plasma membrane and accumulates in the cell nucleus. *J Biol Chem*. 272:16010-7.

Vives, E., J.P. Richard, C. Rispal, and B. Lebleu. 2003. TAT peptide internalization: seeking the mechanism of entry. *Curr Protein Pept Sci*. 4:125-32.

Wadia, J.S., and S.F. Dowdy. 2002. Protein transduction technology. *Curr Opin Biotechnol*. 13:52-6.

Wadia, J.S., and S.F. Dowdy. 2003. Modulation of cellular function by TAT mediated transduction of full length proteins. *Curr Protein Pept Sci*. 4:97-104.

Wadia, J.S., and S.F. Dowdy. 2005. Transmembrane delivery of protein and peptide drugs by TAT-mediated transduction in the treatment of cancer. *Adv Drug Deliv Rev*. 57:579-96.

Wadia, J.S., R.V. Stan, and S.F. Dowdy. 2004. Transducible TAT-HA fusogenic peptide enhances escape of TAT-fusion proteins after lipid raft macropinocytosis. *Nat Med*. 10:310-5.

Wang, S., W.R. Trumble, H. Liao, C.R. Wesson, A.K. Dunker, and C.H. Kang. 1998. Crystal structure of calsequestrin from rabbit skeletal muscle sarcoplasmic reticulum. *Nat Struct Biol*. 5:476-83.

Watarai, M., S. Makino, Y. Fujii, K. Okamoto, and T. Shirahata. 2002. Modulation of Brucella-induced macropinocytosis by lipid rafts mediates intracellular replication. *Cell Microbiol*. 4:341-55.

Way, M., and R.G. Parton. 1995. M-caveolin, a muscle-specific caveolin-related protein. *FEBS Lett*. 376:108-12.

Wigge, P., and H.T. McMahon. 1998. The amphiphysin family of proteins and their role in endocytosis at the synapse. *Trends Neurosci*. 21:339-44.

Wu, H.Y., K. Tomizawa, M. Matsushita, Y.F. Lu, S.T. Li, and H. Matsui. 2003. Poly-arginine-fused calpastatin peptide, a living cell membrane-permeable and specific inhibitor for calpain. *Neurosci Res*. 47:131-5.

Xiao, R.P., H.H. Valdivia, K. Bogdanov, C. Valdivia, E.G. Lakatta, and H. Cheng. 1997. The immunophilin FK506-binding protein modulates Ca2+ release channel closure in rat heart. *J Physiol*. 500 (Pt 2):343-54.

Xu, L., G. Mann, and G. Meissner. 1996. Regulation of cardiac Ca2+ release channel (ryanodine receptor) by Ca2+, H+, Mg2+, and adenine nucleotides under normal and simulated ischemic conditions. *Circ Res*. 79:1100-9.

Yoon, H.Y., S.H. Lee, S.W. Cho, J.E. Lee, C.S. Yoon, J. Park, T.U. Kim, and S.Y. Choi. 2002. TAT-mediated delivery of human glutamate dehydrogenase into PC12 cells. *Neurochem Int*. 41:37-42.

Zamudio, F.Z., G.B. Gurrola, C. Arevalo, R. Sreekumar, J.W. Walker, H.H. Valdivia, and L.D. Possani. 1997. Primary structure and synthesis of Imperatoxin A (IpTx(a)), a peptide activator of Ca2+ release channels/ryanodine receptors. *FEBS Lett*. 405:385-9.

Zaro, J.L., T.E. Rajapaksa, C.T. Okamoto, and W.C. Shen. 2006. Membrane transduction of oligoarginine in HeLa cells is not mediated by macropinocytosis. *Mol Pharm*. 3:181-6.

Zaro, J.L., and W.C. Shen. 2003. Quantitative comparison of membrane transduction and endocytosis of oligopeptides. *Biochem Biophys Res Commun*. 307:241-7.

Zaro, J.L., and W.C. Shen. 2005. Evidence that membrane transduction of oligoarginine does not require vesicle formation. *Exp Cell Res*. 307:164-73.

Zhao, M., M.F. Kircher, L. Josephson, and R. Weissleder. 2002. Differential conjugation of tat peptide to superparamagnetic nanoparticles and its effect on cellular uptake. *Bioconjug Chem*. 13:840-4.

Zhao, M., P. Li, X. Li, L. Zhang, R.J. Winkfein, and S.R. Chen. 1999. Molecular identification of the ryanodine receptor pore-forming segment. *J Biol Chem*. 274:25971-4.

Zhu, S., H. Darbon, K. Dyason, F. Verdonck, and J. Tytgat. 2003. Evolutionary origin of inhibitor cystine knot peptides. *FASEB J*. 17:1765-7.

Zhu, X., F.Z. Zamudio, B.A. Olbinski, L.D. Possani, and H.H. Valdivia. 2004. Activation of skeletal ryanodine receptors by two novel scorpion toxins from Buthotus judaicus. *J Biol Chem*. 279:26588-96.

Ziegler, A., and J. Seelig. 2004. Interaction of the protein transduction domain of HIV-1 TAT with heparan sulfate: binding mechanism and thermodynamic parameters. *Biophys J*. 86:254-63.

Zielinski, J., K. Kilk, T. Peritz, T. Kannanayakal, K.Y. Miyashiro, E. Eiriksdottir, J. Jochems, U. Langel, and J. Eberwine. 2006. In vivo identification of ribonucleoprotein-RNA interactions. *Proc Natl Acad Sci U S A*. 103:1557-62.